

FOREWORD

This report was prepared by Materials Technology, TAPCO, a division of Thompson Ramo Wooldridge Inc. under Contract No. AF 33(616)-7796. The contract was initiated under Project No. 7351, "Metallic Materials," Task No. 735102, "Welding and Brazing of Metals." The work was administered under the direction of Directorate of Materials and Processes, Deputy Commander/Technology, Aeronautical Systems Division, Wright-Patterson Air Force Base, Ohio. Mr. J. T. Gow was the project engineer.

This report covers work done from 16 January 1961 to 15 January 1962.

The investigation was conducted by J. M. Gerken, Research Supervisor and J. M. Faulkner, Research Metallurgist, under the direction of A. H. Grobe. The report includes the results of welding studies of FS82, D31 and F48 columbium alloys.

Electron micrographs included in this report were prepared under the direction of R. A. Jefferys of Materials Processing Department. Flash welding was performed at Taylor Winfield Corporation through the cooperation of W. F. Haessly.

# Contrails

# Contrails

## ABSTRACT

An investigation was made of the welding characteristics of three commercial columbium base alloys, FS82, D31, and F48. Tungsten inert gas, electron beam, spot, and flash butt welding methods were included in this investigation. The effect of the welding variables travel speed, shielding gas composition and purity, filler metal additions, preheat and post heat were studied. Thermal cycles were measured in the fusion zone and heat affected zone of TIG welds to help explain mechanical properties and microstructure on the basis of physical metallurgy of each alloy.

The effect of welding on all alloys investigated was to increase the ductile to brittle transition temperature. This temperature was increased 200°F for FS82, 800°F for D31, and 500° to 800°F for F48 over that of the as-received wrought sheet. Of several post heat treatments investigated those most beneficial in lowering the transition temperature of welds were; 2000°F for 4 hours for FS82, 2100°F for 24 hours for D31, and 2500°F for 4 hours for F48.

The electron beam welding process consistently produced more ductile welds than the TIG process.

Ductile spot welds could be made readily in FS82 alloy; however, a relatively high electrode force is required to minimize center porosity and electrode sticking. Tungsten and molybdenum tipped electrodes were tried but neither offered an advantage over Class I copper electrodes in regard to sticking. Solid phase recrystallization spot welds were recommended for D31 and F48 to minimize cracking which usually occurs in fused spot welds.

A limited effort on flash welding has shown that a post weld heat treatment is required with FS82 and D31 alloys to achieve adequate room temperature ductility at the weld interface. F48 flash welds were not ductile at room temperature even after heat treatment. It is believed that the upset fibrous structure at the weld interface oriented normal to the sheet surface and rolling direction is in part responsible for the low ductility of flash welds.

## PUBLICATION REVIEW

This report has been reviewed and is approved.

FOR THE COMMANDER:



I. PERLMUTTER  
Chief, Physical Metallurgy Branch  
Metals and Ceramics Laboratory  
Directorate of Materials & Processes

# Contrails

## TABLE OF CONTENTS

	<u>Page</u>
I Introduction. . . . .	1
II Literature Review . . . . .	3
III Materials . . . . .	8
A. Source, Thickness and Analysis. . . . .	8
B. Microstructure. . . . .	8
C. Material Preparation. . . . .	17
IV Experimental Procedure. . . . .	17
A. Tungsten Inert Gas Fusion Welding . . . . .	17
1. Vacuum Purge Chamber Welding. . . . .	17
2. Non-Chamber Welding . . . . .	25
3. Preheat of Welds. . . . .	28
4. Filler Metal Additions. . . . .	28
5. Fusion Weld Thermal Cycle Studies . . . . .	28
B. Resistance Welds. . . . .	31
1. Spot and Projection Welds . . . . .	31
2. Flash Butt Welds. . . . .	31
C. Electron Beam Welds . . . . .	33
D. Weld Heat Treatment . . . . .	33
E. Weld Evaluation . . . . .	33
V Discussion of Results . . . . .	38
A. FS82 Alloy - TIG Welds. . . . .	38
B. D31 Alloy - TIG Welds . . . . .	60
C. F48 Alloy - TIG Welds . . . . .	81
D. Electron Beam Welds . . . . .	93
1. FS82 and FS82HS Alloy . . . . .	99
2. D31 Alloy . . . . .	99
3. F48 Alloy . . . . .	99
E. Spot and Projection Welds . . . . .	106
F. Flash Welds. . . . .	118
VI Summary. . . . .	127
VII Conclusions . . . . .	127
References. . . . .	129
Appendix. . . . .	131



# Contrails

## LIST OF ILLUSTRATIONS

	<u>Page</u>
1. Diagram Showing Locations of Hardness Impressions and Metallographic Samples Taken on Each Sheet of Material. . . . .	11
2. Microstructure of FS82 Alloy Sheet, Hardness 166DPH. . . . .	12
3. Microstructure of FS82 Alloy Sheet AD, Hardness 172DPH . . . .	13
4. Microstructure of FS82HS Alloy Sheet BC, Hardness 152DPH . . .	14
5. Microstructure of D31 Alloy Sheet CA, Hardness 234DPH. . . . .	15
6. Microstructure of D31 Alloy Sheet CE, Hardness 288DPH. . . . .	16
7. Microstructure of F48 Alloy Sheet D, Hardness 290DPH . . . . .	18
8. Microstructure of F48 Alloy Sheet DA, Hardness 309DPH. . . . .	19
9. Microstructure of F48 Alloy Sheet DB, Hardness 275DPH. . . . .	20
10. Vacuum Purge Welding Chamber . . . . .	21
11. Vacuum Purge Welding Chamber Showing Cart with Fixture Ready to be Loaded . . . . .	23
12. Fixture Used for Welding . . . . .	24
13. Automatic Tungsten Inert Gas Shielded Welder and Control . . .	26
14. Inert Gas Shielded Tungsten Electrode Welding Torch, Showing Trailer Shield and Filler Wire Positioner. . . . .	27
15. Oscillograph Traces from Tungsten-Tungsten 20% Rhenium Thermocouples in Welds . . . . .	30
16. AWS Recommended Projection Dimensions. . . . .	32
17. Electron Beam Welder and Control Panel . . . . .	34
18. Work Chamber of Electron Beam Welder Showing Gun and Work Table. . . . .	35
19. Drawings of Test Specimens . . . . .	37
20. Bend Ductility of 0.060 in. FS82, D31 and F48 Sheet. . . . .	39
21. Bend Ductility of FS82 As-Welded . . . . .	40

# Contracts

## LIST OF ILLUSTRATIONS (continued)

	<u>Page</u>
22. Bend Ductility of FS82HS As-Welded. . . . .	42
23. Bend Ductility of FS82 Welded in Helium at 15 ipm with Filler Metal Additions . . . . .	43
24. Microstructure of FS82 Welds. . . . .	45
25. Microstructures of FS82 Welds . . . . .	46
26. Microstructures of FS82 Welds . . . . .	47
27. Microstructure of FS82HS Welds. . . . .	48
28. Microstructure of FS82 and FS82HS Alloy Sheet . . . . .	49
29. Hardness Surveys of FS82 Welds. . . . .	51
30. Hardness Surveys of FS82 and FS82HS Welds . . . . .	52
31. Bend Ductility of FS82 Welded in Helium with Air at 15 ipm. . .	54
32. Bend Ductility of FS82 Welded in Helium at 15 ipm Then Aged at 1400 or 1600°F. . . . .	55
33. Bend Ductility of FS82 Welded in Helium at 15 ipm Then Aged at 1800 or 2000°F. . . . .	56
34. Bend Ductility of FS82 Welded in Helium at 15 ipm Then Double Aged at 2000, 2200 or 2400°F plus 1800°F. . . . .	57
35. Electron Micrographs of Heat Treated FS82 Welded at 15 ipm in Helium. . . . .	58
36. Thermal Cycle of Welds in 0.060 in. FS82 Sheet Made at 5, 15 and 30 ipm. . . . .	59
37. Bend Ductility of D31 Welded at 5, 15 or 36 ipm . . . . .	61
38. Cracks in D31 Welded at 36 ipm. . . . .	62
39. Bend Ductility of D31 Welded in Helium at 15 ipm with Pure Cb, FS80, or FS82 Filler Wire . . . . .	64
40. Microstructure of D31 Welded at 5 ipm in Helium . . . . .	65
41. Microstructure of D31 Welded at 21 ipm in Helium. . . . .	66

# Contracts

## LIST OF ILLUSTRATIONS (continued)

	<u>Page</u>
42. Microstructure of D31 Welds. . . . .	67
43. Microstructure of D31 Welds. . . . .	68
44. Microstructure of D31 Weld Made at 15 ipm in Helium with 500°F Preheat . . . . .	70
45. Hardness Surveys of D31 Welds. . . . .	72
46. Hardness Surveys of D31 Welds. . . . .	73
47. Bend Ductility of D31 Welded in Helium with Air at 15 ipm. . .	74
48. Bend Ductility of D31 Welded in Helium at 15 ipm Then Heat Treated at 2100 or 2350°F. . . . .	76
49. Bend Ductility of D31 Welded in Helium at 15 ipm Then Heat Treated at 1900, 2100, or 2550°F . . . . .	77
50. Microstructures of Weld in D31 at 15 ipm in Helium Heat Treated at 2100°F for 24 hours . . . . .	78
51. Microstructures of Welds in D31 at 15 ipm in Helium. . . . .	79
52. Electron Micrographs of D31 Sheet. . . . .	80
53. Microstructure of Weld in D31 at 15 ipm in Helium Heat Treated at 2350°F for 24 hours . . . . .	82
54. Bend Ductility of F48 Welded with a 500°F Preheat and With- out Preheat. . . . .	83
55. Bend Ductility of F48 Welded in Helium at 15 ipm with Pure Cb or FS80 Filler Wire. . . . .	84
56. Microstructures of Welds in F48 at 15 ipm in Helium. . . . .	86
57. Microstructures of Welds in F48 at 15 ipm Helium Preheated at 500°F. . . . .	87
58. Microstructures of Welds in F48 at 15 ipm in Helium. . . . .	88
59. Hardness Surveys of F48 Welds. . . . .	90
60. Hardness Surveys of F48 Welds. . . . .	91

# Contrails

## LIST OF ILLUSTRATIONS (continued)

	<u>Page</u>
61. Bend Ductility of F48 Welded in Helium with Air at 15 ipm. . . . .	92
62. Bend Ductility of F48 Welded in Helium at 15 ipm Then Heat Treated at 2350 or 2500°F. . . . .	94
63. Bend Ductility of F48 Welded in Helium at 15 ipm Then Heat Treated at 2100°F. . . . .	95
64. Microstructure of F48 Welds at 15 ipm in Helium. . . . .	96
65. Microstructures of Welds in F48 at 15 ipm in Helium Heat Treated at 2350°F for 24 Hours . . . . .	97
66. Electron Micrographs of F48 Alloy. . . . .	98
67. Bend Ductility of FS82 and FS82HS Electron Beam Welds. . . . .	100
68. Microstructure of Electron Beam Weld in FS82 at 40 ipm . . . . .	101
69. Microstructure of Electron Beam Weld in FS82HS at 40 ipm . . . . .	102
70. Bend Ductility of D31 Electron Beam Welds. . . . .	103
71. Microstructure of Electron Beam Weld in D31 at 40 ipm. . . . .	104
72. Bend Ductility of F48 Electron Beam Welds. . . . .	105
73. Microstructure of Electron Beam Welds in F48 at 40 ipm . . . . .	107
74. Photomacrographs of FS82 Spot Welds. . . . .	109
75. Photomacrographs of FS82 Projection Welds. . . . .	110
76. Photomacrographs of D31 Spot Welds . . . . .	117
77. Photomacrographs of F48 Spot Welds . . . . .	119
78. Microstructure of Flash Welds Showing Oxide Phase at Interface	121
79. Flash Weld in FS82, Weld No. 17. . . . .	122
80. Hardness Surveys of Flash Welds. . . . .	123
81. Flash Weld in D31, Weld No. 26 . . . . .	124
82. Flash Weld in F48, Weld No. 27 . . . . .	125

# Contrails

## LIST OF TABLES

	<u>Page</u>
I Sheet Material Data . . . . .	9
II Chemical Analysis of Alloys . . . . .	10
III Post Weld Heat Treatment Schedule . . . . .	36
IV Room and Elevated Temperature Tensile Properties for FS82 and FS82HS . . . . .	50
V Room and Elevated Temperature Tensile Properties for D31. . . . .	71
VI Room and Elevated Temperature Tensile Properties for F48 Alloy . . . . .	89
VII Resistance Welding Parameters and Results, Alloy FS82 . . . . .	111
VIII Resistance Welding Parameters and Results, Alloys D31 and F48 . . . . .	114
IX Spot Weld Hardness and Diameters. . . . .	116
X Flash Weld Mechanical Properties. . . . .	126
A-1 Parameters of Welds Made in Vacuum Atmosphere Welding Chamber . . . . .	131
A-2 Parameters of Welds Made Outside the Vacuum Atmosphere Purge Chamber . . . . .	136
A-3 Parameters of Welds Made by the Electron Beam Process . . . . .	137
A-4 Flash Welding Data. . . . .	138

# *Contrails*



## I INTRODUCTION

This report describes the efforts and results of a one year research program from January 16, 1961 to January 15, 1962 to investigate the welding characteristics of three commercial columbium base alloys. This work was sponsored by the United States Air Force, Aeronautical Systems Division, Directorate of Materials and Processes, Wright-Patterson Air Force Base.

Columbium and its alloys along with other refractory metals are of interest as structural materials for supersonic aircraft, space re-entry vehicles and components of jet engines. Columbium is particularly attractive for these applications when compared to other refractory metals (Mo, Ta, W) because it combines the features of a relatively high melting point with ductility, relatively low density and resistance to catastrophic oxidation at high temperature.

Alloys of columbium have been developed to increase the high temperature tensile properties and to increase the resistance to oxidation at high temperatures. While several alloys have been developed on an experimental basis to achieve these results it has usually been at the expense of fabricability and weldability. In addition, the ductile-to-brittle transition temperature is raised by additions of the alloying elements, W, Mo, and Cr, generally linearly with percentage addition. Titanium, zirconium, tantalum, and hafnium are elements which cause a minor increase in the transition temperature. The elements W, Mo, and Zr are most effective for imparting high temperature strength and creep resistance to columbium alloys. Titanium in small percentages develops a moderate increase in high temperature strength but as the percentage increases strength levels off and drops. On the other hand, titanium is the most effective alloying element in improving oxidation resistance. Its reduction in strength can be offset by additions of other alloys. Tantalum is a moderate strengthener but does not raise the transition temperature significantly and does not improve oxidation resistance.

Although most of the columbium alloys are ductile well below room temperature in the cold worked stress relieved condition, in some alloys recrystallization of the wrought structure results in raising the ductility transition temperature several hundred degrees above room temperature. Since the welding operation produces a zone of fused metal and a recrystallized heat-affected-zone the problem of greatly reduced weld ductility is encountered in most of the higher strength columbium alloys.

The purpose of this program was to investigate the effect of a number of welding methods on the mechanical properties and microstructure of welds in columbium alloys. Welding parameters and filler materials

---

Manuscript released by authors March 1962 for publication as an ASD Technical Documentary Report.

# Contrails

were studied to determine which combination of variables resulted in the smallest loss in ductility. In addition, post weld heat treatments were investigated for the purpose of restoring ductility of the weld zones. The effect of atmosphere purity, material cleanliness and interstitial content of the alloys was also studied.

The alloys included in this program for investigation were FS82, D31, and F48. FS82 (Cb-33%Ta-1%Zr) was developed and is produced by Fansteel Metallurgical Corporation. This alloy was included because it is a moderately high strength material which can be welded by most techniques without seriously reducing ductility or tensile properties. However, the weld zone in this alloy can lose ductility by an aging reaction between 1400° and 1800°F, as this investigation has shown, a range which includes a portion of the service temperature for this material. Most of the basic weld parameter determinations were performed on this alloy to develop base line data which then was translated to the other alloys which were more difficult to weld.

D31 (Cb-10%Ti-10%Mo) was developed by Du Pont Pigments Department and is being produced on a commercial basis by their Metallurgical Products Department. This is a moderate high-temperature-strength good oxidation resistant alloy. In the wrought form it is generally ductile down to -275°F. However, heat treatment causing recrystallization also causes a precipitation reaction which raises the transition temperature to about 600°F. This condition appears in the weld zone of D31.

F48 (Cb-15W-5Mo-1Zr) was developed by General Electric Flight Propulsion Department in cooperation with the G. E. Research Laboratory. It is in the laboratory production stage at both Allegheny Ludlum Steel Corporation and Crucible Steel Corporation. F48 exhibits high strength at elevated temperatures but is not particularly resistant to oxidation at high temperatures. Lack of oxidation resistance is not considered to be a serious handicap because it is agreed that most columbium alloy hardware will require a protective coating for service. Like D31, this alloy becomes severely embrittled by welding.



## II LITERATURE REVIEW

During the past several years a large amount of research has been conducted on the metallurgy of columbium and columbium alloy systems. Before 1961 the important researches on columbium alloy welding were performed at Westinghouse Research Laboratories, General Electric Flight Propulsion Laboratories and Oak Ridge National Laboratories. Prior to these investigations, research efforts were concerned with the welding of commercially pure columbium.

Dr. Yntema (1) indicated that columbium and tantalum can be welded by the same processes; resistance welding, submerged arc welding under carbon tetrachloride, and tungsten inert gas welding. In each case emphasis was placed on joint cleanliness and protection of the weld area from atmospheric contamination during the weld cycle. Resistance welds may be made in thin sheets in air or under a blanket of inert gas, while thicker sheets must be welded under water to insure rapid cooling to minimize contamination. Manual welding with a carbon electrode, of components, while submerged in carbon tetrachloride has been applied extensively to tantalum. Small amounts of carbon are introduced into the weld area with apparently no undesirable effect in the particular application. Tungsten inert gas welding was used more where the process could be automated. The operation was carried out in a chamber flushed with helium and great care was exercised to prevent contamination of the weld with metals in the holding fixture.

The British Welding Research Association (2) reported work on the welding of 0.012 in. and 0.030 in. unalloyed columbium sheet by the tungsten inert gas process. The as-welded hardness of the fusion zone in work hardened sheet was comparable to the annealed hardness of this sheet. However, after annealing at 1832°F in vacuo, weld zone hardening occurred as a result of surface oxides diffusing into the metal. This effect was reduced considerably by welding in an inert gas purge chamber or in a vacuum purge chamber where surface contamination during welding was minimized. Spot welding was performed in air with 1 or 2 cycles heating time. It was recommended that seam welding be done under water to cool the welds as quickly as possible.

Hardness measurements, mechanical tests and metallographic examinations were used by Begley (3) to evaluate the effects of atmospheric impurities and alloying additions on welds. Bead-on-plate type of welds were used. Nitrogen additions of 1 and 10% to the welding atmosphere caused slight weld discoloration while 0.63% oxygen caused severe discoloration. However, nitrogen in these amounts raised the bend transition temperature above 482°F while the 0.63% oxygen welds were ductile at 77°F. Hardness measurements of welds made in purified argon, commercial welding grade argon and argon with 1 and 10% nitrogen and 0.63% oxygen additions indicated that nitrogen was the principle cause of hardening in the weld zone. Since commercial argon was found to contain 0.08% nitrogen it was recommended that helium, which normally contains less nitrogen, be used as the shielding gas. Hardness surveys were run on welds in binary columbium base alloys of V, W, and HF. Porosity observed at the fusion line was believed to be the result of

# Contrails

a reaction of O and C to form CO which was trapped because the metal at this location solidified rapidly.

Further work by Begley and Platte (4) was performed in a vacuum purge chamber after evacuating to  $1 \times 10^{-5}$  mm of mercury pressure and back filling with tank helium. Bead-on-plate welds were made in which the weld was started and stopped on the plate about  $3/4$  in. from each end to induce high shrinkage stresses and thereby expose any tendency for hot cracking in each alloy welded. All welding was done with a tungsten electrode, straight polarity and at a speed of 3 ipm. Binary alloys of Cb plus 1, 5, 10 and 20%Ti, 0.5, 1, 5, and 10%Zr, 1%Hf, 1 and 5%W and 1 and 5%V were studied. Before welding the sheets were surface ground, etched in 60%HNO<sub>3</sub>-40%HF solution then annealed at 2732°F in vacuum for 1 hour. Compared with a 30 point VPN hardness increase in the weld fusion zone of unalloyed columbium the Cb-12Zr exhibited a 120 point increase in the fusion zone and the Cb-10Zr a 100 point increase in the fusion and heat affected zones. The fusion zone hardness of Cb-1Ti increased 160 points while the Cb-16Ti fusion zone hardness decreased 60 points. Weld porosity at the fusion line was noted as in the earlier work on unalloyed columbium.

Fugardi and Zambrow (5) discussed the welding of columbium clad stainless steel in which an iron barrier layer was used between the two sheets. Butt joints were prepared by machining the stainless steel back  $5/16$  in. so that when the higher melting columbium was welded first there would be no alloying with stainless steel. Welding was performed in a dry box under an argon atmosphere. Atmosphere purity was checked by applying 4.5 volts to a 3 volt flashlight bulb without the glass inside the welding chamber. A filament life of 8 minutes indicated a satisfactory atmosphere while a dew point of -50°F or higher caused the filament to burn out in less than 6 minutes. Tensile tests of the composite welds indicated that the columbium was more ductile than the stainless steel.

Franco-Ferreira (6) reported that contamination-free welds in  $1/4$  in. and  $1/2$  in. unalloyed columbium were produced in air with a trailer gas shield and machine welding techniques. The procedure was to fuse the root of a groove butt joint with the tungsten inert gas process then fill the remainder of the groove employing the consumable electrode inert gas shielded process. Extensive work has also been done on the aging of welds in Cb-12Zr at temperatures from 1300° to 1800°F for times up to 250 hours. Although the Cb-12Zr alloy is completely ductile at room temperature after welding, exposure of the welds for extended periods between 1500° and 1700°F caused loss in ductility. At the higher temperature loss of ductility occurred after a relatively short time (10 hours) but was regained after 100 hours exposure. At the lower temperatures ductility was lost after about 25 hours and was only partly restored after 250 hours. At 1800°F no loss of ductility was observed. When welds were annealed at 2200°F for 1 hour prior to the aging treatments no loss in ductility was found. It appears that an aging reaction occurs in this alloy and that overaging proceeds at the higher temperatures and longer times.

# Contrails

Stacey (7) describes the fabrication of a prototype leading edge structure of .040 in. FS82 columbium alloy. Manual T-melt-down welds were made in a vacuum purge chamber after evacuating to 0.03 microns of mercury pressure and back filling with argon. Fixturing and control of warpage were of primary concern in this work.

Johnson and Derry (8) in welding 1/16 in. Cb to 1/16 in. V sheet observed a tongue of columbium extending into the fusion zone of the weld indicating that a low melting alloy of Cb and V was formed with little direct melting of the columbium. The hardness changed abruptly from 140 VPN in the columbium to 350 VPN in the fusion zone.

Burrows, Schwartz, and Gagola (9) welded FS82 and D31 in a gas purge chamber in both argon and helium atmospheres. Helium was preferred because a hotter arc was attained and a cleaner atmosphere resulted. Atmosphere purity was checked by welding on titanium sheet. FS82 was ductile in the as-welded condition but strength was lowered slightly. Of three fusion welds made in D31 sheet, only one did not crack during welding. They observed what was described as a precipitate or solid solution melting in the interface between the fusion zone and the heat-affected zone. High temperature heat treatments were tried for improving weld ductility with limited success. Satisfactory spot welds were made in FS82 sheet from 0.002 in. to 0.032 in. thicknesses. Electrode sticking and need for frequent reshaping of tips were the main problems with this alloy. Harder, Class 2 electrode material maintained its shape longer and required less dressing than the softer, higher conductivity Class 1 material. It was necessary to use a multi-impulse welding technique on D31 to eliminate sticking and to give a fine grained solid phase weld. Both D31 and FS82 were brazed with Ti, Pd, 90Pt-10Ir, 90Pt-10Rh and Pt at temperatures from 2900° to 3450°F. Of these, only Ti produced joints with good ductility and limited erosion of the base metal. The 90Pt-10Rh alloy caused severe erosion and very brittle joints. Brazing was done in a cold wall vacuum furnace.

Work performed by Young (10) at the G. E. Flight Propulsion Laboratory has shown that welds made in He in a vacuum purge chamber on pure columbium and on Cb-0.7Zr can be bent 180° in a sharp radius. However, when pure Cb is welded in air with no trailer shield the weld zone becomes brittle. After removal of the surface layers a 105° LT bend can be achieved. Welds have been reported in .042 in. FS82 made in a vacuum purge chamber in He with the addition of .045 in. diameter FS82 filler wire. Although ductile as welded, ductility was reduced by a 1950°F 1-hour heat treatment. However, ductility could be restored by a subsequent 2100°F 1-hour treatment. A double heat treatment of 2100°F for 1 hour followed by 1950°F for 1 hour did not reduce ductility probably because the 2100°F causes overaging by non-coherent precipitation of the embrittling phase. Since aging may occur during service of a welded part or during application of an oxidation resistant coating, it was recommended that welds in FS82 be overaged at 2100°F for 1 hour. Welds made in FS82 without a shielding chamber but with a trailing shield and inert gas backup were ductile as welded. An aging behavior similar to that occurring



# Contrails

in the chamber welds was encountered.

F48 welds were made in a vacuum purge chamber back filled with Grade A helium. Prior to welding, samples were vapor blasted then etched in a  $\text{HNO}_3$ -HF solution. Filler metals consisting of Cb-1Zr, Cb-8Ti, Cb-5 and 10Y, Cb-1Ce, Cb-1 mischmetal, and FS82 were added to manual welds. Filler materials were etched prior to welding to minimize the amount of impurities introduced into the weld from surface films. Tight fixturing of F48 welds caused cracking during cooling. Looser fixturing corrected this condition but allowed more distortion to take place. A 500°F preheat was provided by a quartz lamp in the fixture to allow weld stresses to become equalized while above the transition temperature. Of this combination, only welds made with the Cb-1Zr filler material and annealed at 2500°F for 2 hours produced ductile welds at room temperature. The Cb-1Zr filler metal welds annealed at 2200°F for 10 hours yielded some ductility with failure occurring in the heat-affected zone. It was speculated that the brittle fracture was caused by precipitation of carbides in grain boundaries of that part of the recrystallized heat-affected zone which had exceeded 3000°F. As-welded hardnesses in F48 welded with Cb-1Zr filler metal were: fusion zone 214 VPN, heat affected zone 252 VPN, and parent metal 248 VPN. After aging at 2200°F the heat-affected zone hardness increased to 330 VPN, while the fusion zone and parent metal each increased about 10 points VPN.

FS82 was spot welded in thicknesses of 0.010 in., 0.025 in., and 0.070 in. Tensile shear strengths of 850 and 950 lbs. in the 0.025 in. sheet were obtained with 4-cycle weld times and 4000 lbs. electrode force. Solid phase welds thus obtained did not present a problem of electrode sticking. Both FS82 and F48 sheet were cleaned before spot welding by rubbing with steel wool then rinsing with acetone. There is a possibility that this procedure applied a microfilm of iron to the surfaces which helped in solid phase bonding. Spot welds were made in 0.040 in. F48 sheet at the following sequence: preheat 60 cycles - 3500 amps - 650 lbs. electrode force, weld 2 cycles - 17,500 amps - 1500 lbs. electrode force. Titanium shims, 0.001 in. and 0.003 in. thick, improved the as-welded strength of spots. A 2500°F 2-hour diffusion heat treatment increased the strength of welds with and without Ti foil to the extent that they were nearly equal. Heat treatment also decreased the tendency for failure to occur by cleavage at 45° with the rolling direction. Room temperature tensile strength of 870 to 1270 lbs. were reported with the 0.001 in Ti foil plus 2500°F 2-hour heat treatment. At 350°F ductility increased and loads of approximately 1500 lbs. were obtained.

McDonnell Aircraft Corporation (11) performed extensive work on the spot welding of F48 alloy in thicknesses from 0.012 in. to 0.080 in. Although difficulty was encountered in welding this material, satisfactory welds could be obtained under carefully controlled conditions in uniform quality material. In general, a recrystallization or solid phase type spot weld produced better properties than a fusion or cast nugget type spot weld. Inert gas arc butt and T welds were performed in FS82 alloy in thicknesses from 0.1 to 0.5 in. It was found that cleanliness (atmosphere, sheet and

# Contrails

filler wire) was the most important factor in producing ductile welds in this alloy.

Trabold and Bank (12) of Grumman Aircraft in a study of the fabricability of D31 alloy tried high energy rate techniques such as spot welding and electron beam welding which would minimize the heat affected zone. In both cases extreme brittleness and low strength were observed. Cracks extended from the fused nugget of spot welds out to the surface.

Robertshaw (13) has reported the results of welding studies on F48 alloy sheet produced from hot pressed powder compacts. Full penetration bead-on-plate welds were made manually on 0.050 in. sheet in a vacuum purge chamber with a helium atmosphere. Weld specimens heat treated at 2500°F for 2 hours exhibited about the same degree of ductility as welds similarly heat treated in sheet made from arc cast ingots. An average bend angle of 77° was obtained for electropolished weld samples bent at room temperature around a 6T radius.

The solid phase bonding of columbium has been investigated by Paprocki, Hodge and Gripshover (14, 15, 16). Unalloyed columbium was bonded to itself at a temperature of 2100° to 2400°F and a pressure of 10,000 psi for 3 hours. The surfaces to be bonded were etched in a solution of 65% HNO<sub>3</sub> and 35% HF to remove 0.001 in. of material. The components were then enclosed in an evacuated envelope or welded around the edge to form a gas tight assembly. This method of bonding has produced joint strengths of 40,000 psi with 90% reduction of area. Metallographically this produces a bond in which there is complete grain growth across the original interface.

Ultrasonic welding techniques have been considered as a logical method of joining the columbium alloys which become embrittled in normal fusion welding. Since bonding is accomplished by relative mechanical motion at the joint and relatively little heat is generated, recrystallization and formation of brittle intermetallic compounds is eliminated. Equipment for ultrasonic welding refractory metals has been developed by Jones et al (17) and data on D31 alloy weld properties have been reported. Weare and Monroe (18) reported the results of their efforts to ultrasonically weld 0.020 in. columbium sheet to 0.018 in. type 316 stainless steel and to 0.018 in. Inconel sheet. A tensile shear strength of 90 - 100 lbs. was obtained between columbium and stainless steel and a strength of 130 - 145 lbs. between columbium and Inconel when these materials were welded to each other directly. Use of a 0.005 in. iron insert between the columbium and stainless steel increased the tensile shear strength to 160 - 175 lbs.

Rajala and VanThyne (19) in developing improved vanadium - columbium base alloys observed that V-60Cb alloy was strongest at 2000°F with an ultimate strength of 62,000 psi. A V-5Ti-20Cb alloy exhibited a tensile strength of 50,000 psi at 2000°F and when welded passed a 180° 3T bend without post heat treatment. No welding studies were reported on the V-60Cb alloy.

An evaluation of brazing materials for columbium base alloys was conducted by Young (20). From a study of the brazing behavior on F48 and Cb-12r, four brazing alloys were selected for further investigation. These alloys, Zr-28V-16Ti, Ti-6Fe-4Cr, Ti-30V, and V-35Cb exhibited useful brazing strength and little effect on the ductility of the base metal.

### III MATERIAL

#### A. Source, Thickness and Analysis

As far as possible material for this investigation was obtained in three thicknesses, 0.020 in. for resistance welding, 0.060 in. for tungsten arc, electron beam and resistance welding and 1/8 in. for flash butt welding. The source, quantities, thicknesses, and hardness of each alloy are given in Table I. While the FS82 and D31 were obtained from Fansteel and Du Pont their respective developers and producers, the F48 alloy was obtained from three sources, Allegheny Ludlum, General Electric and Wright Field. The F48 obtained from Wright Field was through the courtesy of Sgt. Jesse Ingram from material produced on the McDonnell Refractory Metals Structural Development Program. Chemical analysis of these materials are listed in Table II.

#### B. Microstructure

Rockwell hardness measurements and metallographic sections were taken at several locations on each individual sheet as shown in Figure 1. Representative microstructures of each heat of material are presented in Figures 2 through 9.

Two heats of FS82 alloy were obtained for this program, one having what is considered a standard oxygen level of 500 to 1000 ppm and the other designated HS (high strength) with the oxygen between 1000 and 1500 ppm. Both grades of FS82 were included because it was believed that the oxygen content would effect the ductility and strength of welds. This material was reported by the manufacturer to be shipped in the fully annealed condition. A comparison of Figures 2 and 3 indicate that the recrystallization of the standard alloy was not complete over all areas of the sheet received. These variations could have been caused by variations in composition, amount of cold work or by temperature differences in the annealing furnace. This variation in structure and hardness did not cause any serious difficulty in welding this alloy. As the microstructure and hardness indicate, Figure 4, the high oxygen FS82 received a full recrystallization anneal. There was no indication of rolling direction in the microstructure, therefore it was considered that the greater dimension of the sheet was in the rolling direction.

The microstructure of the two heats of D31 represented in Figures 5 and 6 indicate a stress relief heat treated condition. The lesser degree of recrystallization in Figure 6 indicates a somewhat lower stress relief temperature. It will also be noticed that sheet CA, Figure 5, exhibited larger and less uniformly distributed carbide particles, particularly as shown by the light and dark irregular bands in the flat section.

TABLE I

SHEET MATERIAL DATA

<u>Alloy</u>	<u>Source</u>	<u>Heat No.</u>	<u>Code*</u>	<u>Thickness</u>	<u>Weight Lbs.</u>	<u>Rockwell Hardness</u>		
						<u>Aver.</u>	<u>Max.</u>	<u>Min.</u>
FS82	Fansteel	82-A-111	AA-AI	.060	24.6	76.8B	84B	67B
	Fansteel	82-A-111	AJ	.020	0.67	80.3B	83B	77.5B
	Fansteel	82-A-181	AK-AW	.125	3.6	93.5B	97B	83B
FS82HS	Fansteel	82-A-244	BC-BD	.060	5.6	70.1B	71.5B	67.5B
	Fansteel	82-A-244	BE	.020	0.45	74.1B	75B	73B
	Fansteel	82-A-244	BA-BB	.125	1.08	77.3B	74B	72B
D31	Du Pont	31-007	CA-CC	.060	14.3	81.0G	90G	74.5G
	Du Pont	31-007	CD	.020	0.55	89.5B	93B	85B
	Du Pont	31-038-02	CE	.060	2.64	84.3G	88G	82.5G
	Du Pont	31-038-02	CF	.021	1.18	98.1G	100G	96.5G
	Du Pont	31-038-2	CI	.125	2.1	99B	100B	98B
F48	G.E.	308.422	DA	.057	1.65	85.2G	90G	82G
F48	Allegheny Ludlum		DB-DD	.055	5.8	84.5G	90G	80G
	Allegheny Ludlum		DE	.061	2.2	85.7G	90G	81G
F48	ASD McDonnell	S95A	D or S95A	.090-.147	11.0			

\*Note: In the material code the alloy is identified by the first letter as follows: A=FS82, B=FS82HS, C=D31 and D=F48. The second letter of the code identifies each individual sheet of an alloy and in this way ties in with a particular heat number. For example, sheets marked AA through AI are FS82 heat 82-A-111 0.060 in. thick. Sheet AJ is FS82 heat 82-A-111 0.020 in. thick. F48 heat S95A was received before the coding system was initiated and is identified as either S95A or D.

All fusion weld and resistance weld data for FS82 was determined on heat 82-A-111, flash weld data was obtained from heat 82-A-181. All FS82HS data was obtained on heat 82-A-244. Most fusion weld data for D31 was obtained on heat 31-007, that obtained on heat 31-038 is identified by the code CE on the ductility and hardness curves. Flash weld and 0.020 in. spot weld data were obtained on heat 31-038. Spot weld and most fusion weld data for F48 were determined on one heat marked DB, DC and DD. Data obtained from other heats are identified as DA, DE, and S95A or D as indicated above. F48 flash welds were made from heat S95A.



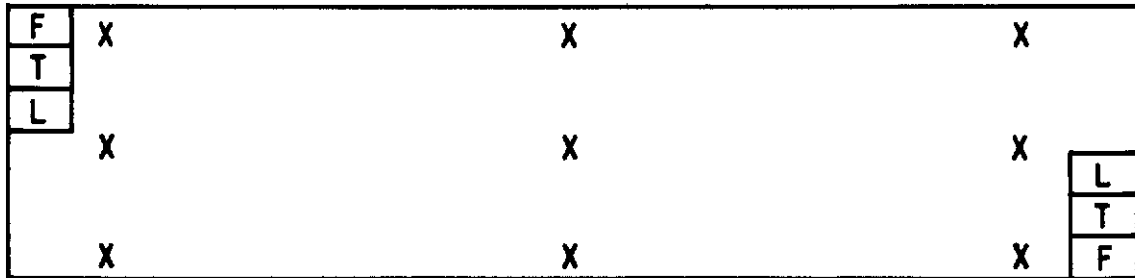
TABLE II

CHEMICAL ANALYSIS OF ALLOYS

<u>ALLOY</u>	<u>LOT NO.</u>	<u>THICK. (IN.)</u>	<u>SOURCE OF ANALYSIS</u>	<u>O</u>	<u>N</u>	<u>H</u>	<u>C</u>	<u>Ta</u>	<u>Zr</u>	<u>W</u>	<u>Mo</u>	<u>Ti</u>
FS82	82-A-111	.060	Tapco	.07	.012	.0017	.004	32.97	.71	-	-	-
			Fansteel	.076	.017	-	.010	30.70	.76	.020	-	-
			Du Pont	.0794	.0267	.0001	.0010	-	-	-	-	-
FS82	82-A-181	.125	Tapco	.056	-	.0059	.00059	33.13	.70	-	-	-
			Fansteel	.093	.030	-	.080	30.7	.59	.25	-	.007
			Du Pont	.12	.032	.0001	.0014	-	-	-	-	-
FS82	82-A-174	.020	Tapco	.12	.006	.00038	.018	32.82	.80	-	-	-
			Fansteel	.10	.031	-	.020	31.50	.58	.043	-	.007
			Du Pont	.12	.0031	.0003	.0029	-	-	-	-	-
FS82HS	82-A-244	.125	Tapco	.05	.004	.001	.000	33.05	.076	-	-	-
			Fansteel	.15	.040	-	.010	33.18	.076	.021	-	.007
			Du Pont	.13	.0218	.0001	.002	-	-	-	-	-
F48	308-422	.060	Tapco	.008	-	.00071	.021	-	.88	14.16	5.21	-
			Du Pont	.0802	.0175	.0001	.0299	-	-	-	-	-
F48	Al. Lud.	.060	Tapco	.017	.002	.0013	.015	-	.62	15.87	4.72	-
F48	S95A	.070	Tapco	.026	-	.0045	.017	-	.88	14.8	5.30	-
D31	31-038-02	.060	Tapco	.032	.003	.005	.065	-	-	-	9.42	13.59
			Du Pont	.0250	.0060	.0002	.1190	-	-	-	10.0	10.0
D31	31-007	.060	Tapco	.034	.002	.0023	.007	-	-	-	9.99	10.64
			Du Pont	.0157	.003	.0018	.0805	.07	.01	-	10.6	9.4
D31	31-001	.030	Tapco	.010	-	.0013	.036	-	-	-	9.60	10.91
			Du Pont	.0104	.0100	.00005	.0884	-	-	-	10.0	8.9
D31	-	.020	Tapco	.067	.001	.0012	.006	-	-	-	9.89	12.55

b





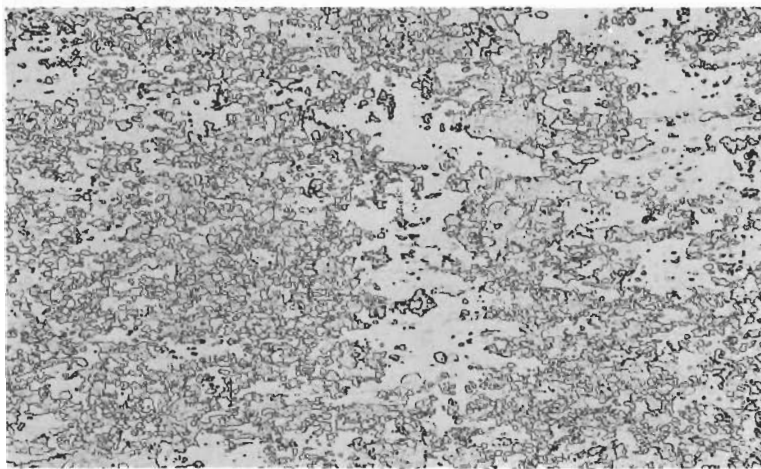
**ROCKWELL-HARDNESS - 3 IMPRESSIONS EACH LOCATION**

**METALLOGRAPHIC SECTIONS**

- F - FLAT**
- L - LONGITUDINAL**
- T - TRANSVERSE**

Figure 1. Diagram Showing Locations of Hardness Impressions and Metallographic Samples Taken on Each Sheet of Material.

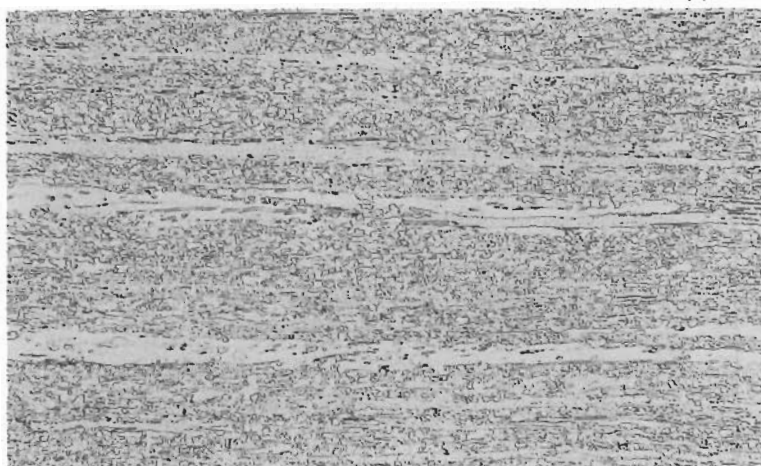
# Contrails



Flat

100X

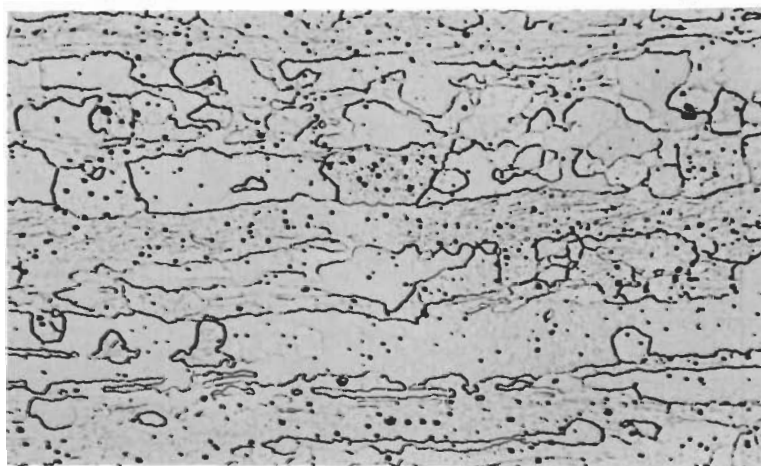
2744



Longitudinal

100X

2743



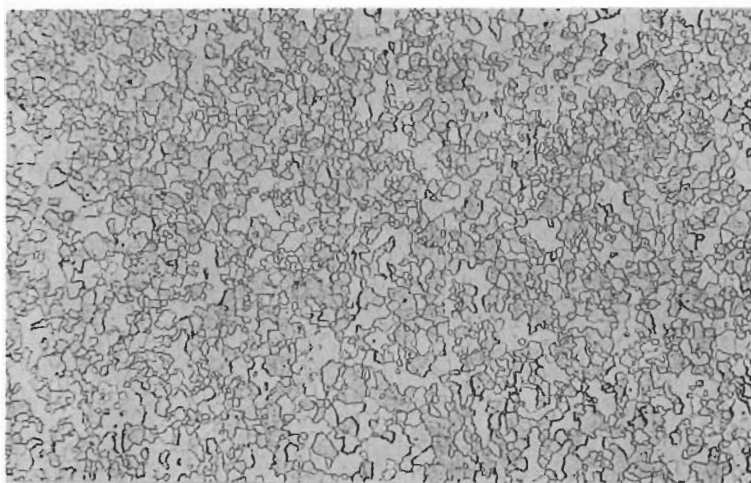
Longitudinal

1000X

2742

Figure 3 Microstructure of FS82 Alloy Sheet AD  
Hardness 172DPH

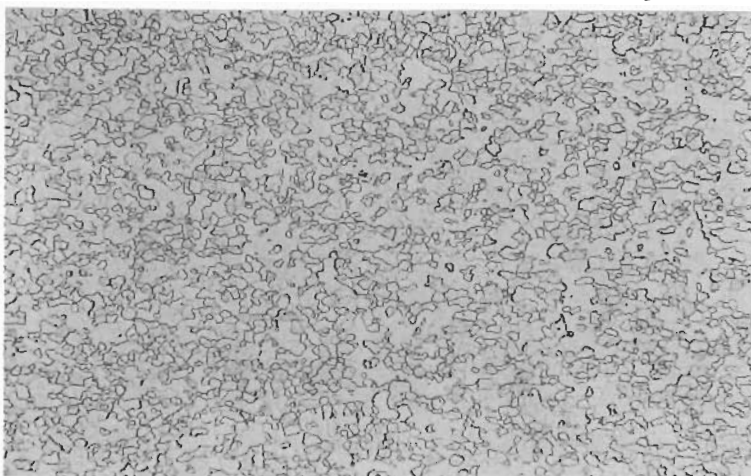
# Contrails



Flat

100X

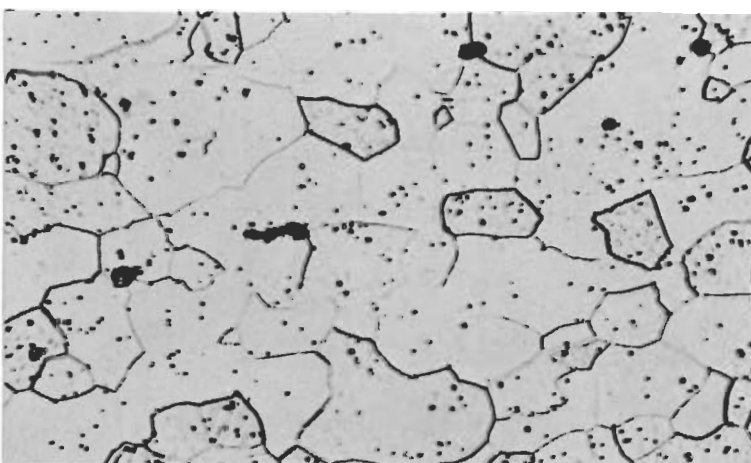
3028



Longitudinal

100X

3027



Longitudinal

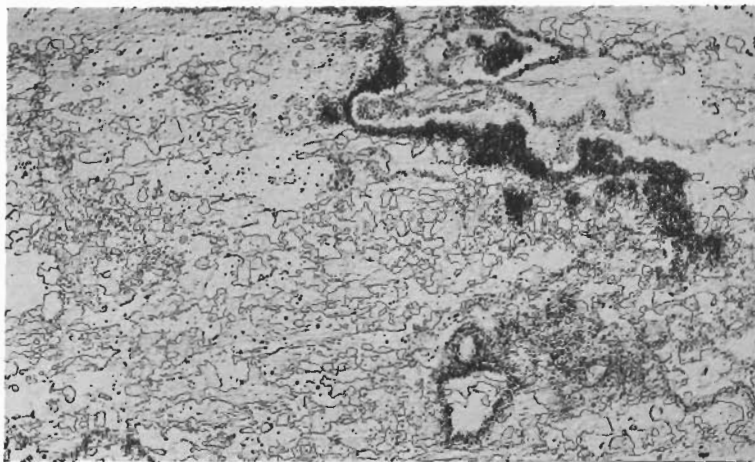
1000X

3030

Figure 4 Microstructure of FS82HS Alloy Sheet  
BC Hardness 152DPH  
14



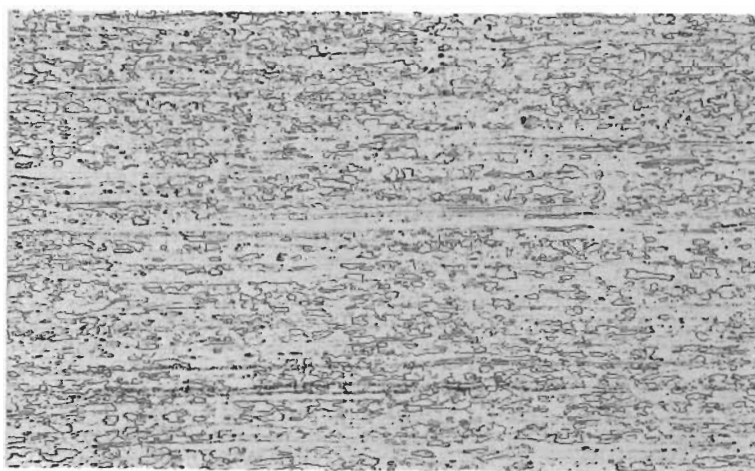
# Contrails



Flat

100X

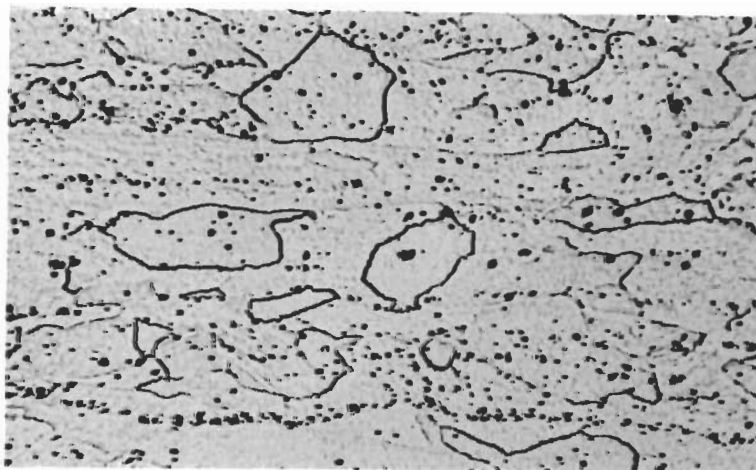
2747



Longitudinal

100X

2746



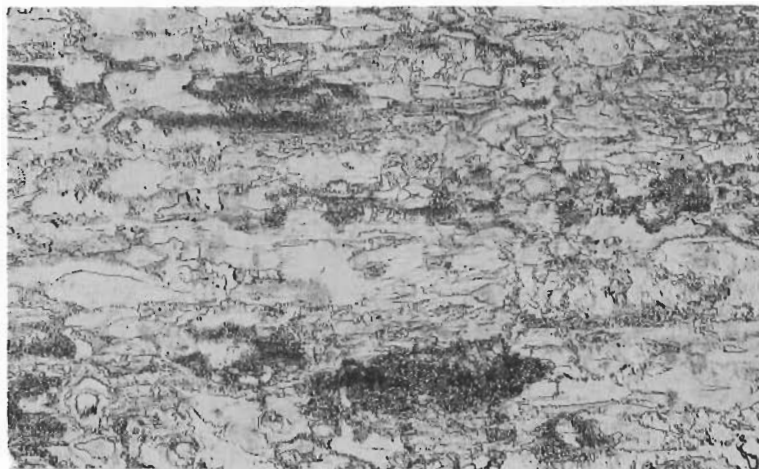
Longitudinal

1000X

2745

Figure 5 Microstructure of D31 Alloy Sheet CA  
Hardness 234DPH

# Contrails



Flat

100X

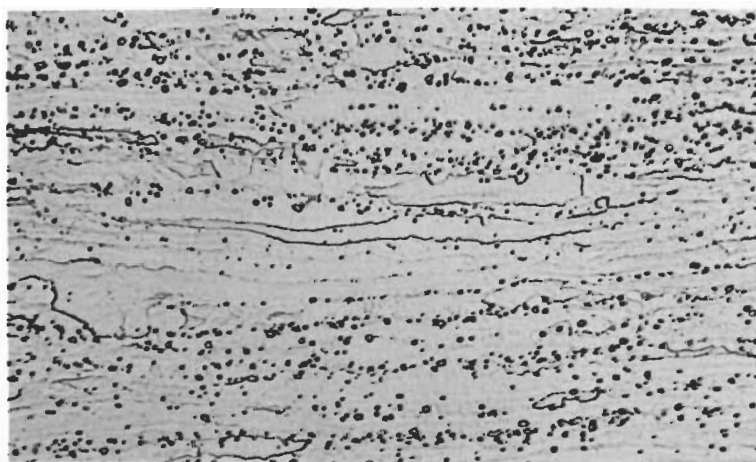
3066



Longitudinal

100X

3067



Longitudinal

1000X

3068

Figure 6 Microstructure of D31 Alloy Sheet CE  
Hardness 288DPH



The structure of the heats of F48 obtained for this program are presented in Figures 7, 8, and 9. It is clear from the flat sections that all these sheets were cross rolled and received approximately equal amounts of work in both directions. The sheet received from Sgt. Ingram, Structures Branch, Flight Dynamics Laboratory, ASD, was obtained from a wide sheet which had cracked on 45 degree angles on rolling leaving pieces large enough for welding samples. This accounts for the 45 degree directionality of the flat section in Figure 7. The larger number of carbide particles indicates a higher carbon content than sheet DA, Figure 8, obtained from General Electric. The microstructure of the F48 received from Allegheny Ludlum is shown in Figure 9. As the microstructure indicates this material is in a cold or warm worked condition.

Bend ductility tests and room and elevated temperature tensile tests were performed on the as-received sheet material. Test methods are discussed in the weld evaluation section under Experimental Procedure. Results are presented in the Discussion of Results under each alloy.

The material obtained for this program was considered to be representative of commercially available sheet at the time procured. Although a variation in microstructure and hardness was observed in each material this is considered a normal consequence of the melting and fabrication methods used.

## C. Material Preparation

Sheet specimens of the D31 and F48 alloys were cut from larger sheets by band sawing out somewhat oversize blanks. The FS82 alloy sheet was sheared on a foot operated platform shear. Edges to be welded were ground straight and square removing approximately 1/32 in. of material per edge. Before welding, samples were cleaned in acetone and the edges to be welded and adjacent sheet surfaces were etched in a solution of 22%HF, 8%HNO<sub>3</sub> and 15%H<sub>2</sub>SO<sub>4</sub> to present an oxide free surface for welding.

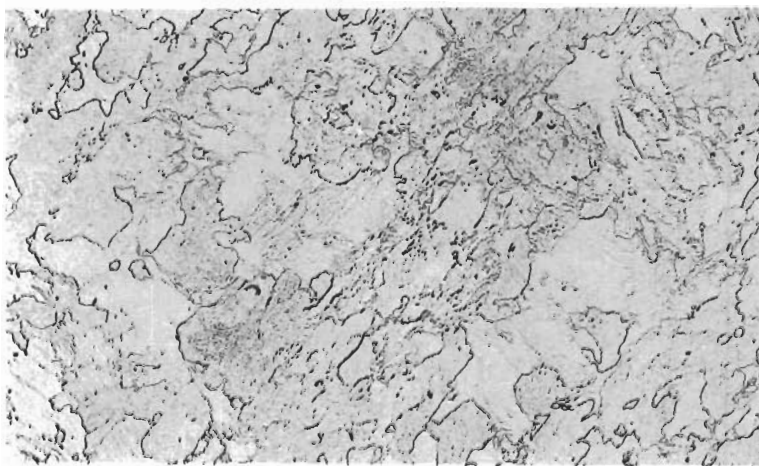
## IV EXPERIMENTAL PROCEDURE

### A. Tungsten Inert Gas Fusion Welding

The majority of the experimental welding for this program was performed by the inert gas shielded tungsten arc process. Two degrees of atmosphere purity were studied to cover this latitude of welding conditions. Welds were made in a vacuum purge atmosphere chamber to represent the best readily attainable atmosphere. In addition, welds were made without a chamber but with inert gas flow in a trailing shield and a backing shield as well as in the welding torch.

#### 1. Vacuum Purge Chamber Welding

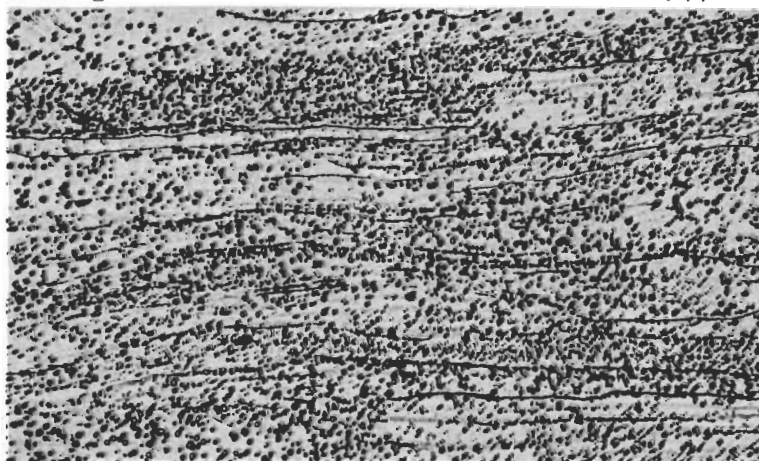
Controlled atmosphere welding was performed in the vacuum purge chamber shown in Figure 10. This equipment could be evacuated to less than



Flat 100X 2943



Longitudinal 100X 2944

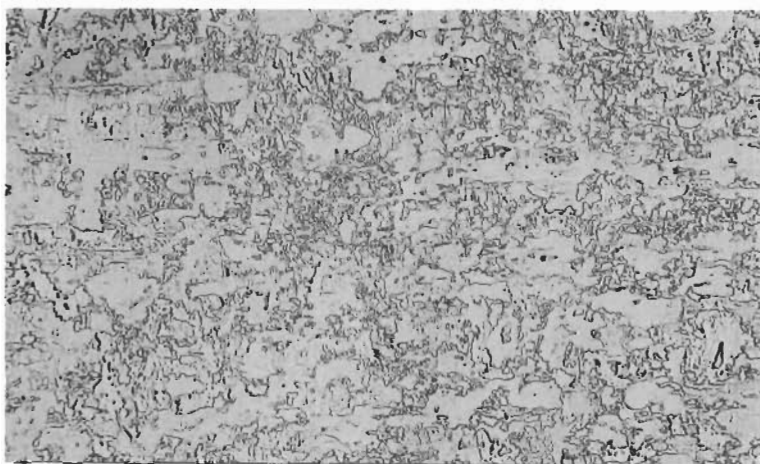


Longitudinal 1000X 2945

Figure 7 Microstructure of F48 Alloy, Sheet D  
Hardness 290DPH  
18



# Contrails



Flat

100X

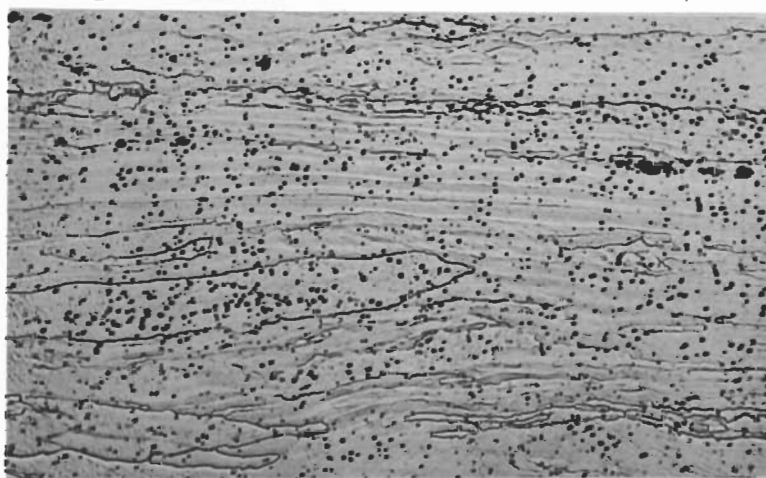
2940



Longitudinal

100X

2941



Longitudinal

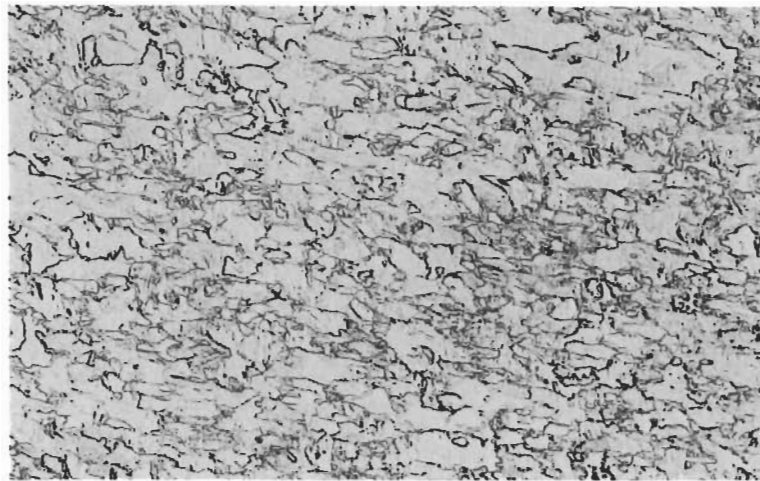
1000X

2942

Figure 8 Microstructure of F48 Alloy Sheet DA  
Hardness 309DPH



# Contrails



Flat

100X

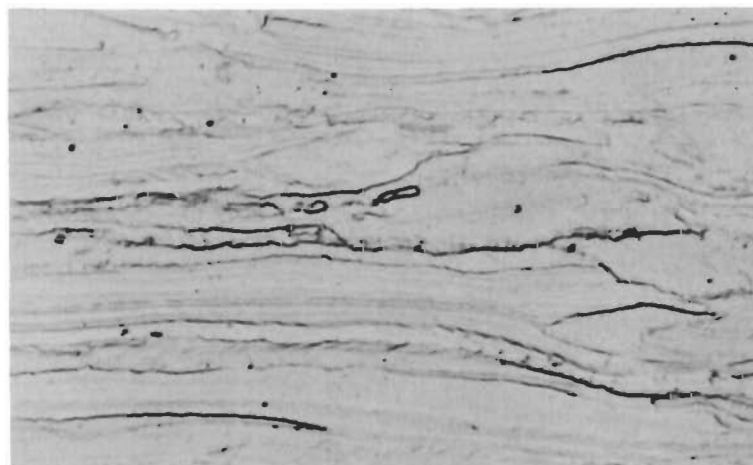
3245



Longitudinal

100X

3246

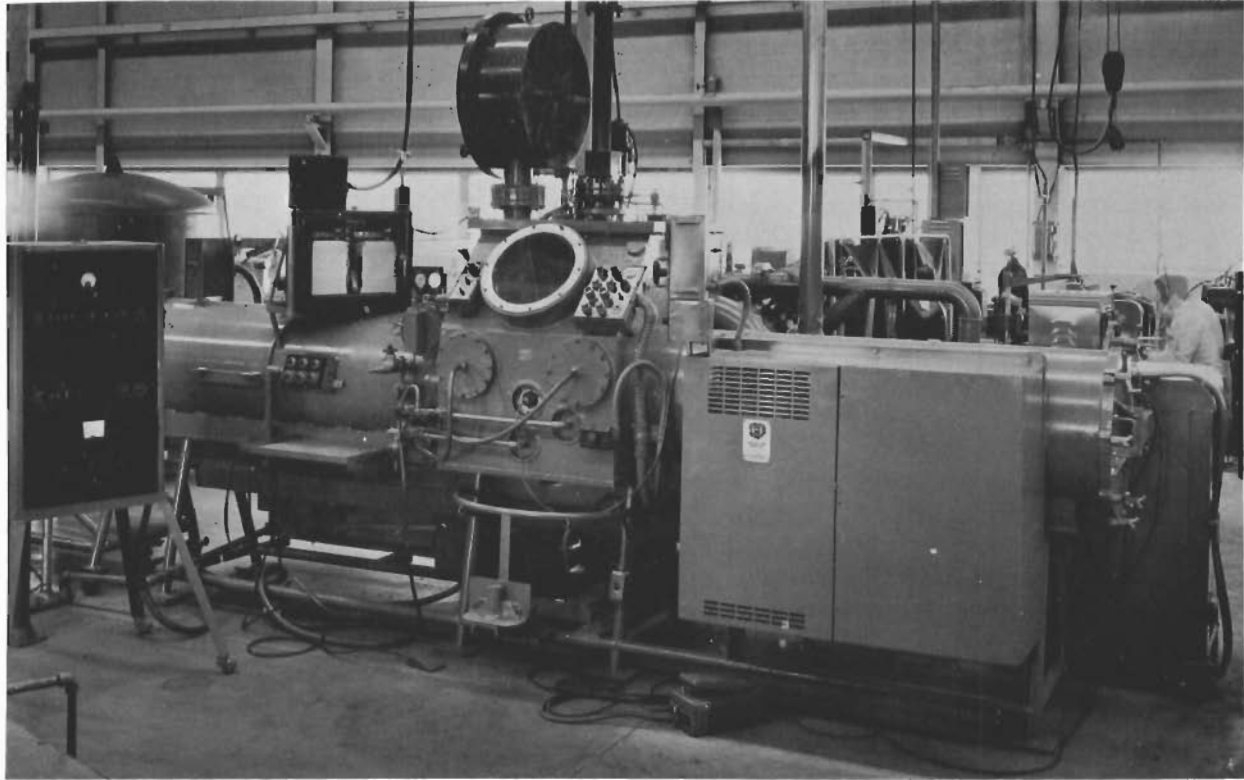


Longitudinal

1000X

3247

Figure 9 Microstructure of F48 Alloy Sheet DB  
Hardness 275DPH



05469-7

Figure 10 Vacuum Purge Welding Chamber

# Contrails

0.1 microns of mercury pressure in approximately 30 minutes. It is equipped with an automatic welding head and electronic controls capable of maintaining arc voltage to preset values within 0.1 volts. The head control also gives transverse motion of the torch, up to 45 ipm. Longitudinal motion of the work up to 39 ipm is provided by cart travel driving through a lead screw powered by a DC motor with thyatron speed control. Figure 11 shows the cart pulled out on a factory dolly to allow material, fixture and tools to be loaded and placed inside the chamber for evacuation. Arc current and voltage were measured and recorded on Esterline-Angus strip chart recording meters.

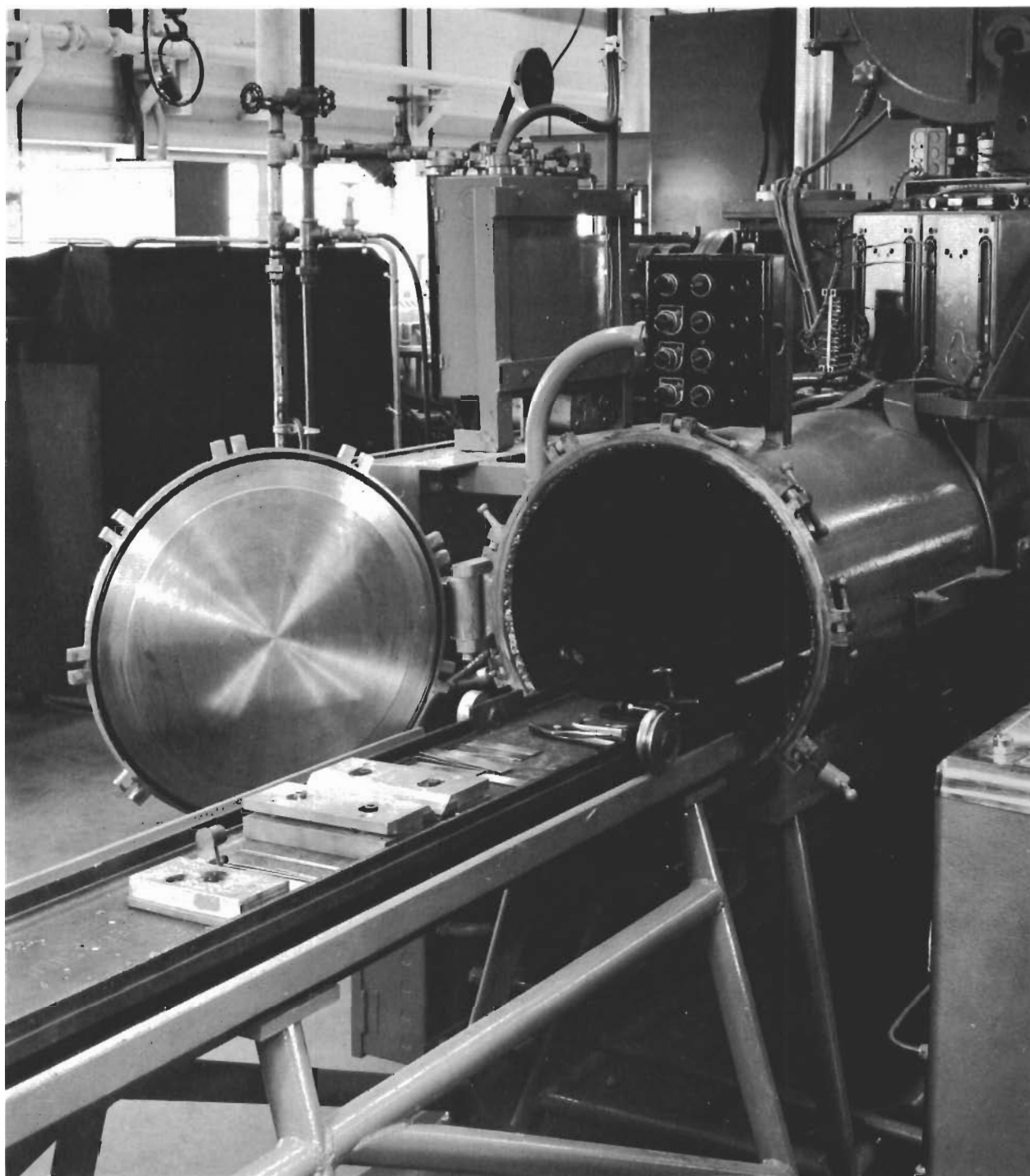
The procedure followed in chamber welding was to place the sheet material, and tools inside the chamber, evacuate to 0.3 microns and then fill to 1 atmosphere pressure with either welding grade argon or tank helium. With the internal pressure equal to atmospheric pressure the glove covers could be removed and fixture loading and positioning could be accomplished manually by the operator working through neoprene gloves. Before any welding was done on the columbium alloys, the purity of the chamber atmosphere was verified by welding on titanium sheet. The titanium sheet was clamped only at one edge and a high heat input was used so that a large area was heated. The titanium absorbed much of the residual contaminants in the inert gas atmosphere and would indicate by color change any serious amount of contamination.

Sheets to be welded were cut to approximately 4 in. by 6 in. rectangles with the primary rolling direction parallel to the 4 in. edges. The 6 in. edges were prepared, butted together and clamped in a steel fixture of the kind shown in Figure 12 with a copper backup bar and copper edged clamping bars. The copper backup bar contained a groove 5/16 in. wide and 1/16 in. deep milled in the top surface to prevent copper contamination and excessive chilling of the root of the weld. The abutting edges of the sheets to be welded were centered over this groove and the clamping bars were tightened to give a 5/32 in. space between the edge of each clamping bar and the butting edges at the center of the weld. This backing groove dimension and the clamping bar separation were found to yield ample chilling and yet not interfere with adequate weld fusion.

Some of the preliminary welding was done with a 1/8 in. wide backing bar groove and 3/16 in. distance from weld centerline to clamping bar edge for the purpose of providing more rapid chilling of the weld. Although close clamping provides rapid chilling of the weld zone, a substantial current increase is required to obtain full weld penetration and increased heat capacity of the fixture is required to soak up the extra heat input.

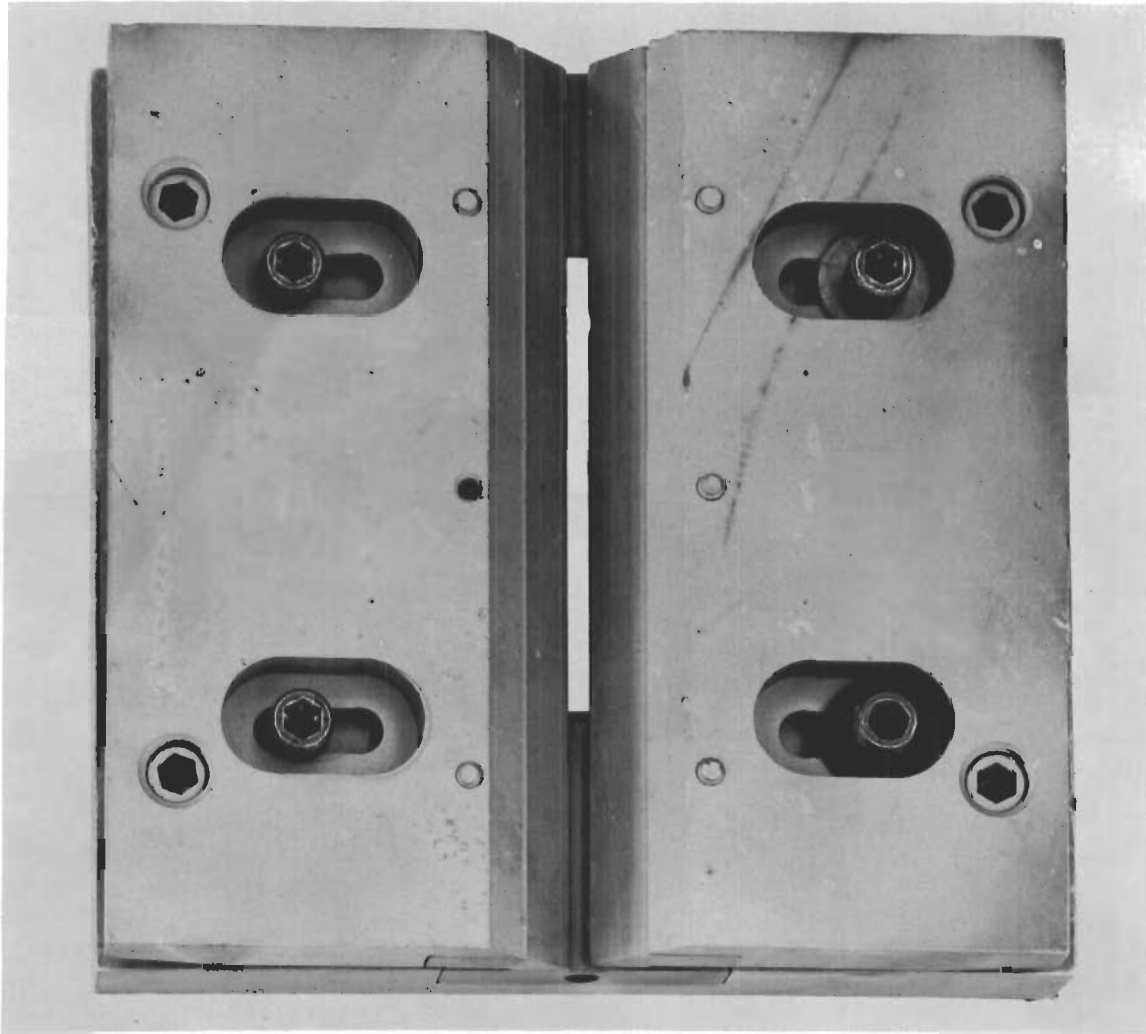
Except for a few welds, welding was done with 2% thoriated tungsten electrodes held in a copper block on the welding head. To prevent mutual contamination of the welds and electrodes the arc was initiated with the aid of a high frequency voltage superimposed on the DC welding voltage. When the arc became established, the high frequency was cut off immediately to prevent it from interfering with the electronic controls of the torch and traversing mechanism.





05469-6

Figure 11 Vacuum Purge Welding Chamber Showing Cart with Fixture Ready to be Loaded



05469-4

Figure 12 Fixture Used for Welding

# Contrails

Most all joints on 1/16 in. sheet were made with 1 in. square tabs at each end of the welds to permit adjustment of current and voltage at the start and also to allow the arc to be stopped on a tab to eliminate a crater in the main weld. Welds were made at speeds of 5, 15, 21, 28, and 36 ipm in atmospheres of argon and helium. Arc currents and voltages were established for each combination of speed, atmosphere and material to obtain adequate fused penetration but not excessive fused width.

The welds and conditions under which they were prepared are compiled in Table A-1 appendix. Most welds were made in the same type fixture without deliberate preheat. However, as successive welds were made by reloading one or two fixtures inside the chamber, a moderate preheat, approximately 150 to 200°F was developed from previous welds.

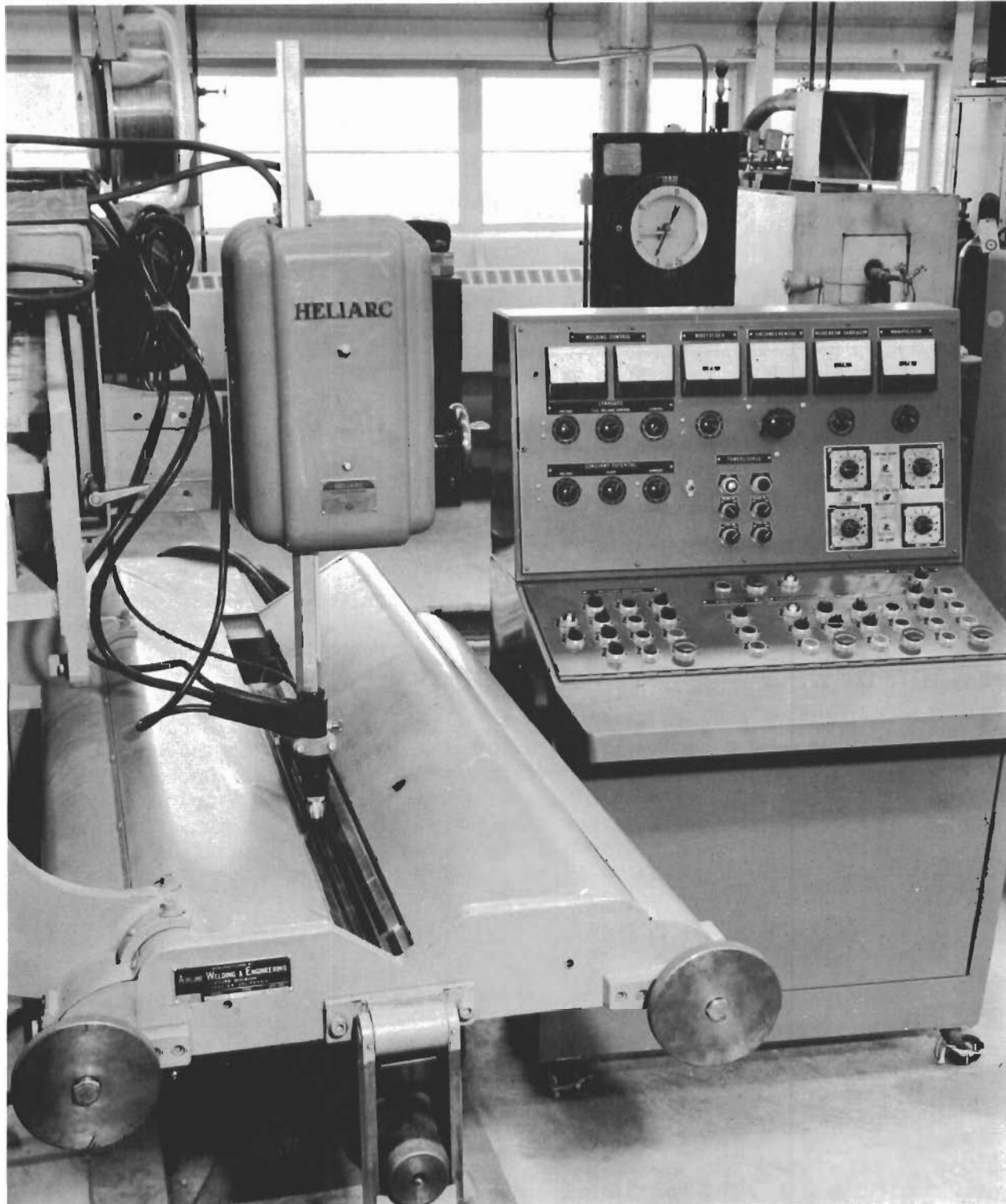
After completing a weld, a strip approximately 9/16 in. wide and 6 in. long containing the weld was sawed from the joined sheets. In this manner, four 1-1/4 in. long bend ductility specimens could be obtained from each weld. The remaining somewhat narrower strips were again prepared for welding by grinding, cleaning and etching the saw cut edges. This procedure was repeated until approximately 1-1/2 in. wide strips remained for rewelding. This procedure permitted cutting bend specimens so the axis of bend would be perpendicular to the welding direction and still would be economical of materials. It was felt that use of narrower than 1-1/2 in. strips would present an unrealistically low stress pattern in the welds and a tendency toward stress cracking during welding would not be detected.

Welds were made in each alloy in the chamber with deliberate air contamination to determine the effect of atmosphere impurity on the weld mechanical properties. Intended atmosphere impurity levels of 200, 600, and 1300 ppm air were sought by evacuating the chamber to 150, 400, and 1000 microns pressure respectively before each back-filling with helium. Ordinarily the chamber is evacuated to 0.3 microns before back-filling so that the impurity level in the chamber is essentially that of the inert gas introduced which usually runs between 50 and 100 ppm.

## 2. Non-Chamber Welding

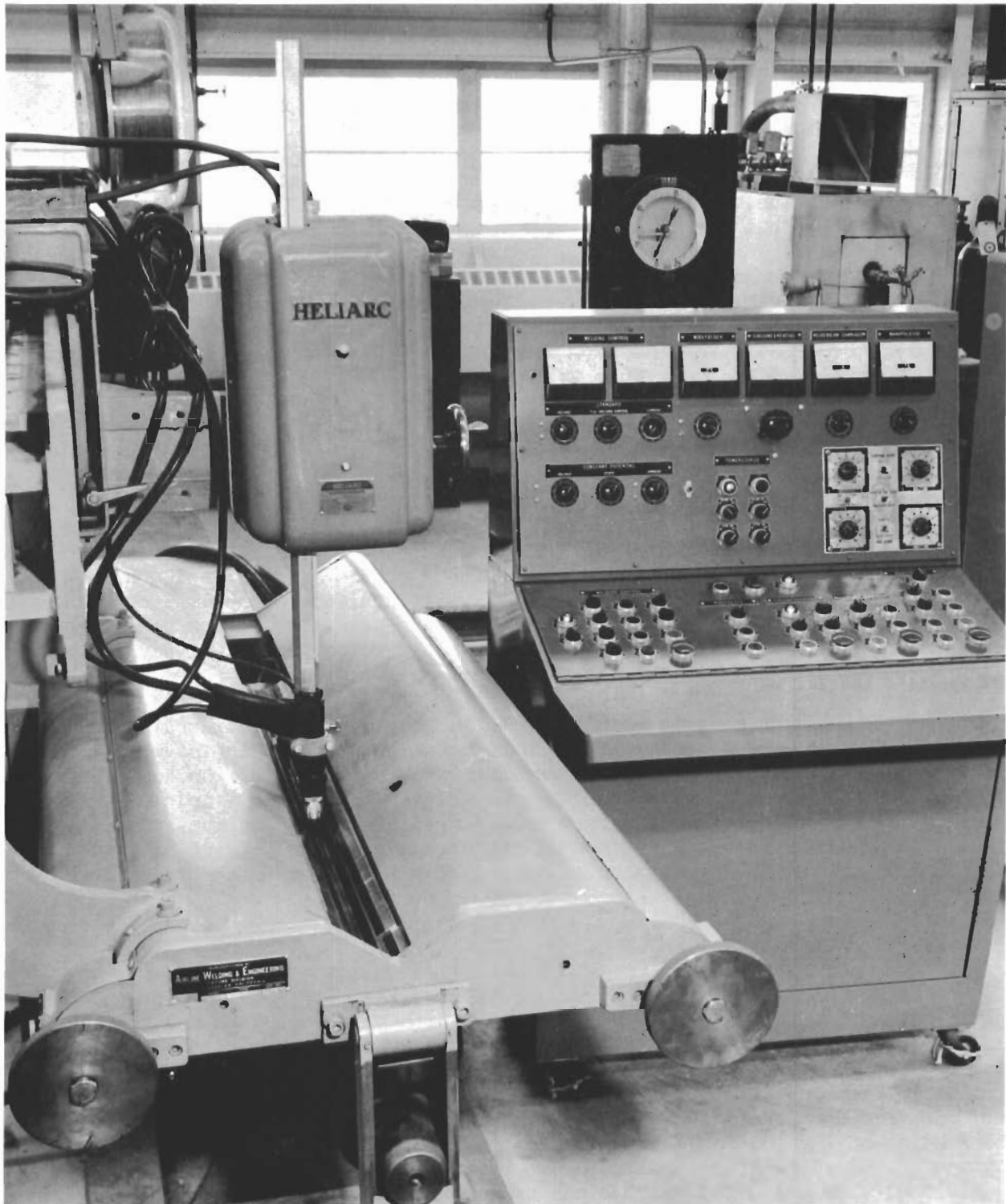
Non-chamber tungsten inert gas welding was performed on the automatic butt welder illustrated in Figure 13. With this equipment arc voltage can be maintained within 0.1 volt of any preset welding potential by the electronic arc voltage control. Uniform travel speeds up to 80 ipm are available with the side beam carriage and electronic governor control. In addition to inert gas flow in the welding torch, gas shielding was provided to the top of the weld by means of a trailing shield, Figure 14, and to the bottom of the weld through holes in the backing bar. The trailer shield was fitted with a 1/4 in. thick piece of porous bronze which allowed the inert gas to blanket the welded area with a minimum of turbulence and air contamination. Arc current and voltage were read from panel meters. As in the case of chamber welds, high frequency arc starting was practiced to prevent weld contamination from the tungsten electrodes. Sheet size and





05000-1

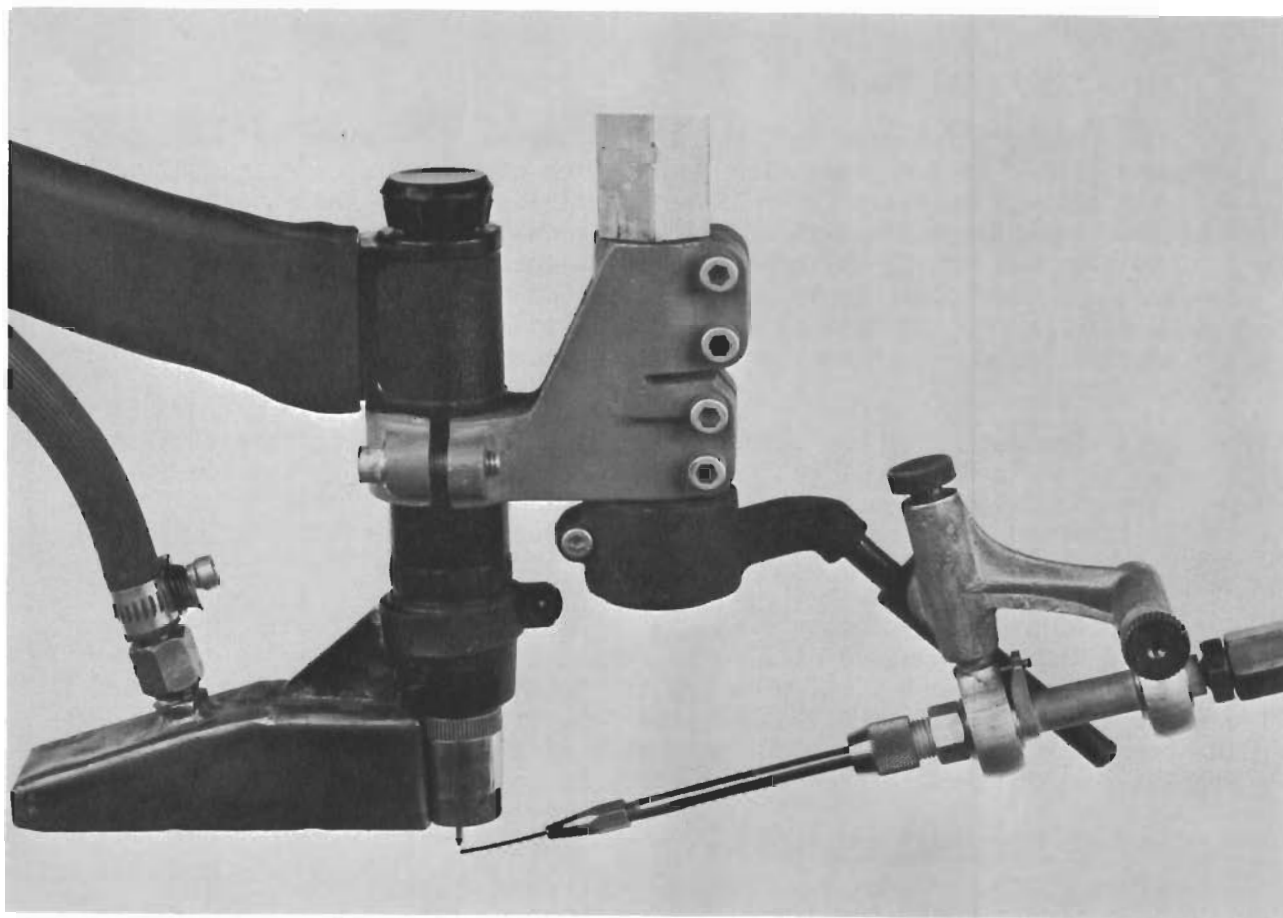
Figure 13 Automatic Tungsten Inert Gas Shielded Welder and Control



05000-1

Figure 13 Automatic Tungsten Inert Gas Shielded Welder and Control





05469-5

Figure 14 Inert Gas Shielded Tungsten Electrode Welding Torch,  
Showing Trailer Shield and Filler Wire Positioner

preparation were the same as used for chamber welds. Welds made without the addition of filler metal or without preheat were made in the same fixture used in the chamber to eliminate the variables of fixturing in comparing the results with chamber welds. Non-chamber weld parameters are given in Table A-2.

### 3. Preheat of Welds

Preheat was used for the single purpose of raising the sheet temperature closer to the transition temperature of the welds and thus allow weld shrinkage stresses to be relieved by yielding while the material is ductile. From the standpoint of preventing embrittling metallurgical reactions from occurring, it is believed that chilling would be desirable to decrease the time that the weld zone is in the embrittling temperature range. But unless the cooling rate is rapid enough to prevent embrittlement, shrinkage stresses produced on cooling can cause transverse and longitudinal weld cracking.

Preheating in the chamber was accomplished in a fixture similar to that shown in Figure 12 but fitted with three 500 watt resistance heating elements. Temperature was controlled and measured by means of a thermocouple inserted in the backup bar of the fixture. Temperatures of up to 500°F could be maintained readily with this arrangement.

Outside the chamber preheated welds were made directly on the butt welder to take advantage of its built in heating bar. Samples to be welded were positioned over a 2 in. wide 1/2 in. thick backing bar so the abutting edges were centered over a 1/4 in. wide 0.04 in. deep groove. The top clamping bars were also 1/2 in. apart with the opening centered over the joint. Preheat temperatures in excess of 500°F were possible on this equipment.

### 4. Filler Metal Additions

Filler metal was added to some welds in the form of 0.045 in. wire of unalloyed columbium, Cb-1%Zr (FS80), and FS82 alloy. The wire was fed into the leading edge of the arc by an automatic wire feeding device at rates of 12 to 22 ipm. The positioning device employed for non-chamber welds is illustrated in Figure 14. A similar wire feeding and positioning device was used for adding metal to welds inside the chamber. In this case the spools of wire and drive rolls were contained inside the atmosphere chamber.

### 5. Fusion Weld Thermal Cycle Studies

Since most alloy properties depend considerably upon previous thermal history, weld metal properties depend to a great extent upon the thermal cycling which occurs during the welding process. The thermal cycles of a weld refer to the heating and cooling behavior of each point included in the fusion zone and heat affected zone.

The temperature of a point in or near a weld raises rapidly to a peak as the arc approaches then cools more slowly as the arc passes the point.

# Contrails

If the time temperature relations of points of increasing distances from the weld centerline are plotted, a family of curves will result in which each curve will at any given time be at a lower temperature than curves representing points closer to the weld centerline. Increasing the weld energy input or the initial sheet temperature has the effect of reducing the cooling rate of all these curves.

Thermal cycles can be determined by attaching thermocouples to the underside of sheets at strategic locations in the weld zone and recording the millivolt signals on an oscillograph. A comprehensive determination of thermal cycles in 1/16 in. columbium alloy sheet would require a separate program and is beyond the scope of this investigation. However, an exploratory study was performed on FS82 alloy in 1/16 in thickness to enable a general pattern to be determined.

Temperature of welds were measured with platinum-platinum 10% rhodium and tungsten-tungsten 26% rhenium thermocouples in contact with the bottom surface of the sheets.

Tungsten-tungsten 26% rhenium thermocouples were used to record temperatures in the fusion zone and the hotter regions of the heat affected zone. The lower temperature regions were measured with platinum-platinum 10% rhodium thermocouples. To simplify the thermocouple attachment problem, full penetration bead-on-plate welds were made on approximately 2 in. by 6 in. sheets. As a result of difficulty in welding the tungsten and tungsten 26% rhenium wires to the columbium sheet, the individual wires were held in spring contact with the underside of the sheet in the required location. As melting of the sheet occurred the wires were fused into the bottom of the weld forming excellent thermal contact of the hot junction. Where fusion did not occur the sharp cut ends of the thermocouple wires made spring contact with the sheet surface and yielded reproducible results in most cases.

The platinum-platinum 10% rhodium wires were readily spot welded to the under surface of the sample sheet to form hot junctions. In all cases the distance between wires was approximately 0.10 in. The use of platinum-platinum 10% rhodium thermocouples was limited to the outer edges of the heat affected zone because melting occurred at the junction of the wires and sheet when welding.

Thermocouple millivoltages were recorded in a 6 channel, direct recording oscillograph. Four of the amplifier units were rewired to provide two recorder channels, each with two amplifier units in series. This arrangement was necessary to obtain readable pen deflections from the thermocouples. Thermal cycle determinations have been made by welding outside the chamber on the original standard fixture used for most of this work. A trailing shield and gas backup were used on all runs. Representative oscillograph traces are reproduced in Figure 15.

Weld temperatures were recorded on FS82 alloy at welding speeds of 5, 15, and 30 ipm with helium and at 15 ipm with argon torch gas. Attempts made to measure temperature at locations of the hottest point directly under



# Contrails

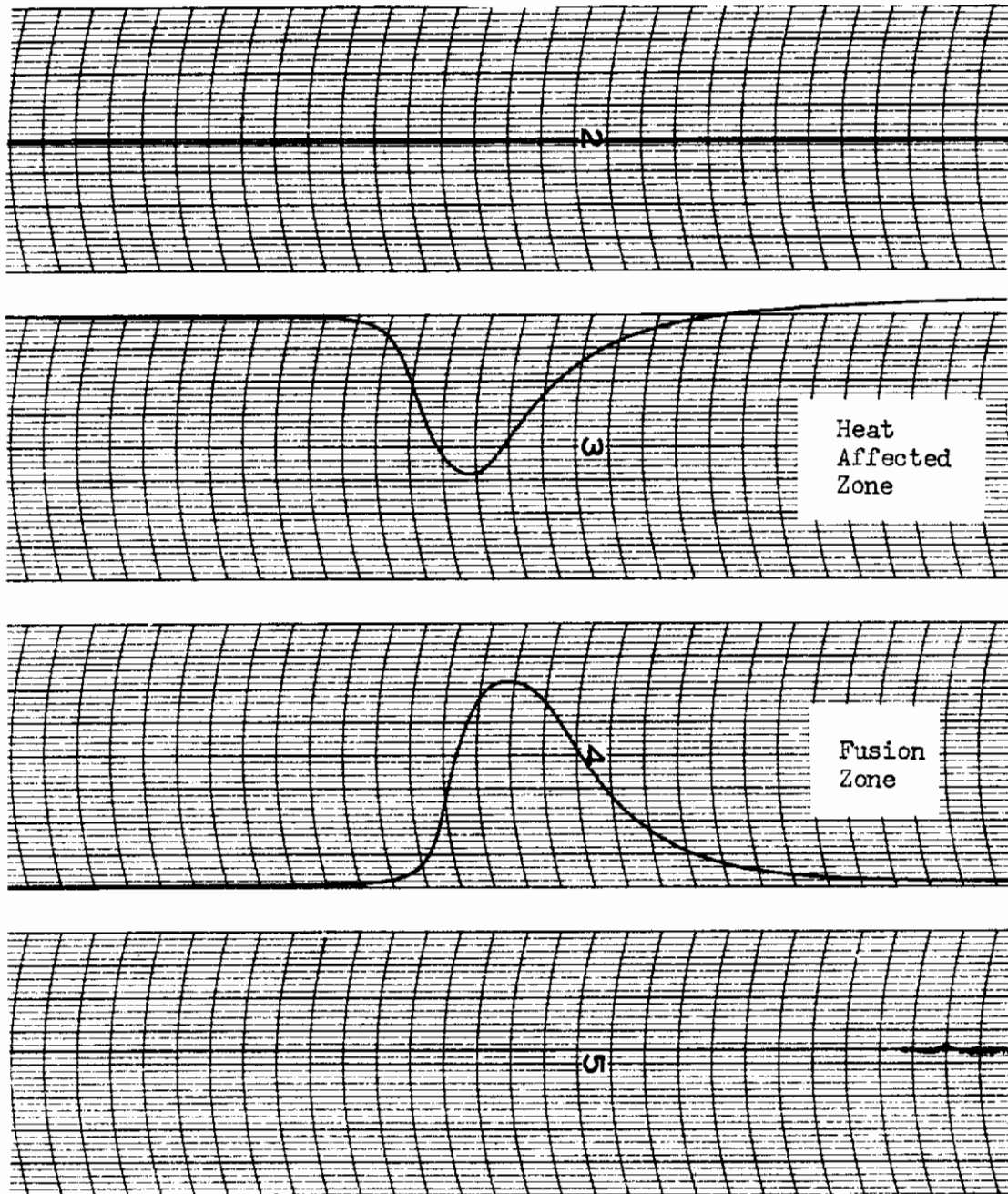


**Figure 15.** Oscillograph Traces from Tungsten-Tungsten 20% Rhenium Thermocouples in Welds.

the center of the weld and at a point approximately 1/16 in. from the weld centerline.

## B. Resistance Welds

### 1. Spot and Projection Welds

Spot and projection welding was performed on a 75 KVA air operated spot welder capable of applying a maximum electrode force of 1560 pounds. This machine was equipped with a phase shift heat control and weld timer which provided the functions of squeeze, weld, hold and off time.

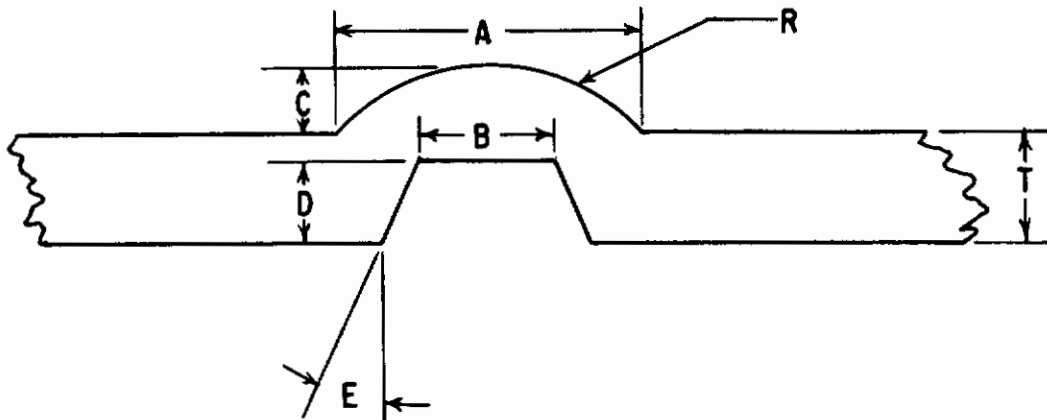
Welding current was determined by measuring primary current then multiplying by the turns ratio of the transformer. Electrode force was measured as air pressure on a dial gage which was previously calibrated against an electrode force gage. Electrode tip materials included Group A Class I copper alloy, molybdenum, and tungsten.

Tip radii of 4 to 12 in. were used for spot welding like thicknesses of sheets. When welding thin to thick sheet, a small tip radius was used against the thin sheet and a large radius or flat electrode was used against the thick sheet to obtain proper heat balance for location of the fused nugget at the interface. The AWS considers that the fused nugget diameter of a spot weld should be three times the sheet thickness plus 0.06 in. This criterion was set as an arbitrary goal when determining spot weld parameters. Electrode tips were cleaned with fine aluminum oxide cloth after each weld to remove the variable of electrode deterioration as welds were made. Initially, dies and punches for forming projections in sheet were made according to AWS recommended practice for 0.020 in. and 0.062 in. thicknesses in stainless steel. As the work progressed, it was obvious that the projections in FS82 0.062 in. sheet were collapsing prematurely causing undersize weld nuggets. In fact the weld diameters were considerably smaller than spot welds formed in the same materials and thicknesses. Therefore, a punch and die set was made to form somewhat larger and stiffer projections, than that recommended for 0.078 in. sheet. The contours and dimensions of the AWS recommended projections are shown in Figure 16.

One-inch square pieces of sheet in thickness combinations of 0.020 to 0.020 in., 0.020 to 0.060 in., and 0.060 to 0.060 in. were welded together at the center then were sectioned so that the metallographic structure, size and type of bond could be determined. With this method, it was possible to narrow-down the welding parameter ranges with the use of a minimum of material. After this, a number of tensile shear specimens were welded over a narrow range of current for determination of weld strength.

### 2. Flash Butt Welds

All flash butt welding for this program was performed on a 100 KVA experimental flash welder at the Taylor Winfield Corporation in Warren, Ohio. This machine was equipped with a servo-hydraulic system for controlling the



<u>T</u> <u>in.</u>	<u>A</u> <u>in.</u>	<u>B</u> <u>in.</u>	<u>C</u> <u>in.</u>	<u>D</u> <u>in.</u>	<u>E</u> <u>degrees</u>	<u>R</u> <u>in.</u>
0.020	0.067	0.039	0.017	0.020	23	0.042
0.062	0.156	0.081	0.035	0.043	23	0.105
0.078	0.187	0.104	0.041	0.055	23	0.128

Figure 16. AWS Recommended Projection Dimensions.

flashing and upset portions of the weld cycle. The flashing curve exponent as well as the total flashing time and distance could be varied independently to achieve a wide range of flashing parameters. In addition, the variables of initial clamping distance, upset distance and upset current were investigated. Flashing was done in air with no inert gas coverage of the weld area. Specimens of  $1/8$  in. x 1 in. section were used for this investigation. Flash welding data are given in Table A-4 Appendix.

## C. Electron Beam Welds

Electron beam butt welds were made in 0.060 in. sheet of all three alloys on the beam welder illustrated in Figures 17 and 18. This equipment is rated at a beam current of 300 ma at 25 KV. A movable electron gun and cart produce travel speeds up to 70 ipm. Welding was done in a vacuum of less than 0.1 micron pressure. Weld data are presented in Table A-3 Appendix.

## D. Weld Heat Treatment

Alloys which generally became embrittled on welding were post weld heat treated to try to restore some ductility. This included D31 and F48. Welds in FS82, which normally is not greatly embrittled by welding, were aged at a number of temperatures to determine whether embrittlement could occur in service at elevated temperatures after welding. All heat treatment was performed in a cold-wall vacuum furnace in a vacuum of less than 0.1 micron pressure. Temperatures below 2350°F were measured with a platinum-platinum 10% rhodium thermocouple. Above this temperature measurement was by optical pyrometer calibrated against the thermocouple at 2350°F. Heat treating times and temperatures are given in Table III.

In addition to heat treatments, the effect of applying a Cr-Ti-Si oxidation protective coating on ductility was studied by applying this coating to welds for bend testing.

## E. Weld Evaluation

Welds and as received sheet were evaluated for bend ductility transition temperature, room and elevated temperature tensile strength, hardness, and microstructure. Before performing mechanical tests, welds in 0.060 in. sheet were radiographed at an exposure of 120 KV 10 ma and 7.5 min. to determine the extent of porosity.

Drawings of the test specimens are shown in Figure 19. Bend test specimens of TIG and electron beam butt welds were cut with weld centered and parallel to the length of the specimen as indicated. Thus in testing the axis of the bending probe radius was normal to the direction of the weld so that fusion zone, heat affected zone (HAZ) and parent metal all experienced the same angle of bend. Specimens were supported on two  $3/8$  in. diameter bars resting on a fixture so that their centers were  $3/4$  in. apart. Bending was performed around a  $1/16$  in. radius tipped probe at a speed of 0.2 ipm to give a 1T bend radius



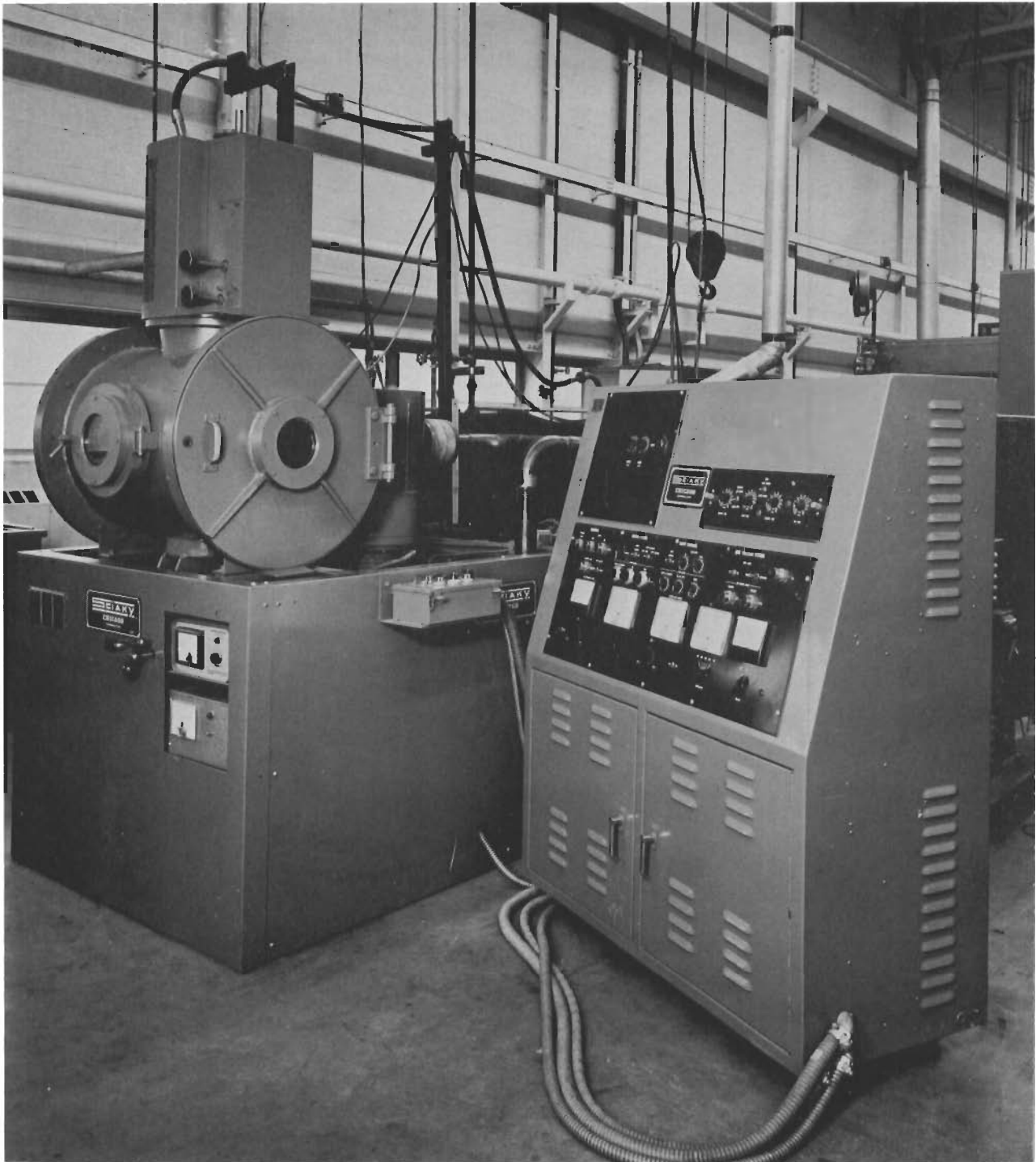


Figure 17 Electron Beam Welder and Control Panel

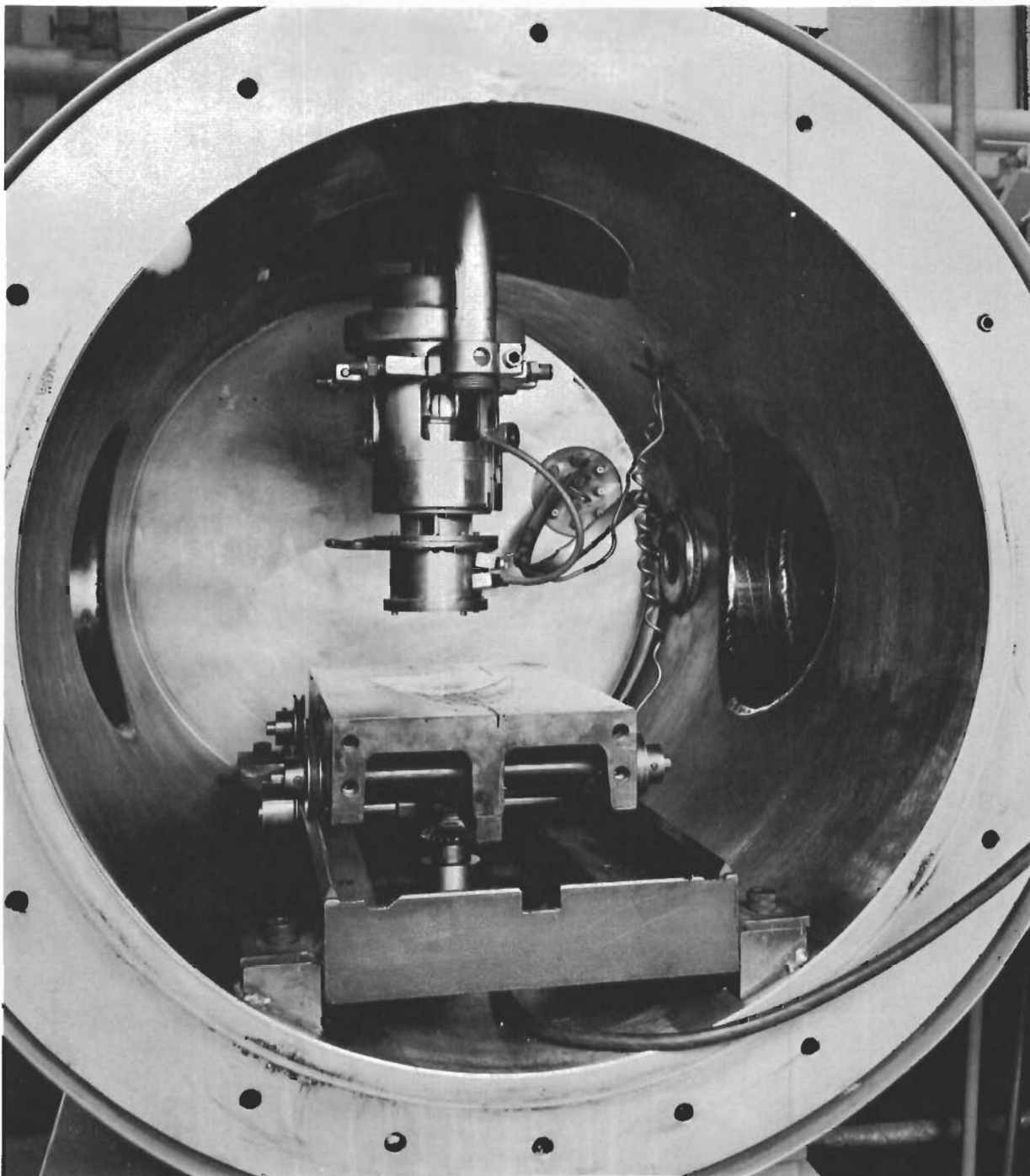


Figure 18 Work Chamber of Electron Beam Welder Showing Gun and Work Table

TABLE III

POST WELD HEAT TREATMENT SCHEDULE

<u>Alloy</u>	<u>Temperature, °F</u>	<u>Time - Hours</u>
D31	1900	24, 72
	2100	4, 24, 72
	2350	24, 72
	2550	4
F48	2100	4, 24, 72
	2350	4, 24, 72
	2500	4
FS82	1400	4, 16, 72
	1600	4, 16, 72
	1800	4, 16, 72
	2000	4, 24
	2000	4
	1800	4, 16
	2200	2
	1800	16
	2400	1
	1800	16

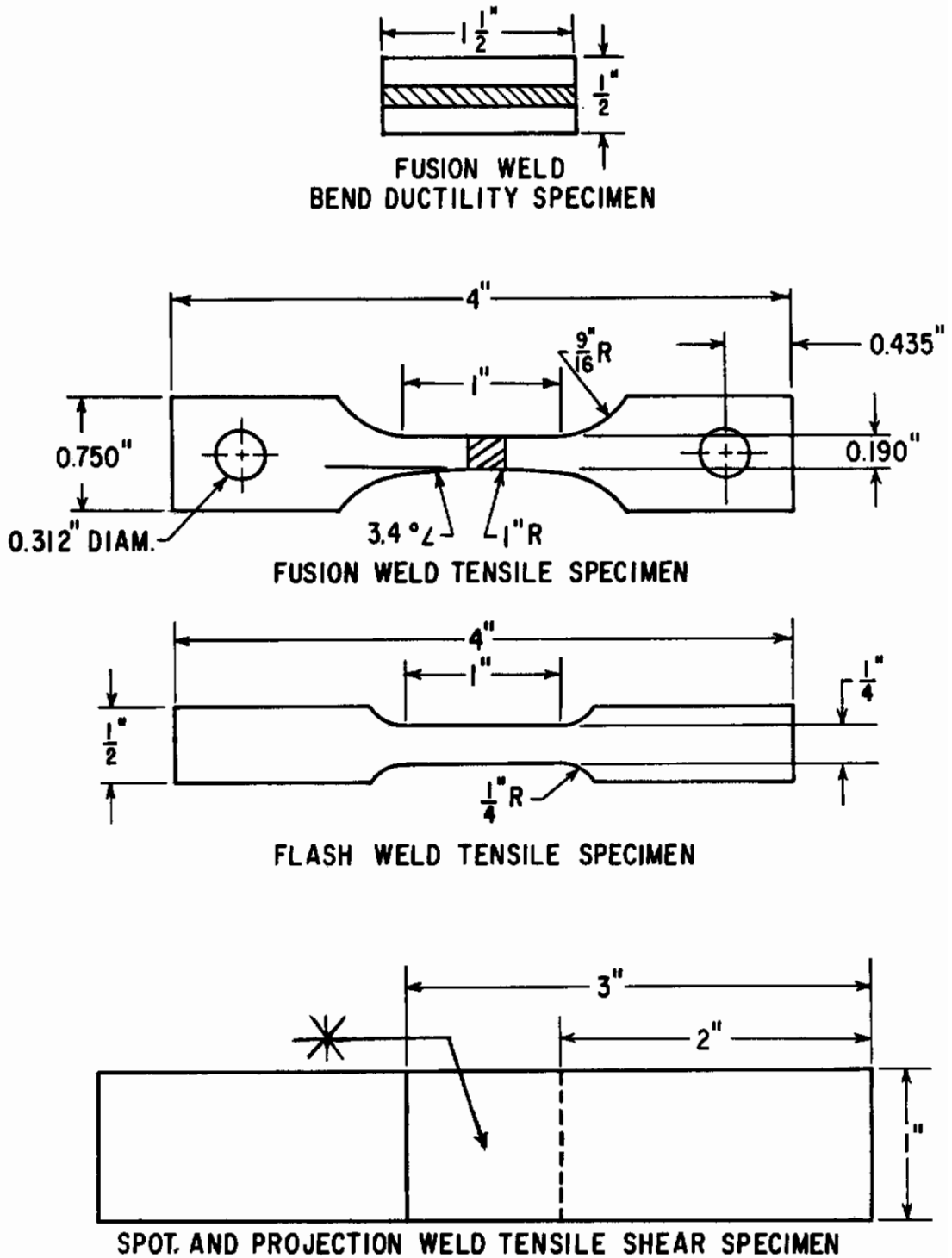


Figure 19. Drawings of Test Specimens.

on the 0.060 in. sheet. Load-deflection curves were recorded for each specimen on an Instron testing machine. Crosshead movement was stopped at the first sharp drop in load or when the deflection corresponding to a 90° to 100° bend was reached. Elevated temperature testing up to 800°F was performed with the fixture placed inside a cylindrical furnace. For cryogenic testing the fixture was placed inside an insulated box. A dry ice-acetone mixture was used for attaining temperatures down to -95°F, while temperatures below this and down to -320°F were obtained by spraying liquid nitrogen through glass wool packed around the fixture. Temperature was measured by two thermocouples in contact with the specimen surface on each side of center. Chromel-alumel thermocouples were used for elevated temperature measurements while copper-constantan thermocouples were used to measure below room temperatures. Ductile to brittle transition temperatures were determined by plotting angle of bend versus test temperature and selecting the temperature from the curve at which a 45° bend angle was obtained.

Tensile specimens were taken with the welding direction normal to the specimen length and direction of loading. The weld was located at the center of a reduced section as illustrated in Figure 19. This testing was performed in an Instron testing machine obtaining load deflection curves. Elevated temperature tensile tests were performed at 2200°F with a resistance heated tube furnace for the heat source. To minimize air contamination of the specimens at 2200°F, specimens were spray coated with an aluminum powder slurry, flowed at 1370°F for 30 min. in argon then diffused at 1900°F for 1 hour in argon. During testing argon was passed through the furnace at a rate of 35 cfm.

Spot and projection welds were evaluated metallographically by sectioning welds made between two 1-in. square pieces. Tensile shear test welds were made by overlapping 1 in. x 3 in. pieces of sheet 1 in. and welding at the center of the overlapped area. Reduced section tensile specimens were machined from flash welds as shown in Figure 19.

## V DISCUSSION OF RESULTS

### Tungsten Inert Gas Welds

Fusion welds were made both inside and outside the vacuum purge atmosphere chamber on the FS82, D31, and F48 columbium alloys. Those welds made in the chamber are termed chamber welds. Welds made outside the chamber are referred to as non-chamber or open-air welds. As was pointed out before, great care was exercised to protect non-chamber welds from atmospheric contamination by providing an inert gas flow through the backing bar and a trailer shield as well as in the welding torch. Bend ductility curves for the as-received sheet material are presented in Figure 20 for comparison with weld ductility in the discussions to follow.

#### A. FS82 Alloy

Figure 21 furnishes the bend ductility data for FS82 columbium alloy,



# Contrails

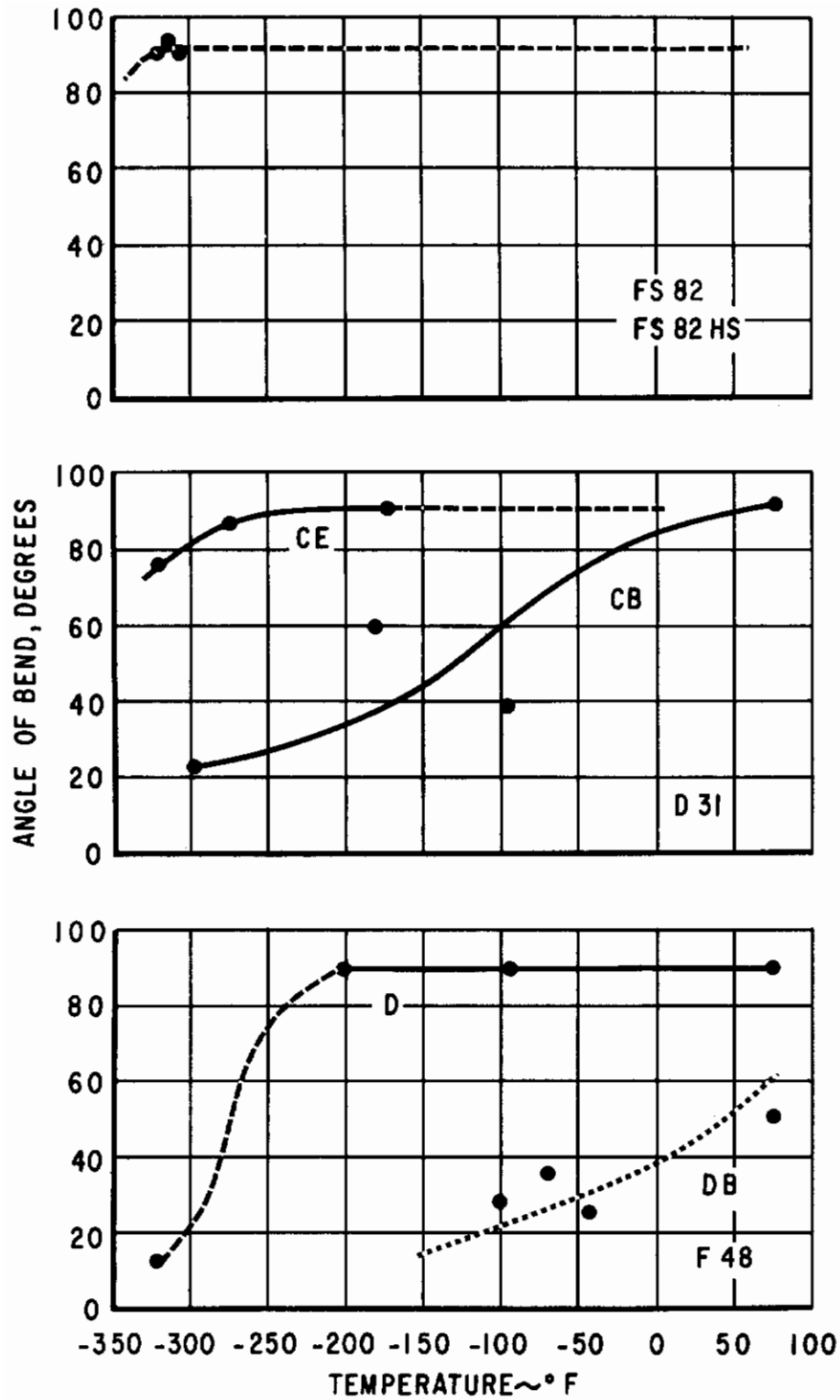


Figure 20. Bend Ductility of 0.060 in. FS82, D31 and F48 Sheet.

# Contrails

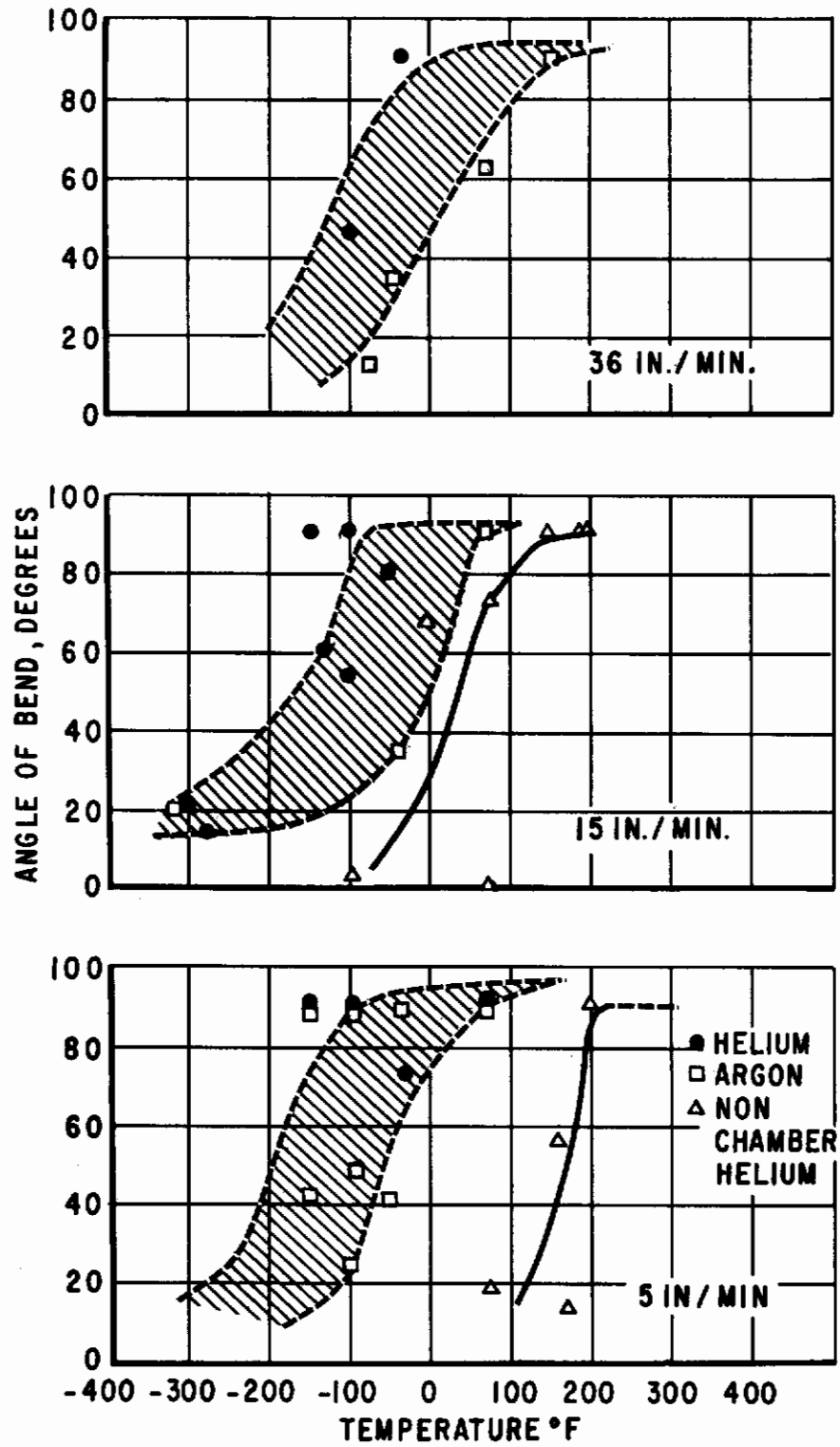


Figure 21. Bend Ductility of FS82 As-Welded.

# Contrails

welded without filler metal addition. Very little change in ductility was observed by increasing the welding speed from 5 to 15 or 36 ipm. However, indications are that at 15 and 36 ipm, welds made in helium yield a lower transition temperature than welds made in an argon atmosphere. It is apparent, regardless of the welding speed chosen, that the transition temperature of the FS82 alloy in the as welded condition is below room temperature, but some 200°F above the transition temperature of the unwelded wrought sheet. The transition temperatures for non-chamber welds made at 5 and 15 ipm are approximately 300° and 150°F respectively above that for chamber welds made at the same speed. Although the welds produced outside the vacuum purge atmosphere chamber compared favorably in color to those produced inside the chamber, it is obvious from the bend test results that contamination to some degree occurred in open-air. The higher welding speeds appear to reduce the contamination when welding in open air.

A speed of 15 ipm was established as a standard and practical welding speed for tensile and post heat treatment specimens.

The bend ductility data for FS82HS columbium alloy welded at 15 and 36 ipm in the vacuum purge atmosphere chamber is displayed in Figure 22. The limited amount of data collected for welds at 36 ipm indicate that no ductility advantage would be gained by using this welding speed. These results show that the transition temperature of the FS82HS alloy is in the range of 100° to 200°F. A comparison of these results with those of the low oxygen alloy indicates that raising the oxygen content of the FS82 to 1500 ppm or more, as is done in the FS82HS raises the weld transition temperature some 200° to 300°F. This same trend is noted with bend ductility curves of welds made in open-air on the FS82 alloy, Figure 21 where the transition temperature is above the transition temperature of this same alloy welded in the chamber. However, the open-air welds still appear to have a lower transition temperature than the FS82HS alloy welded in the chamber.

The bend ductility data for the FS82 alloy welded with pure columbium, FS80 and FS82 filler wire are shown in Figure 23. In each case the transition temperature is higher than welds made without filler wire added. It appears that the FS82 wire produces a somewhat lower transition temperature than developed with the other two wire additions. Furthermore, it can be noticed that the FS82HS and FS82 with wire addition in air have higher transition temperatures than the FS82 alloy. Comparing Figure 22 with Figure 23 it appears that the addition of FS82 filler wire to the high strength material lowers the transition temperature some 50° to 100°F. It is thought that the oxygen level in the weld is reduced by dilution in the filler material thus lowering the weld transition temperature.

Instead of adding filler metal as wire, T-melt down welds were made in which the filler metal was added in the form of a 0.020 x 0.080 in. FS82 shim placed between the abutting edges of the sheet to be welded. The bend ductility data for these welds, also plotted in Figure 23, correlated quite well with that for welds made with FS82 wire as the filler metal.

Non-chamber welds were made in FS82 with FS82 filler wire added to the weld puddle. The transition temperature was about the same as those made at 5 ipm but higher than those made at 15 ipm and higher than welds made in the

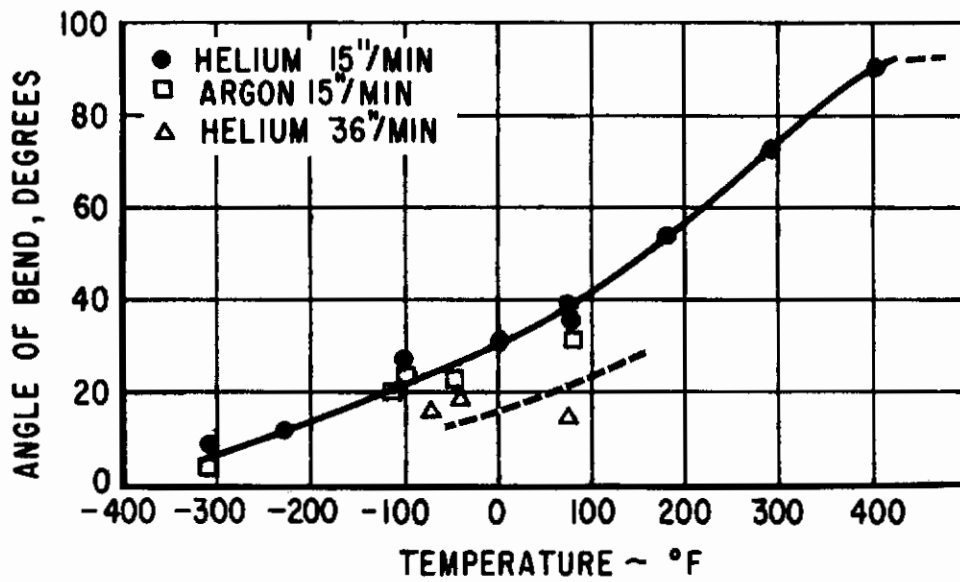


Figure 22. Bend Ductility of FS82HS As-Welded.



# Contrails

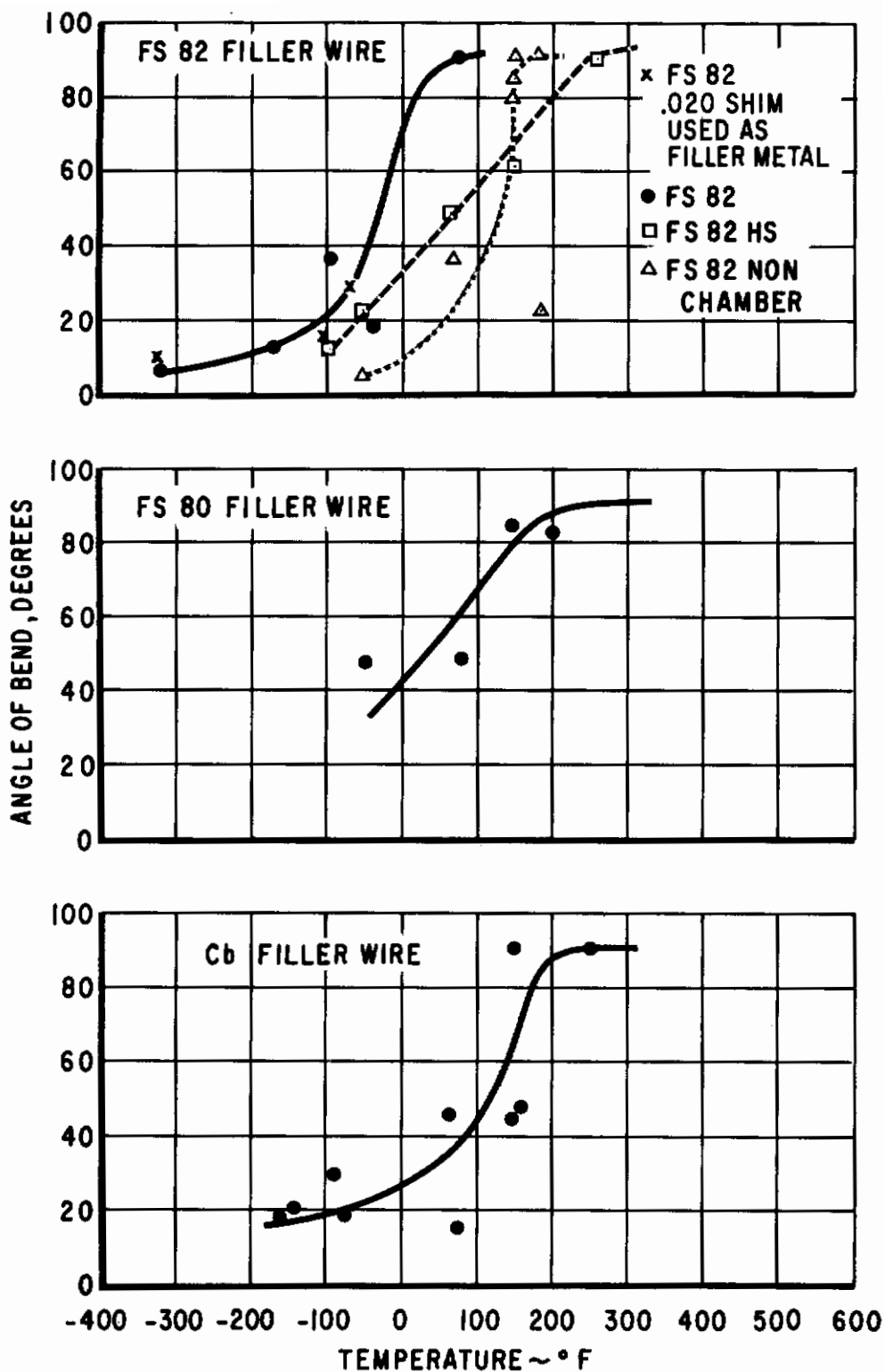


Figure 23. Bend Ductility of FS82 Welded in Helium at 15 ipm with Filler Metal Additions.

# Contrails

chamber with filler metal additions. The addition of filler metal in open-air has not appreciably affected the transition temperature.

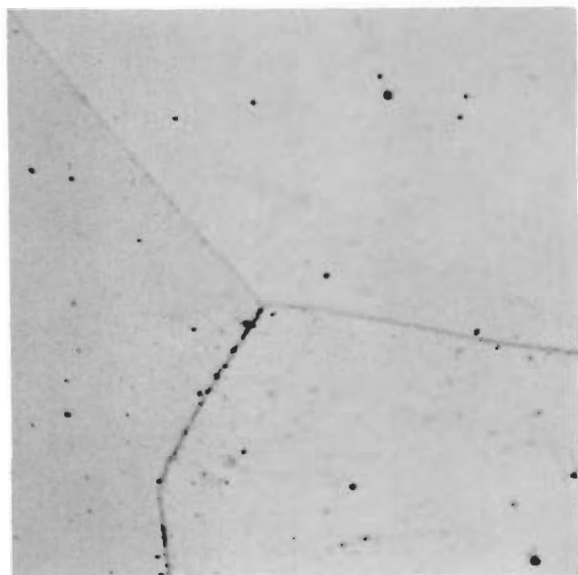
Photomicrographs of welds made at 5, 15 and 36 ipm showing the heat affected zone, and the fusion zone are presented in Figures 24, 25, and 26. The absence of dendritic coring in the fusion zone is obvious in all of these welds. This factor makes it difficult to determine the precise location of the interface between the fusion zone and heat affected zone because there is a gradual reduction in grain size as the distance from the weld center increases. Lack of a cored structure is a result of the narrow melting range of this alloy. As the center of the weld is approached the microstructure changes from a fine recrystallized grain structure containing numerous particles of a second phase to large solidification-oriented grains containing only a few particles. It is believed that most of the particles are dissolved in the fusion zone leaving few nuclei to initiate precipitation. The high temperature side of the heat affected zone is dotted with fewer particles of this second phase than the cooler side indicating that some solution has taken place here. Very little difference appears in the microstructure of this alloy between the welding speeds of 5 and 15 ipm. However, it appears that the fusion zone and heat affected zone in the 36 ipm weld contains fewer of the fine particles compared to similar areas of the microstructure in welds made at the slower speeds. It is possible that at the faster cooling rate in the 36 ipm weld, Figure 26, that the particles go into solution but do not have time to precipitate on cooling.

Photomicrographs of welds made in the FS82HS alloy in helium at a speed of 15 ipm showing the heat affected zone and fusion zone are presented in Figure 27. The microstructure of the heat affected zone is very similar to that of the FS82 alloy except that oxide inclusions which were present in the parent material still appear in the heat affected zone. These inclusions are taken into solution in the fusion zone then appear as many finer particles on cooling. The presence of this secondary phase suggests that lower ductility, compared to the FS82 alloy, is caused by supersaturation of the matrix with oxygen which may form a coherent precipitate on further cooling or result in solid solution strengthening. The electron micrographs at 10,000X in Figure 27 show a fine precipitate which appears to have been formed on cooling after welding. Electron micrographs, at 6000X, of the FS82 and FS82HS parent material are shown in Figure 28 for comparison. Large oxide particles shown in FS82HS at 1000X were not included in the electron micrographs.

Room and elevated temperature tensile properties for FS82 and FS82HS are listed in Table IV, page 50. The effect of high oxygen in the FS82HS alloy is apparent in the higher yield strength and lower elongation of the welded room temperature tensile specimens. Although the room temperature tensile strength of the FS82 sheet is much lower than for the D31 sheet. Table V, page 70, the FS82 appears to have more strength at 2200°F.

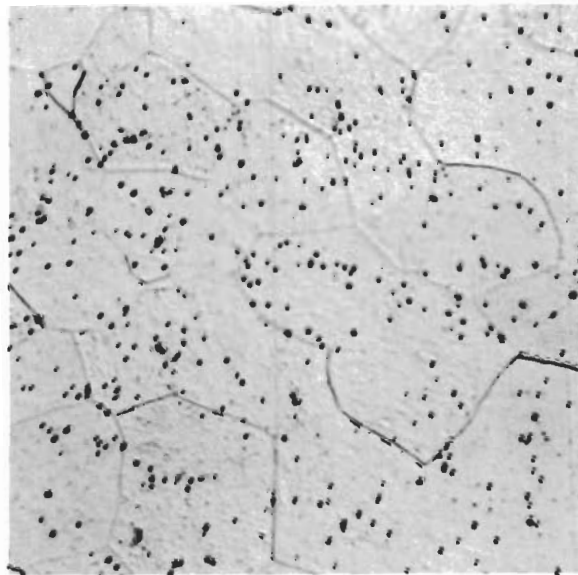
Hardness surveys of FS82 welds are displayed in Figures 29 and 30. The increase in hardness in the welds is probably a result of the solution of oxygen from an oxide phase causing interstitial solid solution strengthening or precipitation hardening. Either of these mechanisms could account

# Contrails



Fusion Zone

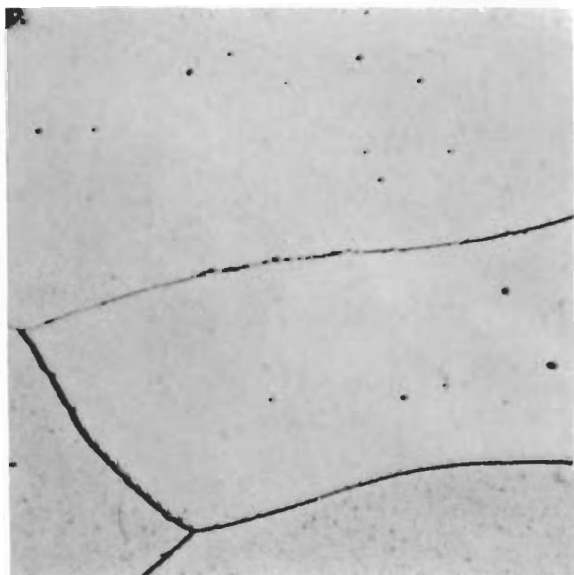
3160



Heat Affected Zone

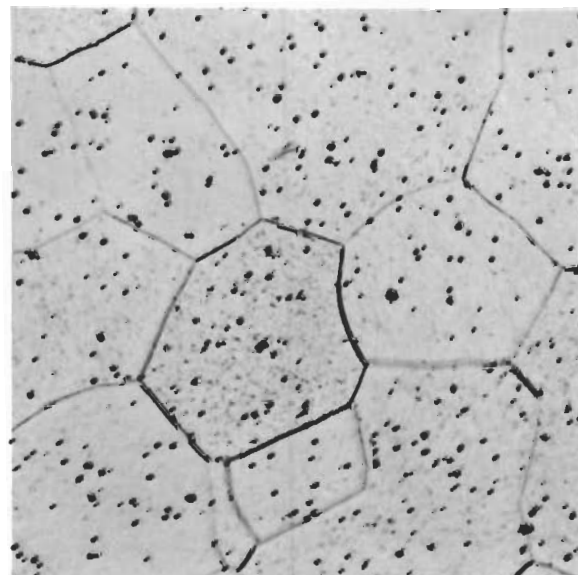
3162

5 ipm Helium



Fusion Zone

3169



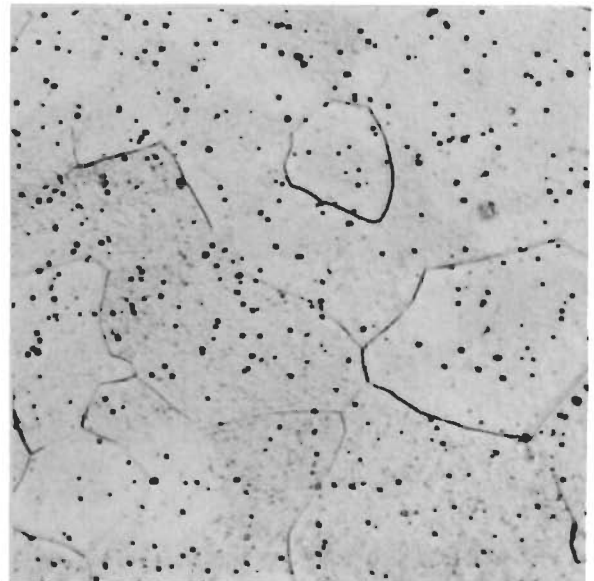
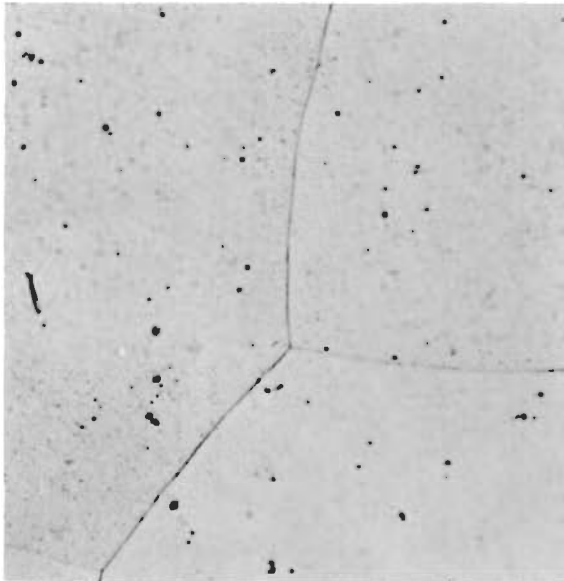
Heat Affected Zone

3171

5 ipm Argon

Figure 24 Microstructure of FS82 Welds 1000X

# Contrails



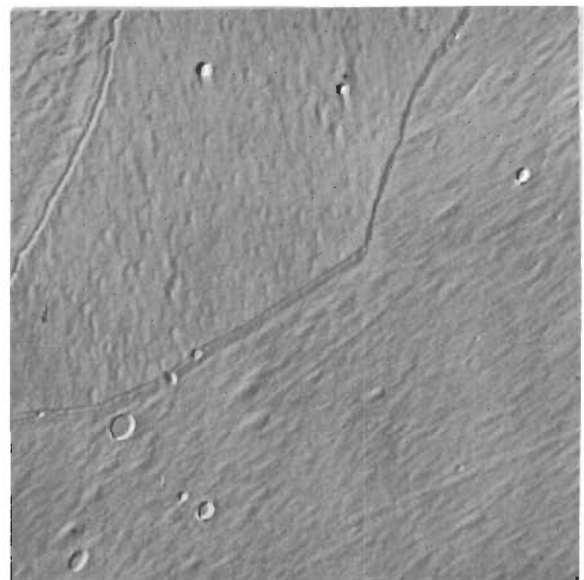
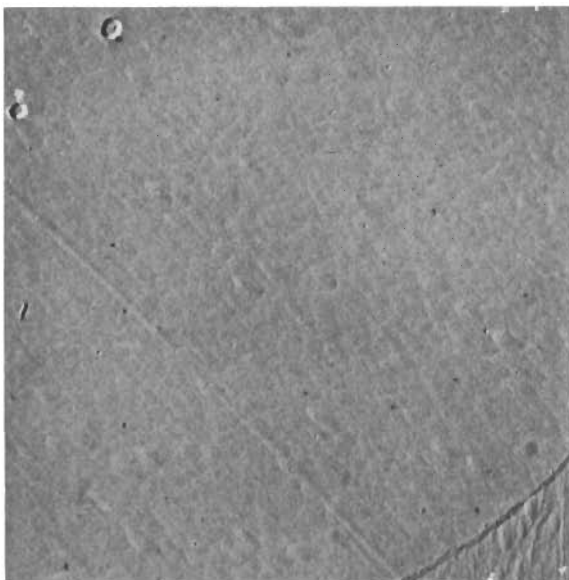
Fusion Zone

3175

Heat Affected Zone

3177

15 ipm Helium  
1000X



Fusion Zone

0643

Heat Affected Zone

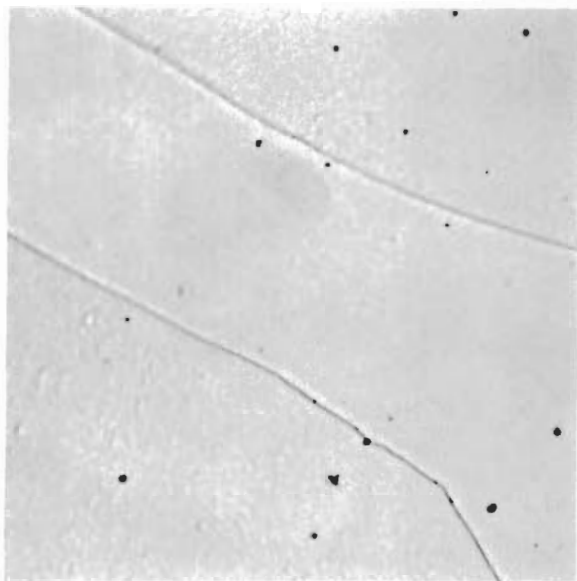
0641

15 ipm Helium  
6000X

Figure 25 Microstructures of FS82 Welds

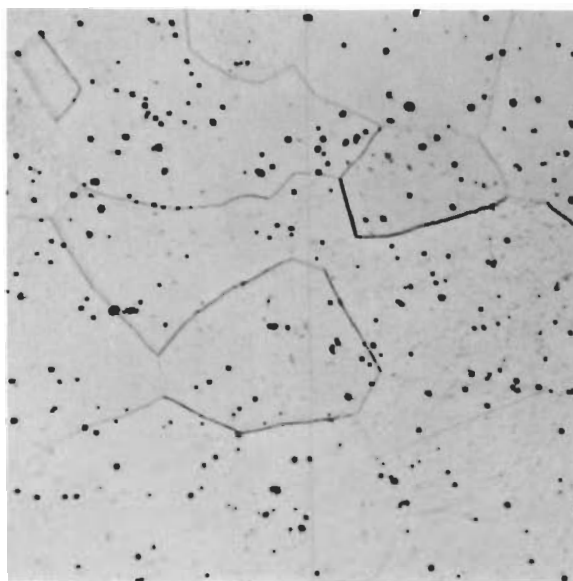


# Contrails



Fusion Zone

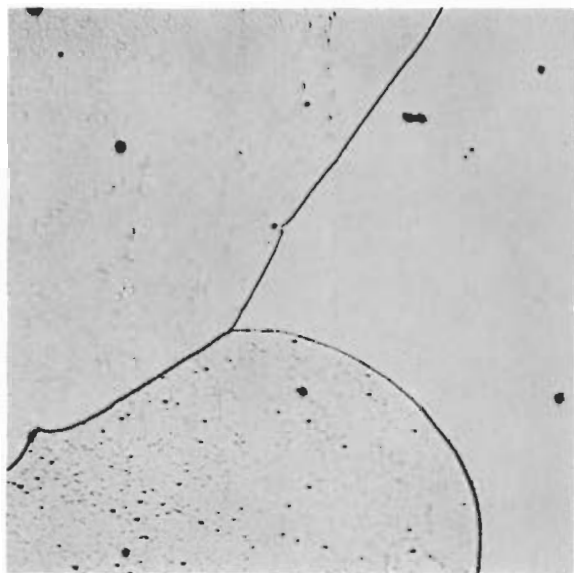
3172



Heat Affected Zone

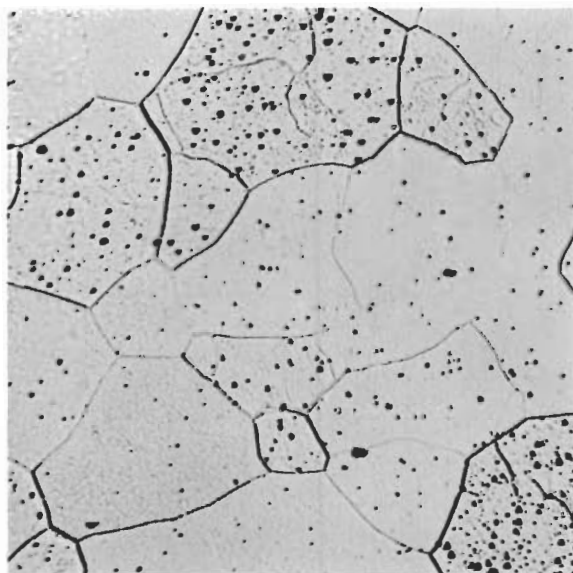
3174

36 ipm Helium



Fusion Zone

4449

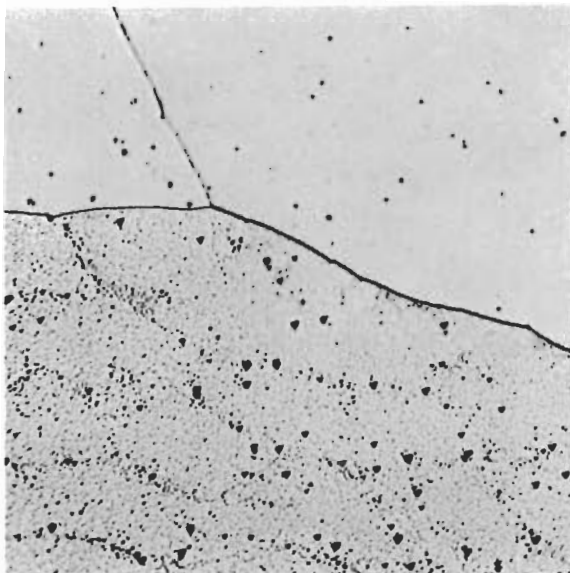


Heat Affected Zone

4450

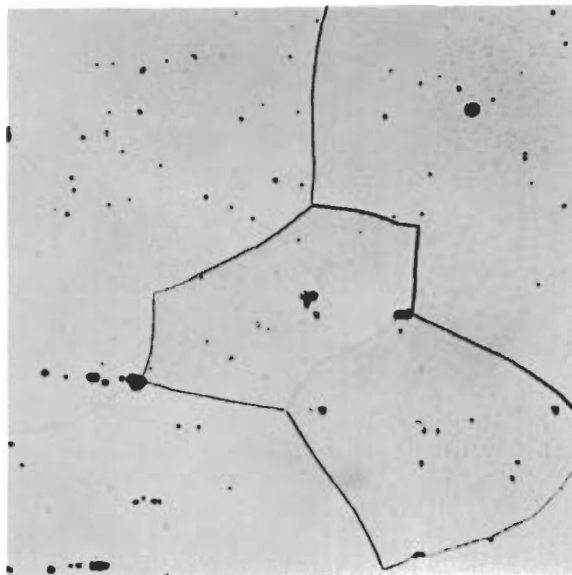
15 ipm Helium  
FS82 Wire Addition

Figure 26 Microstructures of FS82 Welds 1000X



Fusion Zone

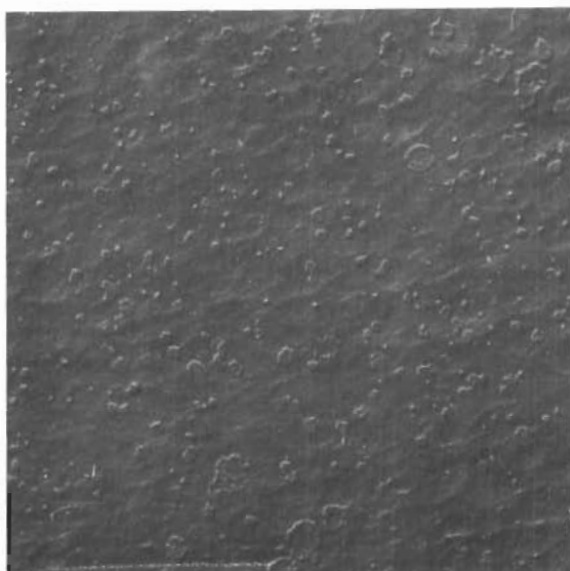
3831



Heat Affected Zone

3832

15 ipm Helium  
1000X



Fusion Zone

0609

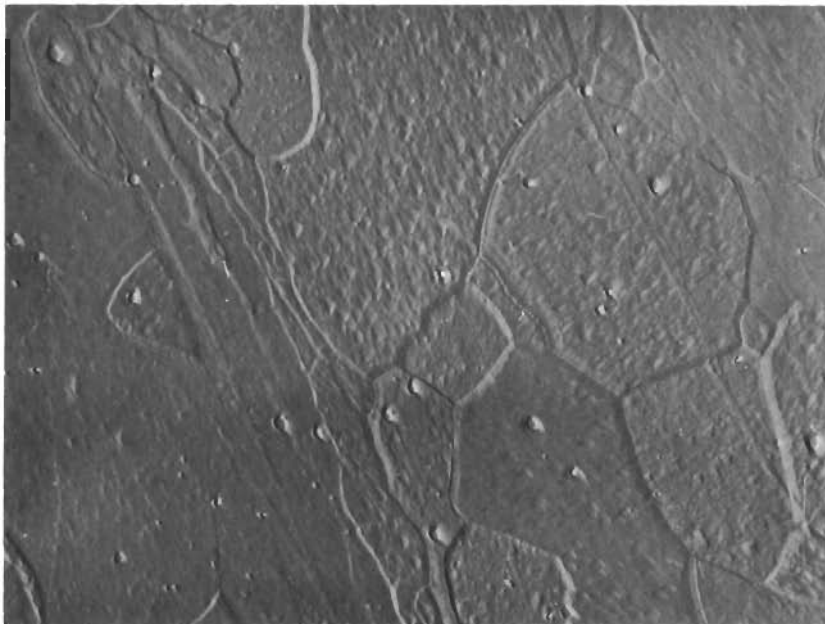


Heat Affected Zone

0608

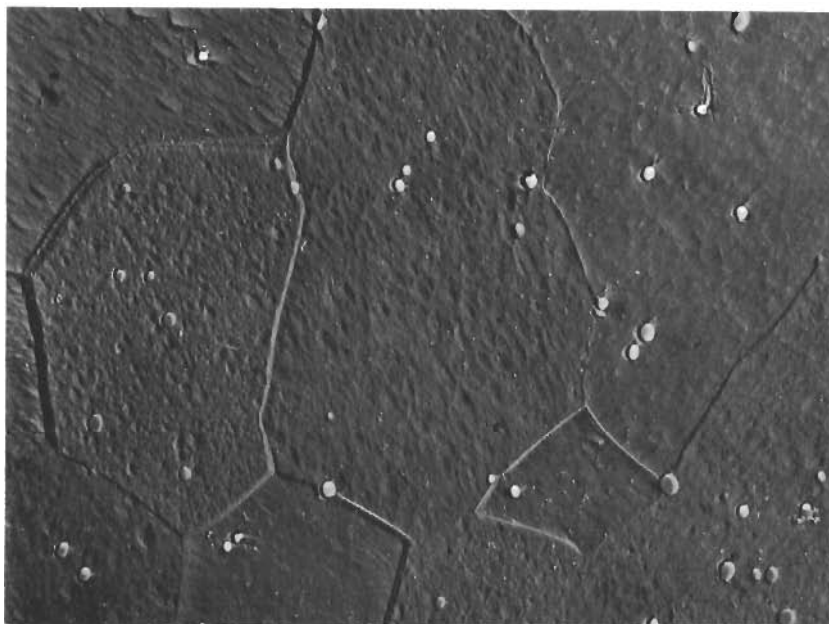
15 ipm Helium  
10,000X

Figure 27 Microstructure of FS82HS Welds



FS82 Longitudinal

0595



FS82HS Longitudinal

0596

Figure 28 Microstructure of FS82 and FS82HS Alloy Sheet 6000X

TABLE IV

ROOM AND ELEVATED TEMPERATURE  
TENSILE PROPERTIES FOR FS82 AND FS82HS

<u>Specimen</u>	<u>Type</u>	<u>Test Temperature</u>	<u>Ultimate Strength</u>	<u>0.2% Offset Yield Strength</u>	<u>% Elong.</u>	<u>% Reduction Of Area</u>
* AFFM 1-1	PM	RT	71,350	57,300	32.7	77.0
* AFFM 2-2	PM	RT	71,350	57,400	31.9	75.7
AFFM 2-6	PM	RT	68,100	57,300	35.6	74.3
AFFM 2-7	PM	RT	68,200	55,300	33.3	82.4
* BDPM 2-1	PM	RT	64,200	48,400	35.8	70.6
* BDPM 2-2	PM	RT	64,000	48,000	35.8	72.5
BDPM 2-5	PM	RT	64,100	46,500	38.6	69.9
BDPM 2-6	PM	RT	63,500	46,500	37.3	60.5
*** AA7	Weld	RT	84,100	70,900	25.6	43.9
*** AA8	Weld	RT	83,200	70,400	31.4	43.7
*** AD4	Weld	RT	82,600	71,400	23.9	56.9
*** AH4	Weld	RT	89,000	69,400	25.6	39.6
*** BC1	Weld	RT	86,800	73,500	16.9	27.8
*** BD5	Weld	RT	91,400	75,500	16.1	22.0
**** AC 5-2	Weld	RT	79,900	-	-	-
**** AC 5-3	Weld	RT	80,000	-	-	-
**** AD 5-1	Weld	RT	75,200	-	-	-
**** AD 5-2	Weld	RT	77,200	-	-	-
FS82	PM	2200°F	26,600	-	-	-
**** AD 5-3	Weld	2200°F	26,100	-	-	-
**** AD 5-4	Weld	2200°F	25,000	-	-	-
**** AD 5-5	Weld	2200°F	26,300	-	-	-
**** AD 5-6	Weld	2200°F	24,900	-	-	-
BCPM 1	PM	2200°F	19,000	-	-	-
* BCPM 2	PM	2200°F	16,900	-	-	-
*** BC 1	Weld	2200°F	16,900	-	-	-
*** BC 2	Weld	2200°F	16,700	-	-	-

\* Direction of loading transverse to direction of rolling.

\*\* Sheet material was cross rolled.

\*\*\* Direction of loading transverse to direction of rolling and parallel to weld.

\*\*\*\* Direction of loading transverse to weld and parallel to direction of rolling.

All elevated temperature specimens were aluminum coated.

Rate of loading 0.050 in/min.

Note: The first letter of the specimen number identifies the material; A = FS82, B = FS82HS



# Contrails

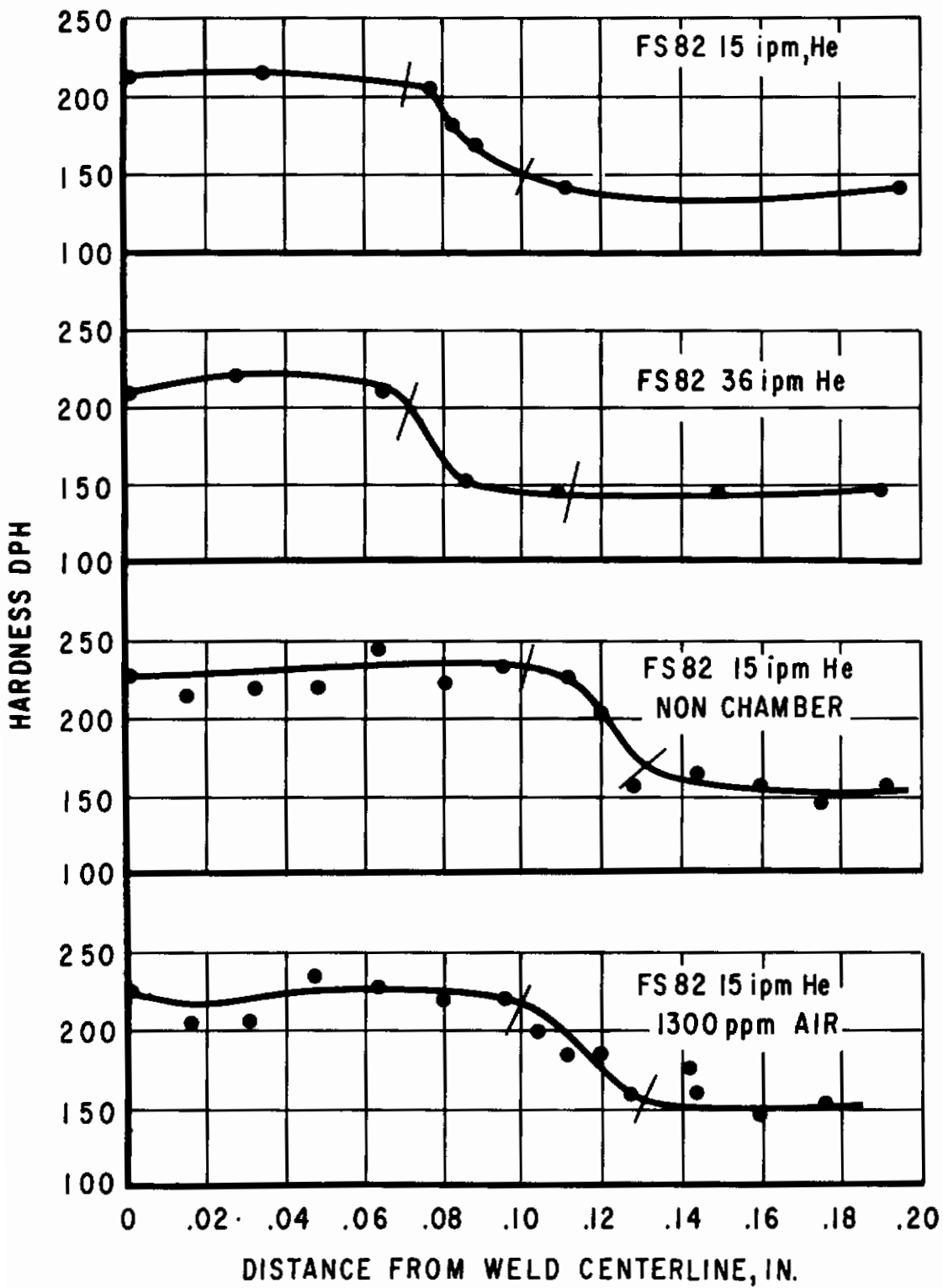


Figure 29. Hardness Surveys of FS82 Welds.

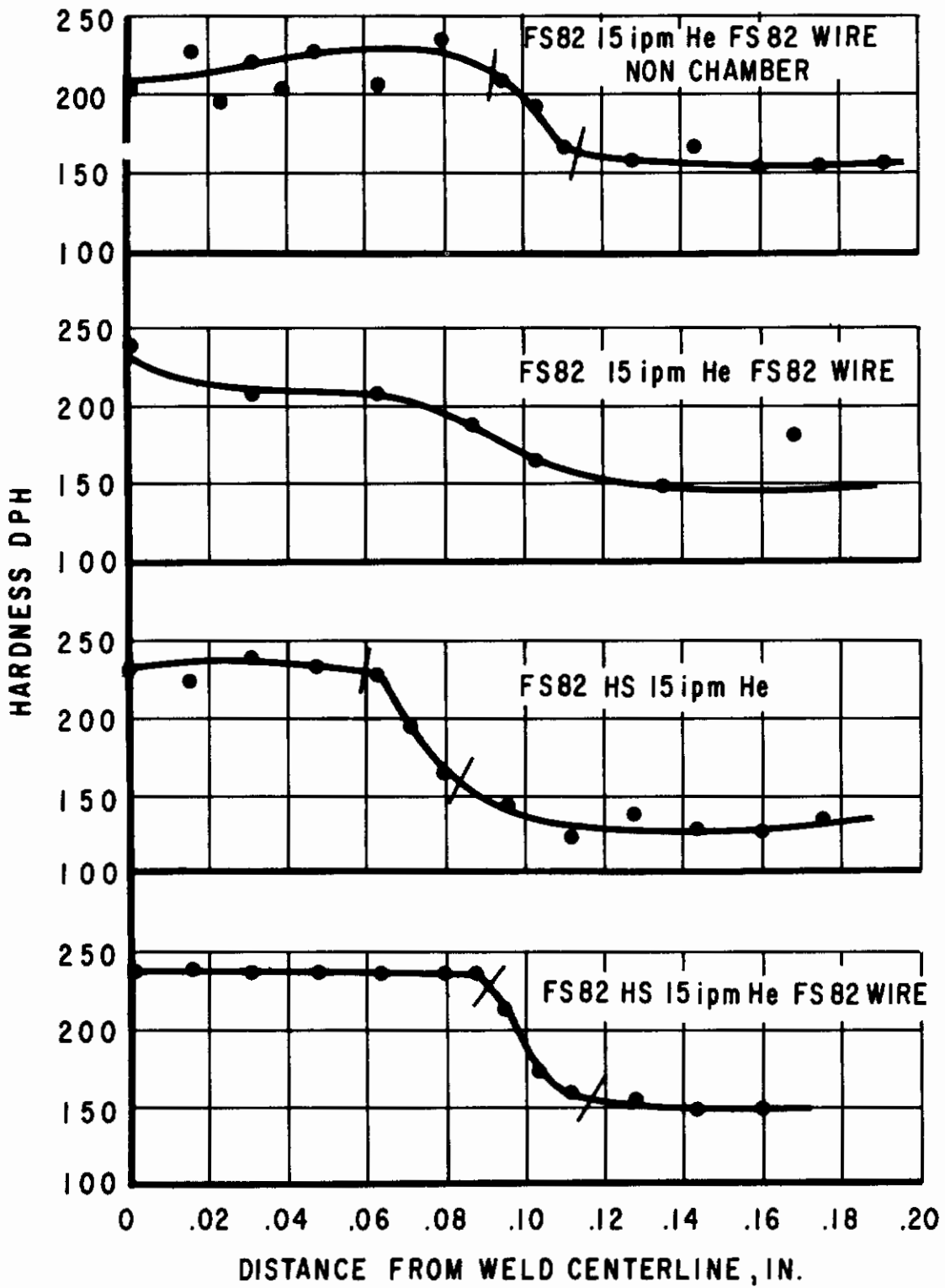


Figure 30. Hardness Surveys of FS82 and FS82HS Welds.

# Contrails

for the increased transition temperature of the weld over base metal. The non-chamber welds and welds made with the addition of 1300 ppm air to the atmosphere appear to have increased hardness at a greater distance from the weld centerline than the chamber welds. This hardening could be caused by oxygen and nitrogen pickup.

The bend ductility curves for FS82 welds made in an atmosphere purposely contaminated with controlled amounts of air are described in Figure 31. A small but noticeable decrease in ductility is apparent as the amount of air is increased from 200 ppm to 1300 ppm.

Bend ductility curves for FS82 alloy aged at a number of temperatures and times after welding are displayed in Figures 32 and 33. Considering that as-welded FS82 exhibited a transition temperature of approximately  $-100^{\circ}\text{F}$ , it is obvious that a loss of ductility has occurred at  $1400^{\circ}$ ,  $1600^{\circ}$ , and  $1800^{\circ}\text{F}$ . The transition temperature increase is most pronounced after the  $1600^{\circ}$  and  $1800^{\circ}\text{F}$  aging treatments. However, the  $2000^{\circ}\text{F}$  treatments lower the transition temperature to between  $-250^{\circ}$  and  $-300^{\circ}\text{F}$  resulting in an improvement in ductility over the as-welded condition. The results seem to indicate that the aging reaction follows a normal C-curve behavior where the loss of ductility occurs at shorter aging times as the temperature is raised from  $1400^{\circ}$  to  $1800^{\circ}\text{F}$ . At  $2000^{\circ}\text{F}$  treatments it is believed that the ductility is increased because over-aging occurs giving a non-coherent precipitate and reduction in solid solution strengthening. To verify this, welds were aged at  $2000^{\circ}$ ,  $2200^{\circ}$ , and  $2400^{\circ}\text{F}$  then subsequently heat treated at  $1800^{\circ}\text{F}$ . The bend ductility data are presented in Figure 34. This shows that the subsequent heat treatment of  $1800^{\circ}\text{F}$  does not embrittle the material as in the case of the  $1800^{\circ}\text{F}$  at 4 and 16 hours without the preceding over-aging heat treatments. It is expected that much longer aging times at  $1800^{\circ}\text{F}$  would cause over-aging and thus would restore ductility. Electron micrographs, Figure 35, help to substantiate this. The fusion zone and heat affected zone after  $1800^{\circ}\text{F}$  for 70 hours show no evidence of a precipitate indicating that a coherency precipitate could have occurred. After  $2000^{\circ}\text{F}$  for 24 hours a precipitate is readily distinguished showing that over-aging probably did occur.

Fusion welds made in the vacuum purge atmosphere chamber were coated with the TRW Cr-Ti-Si vapor deposited coating which involved temperatures of  $2050^{\circ}$ ,  $2300^{\circ}$ , and  $2150^{\circ}\text{F}$ . It was found that the welds were fully ductile down to  $-320^{\circ}\text{F}$ . After an oxidizing treatment of  $2500^{\circ}\text{F}$  for 50 hours the welds were still fully ductile down to  $-200^{\circ}\text{F}$ , the lowest temperature at which they were tested.

Thermal cycle measurements of the weld and heat affected zone were taken on the FS82 alloy, and the results of these measurements are presented in Figure 36. It is immediately obvious that the higher welding speeds cause faster heating and cooling rates and considerable less time at elevated temperatures than the slower welding speeds. The reason for this is apparent when one considers the energy input in watt second or joules per inch of weld to achieve full fused penetration for each speed

# Contrails

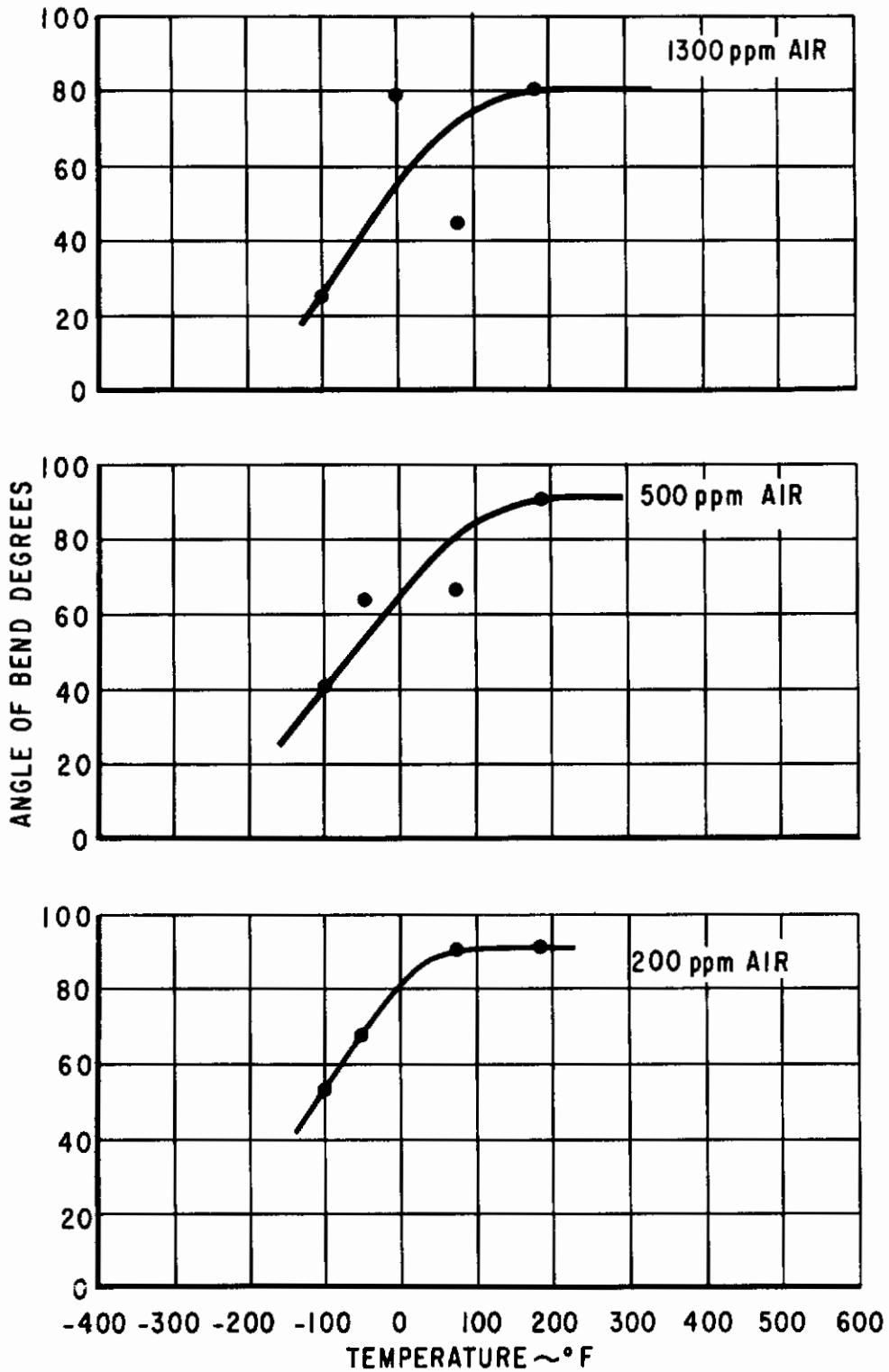


Figure 31. Bend Ductility of F982 Welded in Helium with Air at 15 ipm.



# Contrails

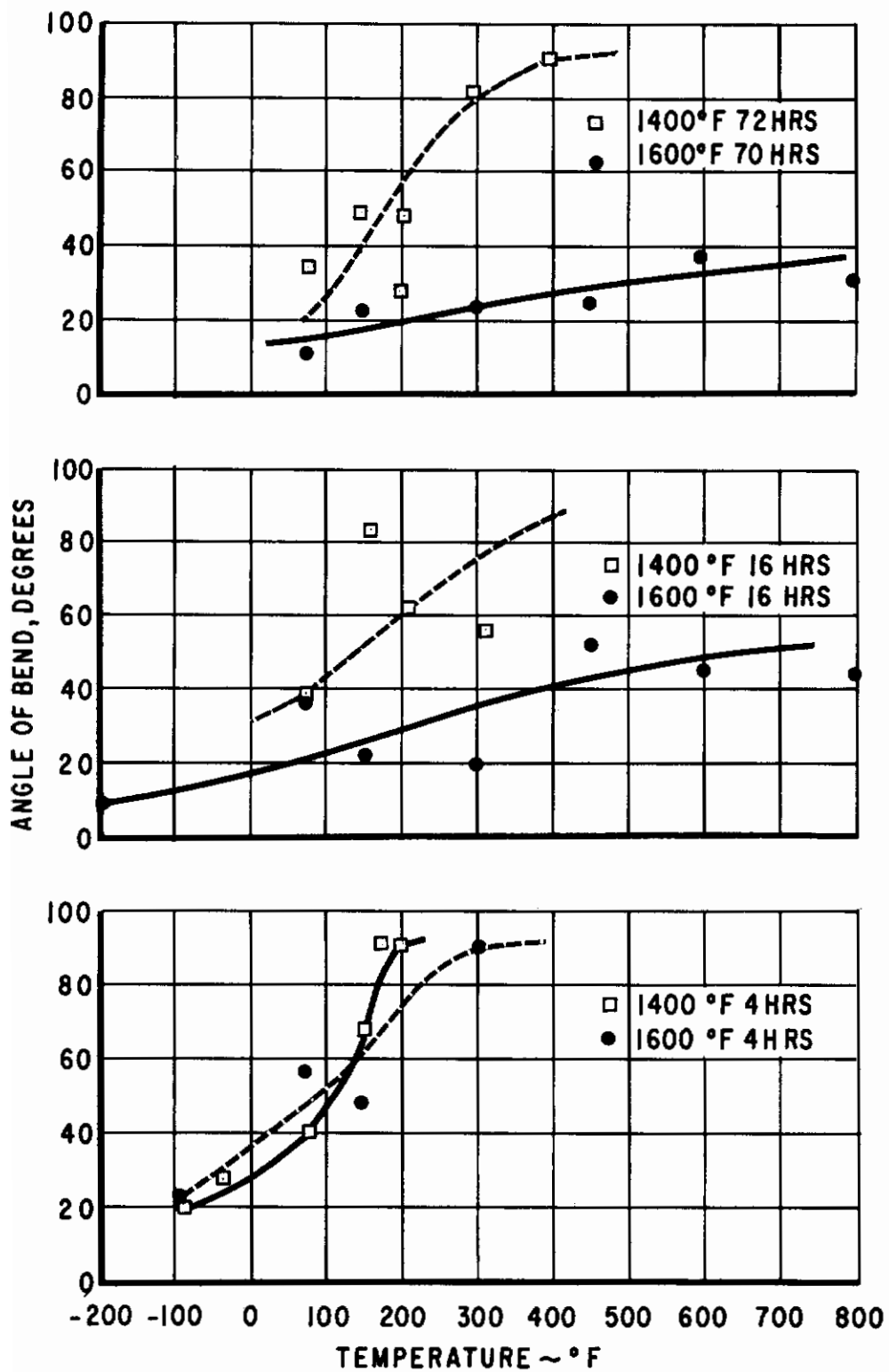


Figure 32. Bend Ductility of FS82 Welded in Helium at 15 ipm Then Aged at 1400 or 1600°F.

# Contrails

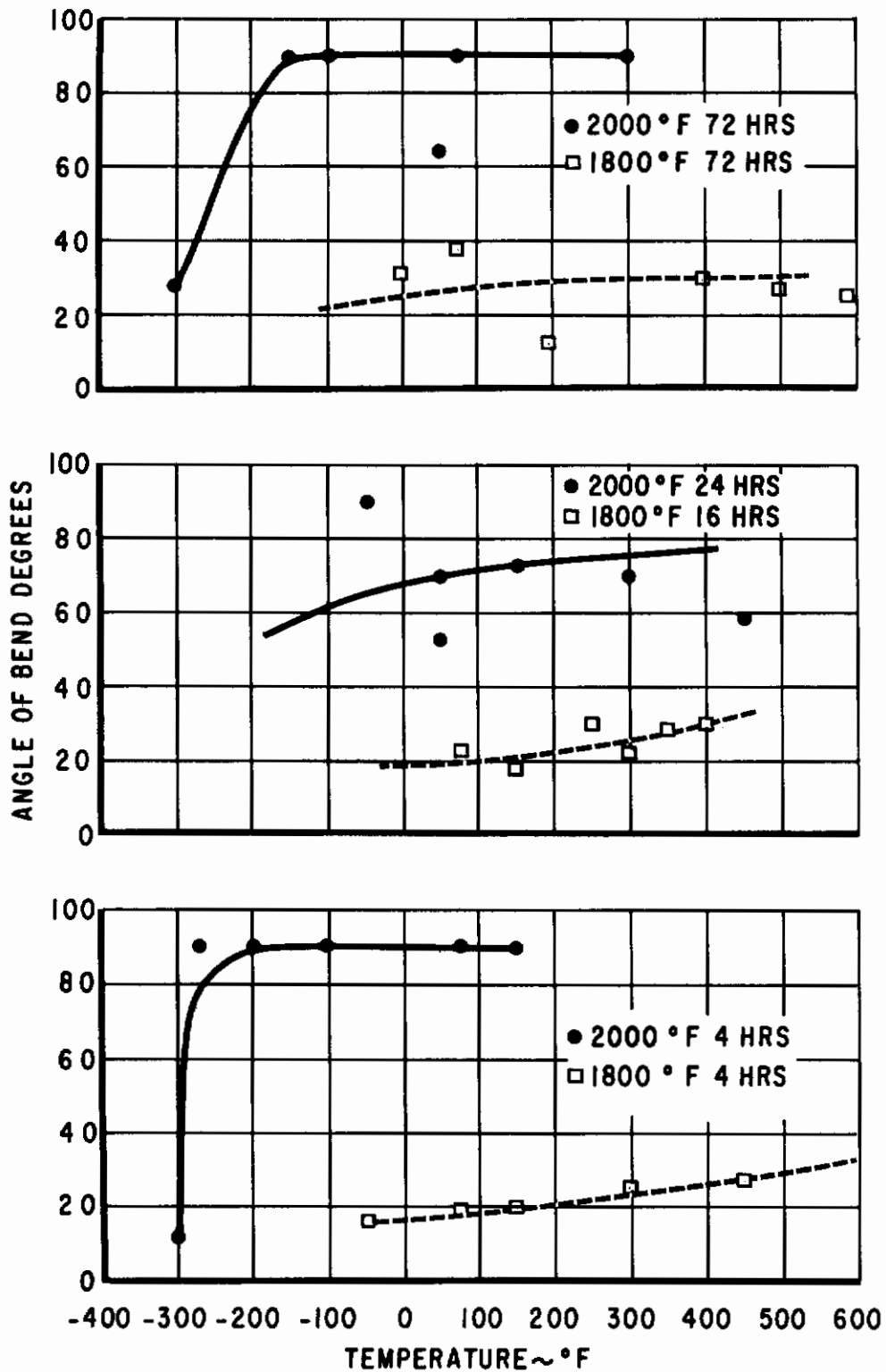


Figure 33. Bend Ductility of FS82 Welded in Helium at 15 ipm Then Aged at 1800 or 2000°F.

# Contrails

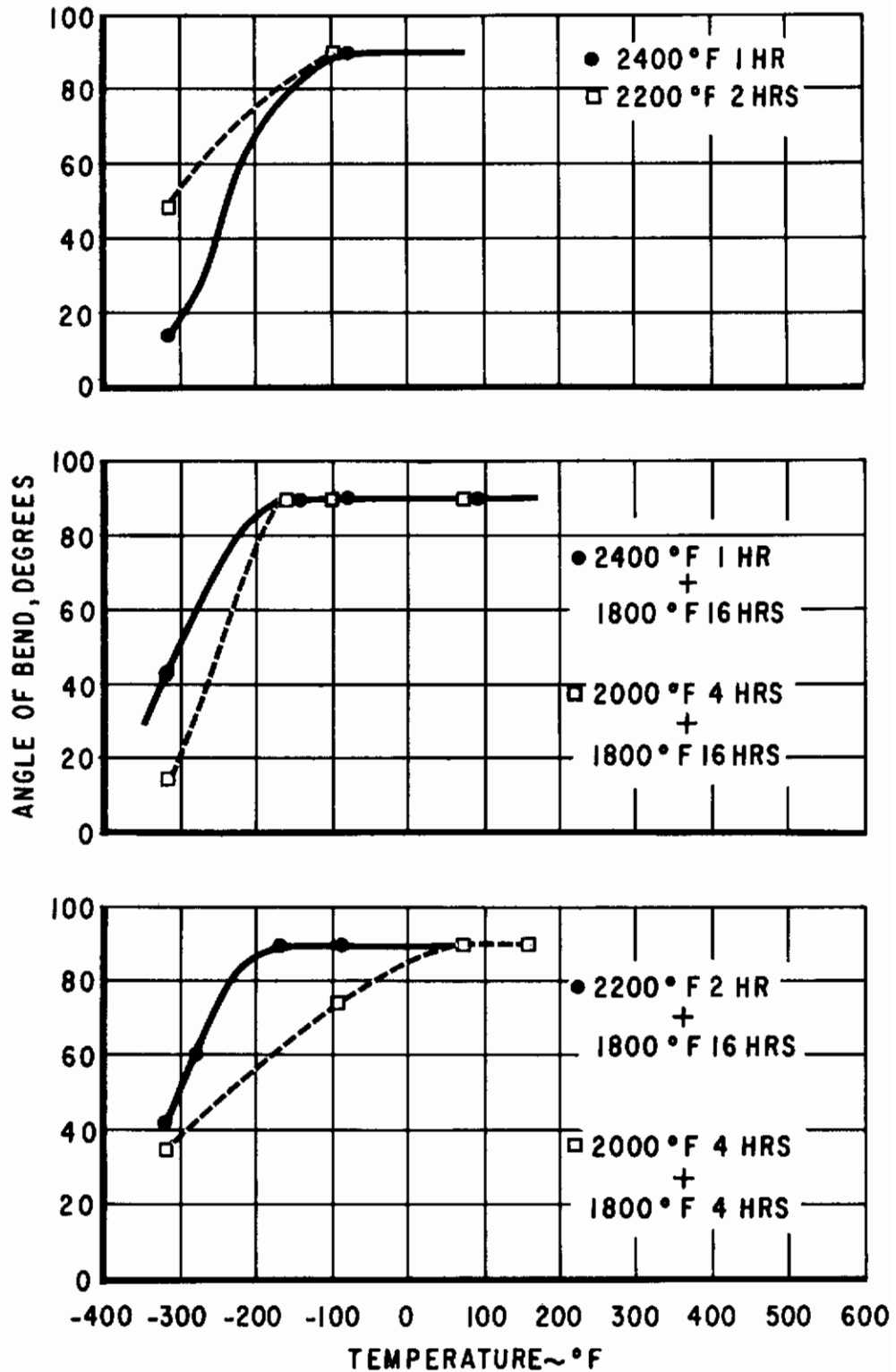
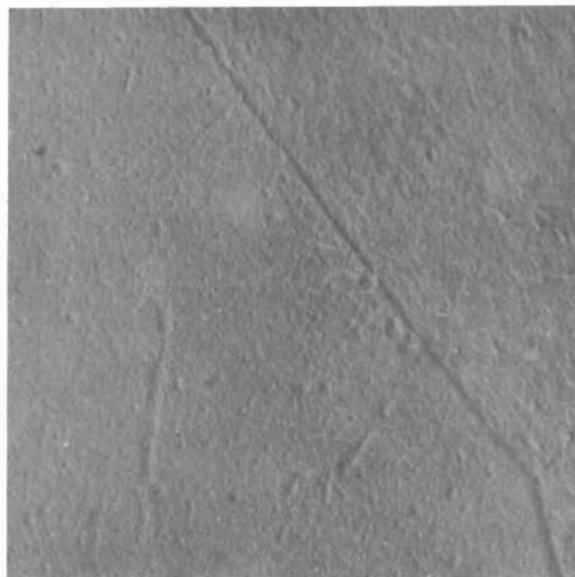
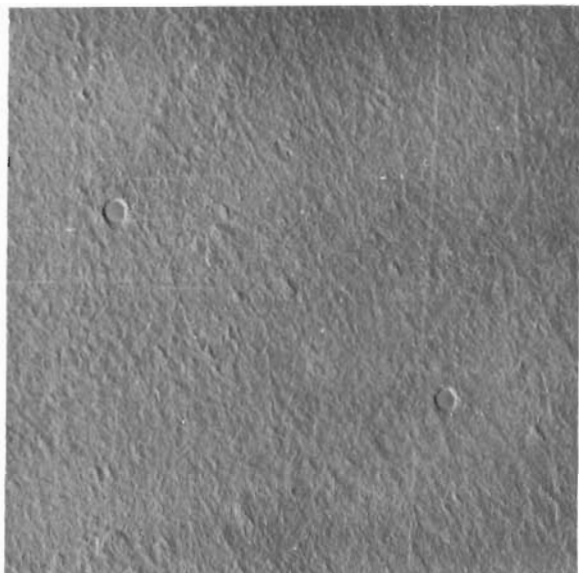


Figure 34. Bend Ductility of FS82 Welded in Helium at 15 ipm Then Double Aged at 2000, 2200 or 2400°F plus 1800°F.



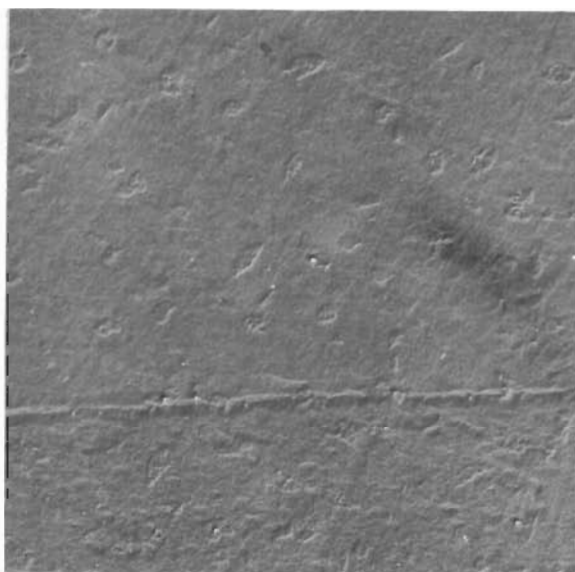
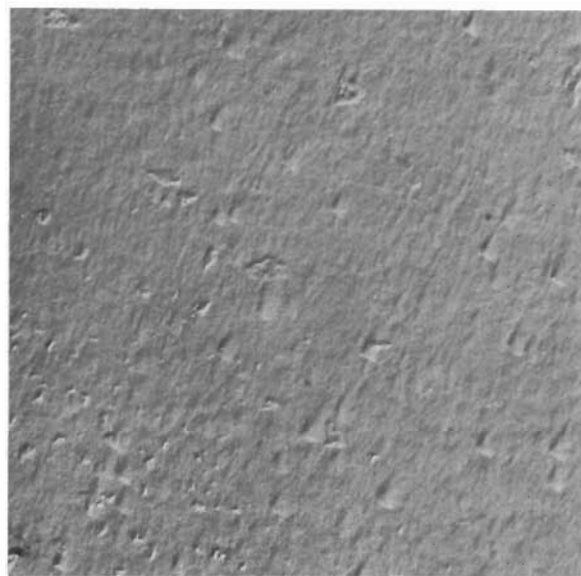
Fusion Zone

0606

Heat Affected Zone

0607

1800°F 70 Hours  
6000X



Fusion Zone

0605

Heat Affected Zone

0604

2000°F 24 Hours  
10,000X

Figure 35 Electron Micrographs of Heat Treated FS82  
Welded at 15 ipm in Helium



# Contrails

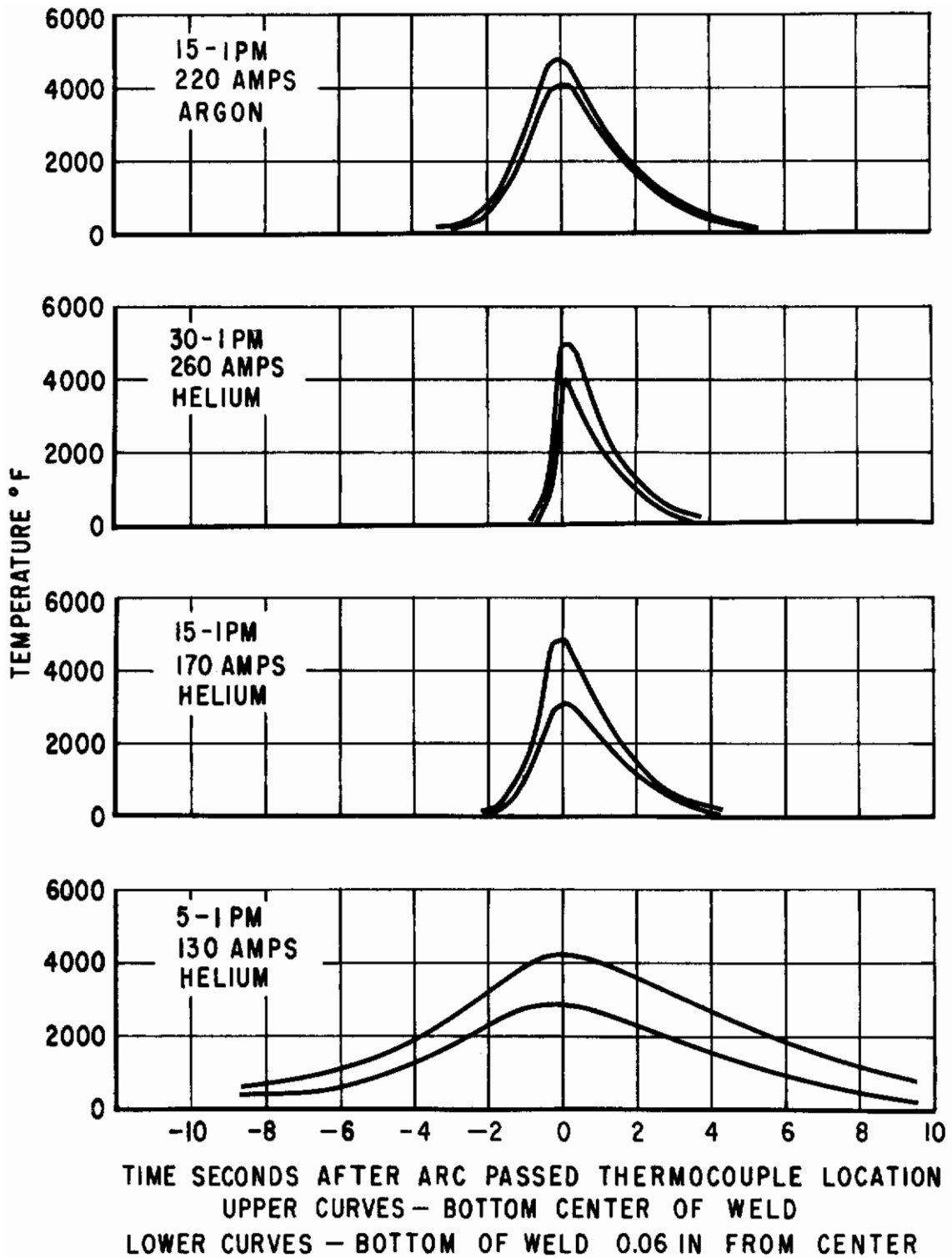


Figure 36. Thermal Cycle of Welds in 0.060 in. FS82 Sheet Made at 5, 15 and 30 ipm.

of travel. At low welding speeds this heat is lost by conduction to the fixture. The heat energy supplied by the arc must equal that needed to heat and melt the joint plus that lost to the adjacent plate and fixture. Another way to consider this is that at the slow speed the effective dwell time of the arc at any point is longer than for fast speeds hence the extended time at temperature.

A comparison of the effect of helium and argon shielding gases is shown in Figure 36. The higher energy input required to obtain full penetration with argon causes slower cooling rates and a longer time at elevated temperatures.

It is observed that the effect of increasing travel speed from 15 to 30 ipm did not produce as great a change in heating and cooling rate as occurred on increasing from 5 to 15 ipm. This indicates that the benefits of further shortening the time at elevated temperature by increasing welding speed is marginal above 15 ipm for tungsten inert gas welds.

Since weld thermal cycles indicate the time that every point in a weld remains at a given temperature and cooling rate, information of this nature is useful in predicting and understanding the properties at each of these points in the weld.

High quality welds in 0.060 in. FS82 and FS82HS sheet can be made in helium in a vacuum purge chamber at 150 - 160 amperes, 14 - 16 volts and a speed of 15 ipm. Transition temperatures of  $-100^{\circ}\text{F}$  for the FS82 and  $150^{\circ}\text{F}$  for the FS82HS can be expected under these conditions. Addition of FS82 filler wire to the puddle raises the transition temperature of FS82 welds approximately  $70^{\circ}\text{F}$  and lowers the transition temperature of FS82HS welds approximately  $50^{\circ}\text{F}$ . Welds can be made outside the chamber with very careful helium shielding at 180 amperes, 16 volts and at a speed of 15 ipm. A ductile to brittle transition temperature of  $50^{\circ}\text{F}$  can be obtained for FS82. Over-aging at  $2000^{\circ}\text{F}$  for 4 hours is necessary if service temperatures in the range of  $1400^{\circ}$  to  $1800^{\circ}\text{F}$  are expected.

## B. D31 Alloy

The bend ductility curves for D31 alloy welded at 5, 15, and 36 ipm in the vacuum purge atmosphere chamber, are presented in Figure 37. Contrary to the belief that a fast welding speed can minimize the embrittling reaction in this alloy the faster welding speeds tend to produce a somewhat higher transition temperature than the slow speeds. It was observed that all but one D31 weld made at 36 ipm contained transverse cracks across the fusion and heat affected zone as illustrated in Figure 38. The dimples at the end of the crack indicate ductility in the unaffected base metal. It is believed that the magnitude of restraint and steep thermal gradient developed during welding are partly responsible for this crack formation. This restraint may produce a number of microfissures in the weld which tend to increase the bend ductility transition temperature by forming stress raisers. An apparent microfissure is shown in the heat affected zone, Figure 42, of a weld made

# Contrails

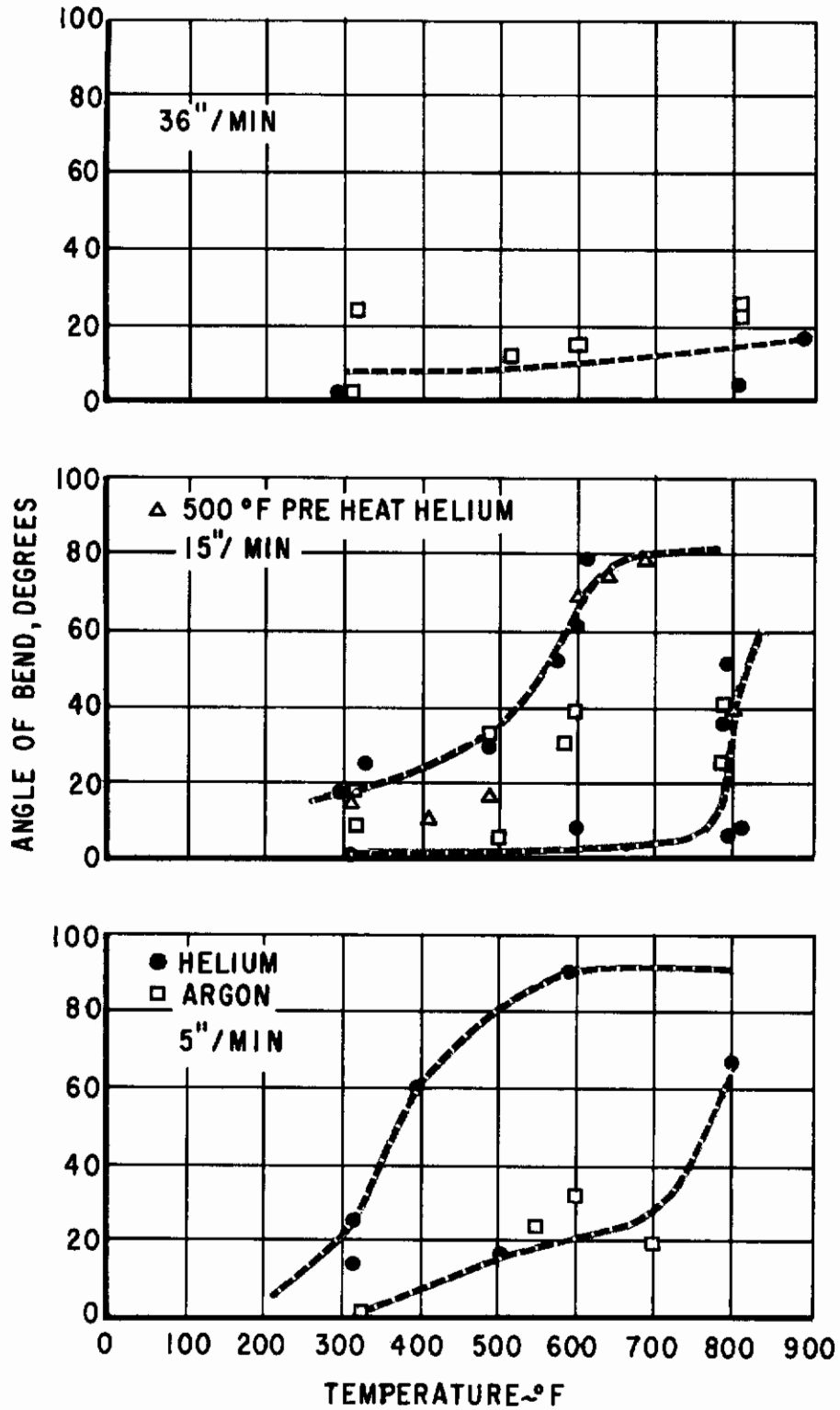
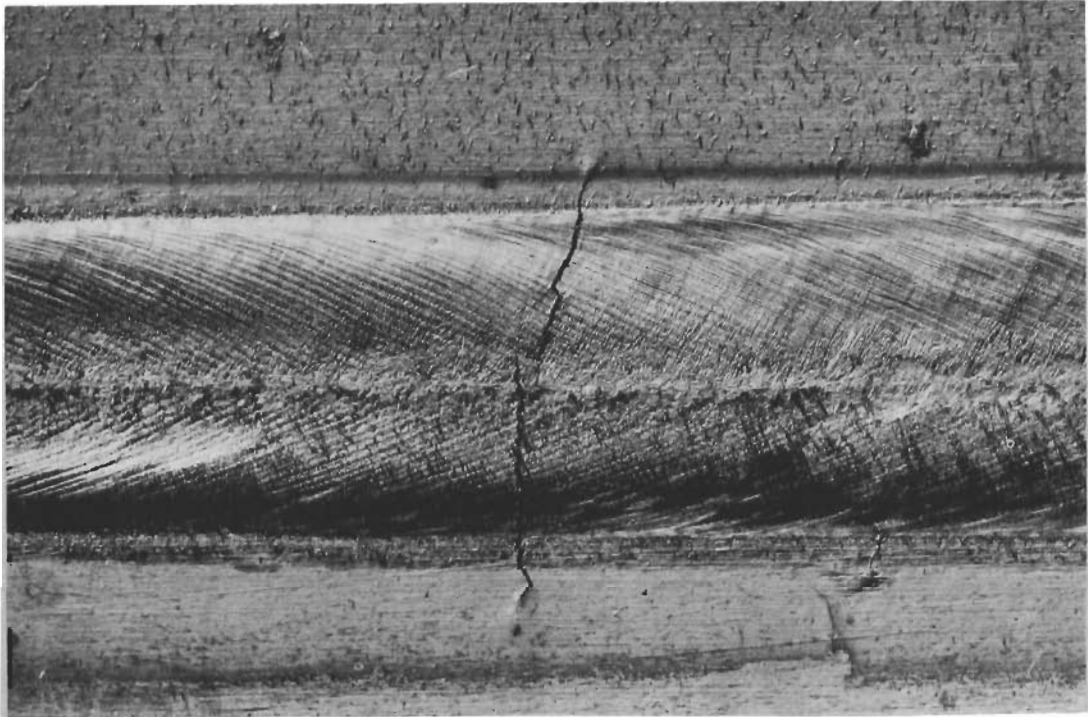


Figure 37. Bend Ductility of D31 Welded at 5, 15 or 36 ipm.

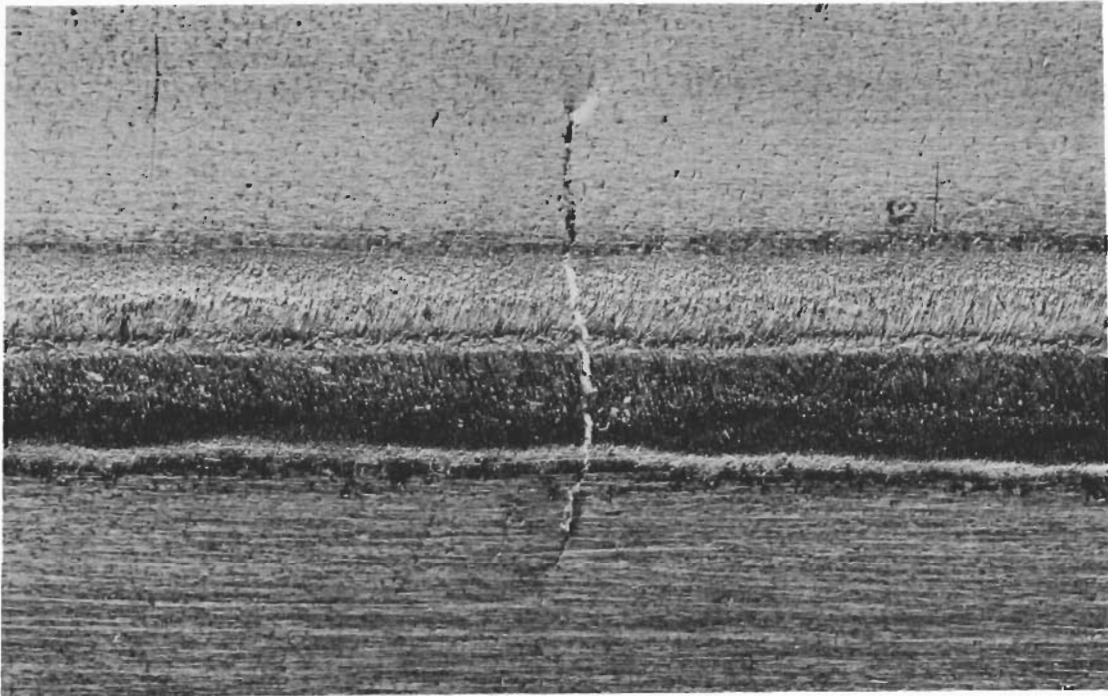
# Contrails



Top Surface

10X

05613-1



Bottom Surface

10X

05613-2

Figure 38 Cracks in D31 Welded at 36 ipm



# Contrails

at 36 ipm. These could be the cause of extremely poor ductility of the bend specimens obtained from 36 ipm welds. The rough surface condition of the D31 alloy visible in Figure 38 could be partly responsible for weld cracking and contribute to the high transition temperature of some of the as-received sheet.

One weld, made at 21 ipm, had no visual signs of cracking, however, of 13 welds made at 15 ipm transverse cracking did appear in three of them. Additional welds were made at 15 ipm in cold fixtures and after the fixture had been preheated to 150° to 200°F by a previous weld. There was no significant difference in the influence of this amount of preheat on weld cracking. To study the effect of preheat temperatures on weld cracking, chamber welds were made at 15 ipm with a 500°F preheat. The bend ductility curve for these welds is presented in Figure 37 along with the 15 ipm chamber welds. The curve tends to fall in the same general area of the other welds, however, the results are not as scattered.

Welds made at 5 and 15 ipm exhibit a fairly broad scatter in bend ductility in the temperature range of 600° to 800°F. The scatter in results could be caused by random occurrence of microfissures in welds. The drop in ductility as 800°F is approached could be caused by strain aging at this temperature with diffusion of oxygen or nitrogen into the material a contributing factor.

The use of argon or helium at 15 and 36 ipm did not make a significant difference in ductility, but at 5 ipm welds made in helium generally were more ductile than those made in argon.

The bend ductility curves for chamber welds made with the addition of FS82, FS80, and pure columbium filler wire to the weld puddle are demonstrated in Figure 39. It appears that welds made with FS80 wire have the most consistent results and a lower transition temperature than welds made with FS82 and pure columbium wire additions.

Microstructures of the D31 welds made at 5, 21, and 36 ipm are presented in Figures 40, 41, and 42 respectively. An outstanding difference between the fusion zone in D31 and FS82 is the cored network in the D31. At 36 ipm the segregations are sharper and these appear to contain some microporosity. The coring at 5 ipm is more diffuse and contains an acicular phase. In the heat affected zone, most of the carbide particles have been taken into solution.

The electron micrographs of D31 show a somewhat larger acicular precipitate in the 5 ipm welds as a result of the slower cooling rates involved. A comparison of these structures with parent metal structure, Figure 52, shows that the banded particles of carbide have been dissolved and reprecipitated as fine acicular particles.

Microstructures of welds made with the addition of filler metal are shown in Figure 43. The fusion zones contain the typical cored network found in welds made without filler metal. However, the heat affected zone of the

# Contrails

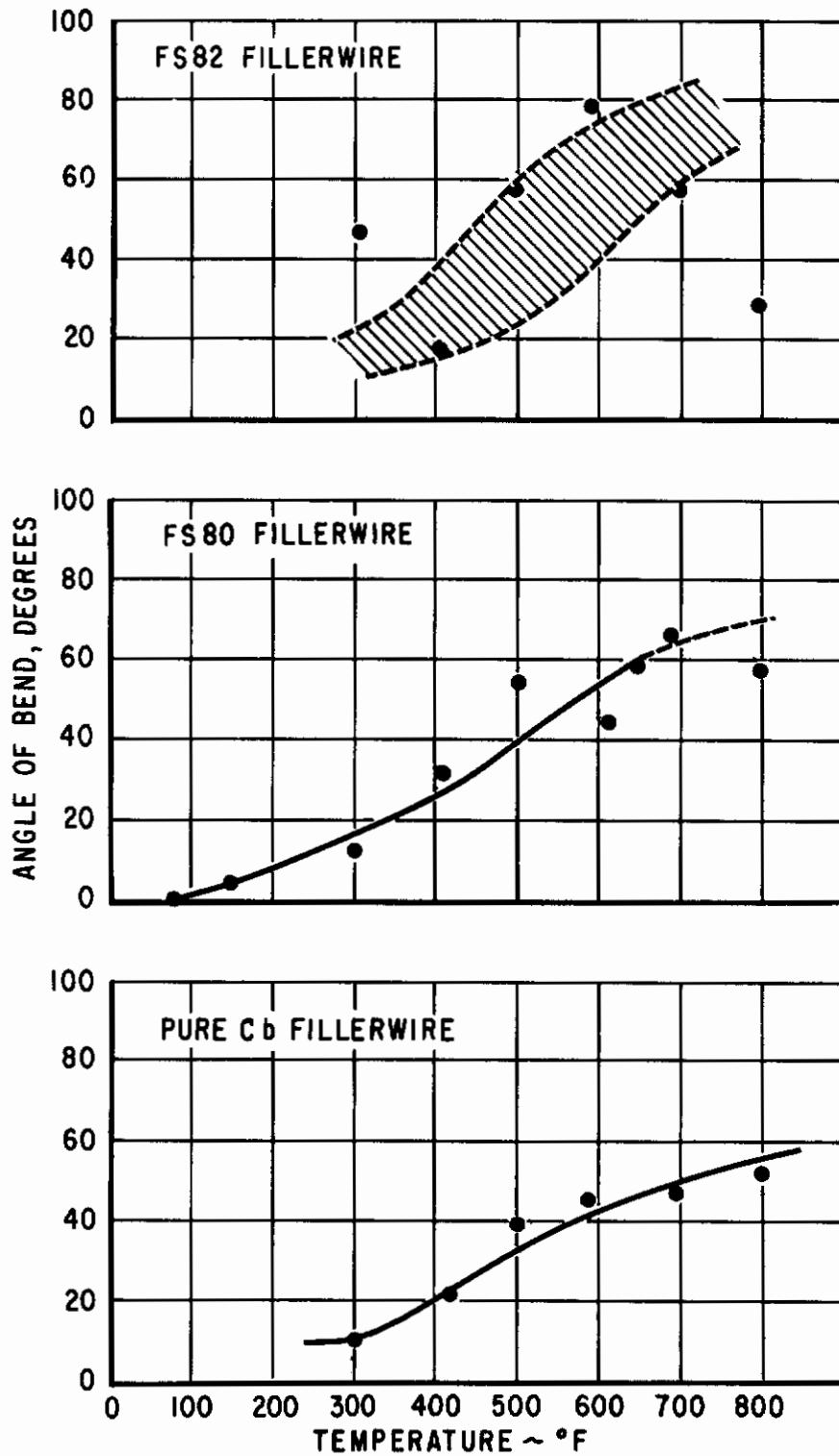
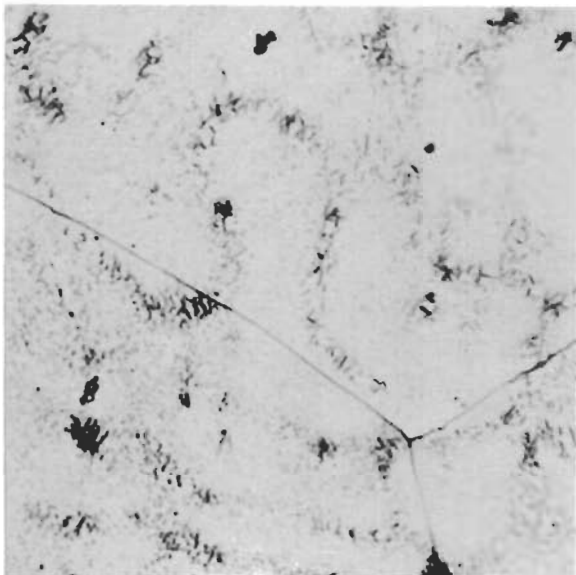


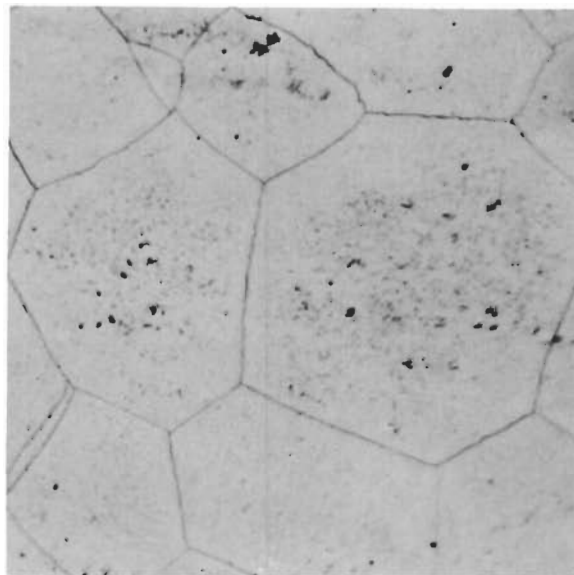
Figure 39. Bend Ductility of D31 Welded in Helium at 15 ipm with Pure Cb, FS80, or FS82 Filler Wire.

# Contrails



Fusion Zone

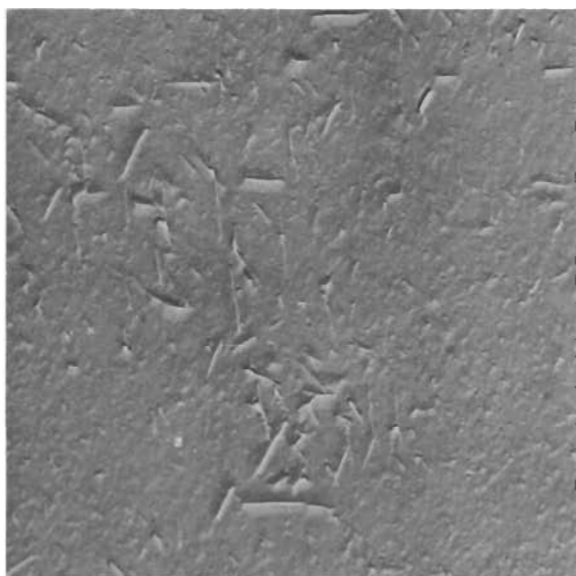
3166



Heat Affected Zone

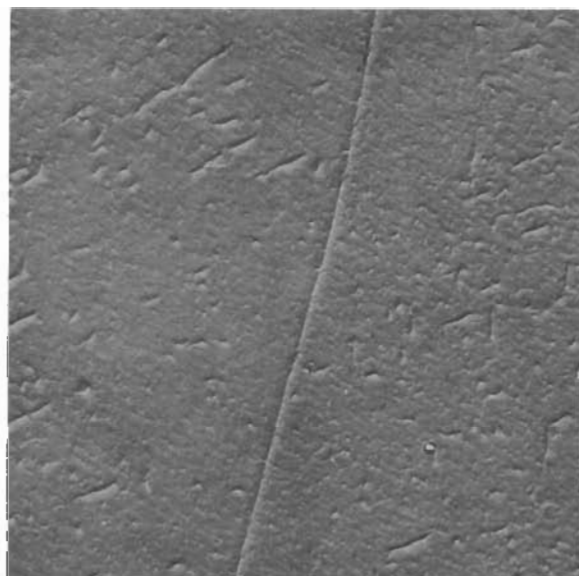
3168

1000X



Fusion Zone

0601

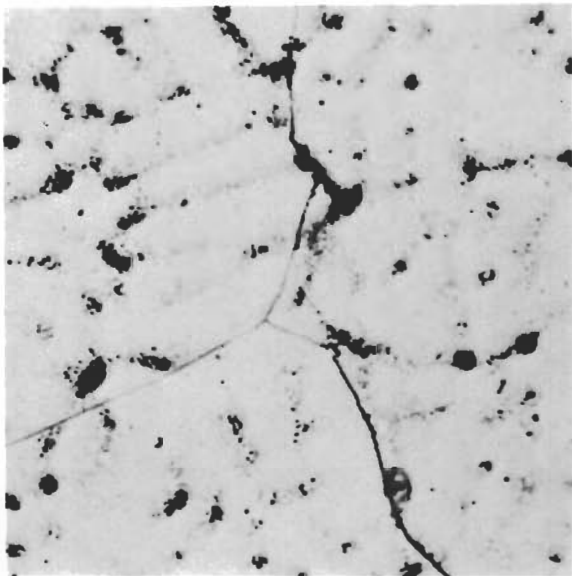


Heat Affected Zone

0600

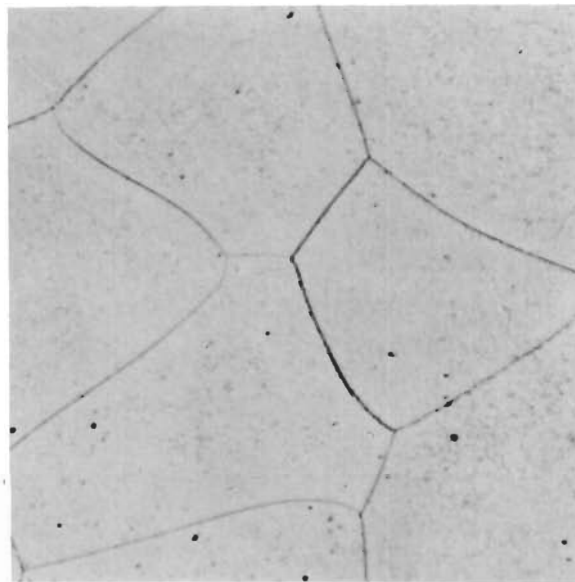
10,000X

Figure 40 Microstructure of D31 Welded at 5 ipm in Helium



Fusion Zone

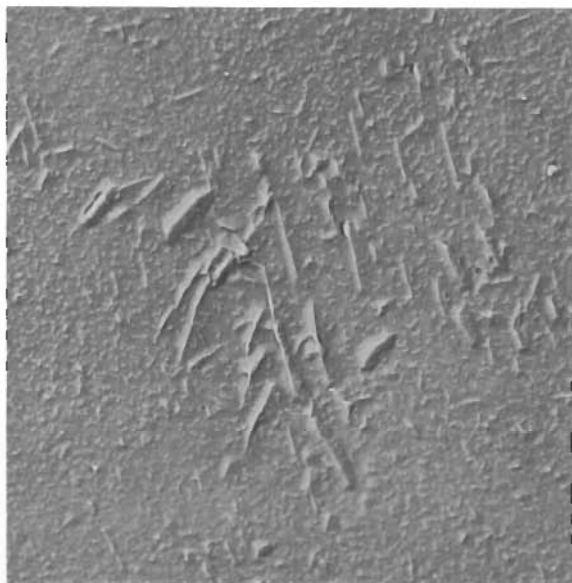
3178



Heat Affected Zone

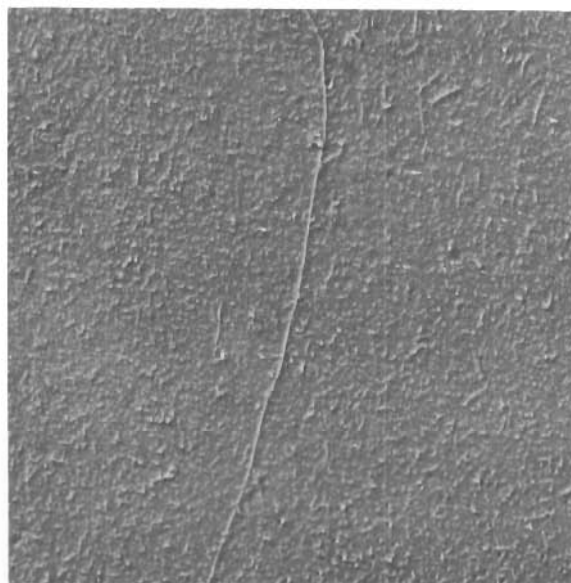
3180

1000X



Fusion Zone

0602



Heat Affected Zone

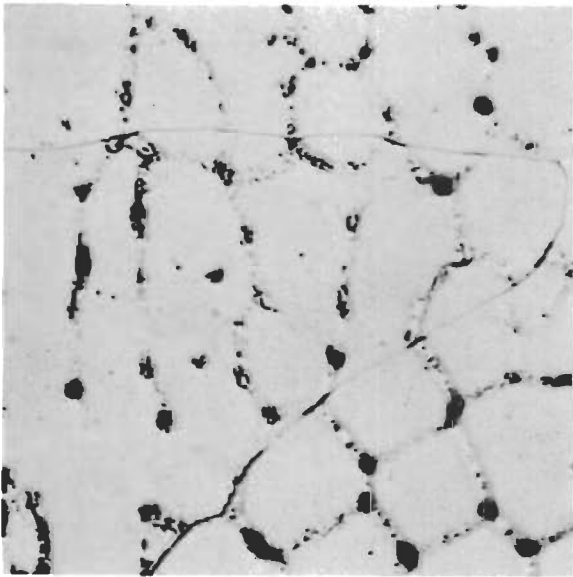
0603

10,000X

Figure 41 Microstructure of D31 Welded at 21 ipm in Helium

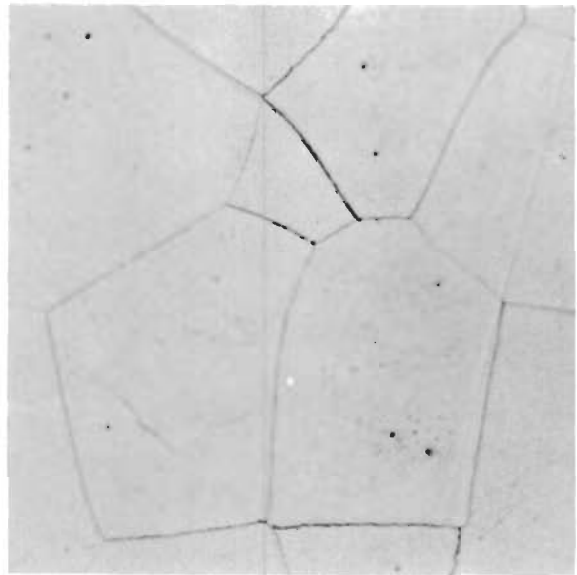


# Contrails



Fusion Zone

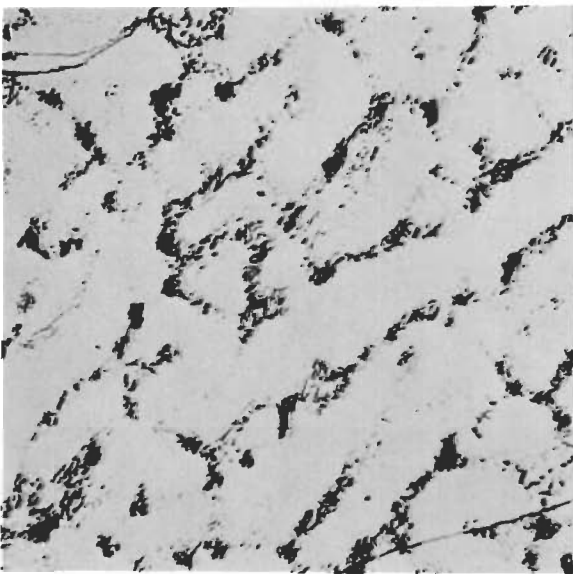
3163



Heat Affected Zone

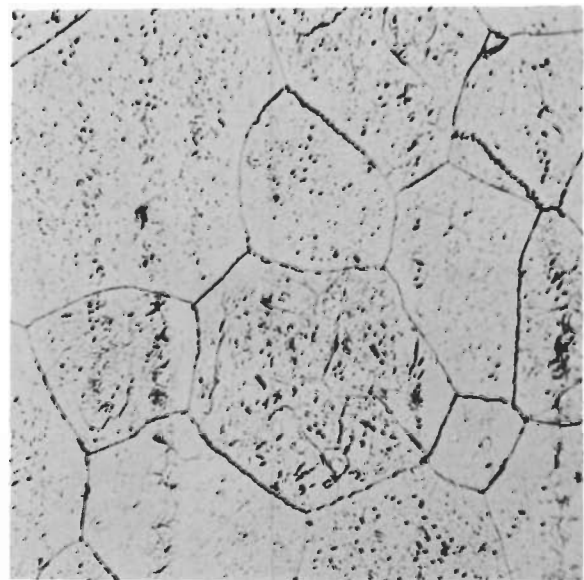
3165

36 ipm Helium



Fusion Zone

4431



Heat Affected Zone

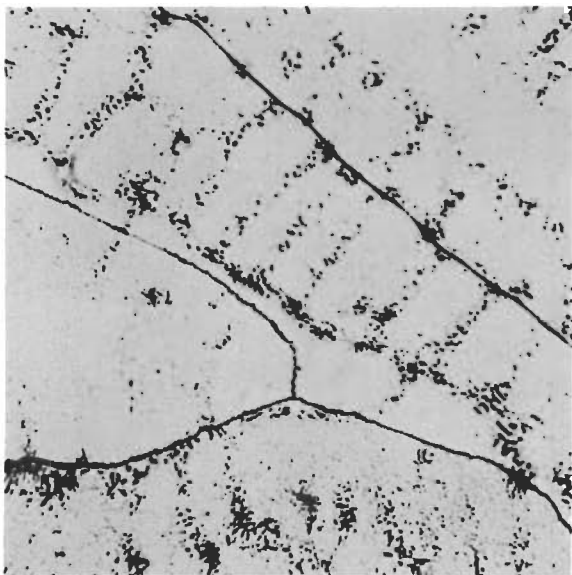
4432

15 ipm Helium Non Chamber

Figure 42 Microstructure of D31 Welds

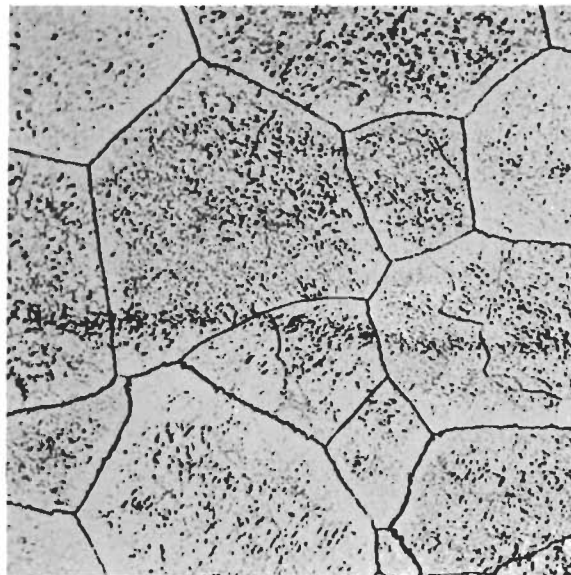
1000X

# Contrails



Fusion Zone

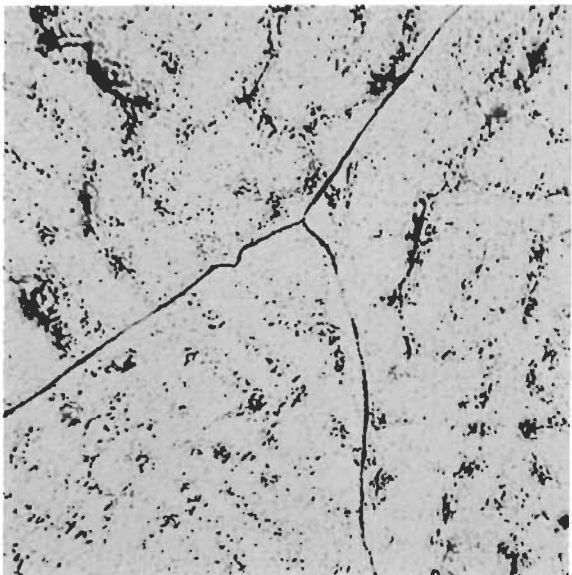
4447



Heat Affected Zone

4448

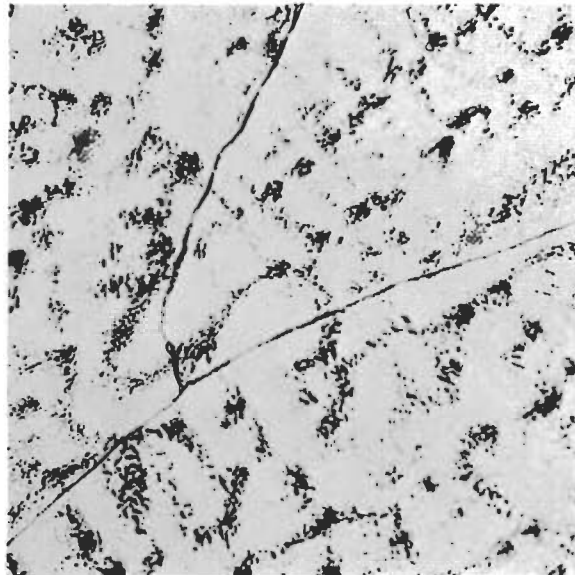
15 ipm Helium - Cb Filler Wire



Fusion Zone

FS80 Filler Wire

4455



Fusion Zone

FS82 Filler Wire

4445

15 ipm Helium

Figure 43 Microstructure of D31 Welds

1000X



weld made with the addition of pure columbium does contain a larger amount of the precipitate found in the welds made at 21 ipm without filler wire addition, Figure 41. This is a function of the slower cooling rate of the welds made with filler wire additions.

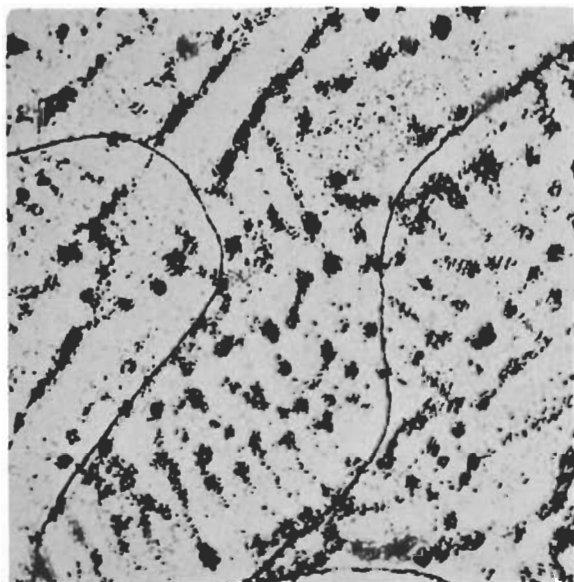
Microstructures of D31 welds at 15 ipm with a 500°F preheat are shown in Figure 44. The effect of preheat and the expected slower cooling rate has produced a structure with a greater amount of coring in the fusion zone and the appearance of a network phase in the heat-affected zone. The electron micrographs, when compared with the structure of a similar weld made with no preheat show a greater amount of an acicular precipitate both in the fusion and heat affected zones. This would be expected as a normal consequence of the slower cooling rates involved.

A series of fusion welds were made outside the vacuum purge atmosphere chamber on the D31 alloy. These were made on a cold fixture and also on a fixture preheated to 300° and 450°F. In all cases the bend angle for these welds was zero from room temperature to 800°F. Only those welds which were comparable in color to welds made in the chamber were used for testing with the exception of welds made with a preheat of 450°F. It was found that preheating to this temperature caused copper pickup from the clamping jaws on the surface of the alloy in the heat affected zone. It was noticed that whenever this alloy was welded with helium as the shielding gas, a heavy black smut was formed, covering the weld and heat affected zone. It is hypothesized that this smut consists of titanium vaporized by the arc and condensed on the surface of the sheet. This is quite common in titanium base alloy welds.

Room and elevated temperature tensile properties for D31 are furnished in Table V. Although the room temperature results indicate that the ultimate strength of this alloy is high as compared to FS82 the elevated temperature tensile strength is relatively low. The two specimens tested without the aluminum coating show a noticeable increase in strength probably caused by oxygen diffusion and hardening. All specimens fractured in parent metal with the exception of the two uncoated ones which fractured in the weld.

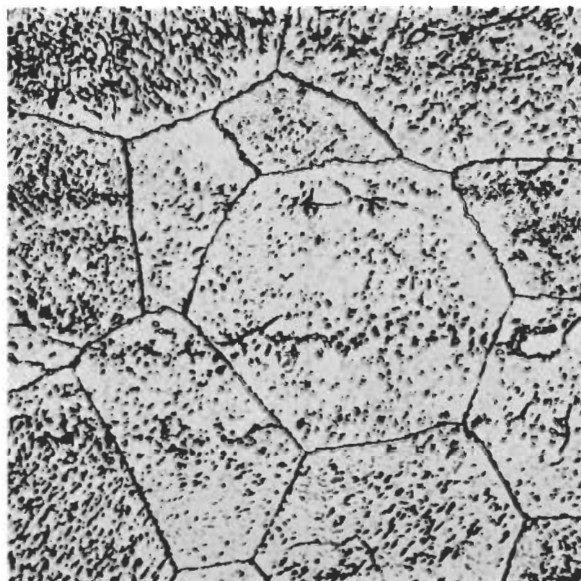
Hardness surveys across the weld in D31 are presented in Figures 45 and 46. After heat treatment the hardnesses of base metal, heat affected zones and fusion zones have leveled off to a value of approximately 235 DPH compared to a hardness of around 280 DPH in the fusion zone as welded. The hardnesses of non-chamber welds and those made in purposely contaminated atmospheres show an increase in hardness in the fusion zone and heat affected zone above 300 DPH.

The bend ductility curves for welds in D31 made in an atmosphere purposely contaminated with controlled amounts of air are illustrated in Figure 47. Although the curves follow the same general shape as those of welds made in uncontaminated atmosphere it is found that full 90° bend ductility is not reached and the maximum bend angle obtained is approximately 40 degrees at 600°F compared to 90 degrees for welds made in an ideal atmosphere.



Fusion Zone

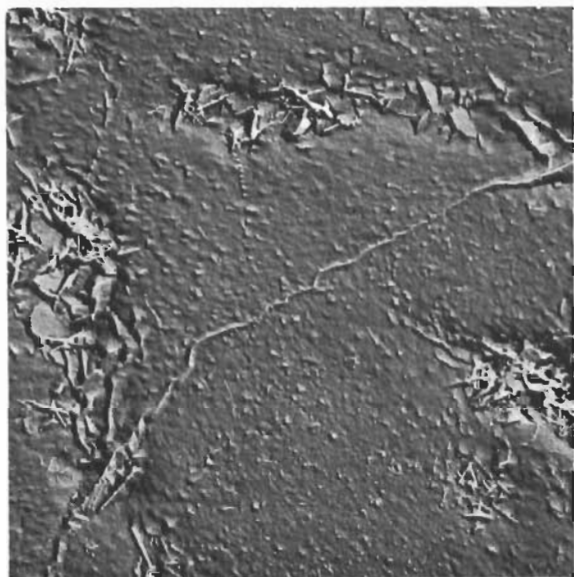
4459



Heat Affected Zone

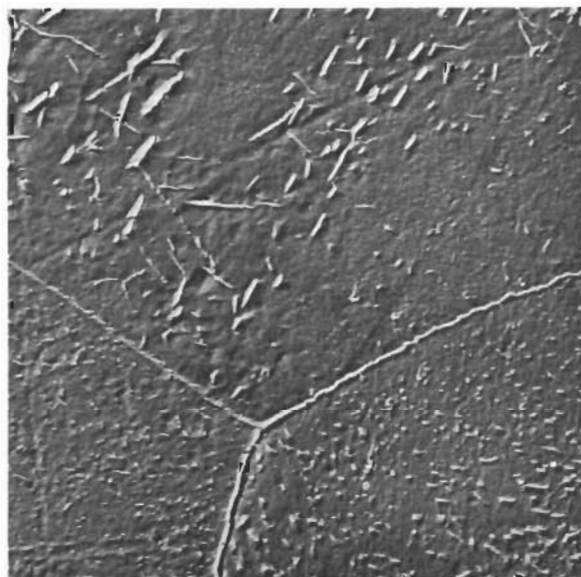
4460

1000X



Fusion Zone

0798



Heat Affected Zone

0795

6000X

Figure 44 Microstructure of D31 Weld Made at 15 ipm in Helium with 500°F Preheat



TABLE V

ROOM AND ELEVATED TEMPERATURE  
TENSILE PROPERTIES FOR D31

	<u>Specimen</u>	<u>Type</u>	<u>Test Temperature</u>	<u>Ultimate Strength</u>	<u>0.2% Offset Yield Strength</u>	<u>% Elong.</u>	<u>% Reduction Of Area</u>
**	CCPM 2-1	PM	RT	100,800	92,300	23.2	39.7
**	CCPM 2-2	PM	RT	99,900	92,100	25.1	42.1
**	CCPM 2-3	PM	RT	101,000	93,100	21.2	41.9
**	CCPM 2-4	PM	RT	99,900	92,300	23.7	48.3
	CEPM 2-1	PM	RT	105,200	100,900	20.9	62.7
*	CEPM 2-3	PM	RT	111,600	103,200	16.8	31.6
	CR 17-1	Weld	RT	112,100	-	14.0	-
	CR 17-2	Weld	RT	113,100	-	8.0	-
	CC 15-1	Weld	RT	121,100	-	-	-
	CC 15-2	Weld	RT	110,400	-	11.0	-
	CA 17-3	Weld	2200°F	19,300	-	-	-
	CC 15-3	Weld	2200°F	23,900	-	-	-
	CC 15-4	Weld	2200°F	18,400	-	-	-
	CC 15-5	Weld	2200°F	21,800	-	-	-
	CC 15-6	Weld	2200°F	19,000	-	-	-
**	CD	PM	2200°F	18,800	-	-	-
**	CC	PM	2200°F	19,400	-	-	-

- \* Direction of loading transverse to direction of rolling.  
 \*\* Sheet material was cross rolled. All elevated temperature specimens except CC 15-3 and CC 15-5 were aluminum coated before testing.

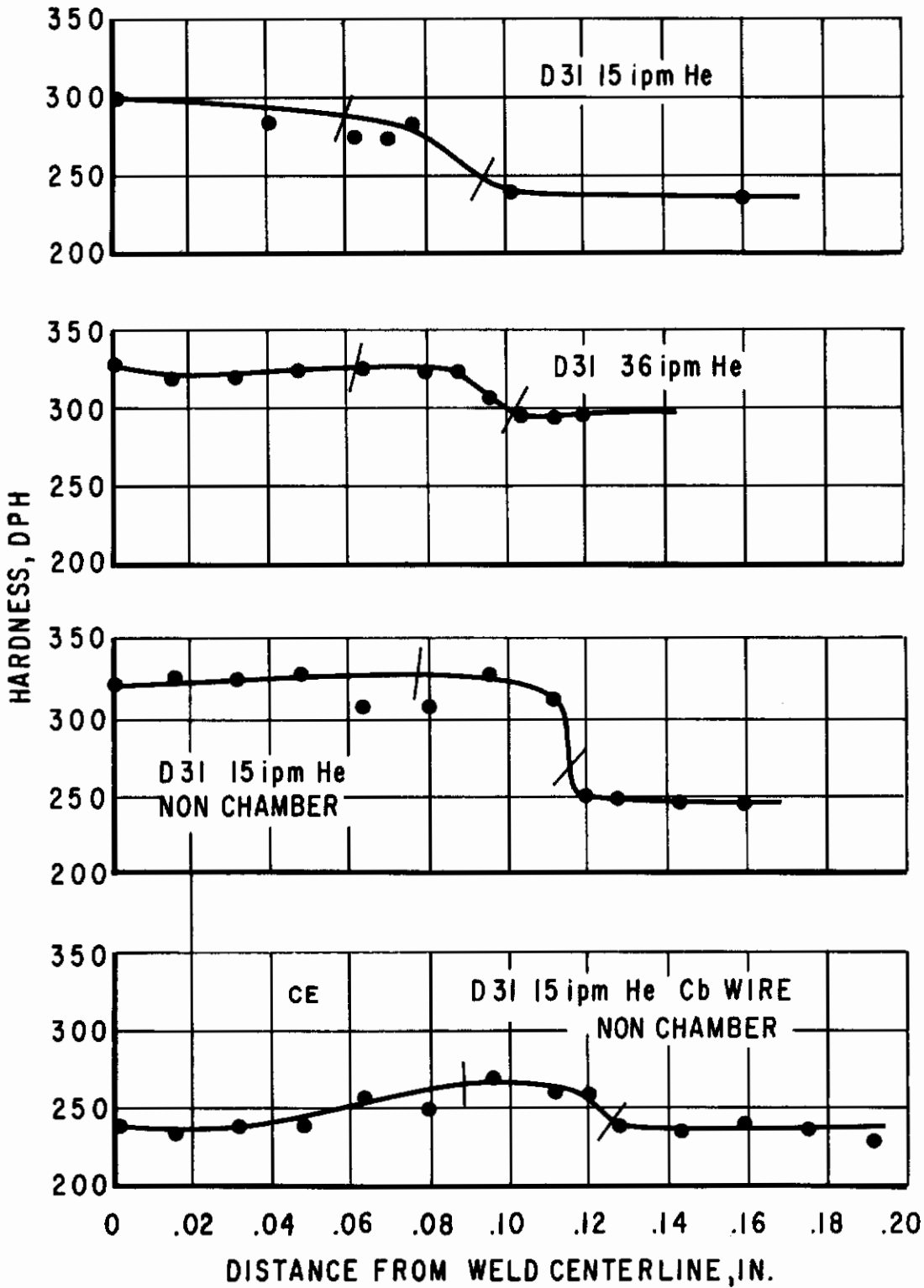


Figure 45. Hardness Surveys of D31 Welds.

# Contrails

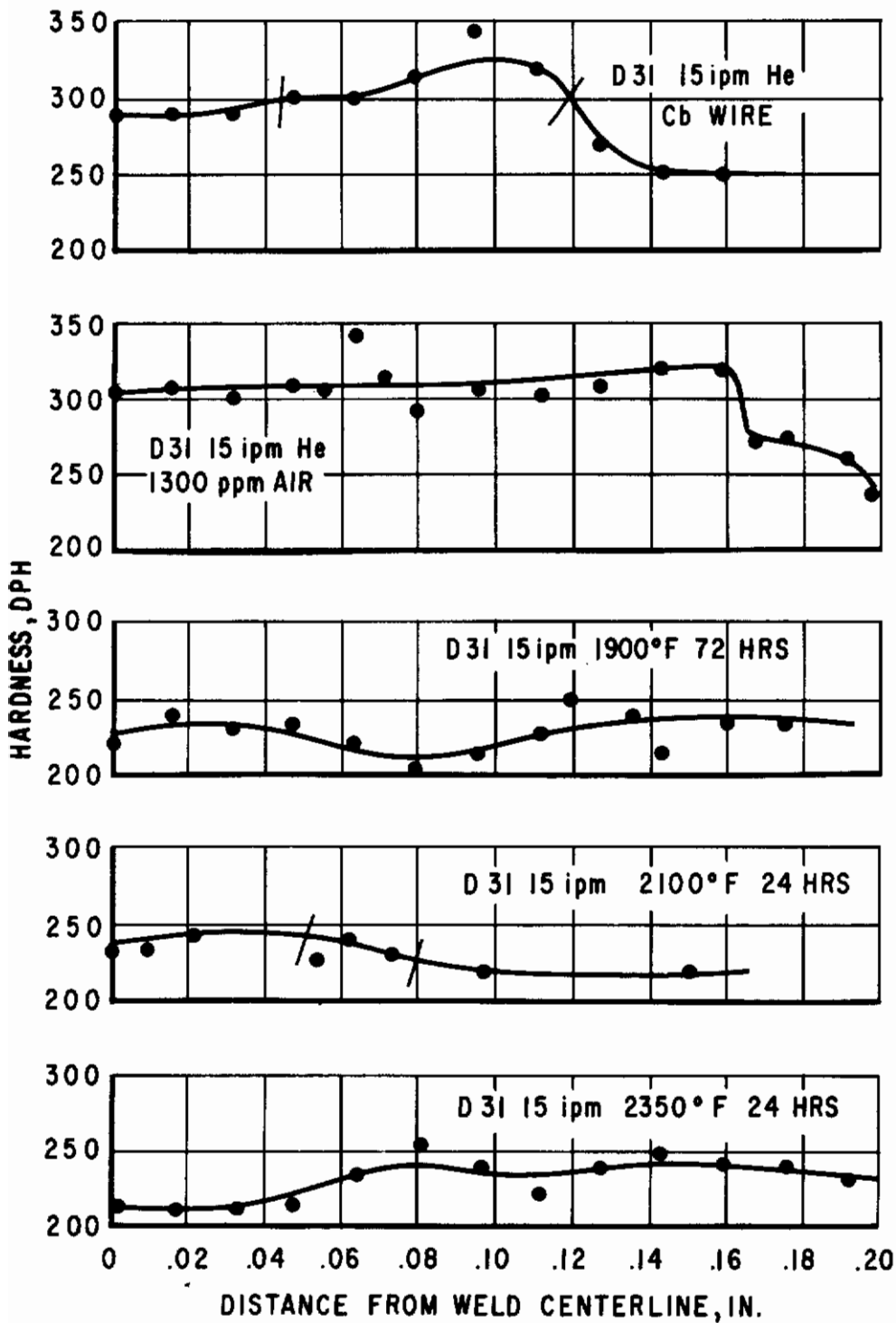


Figure 46. Hardness Surveys of D31 Welds.

# Contrails

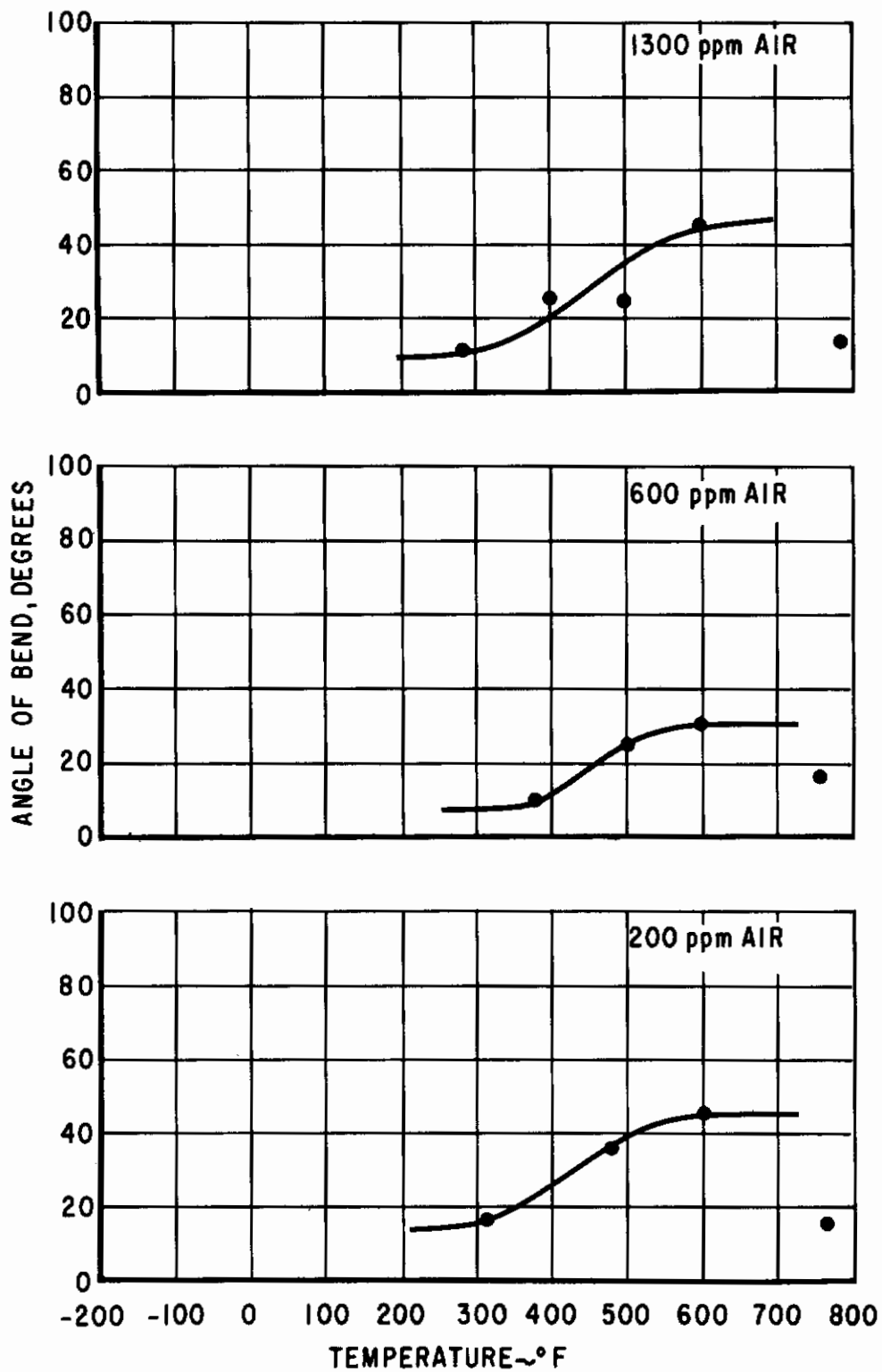


Figure 47. Bend Ductility of D31 Welded in Helium with Air at 15 ipm.



# Contrails

Welds made at 15 ipm in D31 were post heat treated at 2100°F for 24 and 72 hours. The bend ductility curves for these welds are shown in Figure 48. For each treatment the transition temperature was lowered significantly by heat treatment and some ductility was obtained at room temperature. After both 2100°F heat treatments the welds have full ductility down to 150° to 200°F.

Figure 49 demonstrates the affect on bend ductility for D31 alloy welds heat treated at 2100°F 4-hours, 2550°F 4-hours, and 1900 °F 24 and 72 hours. The transition temperature has been lowered some 200°F by post heat treatments of 2100°F 4-hours and 1900°F 72-hours. Very little improvement was observed as a result of the 2550°F 4-hour post heat treatment. The 2100°F 24-hour treatment lowers the transition temperature approximately 450°F for welds in this alloy. Above 24 hours at 2100°F no further gain in ductility was obtained. While 4 hours did not improve ductility as much as 24 hours, it is possible that an intermediate time such as 8 or 12 hours would be adequate.

Photomicrographs of the fusion zones and heat affected zones for the 2100°F 24-hour heat treatment appear in Figure 50. Structures of the 2100°F 72-hour treatment are shown in the lower part of Figure 51. After both times the fusion zone segregated phase has become more distinct than in the welded condition indicating that some additional precipitation has occurred here. Also the carbide particles which apparently had been dissolved in the heat affected zone have reprecipitated as fine platelets, and a grain boundary phase has appeared, possibly a carbide.

These microstructural changes and the improvement in ductility suggest that D31 welds become embrittled by a solution of a phase, probably carbides, and subsequent early-state coherency precipitation. A high temperature over-aging treatment can cause agglomeration of the original precipitate and increased ductility.

Photomicrographs of the heat affected zone and the fusion zone for D31 welded at 15 ipm then heat treated at 1900°F 72-hours are shown in the top of Figure 51. These structures are almost identical to structures resulting from the 2100°F 24 and 72 hour heat treatments. Carbide particles which apparently had been dissolved in the heat affected zone of the as-welded material have reprecipitated as fine platelets and a grain boundary phase appears. The fusion zone segregated phase has become more pronounced.

The effect of the 2100°F 24-hour heat treatment is illustrated by electron micrographs in Figure 50. A comparison with corresponding zones in Figure 41 shows that this heat treatment has caused the formation of additional acicular precipitate and a discontinuous grain boundary phase. The unaffected parent metal which received this heat treatment differs from the as-received metal structure, Figure 52, in that a very fine precipitate has formed in the heat treated material. This fine precipitate is present in the weld structures in Figure 50.

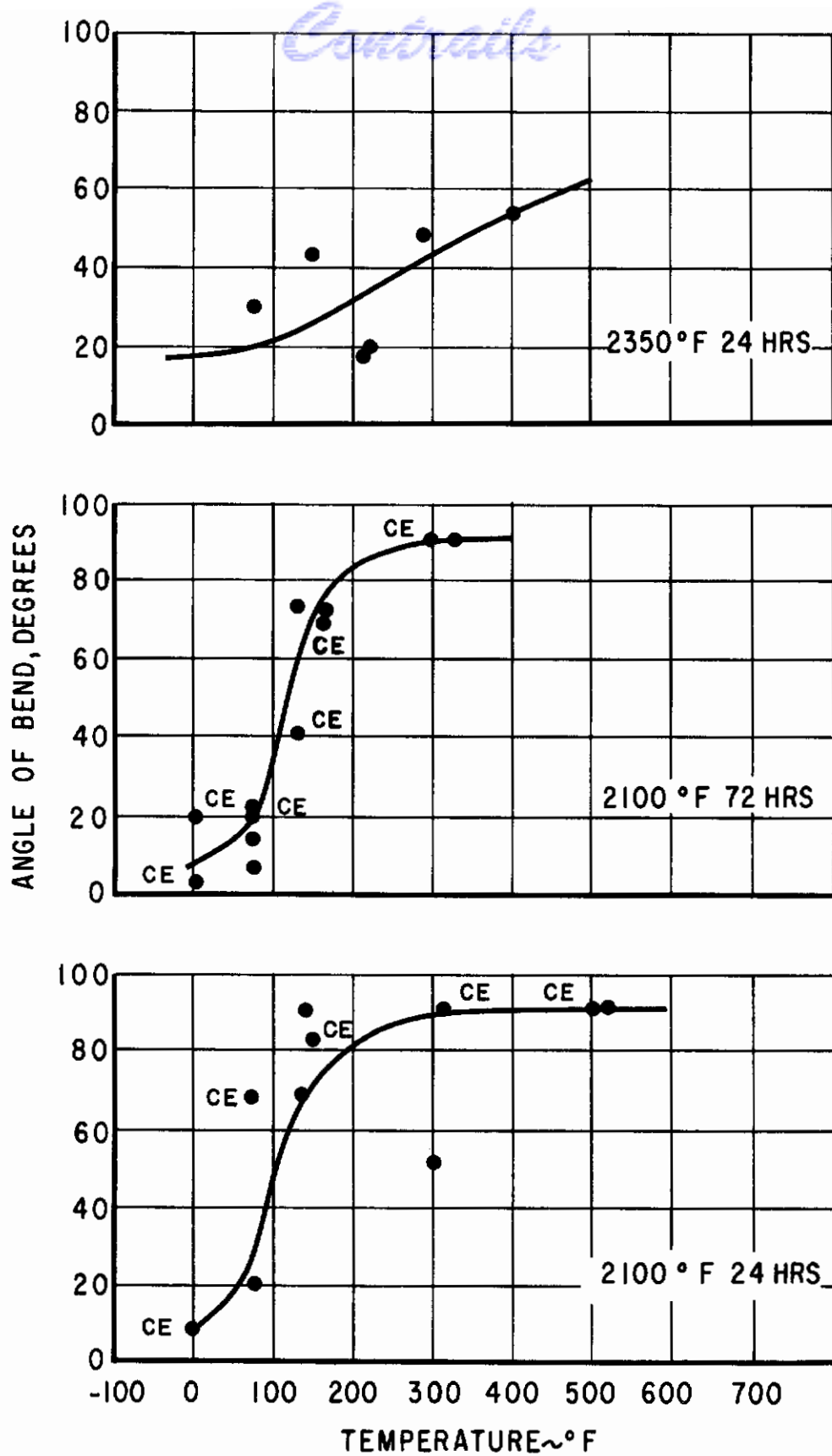


Figure 48. Bend Ductility of D31 Welded in Helium at 15 ipm Then Heat Treated at 2100 or 2350°F.

# Contrails

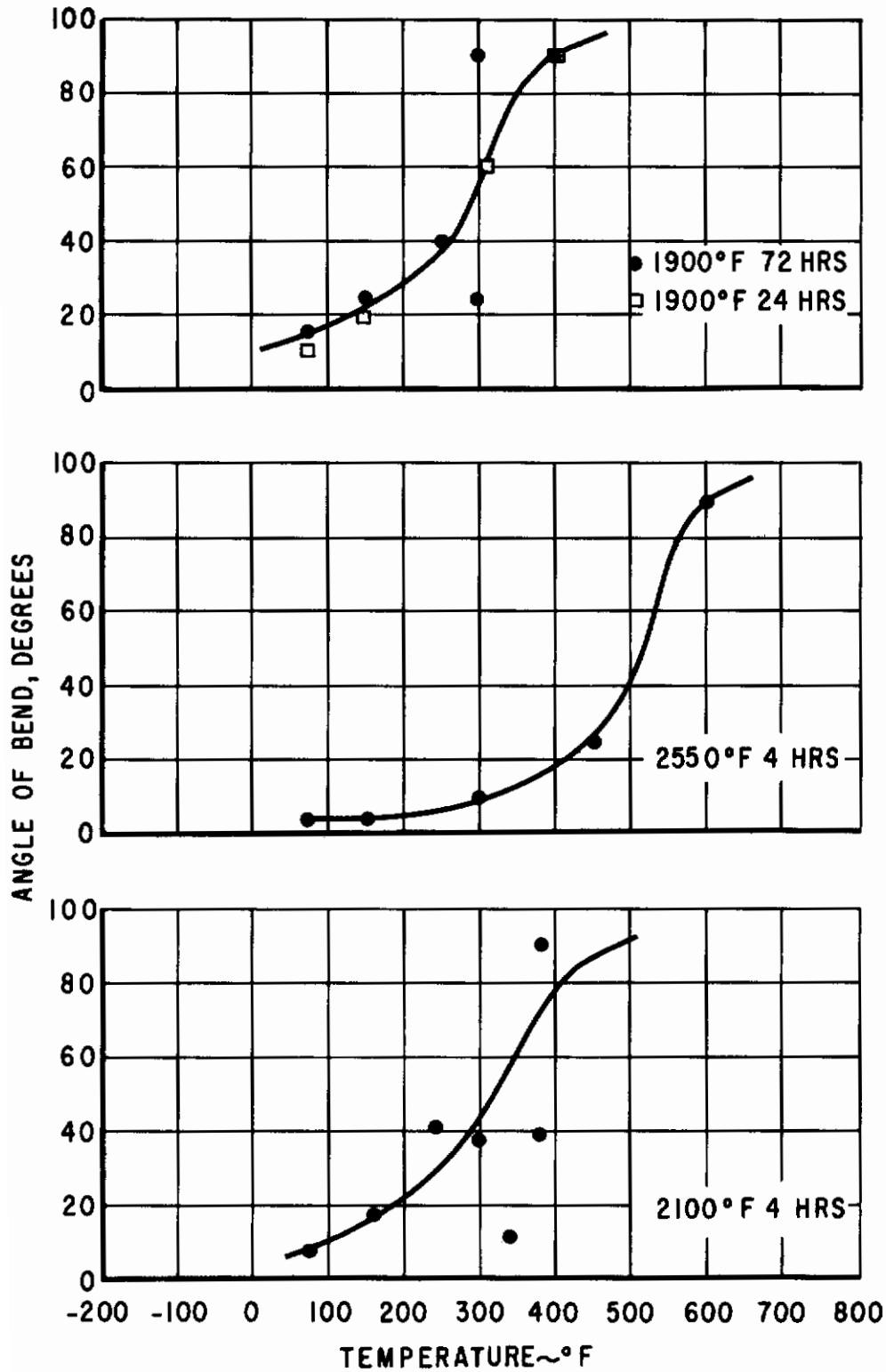
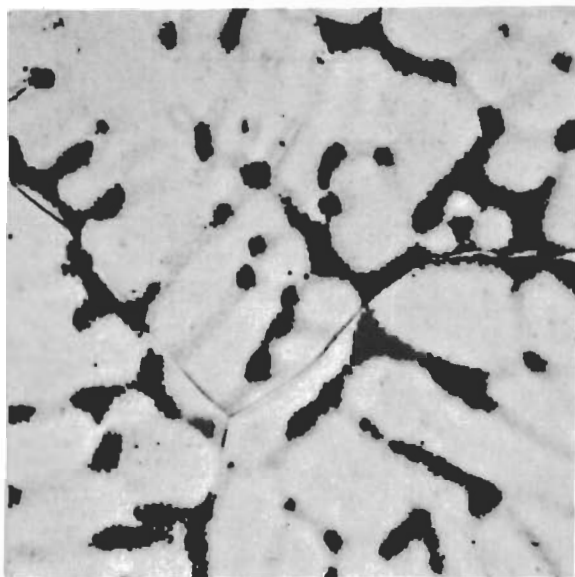
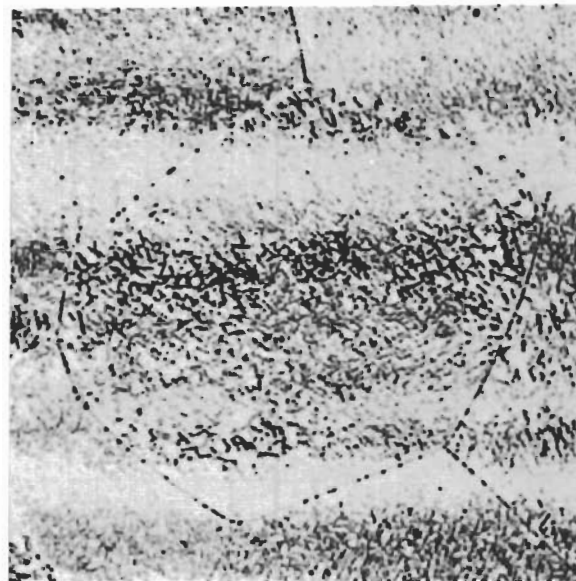


Figure 49. Bend Ductility of D31 Welded in Helium at 15 ipm Then Heat Treated at 1900, 2100, or 2550°F.



Fusion Zone

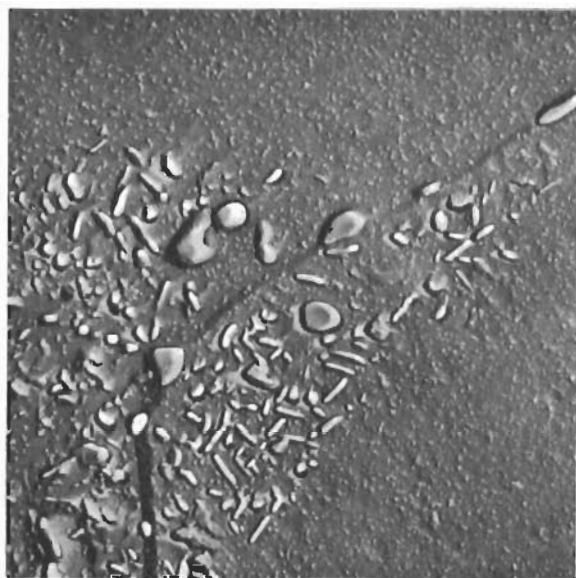
3242



Heat Affected Zone

3244

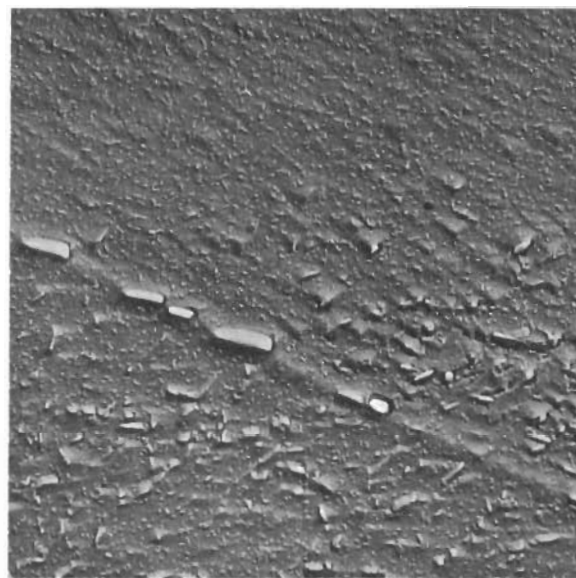
1000X



Fusion Zone

0587

10,000X

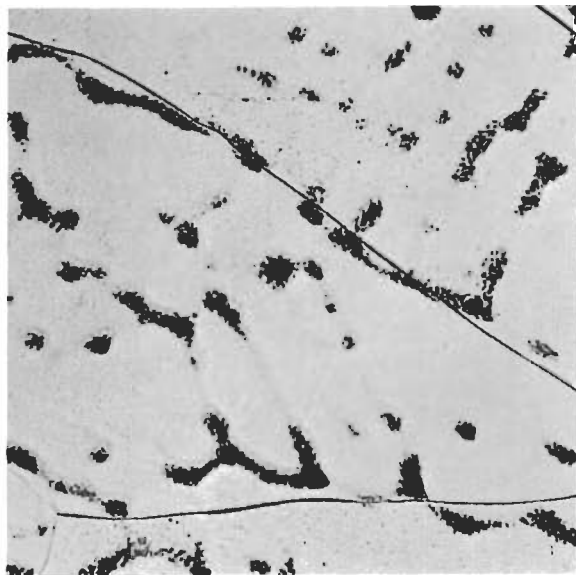


Heat Affected Zone

0590

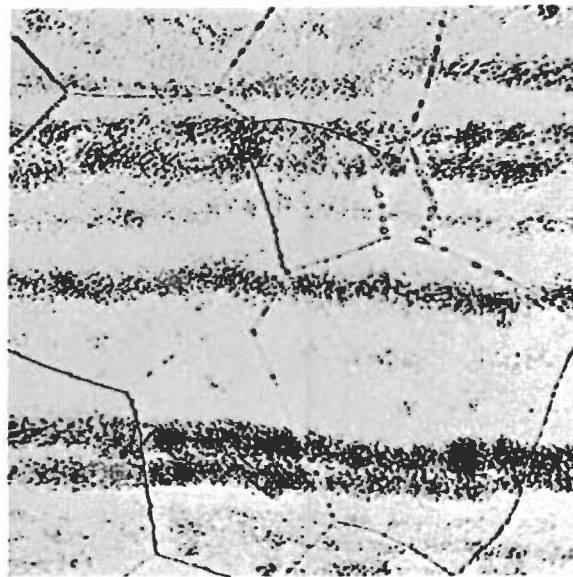
Figure 50 Microstructures of Weld in D31 at 15 ipm in Helium  
Heat Treated at 2100°F for 24 Hours





Fusion Zone

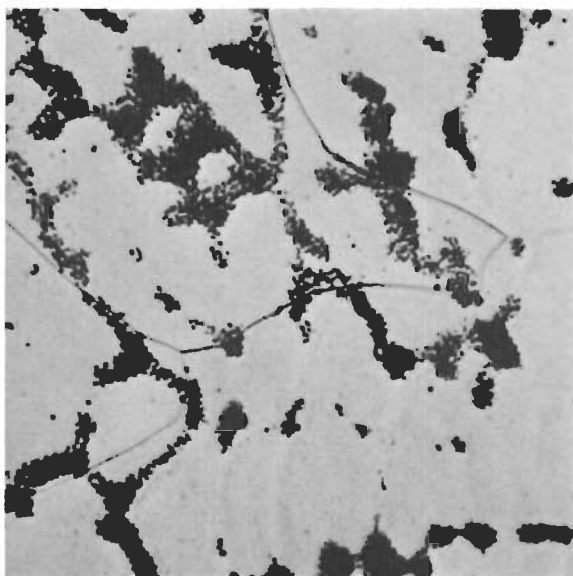
3827



Heat Affected Zone

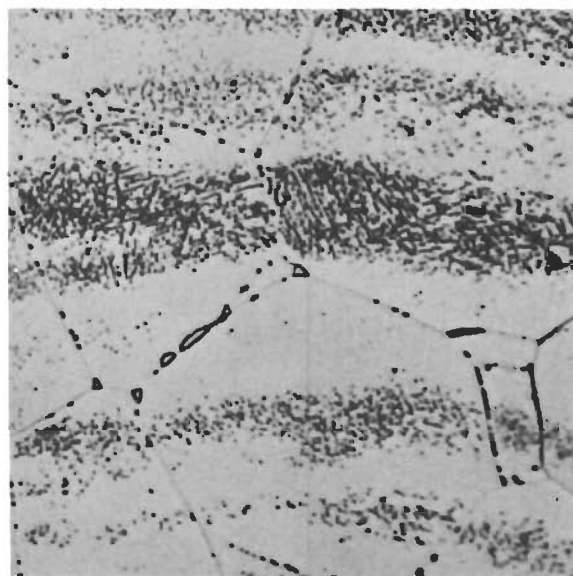
3828

Heat Treated 1900°F 72 Hours



Fusion Zone

3242

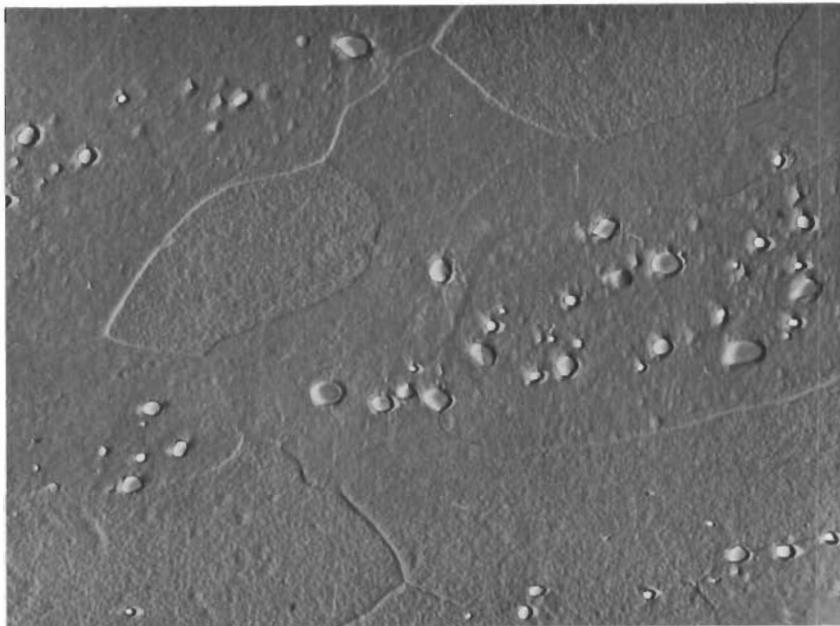


Heat Affected Zone

3241

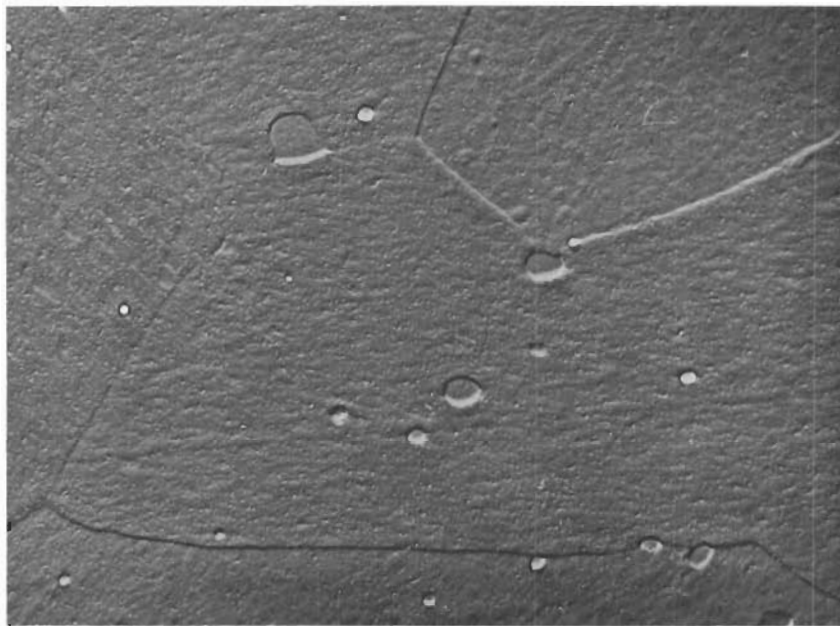
Heat Treated 2100°F 72 Hours

Figure 51 Microstructures of Welds in D31 at 15 ipm in Helium 1000X



As Received

0597



Heat Treated 2100°F 24 Hours

0593

Figure 52 Electron Micrographs of D31 Sheet 6000X

Photomicrographs of the 2350°F 24-hour heat treatment are presented in Figure 53. The banded precipitate in the heat affected zone contains larger particles than the 1900° and 2100°F heat treatment structures and the grain boundary phase is more distinct and continuous. A smaller amount of the cored precipitate in the fusion zone is apparent. The microstructure resulting from this heat treatment gives evidence that the fine carbide platelets are being taken into solution and are being reprecipitated as larger particles at this temperature. The electron micrographs do not show evidence of the very fine evenly distributed precipitate which is present in the 1900° and 2100°F microstructures.

Fusion welds made in the vacuum purge atmosphere chamber and coated with the Cr-Ti-Si coating had a transition temperature above 800°F. It was expected that the coating treatment which involved exposure at 2050° and 2150°F would improve weld ductility. The reason for this behavior probably stems from a thin brittle diffusion layer which can cause cracks to initiate into a notch sensitive material.

The extreme brittleness resulting from TIG welding D31 alloy in open-air necessitates the use of an atmosphere welding chamber. Furthermore, the high transition temperature (550°F) resulting from TIG welding under ideal conditions in a chamber makes post heat treatment desirable. The most satisfactory chamber welds in this alloy were produced in a helium atmosphere at a welding speed of 15 ipm 150 - 160 amperes and 14 - 15 volts followed by a post heat treatment of 2100°F for 24 hours. This procedure has resulted in weld transition temperatures of 100°F.

### C. F48 Alloy

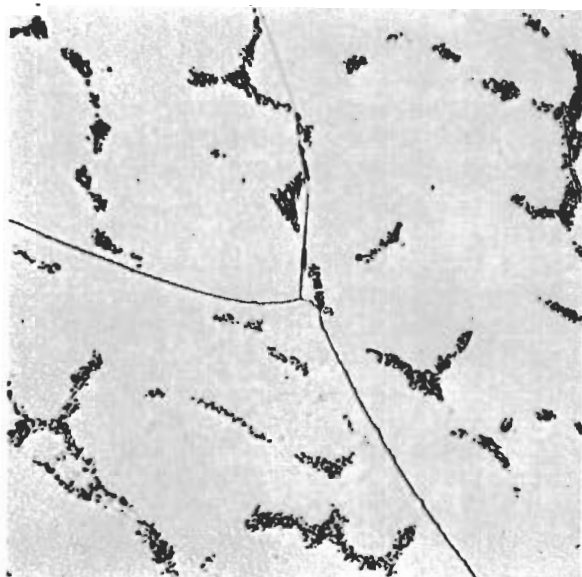
A smaller amount of welding was performed on the F48 alloy than on the other alloys because the material available was limited in quantity. Fusion welds were made at 5 ipm in helium and argon, at 28 ipm in argon and at 15 ipm in helium. It was found that welds in the as-welded condition were quite brittle having maximum bend angles of 26° at 610°F for welds made at 5 ipm, 33° at 585°F for welds made at 15 ipm, and 5° at 400°F for welds made at 28 ipm.

This work showed that preheating was necessary to preclude weld and parent metal cracking when welding F48 sheet. The bend ductility data for F48 welds, preheated to 500°F on material previously vacuum annealed at 2450°F for 1 hour, is presented in Figure 54. These welds have a 45° bend transition temperature of approximately 350°F achieving full ductility at 500°F.

The bend ductility curves for chamber welds made with the addition of pure columbium and FS82 filler wire to the weld puddle are included in Figure 55. Contrary to results obtained outside the chamber, welds made with FS80 filler wire appear to be more ductile than welds made with pure columbium as the filler metal.

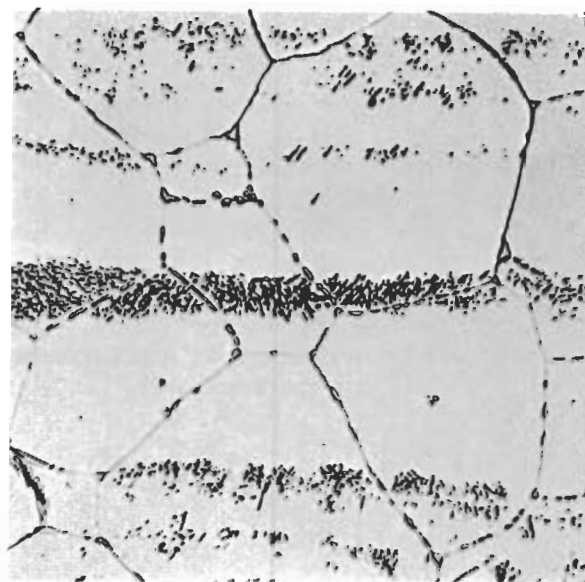


# Contrails



Fusion Zone

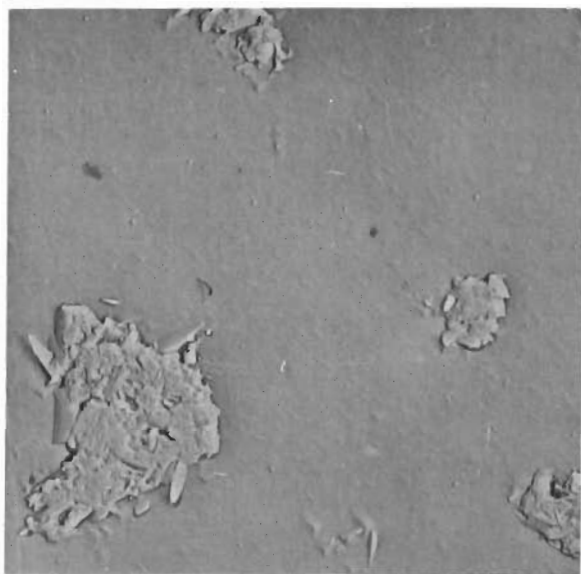
3821



Heat Affected Zone

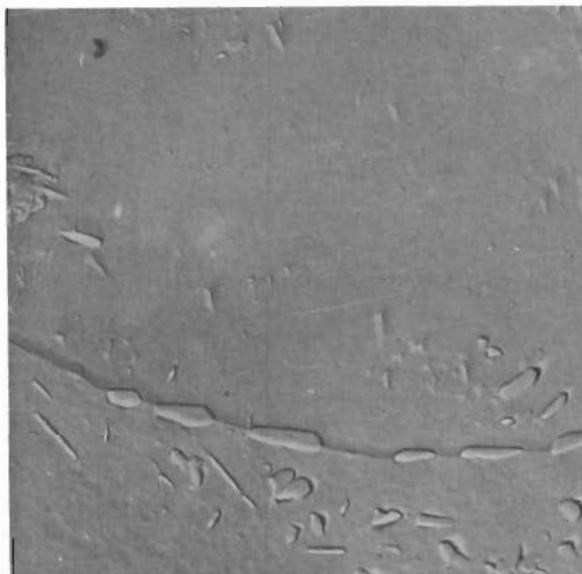
3822

1000X



Fusion Zone

0598



Heat Affected Zone

0599

6000X

Figure 53 Microstructure of Weld in D31 at 15 ipm in Helium  
Heat Treated at 2350°F for 24 Hours



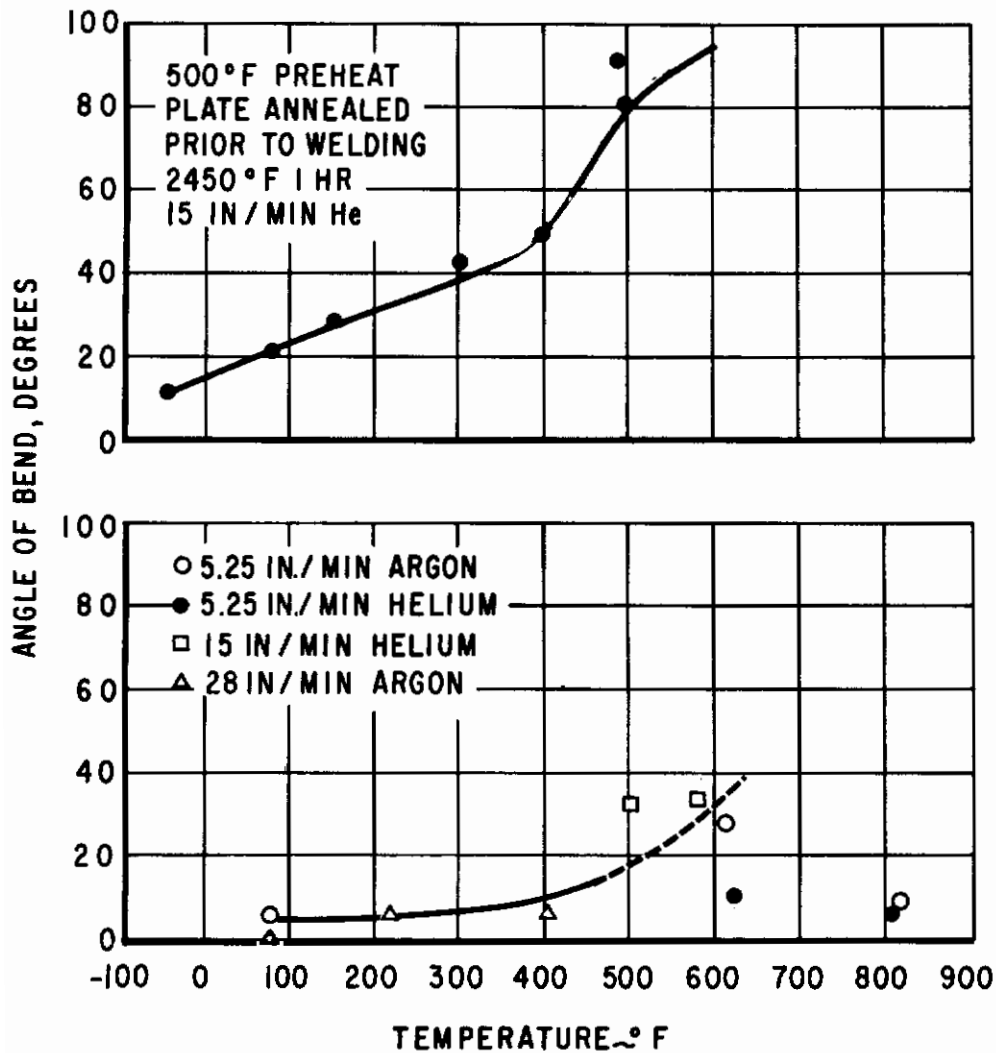


Figure 54. Bend Ductility of F48 Welded with a 500°F Preheat and Without Preheat.

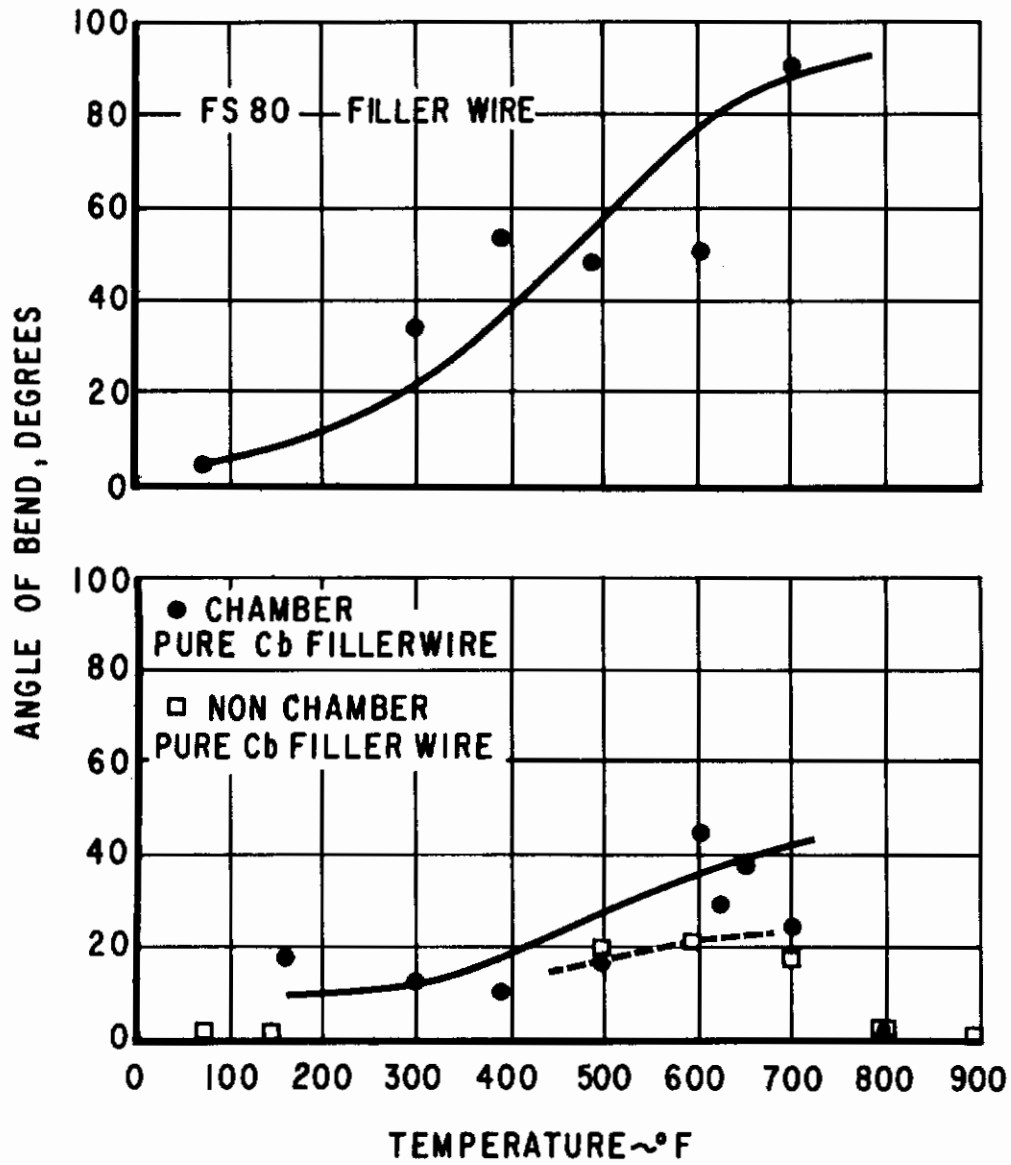


Figure 55. Bend Ductility of F48 Welded in Helium at 15 ipm with Pure Cb or FS80 Filler Wire.

# Contrails

A series of fusion welds were made outside the vacuum purge atmosphere chamber on the F48 alloy. These were made on a cold fixture and on a fixture preheated to 300° and 450°F. The bend ductility for these welds was essentially zero up to 800°F. A maximum bend angle of approximately 8° was obtained in the test temperature range of 600 - 700°F.

Photomicrographs and electron micrographs of an F48 weld made at 15 ipm are presented in Figure 56. The microstructure of the heat affected zone has distinct grain boundaries with little sign of a grain boundary precipitate. The grains contain a fine barely resolved precipitate at 1000X but no indication of fine banding. The fusion zone has sharp grain boundaries and a faint sign of coring. At 6000X, a fine, well defined precipitate is shown in the heat affected zone with some indication of a banded distribution. The fusion zone at 6000X contains a finer more evenly distributed precipitate than the heat affected zone and some semblance of a network phase.

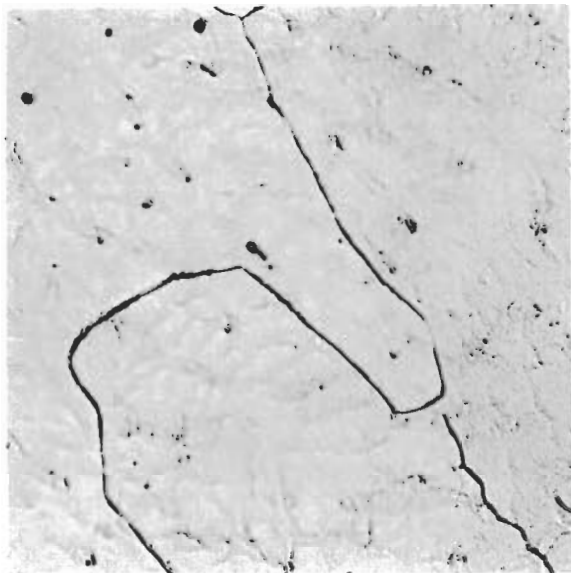
The microstructures of a weld made at 15 ipm with a 500°F preheat in helium are shown in Figure 57. At 1000X the cored structure of the fusion zone has become more distinct and a network phase has appeared in the heat affected zone. At 6000X it can be seen that a larger amount of the second phase has developed in the fusion zone when compared to Figure 56. The heat affected zone does not contain the distinct precipitate revealed in the corresponding zone of Figures 56, but a rough surface indicative of a supersaturated condition.

The microstructures of a weld made with pure columbium filler wire and a weld made outside the chamber, both in helium and at 15 ipm, are illustrated in Figure 58. At 1000X there is no significant difference between the structures of Figures 57 and 58 and the 15 ipm structure of Figure 56.

Room and elevated temperature tensile properties of F48 are presented in Table VI. The extreme brittleness of the alloy in the as-welded condition presented many problems in machining specimens that were not cracked, hence hot tensile properties of welds were not determined. This alloy has a much higher strength at room temperature and at 2200°F than either FS82 or D31.

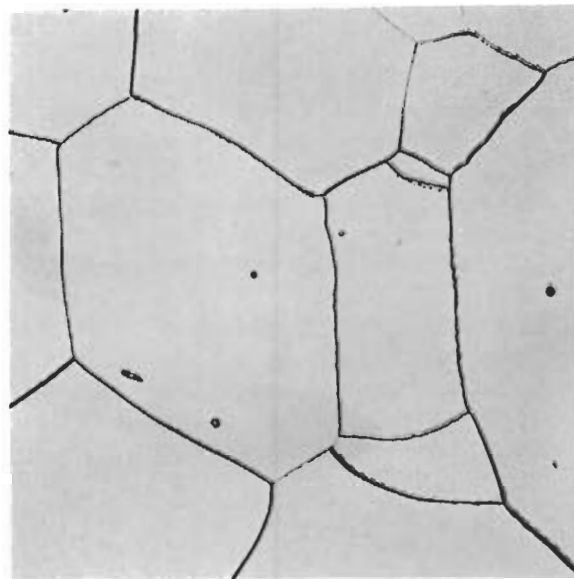
Hardness surveys of welds in F48 as-welded and after heat treatments, are plotted in Figures 59 and 60. Both heat treatments of 2100°F and 2350°F for 24 hours have effected more than 100 DPH reduction in hardness of the fusion and heat affected zone. Approximately 50 DPH reduction of the parent metal occurred at the same time. The slightly higher fusion zone hardness of the 2100°F treatment corresponds to the lower ductility produced by this heat treatment, Figure 63.

The bend ductility curves for welds in F48 made in an atmosphere purposely contaminated with controlled amounts of air are displayed in Figure 61. It should be noted that the F48 welds made under these conditions exhibit a lower transition temperature than the D31 alloy. Also no explanation can be offered for the greater ductility for the F48 weld made with 600 ppm air contamination.



Fusion Zone

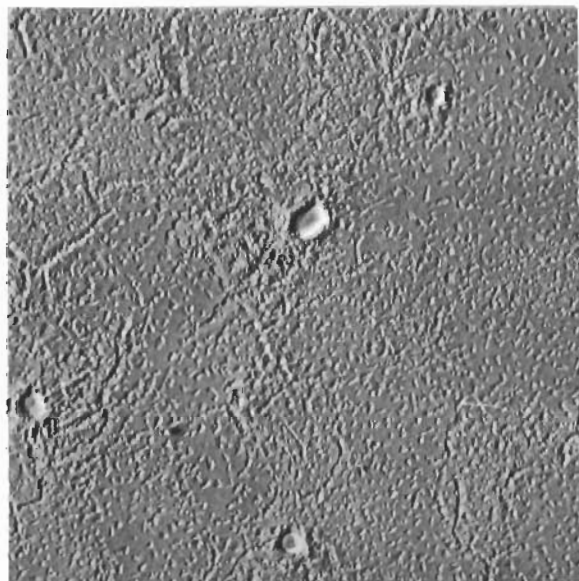
3833



Heat Affected Zone

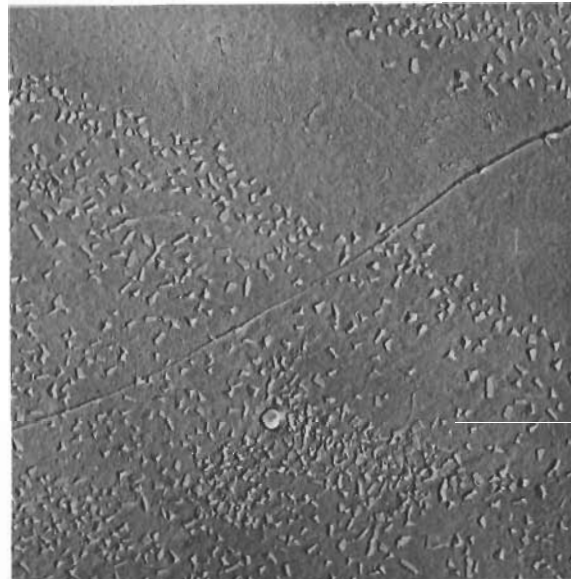
3834

1000X



Fusion Zone

0633



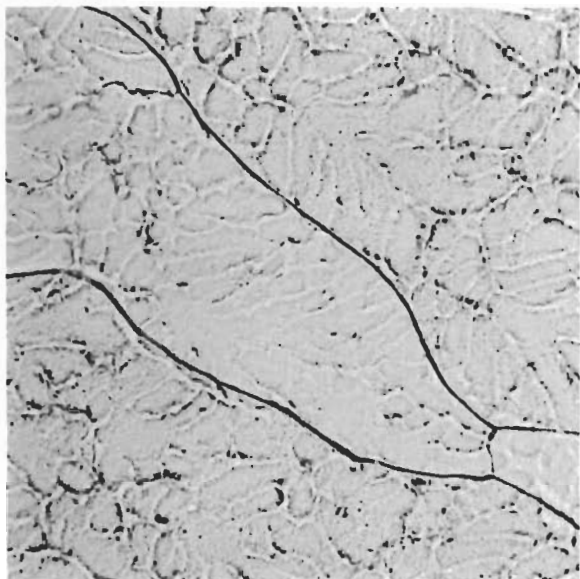
Heat Affected Zone

0631

6000X

Figure 56 Microstructures of Welds in F48 at 15 ipm in Helium





Fusion Zone

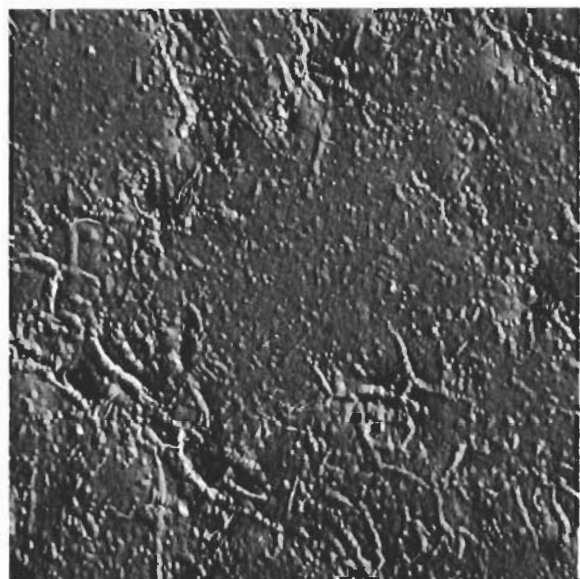
4457



Heat Affected Zone

4458

1000X



Fusion Zone

0790

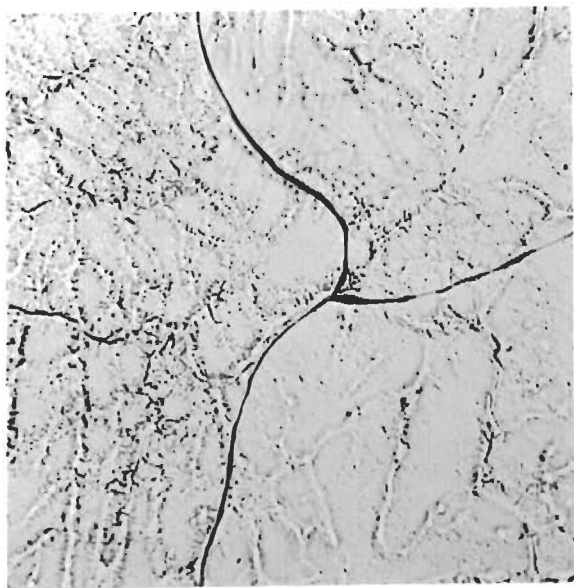


Heat Affected Zone

0792

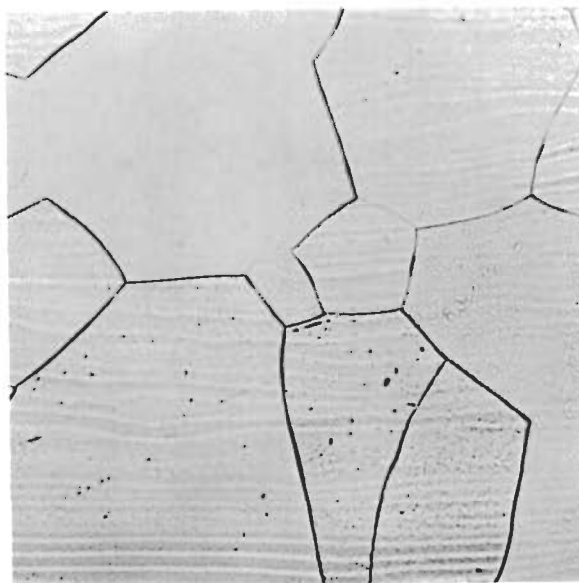
6000X

Figure 57 Microstructures of Welds in F48 at 15 ipm in Helium  
Preheated at 500°F



Fusion Zone

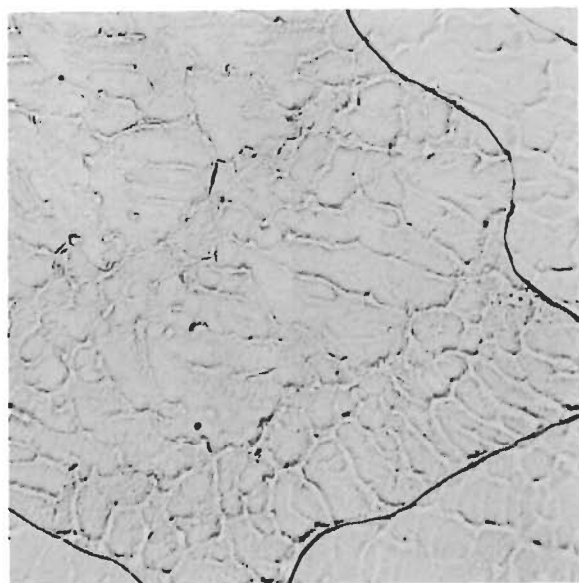
4451



Heat Affected Zone

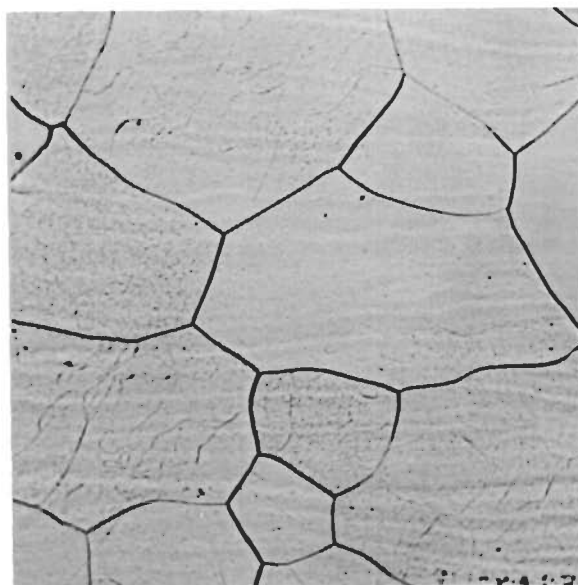
4452

Cb Filler Wire



Fusion Zone

4435



Heat Affected Zone

4436

Non Chamber

Figure 58 Microstructures of Welds in F48 at 15 ipm in Helium 1000X

TABLE VI

ROOM AND ELEVATED TEMPERATURE  
TENSILE PROPERTIES FOR F48 ALLOY

<u>Specimen</u>	<u>Type</u>	<u>Test Temperature</u>	<u>Ultimate Strength</u>	<u>0.2% Offset Yield Strength</u>	<u>% Elong.</u>	<u>% Reduction Of Area</u>
S95APM 1-1	PM	RT	112,400	100,000	10.1	12.4
S95APM 1-2	PM	RT	112,400	98,000	25.0	32.0
DB	PM	RT	121,300	100,700	7.4	10.1
DE9-3	Weld	RT	126,400	-	-	-
DD	PM	2200°F	59,900	-	-	-
F48	PM	2200°F	61,100	-	-	-

All material cross rolled.

All elevated temperature specimens aluminum coated.

# Contrails

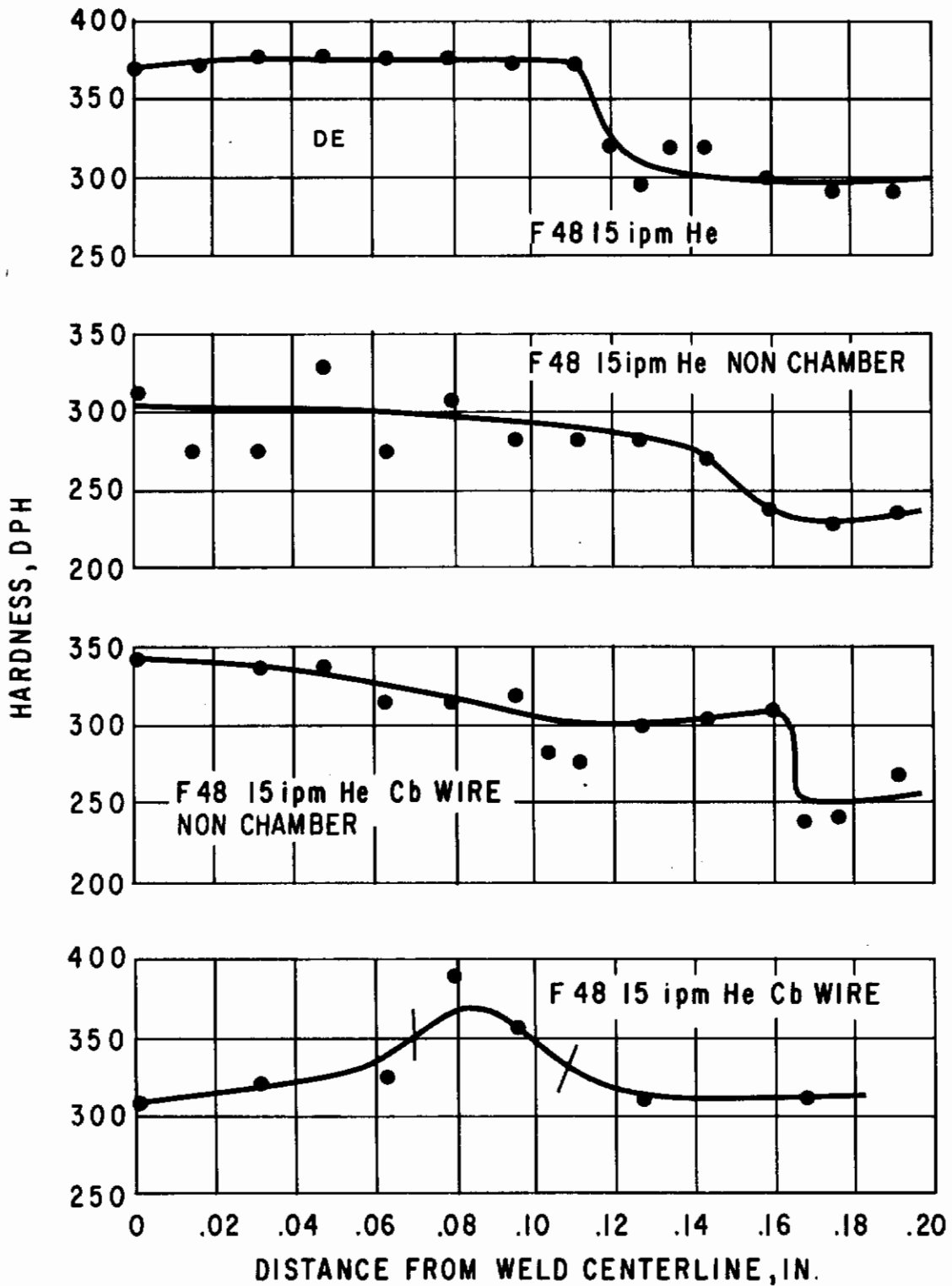


Figure 59. Hardness Surveys of F48 Welds.



# Contrails

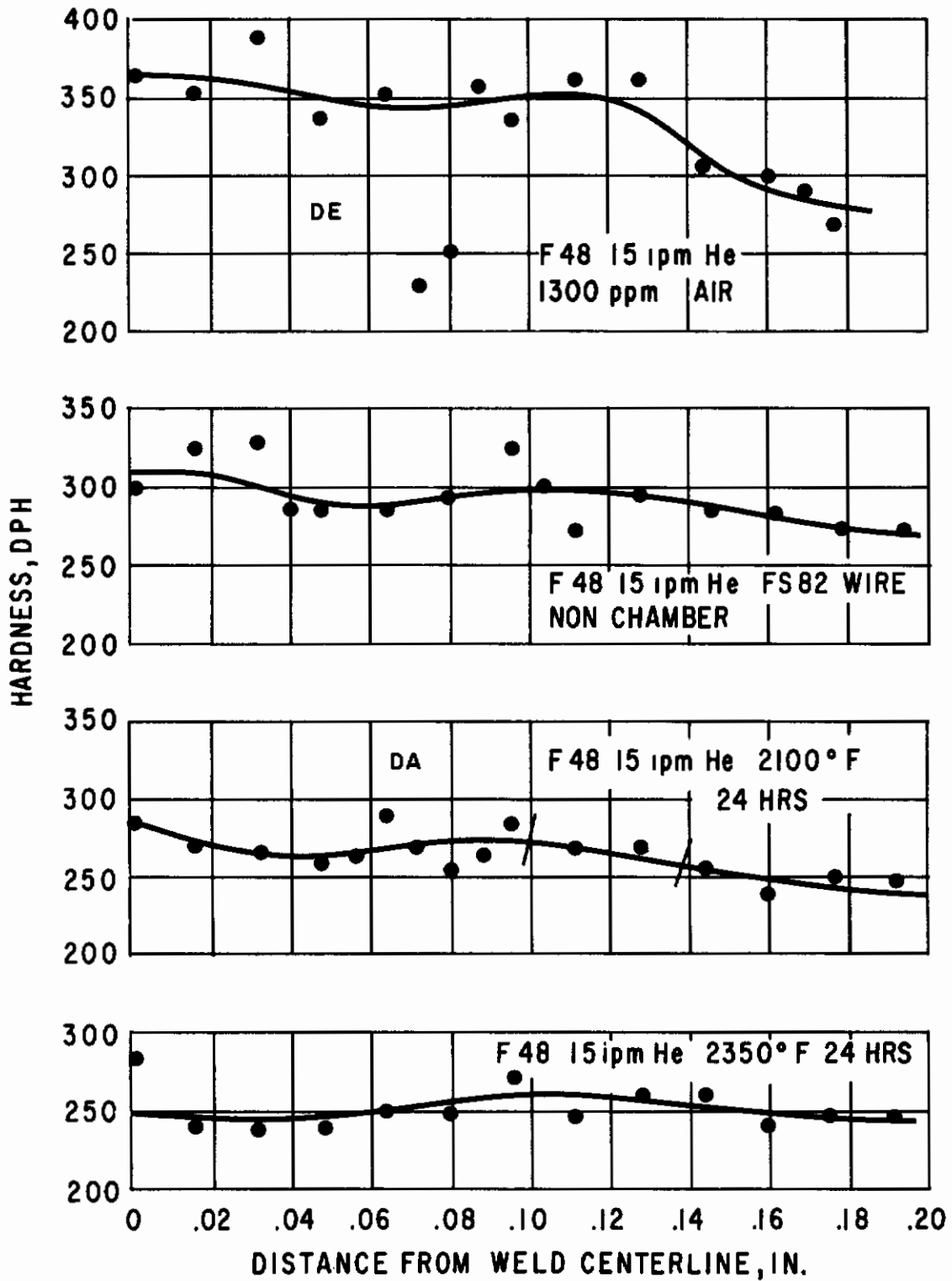


Figure 60. Hardness Surveys of F48 Welds.

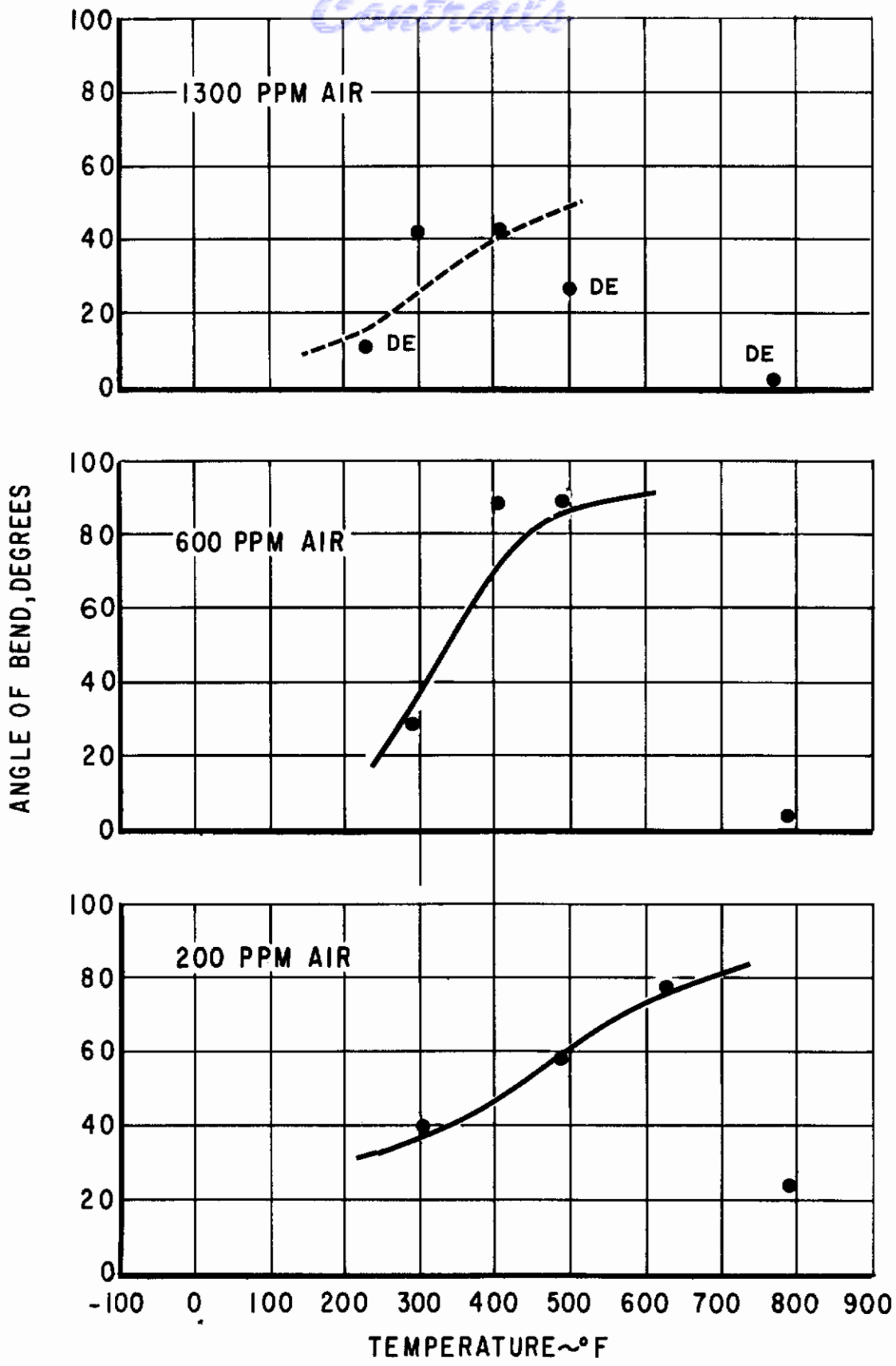


Figure 61. Bend Ductility of F18 Welded in Helium with Air at 15 ipm.

# Contrails

Bend ductility data for F48 alloy heat treated at 2350°F for 4, 24, and 72 hours and 2500°F for 4 hours are illustrated in Figure 62. Post heat treatment in these temperature ranges have effected a significant lowering of the transition temperature to approximately 150° to 200°F.

Figure 63 presents the bend ductility curves for F48 alloy heat treated after welding at 2100°F for 4, 24, and 72 hours. Although the 2100°F heat treatment does lower the transition temperature, it is not as effective as the 2350° or 2500°F heat treatments. Figure 64 depicts the microstructure of the fusion zone and heat affected zone for the 2100°F 72-hours, and 2350°F 72-hours heat treatments. The 2350°F 24-hours microstructures are shown in Figure 65. Referring to the microstructures of these welds, particularly the heat affected zone, it can be noticed that at 2100°F 72-hours a fine banded precipitate is present and a few indications of a grain boundary phase can be seen. In the 2350°F 24-hour treatment, Figure 65, the fine banded precipitate has increased in quantity and a grain boundary phase is present. At 6000X, the fusion zone cored precipitate is more distinct but the banded phase in the heat affected zone is not obvious. Instead, a fine incipient precipitate is found. After 72 hours at 2350°F, the quantity of fine banded precipitate is less than after 24 hours at this temperature. This is probably caused by a variation in the parent material composition. The bend ductility curves corresponding to this heat treatment, Figure 62, suggests that improved ductility stems from an over-aging reaction.

Electron micrographs, Figure 66, of a weld aged at 2100°F for 24 hours show a supersaturated condition and the start of fine precipitation. The structure of the as-received sheet at 6000X is included here for comparison with the weld structures. The start of precipitation after the 2100°F 24-hour age ties in with the moderate improvement in transition temperature to between 400° and 550°F. The 2350°F 72-hour heat treatment lowers the transition temperature to the 200° to 300°F range while the 2350°F 24-hour treatment lowers the transition to between 100° and 200°F. The fusion zones associated with all these conditions are somewhat similar showing signs of a cored precipitate. Fusion welds made in the vacuum purge atmosphere chamber and coated with the Cr-Ti-Si coating exhibited zero bend ductility up to 300°F. Although the coating heat treatment is close in temperature to post heat treatments which improved weld ductility, less ductility was the result. As with D31, the coating produces a brittle diffusion layer which is believed to help initiate cracks in a notch sensitive material.

Maximum as-welded ductility for this alloy can be obtained by welding in an atmosphere chamber with a 500°F preheat, in helium at 15 ipm, a current of 135 amperes and 15 arc volts. These conditions have resulted in a bend transition temperature of approximately 350°F. A transition temperature of approximately 100°F has been obtained in F48 welds which were post heat treated at 2500°F 4-hours.

## D. Electron Beam Welds

Electron beam welds were made on FS82, FS82HS, D31, and F48 columbium alloys to compare the effect of electron beam welding on the transition temperature of these alloys.

*Contrails*

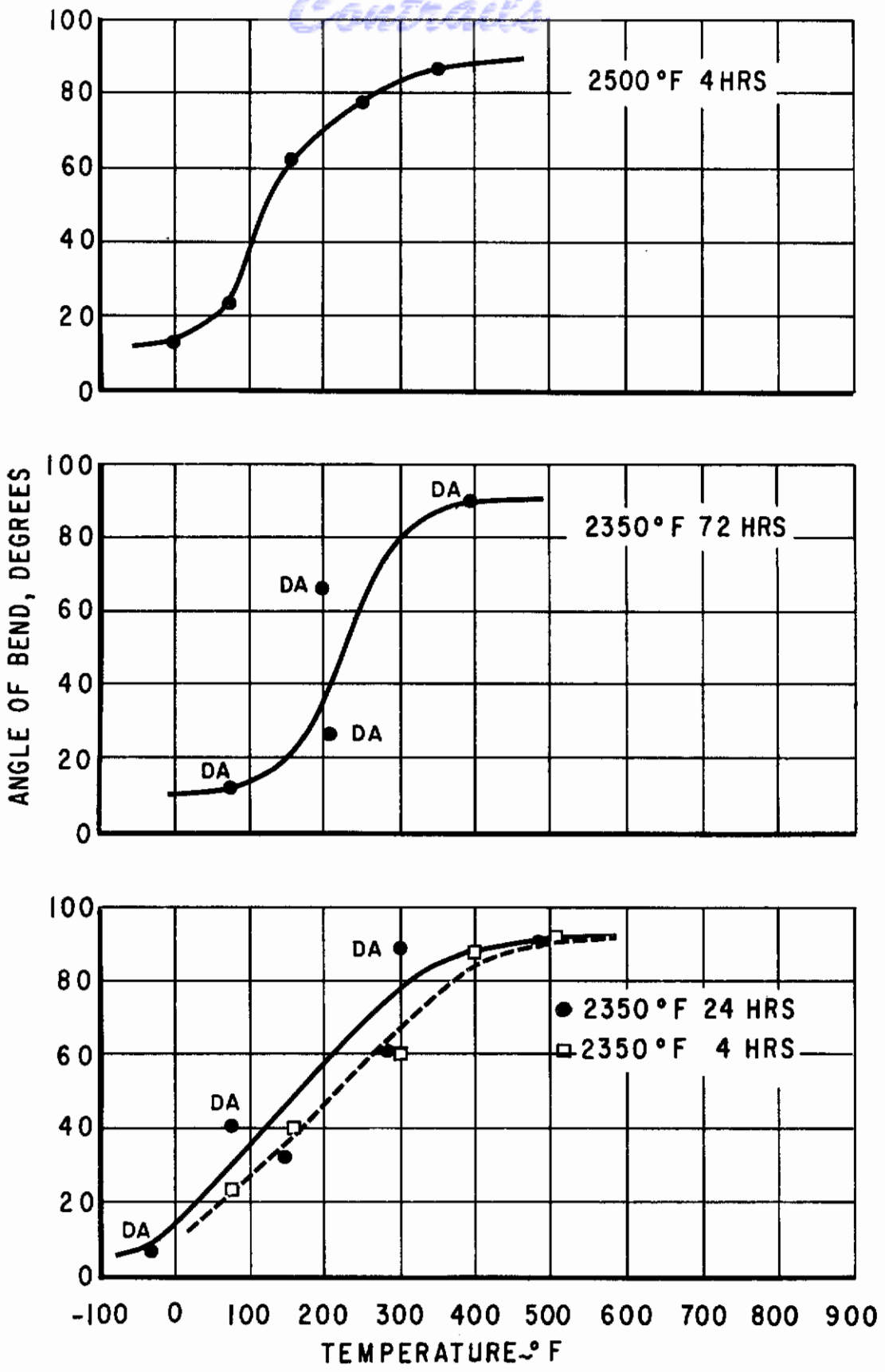


Figure 62. Bend Ductility of F48 Welded in Helium at 15 ipm Then Heat Treated at 2350 or 2500°F.



# Contrails

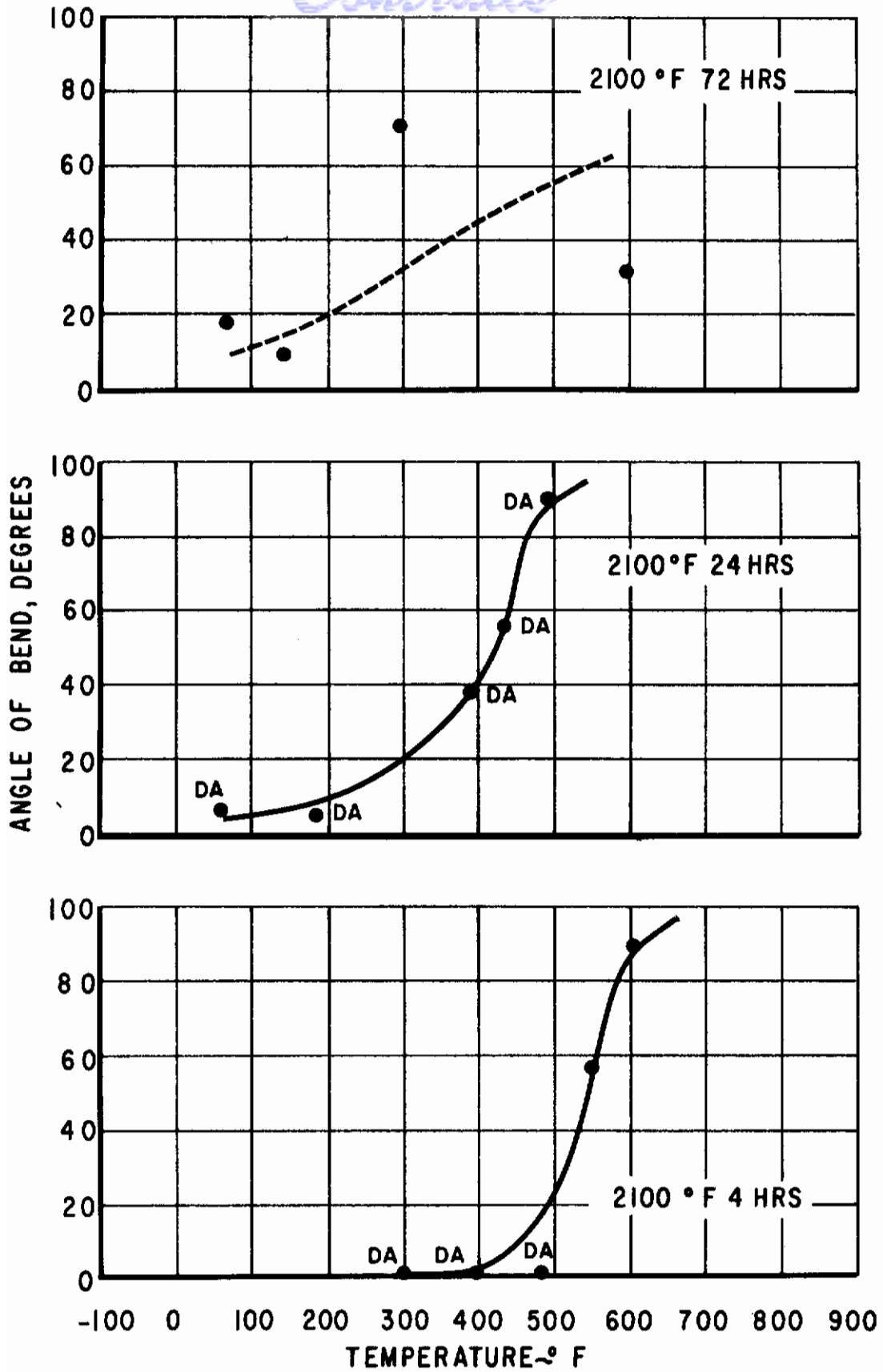
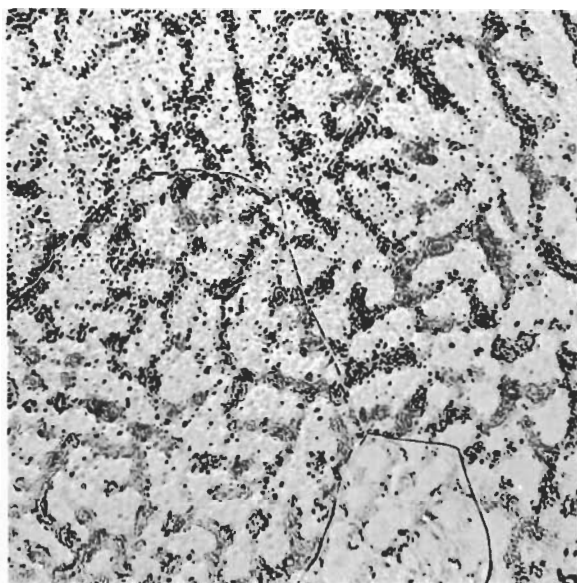


Figure 63. Bend Ductility of F48 Welded in Helium at 15 ipm Then Heat Treated at 2100°F.



Fusion Zone

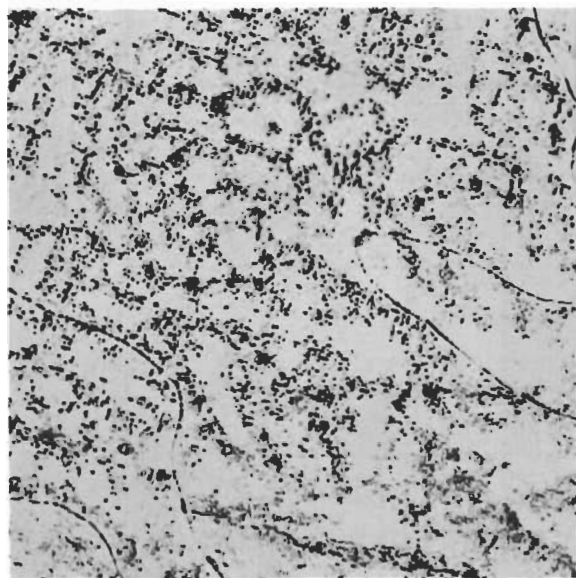
3829



Heat Affected Zone

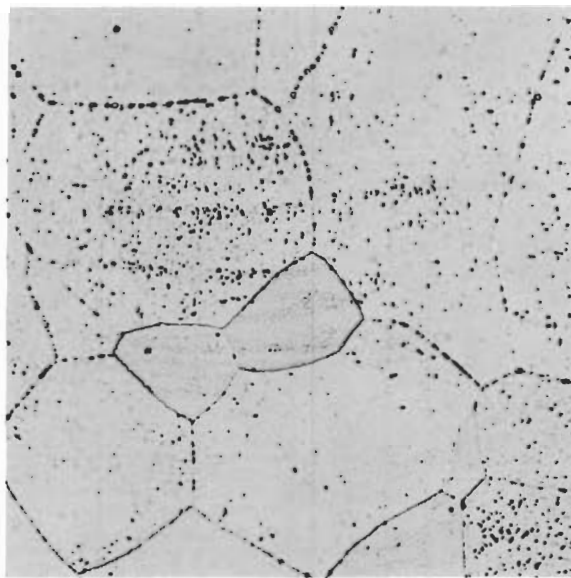
3830

Heat Treated 2100°F 72 Hours



Fusion Zone

3825

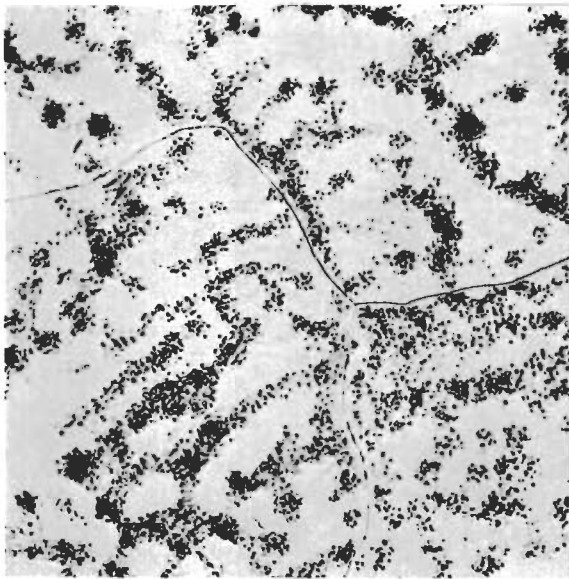


Heat Affected Zone

3826

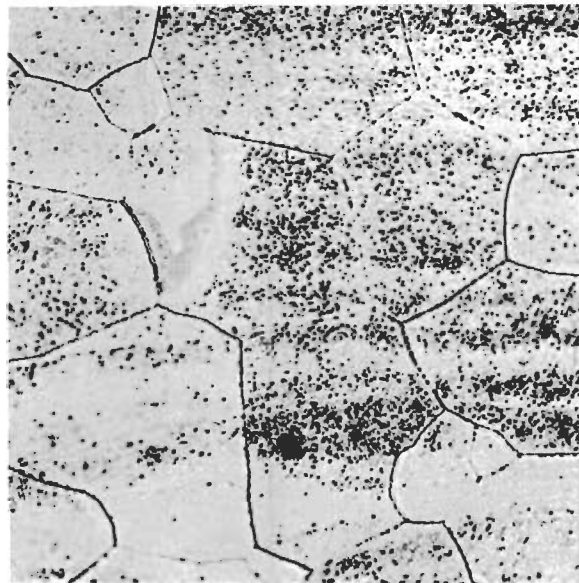
Heat Treated 2350°F 72 Hours

Figure 64 Microstructure of F48 Welds at 15 ipm in Helium 1000X



Fusion Zone

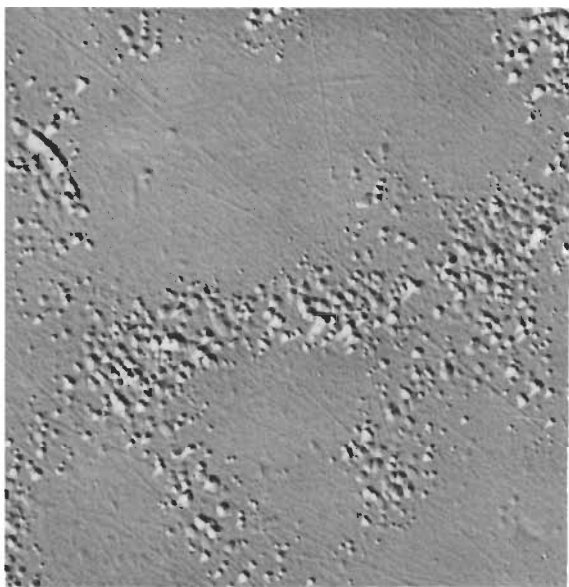
3819



Heat Affected Zone

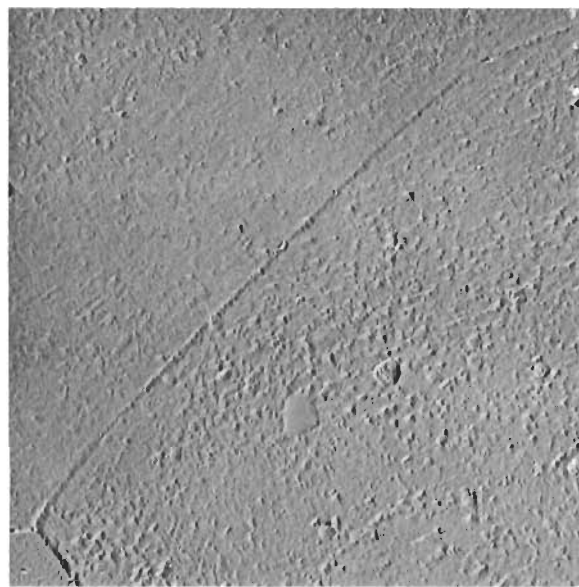
3820

1000X



Fusion Zone

0640



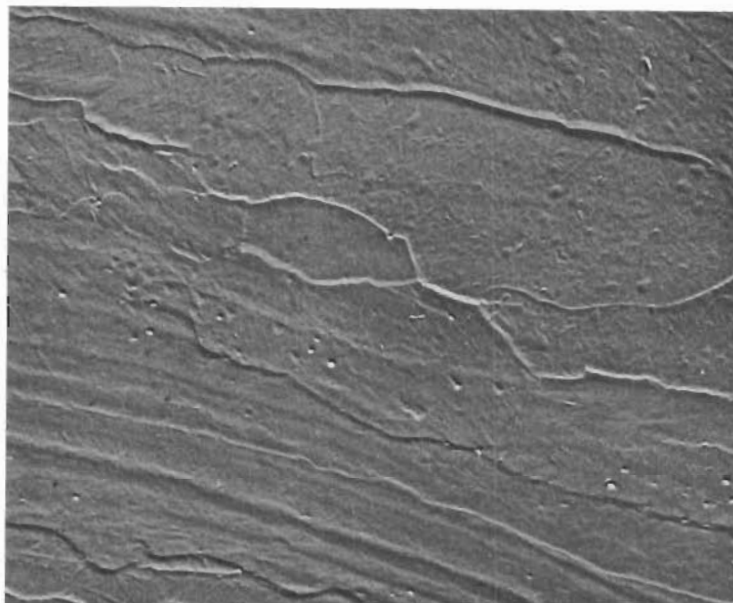
Heat Affected Zone

0637

6000X

Figure 65 Microstructures of Welds in F48 at 15 ipm in Helium  
Heat Treated at 2350°F for 24 Hours





As Received Sheet

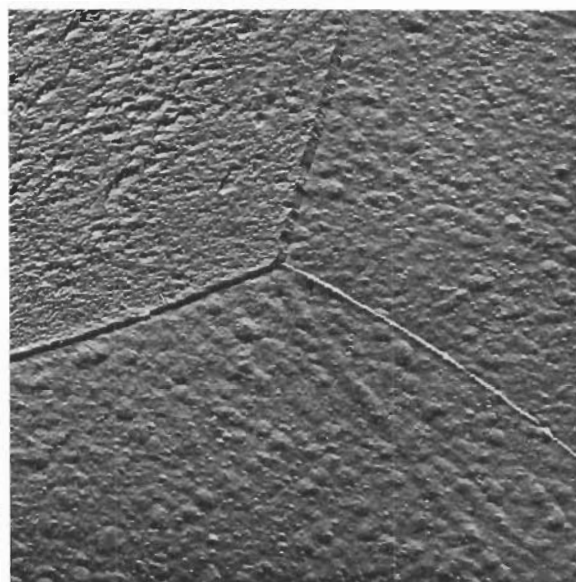
6000X

0636



Fusion Zone

0786



Heat Affected Zone

0787

6000X

Weld 15 ipm Helium Heat Treated 2100°F 24 Hours

Figure 66 Electron Micrographs of F48 Alloy



## 1. FS82 and FS82HS Alloy

The bend ductility curves for FS82 and FS82HS alloy electron beam welded are presented in Figure 67. The 45° bend ductile to brittle transition temperature appears to be at approximately -280°F compared to approximately -200°F for TIG welds. This significant lowering of the transition temperature is attributed to the high purity atmosphere obtained by the electron beam welding equipment, the narrow weld bead, and consequent narrow heat affected zone.

Microstructures of the fusion and heat affected zone for FS82 electron beam welds are presented in Figure 68. These microstructures do not differ greatly from FS82 TIG welded; however, the small grain size in the heat affected zone is quite noticeable. Electron beam welding FS82HS material has lowered the transition temperature more than 200°F from approximately 150°F for TIG welds to -80°F for electron beam welds. Some of this can be attributed to the nature of the process; however, some of it is probably due to a decrease in the oxygen content of the fusion zone while welding. Microstructures of FS82HS electron beam welded are presented in Figure 69. These are almost identical to those for FS82.

## 2. D31 Alloy

Bend ductility data for D31 electron beam welded at 20, 30, 40, and 60 ipm is presented in Figure 70. The effect of welding speed on the transition temperature of this alloy is not noticeable over this range of speed. However, the electron beam process does lower the transition temperature some 100°F to 300°F when compared to TIG welding. Photomicrographs of the fusion zone and heat affected zone of an electron beam weld in D31 are presented in Figure 71. As in the case of TIG welds the fusion zone has a cored structure and a network phase is found within the grains in the heat affected zone. At 6000X, the main difference in the structure from the 15 ipm TIG welds is the smaller amount of a very fine evenly distributed precipitate.

## 3. F48 Alloy

The bend ductility curves for F48 alloy electron beam welded at various welding speeds are presented in Figure 72. The 24 ipm weld appears to be more ductile than the 20 ipm weld. It is believed that a variation in the parent material is the cause for this. The 24 ipm welds were made from material received from Allegheny Ludlum while the 20 ipm welds were made on material procured from Wright Field. The 40 ipm welds were all made on Allegheny Ludlum material. The difference in ductility appears to be the result of the 2450°F vacuum anneal given the one plate prior to welding. It was believed that residual stresses in the material were the cause for parent metal cracking during TIG welding. However, the anneal did not appear to be beneficial in TIG welding. The 60 ipm welds were all made on material furnished by Wright Field.

The bend ductility data presented here indicates that the transition temperature is lowered at least 100°F by comparing electron beam welds

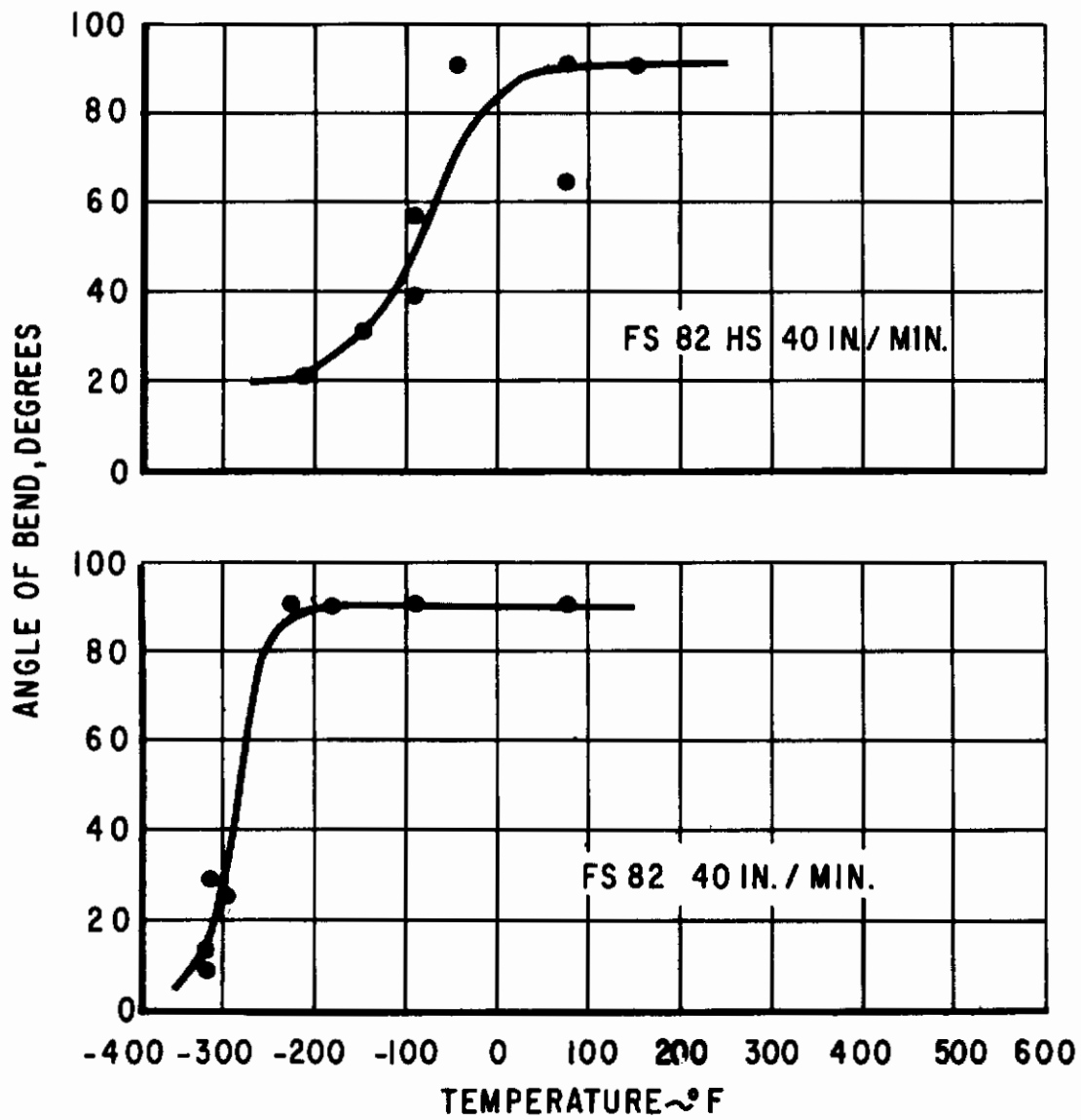
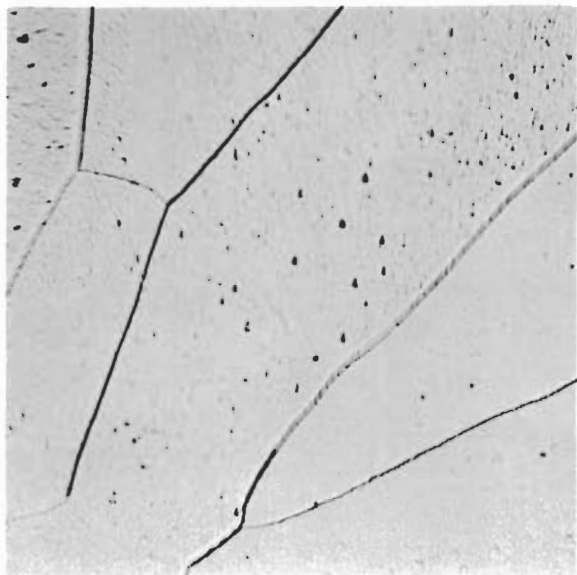
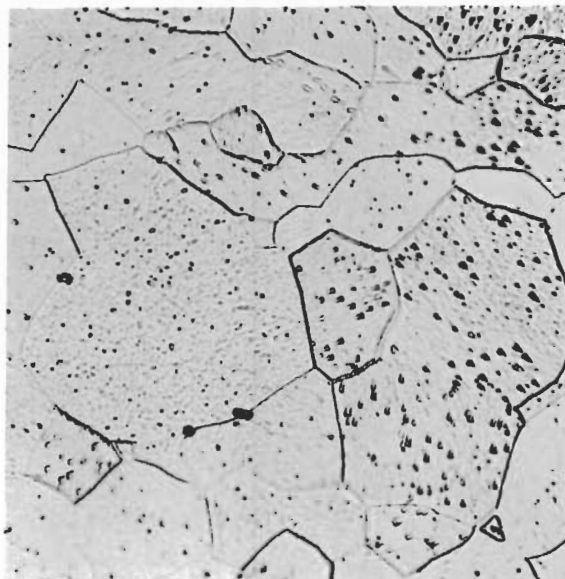


Figure 67. Bend Ductility of FS82 and FS82HS Electron Beam Welds.



Fusion Zone

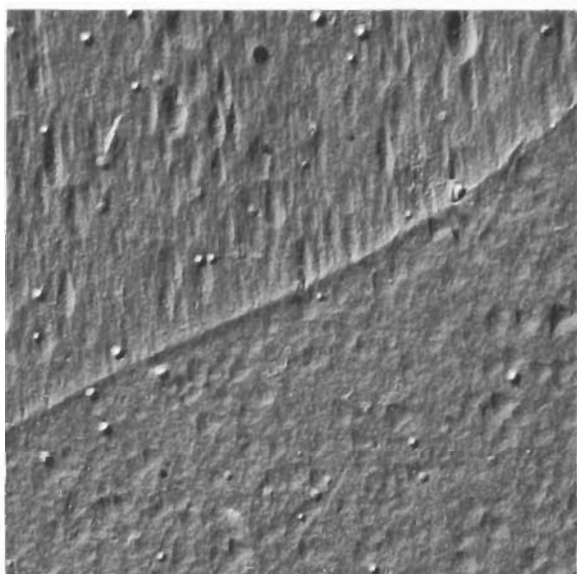
4443



Heat Affected Zone

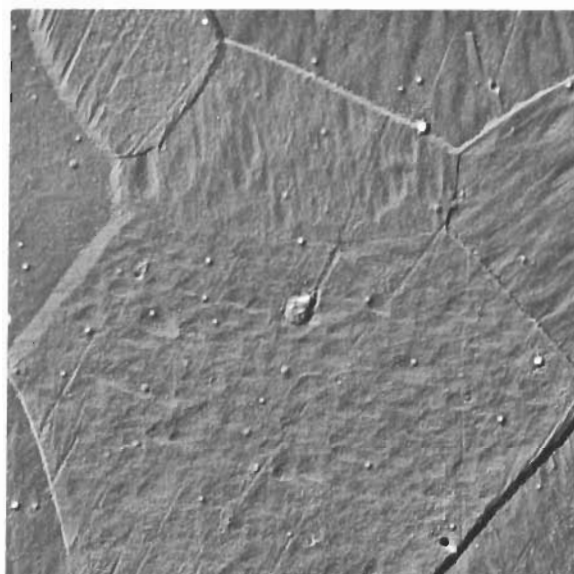
4444

1000X



Fusion Zone

0767

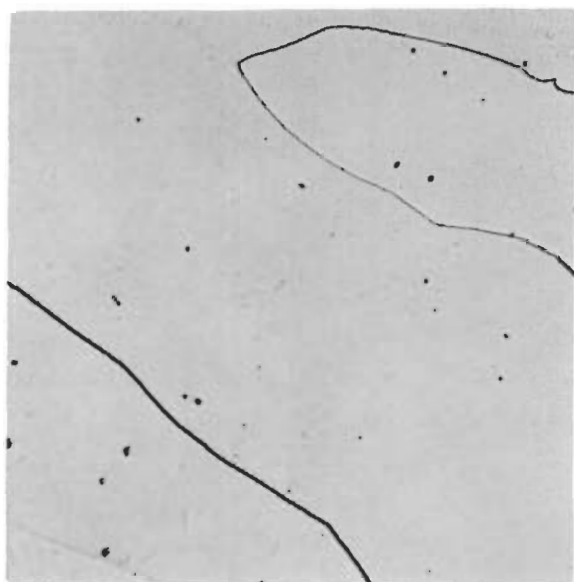


Heat Affected Zone

0765

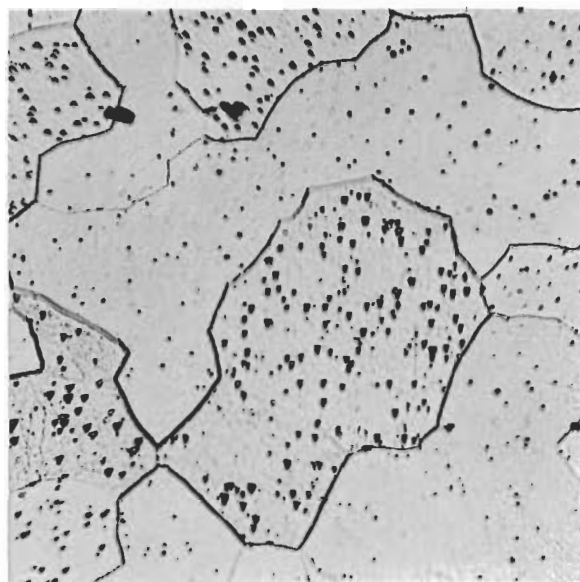
6000X

Figure 68 Microstructure of Electron Beam Weld in FS82 at 40 ipm



Fusion Zone

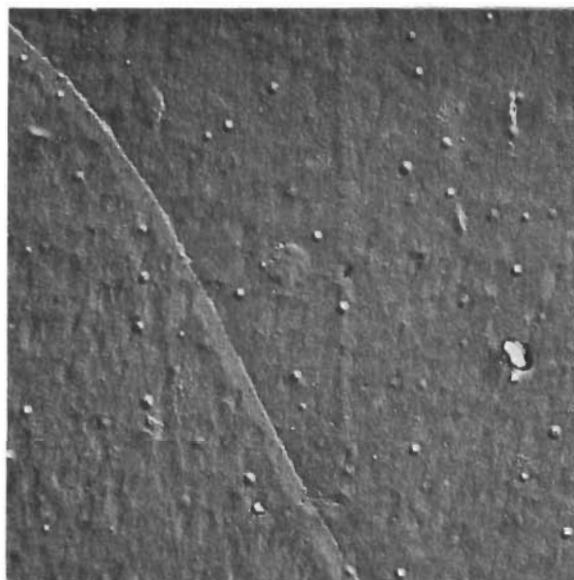
4441



Heat Affected Zone

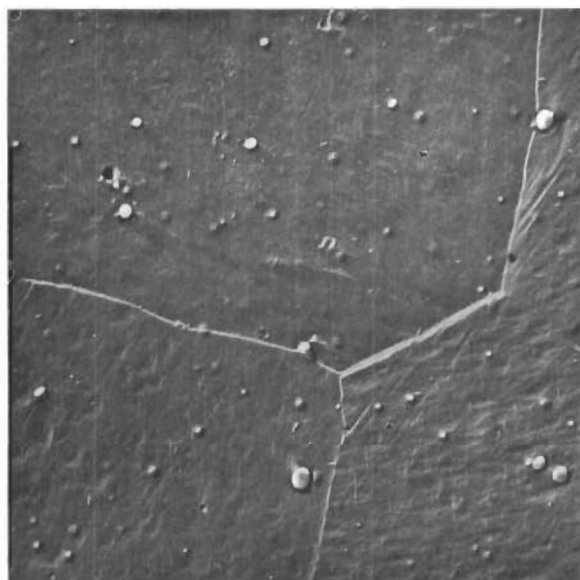
4442

1000X



Fusion Zone

0771



Heat Affected Zone

0769

6000X

Figure 69 Microstructure of Electron Beam Weld in FS82HS at 40 ipm



# Contrails

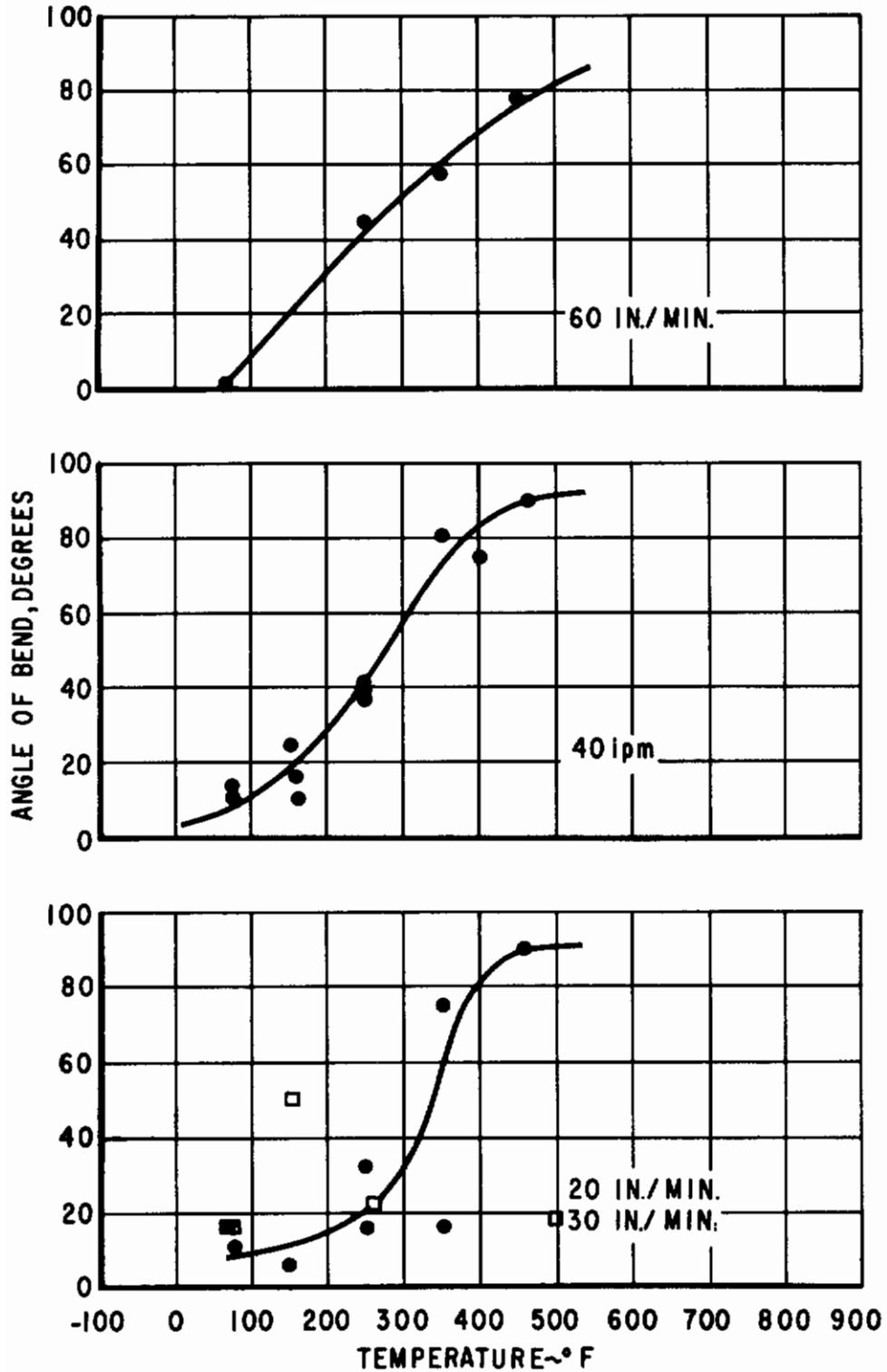
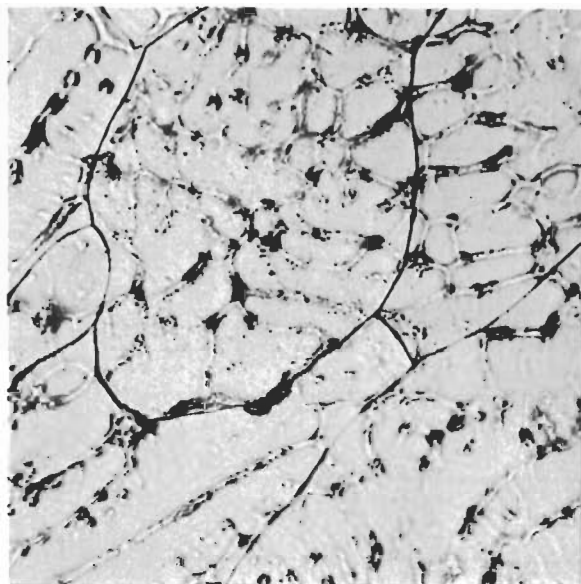
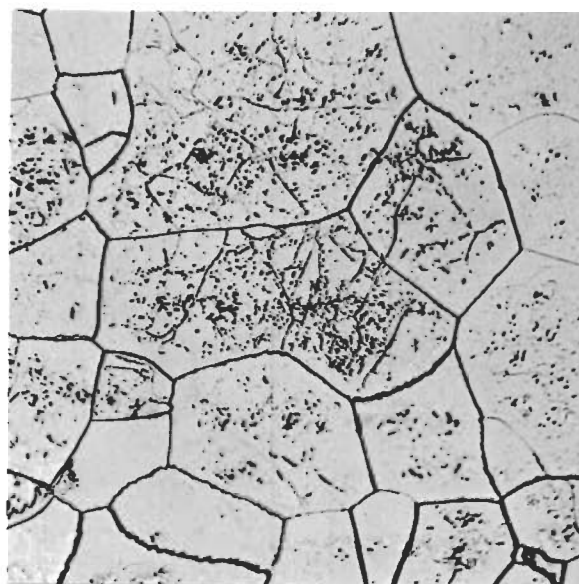


Figure 70. Bend Ductility of D31 Electron Beam Welds.



Fusion Zone

4439



Heat Affected Zone

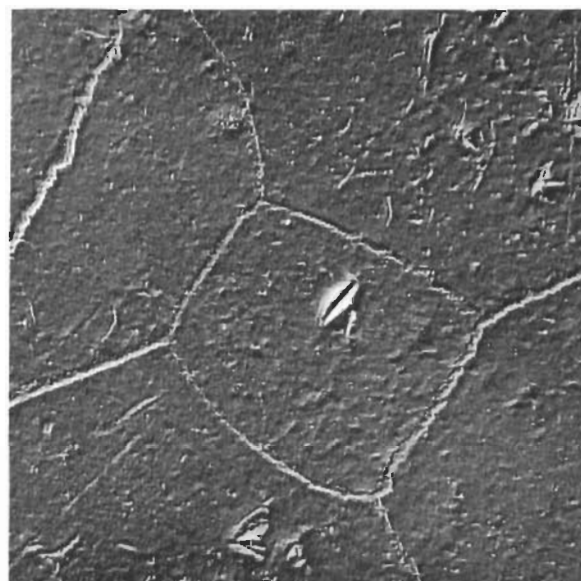
4440

1000X



Fusion Zone

0776



Heat Affected Zone

0773

6000X

Figure 71 Microstructure of Electron Beam Weld in D31 at 40 ipm

# Contrails

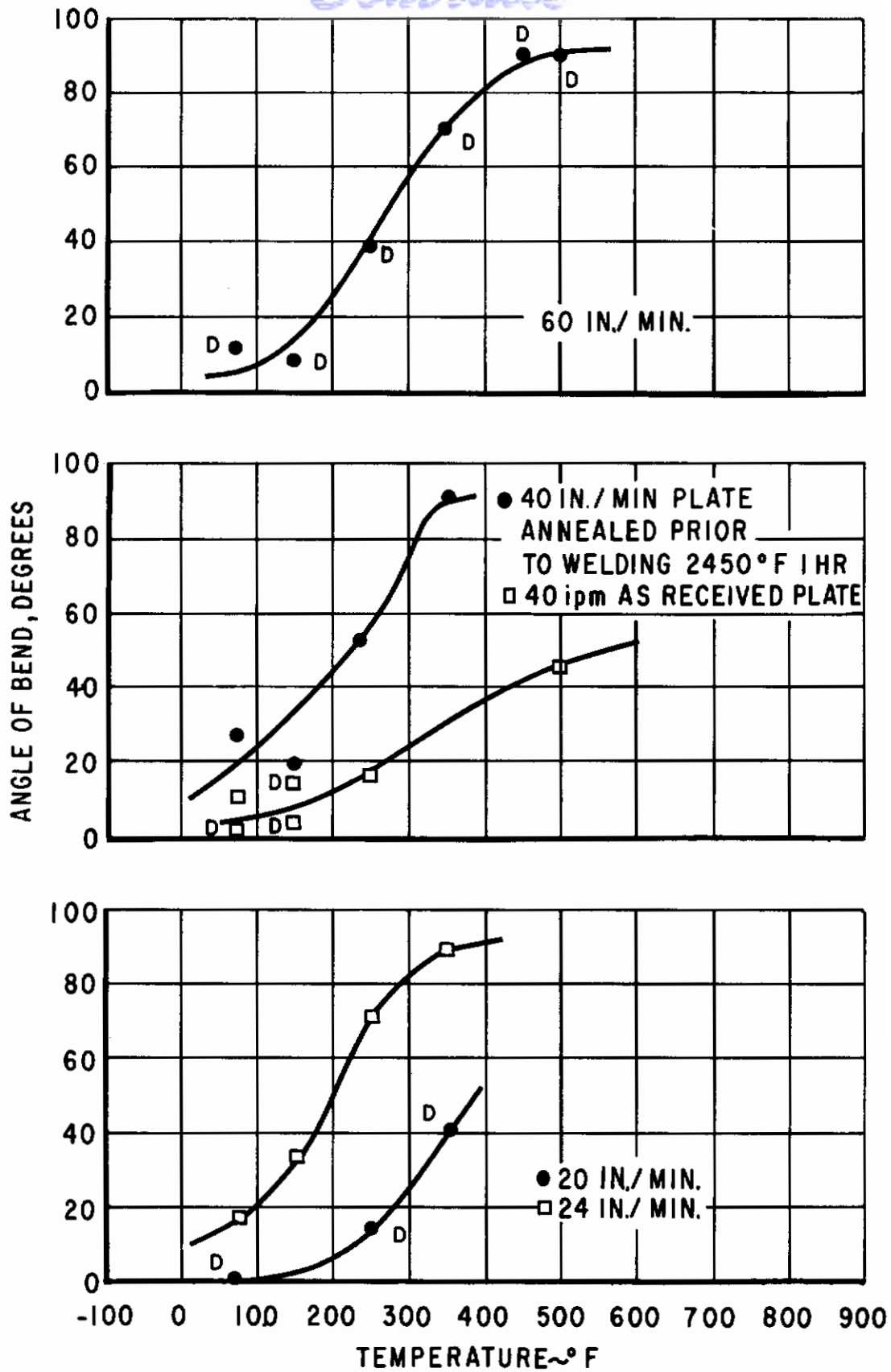


**Figure 72. Bend Ductility of F48 Electron Beam Welds.**

to those made with a preheat of 500°F, Figure 54.

Microstructures of electron beam welds made in F48 are presented in Figure 73. In this case a finer cored structure is found in the fusion zone than in TIG welds and the heat affected zone grains are smaller. At 6000X a supersaturated condition is indicated by the rough appearance. The fast cooling rate probably has prevented the formation of a precipitate.

Electron beam welding has afforded a significant improvement in ductility over TIG welding for all alloys studied. For 0.060 in. sheet a welding speed of 40 ipm was found to be satisfactory. Both FS82 and F48 were welded at a beam energy of 22 KV and 120 MA while D31 was welded at 20 KV and 100 MA. These parameters have given approximate transition temperatures of -280°F for FS82, -80°F for FS82HS, 250°F for D31 and 250°F for F48.

## E. Spot and Projection Welds

One of the major problems encountered in resistance welding columbium alloys and all refractory metal alloys is the tendency of the welding electrodes to weld to the sheet outer surfaces. This is caused by the electrode sheet interfaces becoming sufficiently hot to bond when adequate heat is produced to form a satisfactory weld between the sheets. In addition to sticking, fused nuggets generally contained some degree of porosity and in the case of the more brittle materials weld cracking appeared.

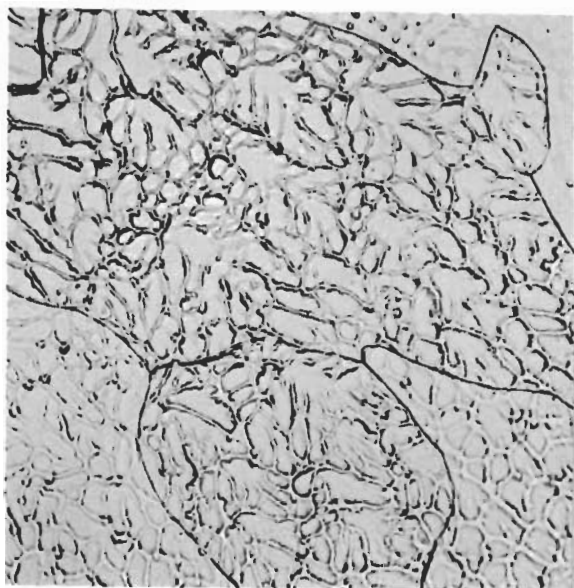
The approaches taken to reduce electrode sticking were to increase electrode force, weld with a low current-long time cycle and use molybdenum or tungsten tips on the electrodes. A solid phase bond was sought with the low current-long time approach which would at the same time eliminate the weld porosity and reduce the cracking tendency.

Most spot welds in the 0.060 in. sheets were made at electrode forces at or near the 1560 lbs. maximum force available. A small number of spot welds were made in FS82 sheet of this thickness at forces up to 3000 lbs. on a machine at Taylor Winfield Corp. The use of the high welding force did not reduce electrode sticking. It was found that the higher current necessary to form an adequate weld at higher forces offsets the gain of lower contact resistance.

The use of Mo or W tipped electrodes was expected to reduce sticking by presenting a higher melting point material at the contacts. Tungsten tips normally stuck slightly less than copper tips but on occasions sticking was great enough to pull a plug of tungsten from the tip. Molybdenum tips stuck somewhat more than Class I Group A copper electrodes. The Mo or W tips apparently reach a considerably higher surface temperature during the weld cycle because their lower thermal and electrical conductivity cause more heat to be generated at the surface and also restricts heat flow away from the surface. The low current long time weld sequence was found to be more effective in minimizing electrode sticking. With the lower current

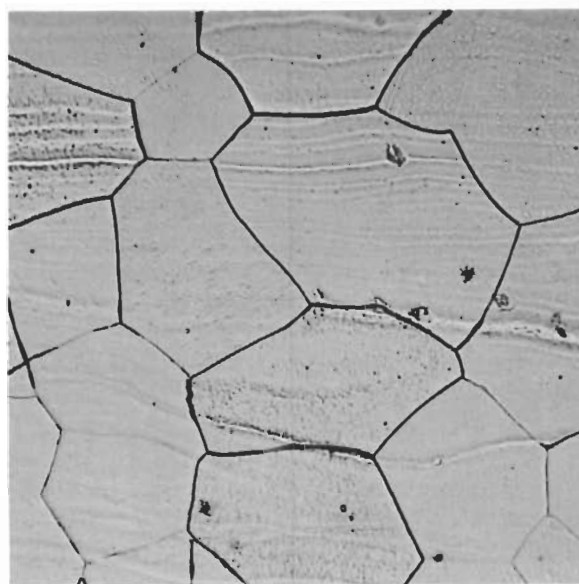


# Contrails



Fusion Zone

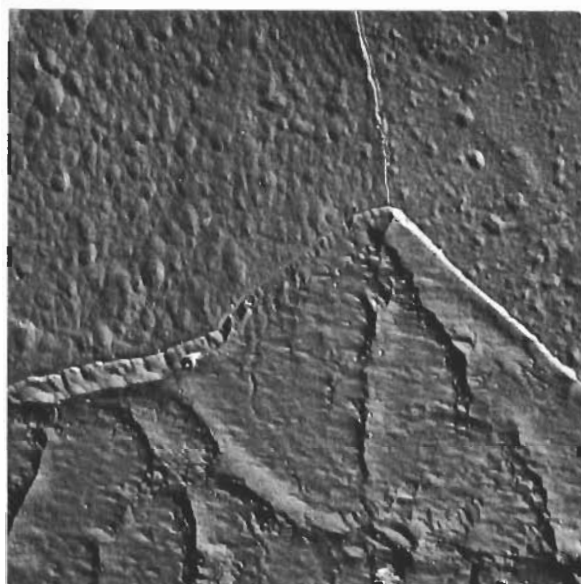
4437



Heat Affected Zone

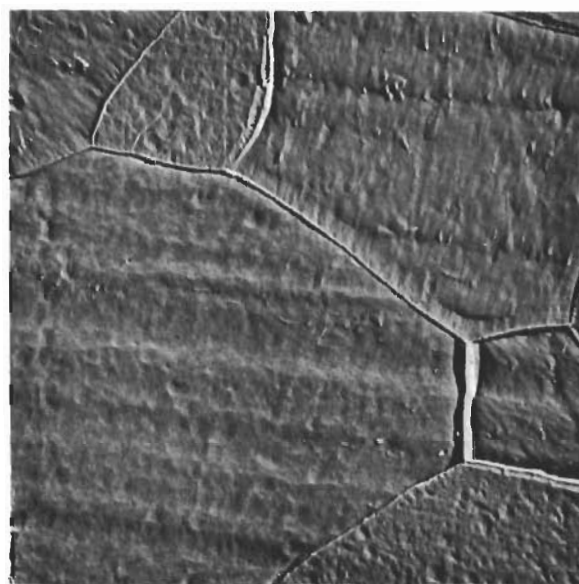
4438

1000X



Fusion Zone

0784



Heat Affected Zone

0782

6000X

Figure 73 Microstructure of Electron Beam Welds in F48 at 40 ipm

# Contrails

the rate at which heat is generated at the contacts apparently is low enough so that the water cooling and superior conductivity of the copper electrodes can maintain this surface below the melting point of copper.

Photomicrographs of representative spot welds in FS82 are shown in Figure 74. In the dissimilar thickness weld it will be noted that the fused nugget is entirely within the 0.060 in. sheet, in spite of the use of a flat electrode on the 0.060 in. sheet and a 1/4 in. radius electrode on the 0.020 in. sheet to achieve heat balance. The two lower micrographs show representative solid phase and fusion type spot welds in 0.060 in. sheet. The projection welding technique was expected to minimize electrode sticking but this was not the case. After a few welds the electrodes became indented under the projection causing higher contact resistance and sticking. Projection welding did provide a method of heat balance for welding dissimilar thicknesses by placing the projection in the thicker sheet. Representative projection weld micrographs of three thickness combinations are included in Figure 75. The AWS recommended projection for 0.062 in., stainless sheet was used for the 0.060 in. to 0.020 in. weld while a larger projection, that recommended for 0.078 stainless sheet, was used for the 0.060 in. to 0.060 in. welds.

Results of tensile shear tests of spot and projection welds for FS82 alloy are given in Table VII. Representative weld hardnesses, fused and recrystallized diameters are listed in Table IX.

At an electrode force of 730 lbs. and 6 cycles weld time, shear strengths of 850 - 900 lbs. were obtained at a current of 10,000 amps and 1080 - 1140 lbs. were obtained at a current of 12,000 amps for 0.041 in. sheet.

Higher electrode forces were used for 0.020 in. sheet than previously used for 0.041 in. sheet to help minimize electrode sticking and to eliminate porosity at the center of the nuggets. Electrode forces up to approximately 1200 lbs. probably would be satisfactory, for the 0.041 in. sheet but this was not verified by experiment.

The tensile shear results for the 0.020 in. sheet show breaking load values from 440 to 520 lbs. over a current range of 8900 to 12,300 amps. When setting up a spot welding schedule it is desirable to operate at a current value where a small variation in current will result in an insignificant change in weld strength. Over this same current range the diameter of the recrystallization bonded area varied from 0.118 in. to 0.142 in. as measured on representative metallographic sections. Only at 12,300 amps was a fair-sized fused diameter of 0.122 in. obtained. A plug type failure occurred in each of these 0.020 in. sheet samples indicating that reliable strength and ductility can be obtained with spot welds in this material with either recrystallization or fusion bonding. In a plug type failure of a spot weld test specimen, failure occurs by shearing around the bonded area in one or both sheets rather than by shearing through the bonded area.

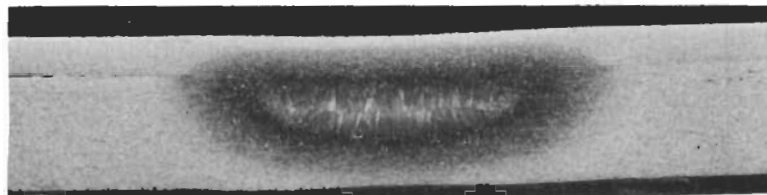
The tensile shear results and mode of failure for spot welds in the 0.060 in. FS82 sheet show a leveling off point at 18,700 to 19,600 amps. Below this value of current the shear strength falls off sharply and the

# Contrails



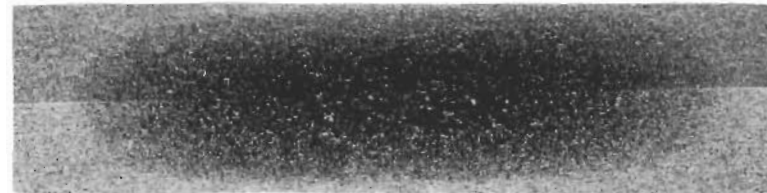
.020 - .020

19R



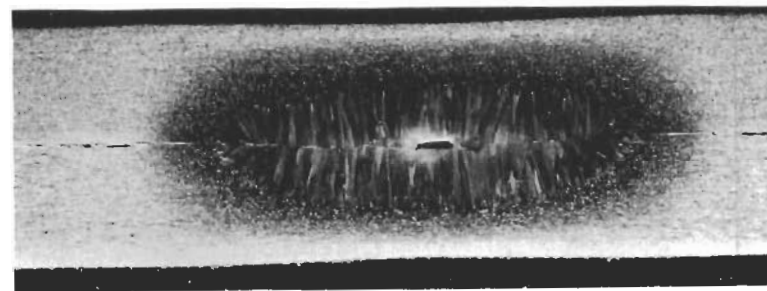
.020 - .060

65R



.060 - .060

136R



06060

.060 - .060

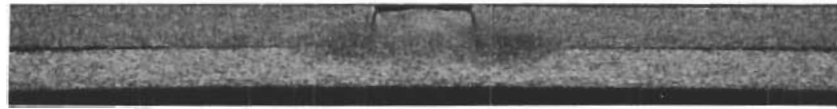
62R

Figure 74 Photomicrographs of FS82 Spot Welds

10X

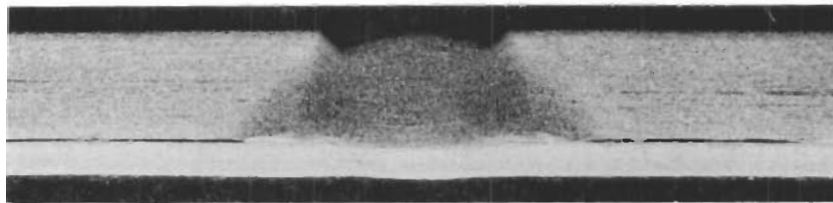


# Contrails



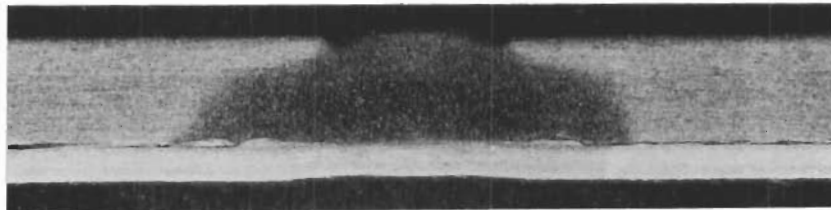
.020 - .020

31R



.060 - .020

288R



.060 - .020

229R



06060

.060 - .060

147R

Figure 75 Photomicrographs of FS82 Projection Welds 10X



TABLE VII

RESISTANCE WELDING PARAMETERS AND RESULTS, ALLOY FS82

<u>Weld No.</u>	<u>Sheet Thickness (In.)</u>	<u>Tip Radius (In.)</u>	<u>Electrode Force Lbs.</u>	<u>Weld Time Cycles</u>	<u>Weld Current Amps</u>	<u>Comments</u>	<u>Shear Strength Lbs.</u>	<u>Type Failure</u>
18R	.020	4	730	3	12,300	2,5		
19R	.020	4	730	3	10,300	1,5		
71R	.020	4	730	3	10,300	2	480	Plug
72R	.020	4	730	3	10,300	2	490	Plug
73R	.020	4	730	3	11,100	2	500	Plug
74R	.020	4	730	3	11,100	2	500	Plug
75R	.020	4	730	3	12,300	3	480	Plug
76R	.020	4	730	3	12,300	3	530	Plug
113R	.020	4	850	3	8,900	1	470	Plug
114R	.020	4	850	3	8,900	1	440	Plug
115R	.020	4	850	3	9,600	1	480	Plug
116R	.020	4	850	3	9,600	1	520	Plug
6R	.041	4	730	6	10,000		900	
7R	.041	4	730	6	10,000		850	
8R	.041	4	730	6	10,000		850	
9R	.041	4	730	6	12,000		1140	
10R	.041	4	730	6	12,000		1125	
11R	.041	4	730	6	12,000		1090	
133R	.060	12	1580	15	17,800	3,5		
134R	.060	12	1580	15	17,800	2	2380	Shear
135R	.060	12	1580	15	17,800	2	2100	Shear
136R	.060	12	1580	15	18,700	4,5		
137R	.060	12	1580	15	18,700	3	2500	Plug
138R	.060	12	1580	15	18,700	3	2610	Plug
139R	.060	12	1580	15	19,600	4,5		
140R	.060	12	1580	15	19,600	4	2710	Plug
141R	.060	12	1580	15	19,600	4	2750	Plug
142R	.060	12	1580	15	16,900	2,5		
143R	.060	12	1580	15	16,900	2	2210	Shear
144R	.060	12	1580	15	16,900	2	2100	Shear
219R	.060	12T	1580	15	16,400	2	2790	Plug
220R	.060	12T	1580	15	16,400	2	2770	Plug
221R	.060	12T	1580	15	16,400	2	2700	Plug
230R	.020-.060	Flat	730	8	10,700	2P	628	Plug
231R	.020-.060	Flat	730	8	10,700	2P	664	Plug
232R	.020-.060	Flat	730	8	10,700	2P	622	Plug
233R	.020-.060	Flat	730	8	12,000	3P	645	Plug
234R	.020-.060	Flat	730	8	12,000	4P	568	Plug
235R	.020-.060	Flat	730	8	12,000	4P	545	Plug

# *Contrails*

TABLE VII (Continued)

Comments: (1) No sticking and electrode pickup. (2) Light electrode sticking and pickup. (3) Moderate electrode sticking and pickup. (4) Heavy electrode sticking and pickup. (5) Metallographic sample.

**ERRATA - July 1962**

**The following correction is applicable to ASD Technical Documentary Report 62-292, entitled "Investigation of Welding of Commercial Columbium Alloys", and dated May 1962:**

**Page 113**

**In Table VIII, insert "7" after "8" under "Comments" opposite Weld Nos. 190R, 191R, 196R, 205R, and 208R.**

**Aeronautical Systems Division  
Air Force Systems Command  
Wright-Patterson Air Force Base, Ohio**

# Contrails

specimen fracture changes from a plug (shearing the sheet material) to shearing through the weld interface. At 19,600 amps, electrode sticking and copper pickup were becoming excessive making this an impractical weld parameter. Metallographic examination indicated a recrystallization diameter of 0.256 in. to 0.272 in. A fused diameter of 0.181 was obtained at 19,600 amps. Welds made at similar parameters with tungsten electrodes attained the same strength level and plug type failures at 16,400 amps as obtained with Class 1 electrodes at 19,700 and 19,600 amps. A fused zone diameter of 0.203 in. had previously been obtained at 1160 lbs. electrode force, 8 cycles and 16,400 amps but the center of the nugget contained a hole approximately 0.02 in. diameter with vertical cracks branching from it. The electrode force and consequently the weld heat were increased to minimize the porosity and cracking.

Results of tensile shear tests and parameters for D31 spot welds are presented in Table VIII. The higher strength obtained in 0.020 in. D31 spot welds compared to 0.020 in. FS82 is attributed to the higher strength of the D31 and a slightly larger weld diameter. When examining microsections of welds made in each material under identical conditions it was observed that a larger fused diameter was obtained in the D31. A lower melting temperature and higher resistivity of D31 could account for this behavior. Although all but sample 119R exhibited plug-type failures, examination of microsections of a series of welds made at similar conditions indicated that only the samples welded at 13,000 amps contained a fused nugget. While most of these welds pulled plugs there were indications of low ductility where cracks first formed in the sheet at the edge of some of the welds.

The spot weld tensile shear strength obtained with the 0.060 in. D31 sheet was approximately half the strength obtained with the same thickness FS82. This behavior, which is inconsistent with the strengths obtained in the 0.020 in. sheet, is probably caused by the longer time at high temperature and resulting embrittlement of the welds in the 0.060 in. sheet. Since shorter time welds at higher current would increase the electrode sticking condition, lower current longer time recrystallization type welds were investigated. The 60 cycle welds were stronger than the 12 cycle welds as listed in Table VIII. Heat treatment of both 12 cycle and 60 cycle welds at 2100°F for 24 hours increased the shear strength but changed the mode of failure to cracking across one of the sheets at the edge of the weld. The heat treatment increased the ductility of the weld area but lowered the ductility of the sheet.

The fact that spot welds in D31 become embrittled in 12 cycles heat time points up the problem of trying to avoid a brittle condition in fusion welds where the time at elevated temperatures is much longer. For example, the time that the fusion zone is above 4000°F in a weld made at 30 ipm is approximately 0.75 second or 45 cycles according to Figure 36. At slower welding speeds the time is correspondingly longer.

Macrosections of D31 spot welds in 0.020 in. and 0.060 in. sheet are displayed in Figure 76. When sufficient heat was developed to form a fused zone in the 0.020 in sheets a transverse crack appeared. This was a common



# Contracts

TABLE VIII

RESISTANCE WELDING PARAMETERS AND RESULTS, ALLOYS D31 AND F48

<u>Weld No.</u>	<u>Thickness (In.)</u>	<u>Tip Radius (In.)</u>	<u>Electrode Force Lbs.</u>	<u>Weld Time Cycles</u>	<u>Weld Current Amps</u>	<u>Comments</u>	<u>Shear Strength No.</u>	<u>Type Failure</u>
117R	.020	4	910	6	10,300	2, 8		
118R	"	"	"	"	"	2	720	Plug
119R	"	"	"	"	"	2	660	Shear
120R	"	"	"	"	11,400	2, 8		
121R	"	"	"	"	"	2	740	Plug
122R	"	"	"	"	"	2	"	Plug
123R	"	"	"	"	13,000	3, 8		
124R	"	"	"	"	"	3	630	Plug
125R	"	"	"	"	"	3	740	Plug
126R	"	"	"	"	14,300	4, 8		
110R	.060	12	1420	12	14,200	1, 8		
127R	"	"	"	"	"	1	1230	Shear
128R	"	"	"	"	"	1	1390	Shear
111R	"	"	"	"	16,400	2, 8		
129R	"	"	"	"	"	2	1230a	Crack
130R	"	"	"	"	"	2	1270b	Crack
112R	"	"	"	"	18,700	2, 8		
131R	"	"	"	"	"	3e	1240	Shear
132R	"	"	"	"	"	3e	1130c	Crack
160R	"	"	"	"	12,800	1, 5	2040	d
161R	"	"	"	"	"	1, 5	2825	d
162R	"	"	"	"	"	1, 5	2320	d
203R	"	"	1500	60	11,000	3, 8		
213R	"	"	"	"	"	2	1425	Shear
204R	"	"	"	"	11,900	4, 8		
215R	"	"	"	"	11,000	2	1420	Plug
217R	"	"	"	"	11,000	2	1270	Plug
214R	"	"	"	"	"	2, 5	2335	d
216R	"	"	"	"	"	2, 5	2280	d
218R	"	"	"	"	"	2, 5	1660	d
190R	.060	12	1500	60	11,900	2, 8 7		
191R	"	"	"	"	10,500	2, 8 7		
196R	"	12T	"	"	7,700	2, 8 7		
205R	"	12	"	"	12,800	4, 8 7		
208R	"	12T	"	"	8,800	2, 8 7		
222R	"	"	"	"	"	2, 6, 7	965	d
223R	"	"	"	"	"	4, 6, 7	740	d

# Contrails

TABLE VIII (continued)

Comments:

- |   |   |
|---|---|
| 1 - No sticking or electrode pickup.          | a - Cracked at 800 pounds.                |
| 2 - Light electrode sticking or pickup.       | b - Cracked at 730 pounds.                |
| 3 - Moderate electrode sticking or pickup.    | c - Cracked at 780 pounds.                |
| 4 - Heavy electrode sticking and pickup.      | d - Sheet cracked across at edge of weld. |
| 5 - Post heat treated at 2100°F for 24 hours. | e - Expulsion                             |
| 6 - Post heat treated at 2350°F for 24 hours. | T - Tungsten tips.                        |
| 7 - F48 alloy, all others are D31.            |   |
| 8 - Metallographic sample.                    |   |

TABLE IX

SPOT WELD HARDNESSES AND DIAMETERS

Weld No. *	Alloy	Hardness DPH			Weld Diameter In.		Comments
		FZ	HAZ	Sheet	Fused	Recryst.	
18R	FS82				0.122	0.142	
19R	"				-	0.122	
133R	"				0.126	0.256	
136R	"	202	181	185	-	0.244	
139R	"				0.181	0.272	P
144R	"						
110R	D31				0.181	0.256	C, P
111R	"	378	374	354	0.224	0.276	C, P
112R	"				0.276	0.276	P
117R	"				-	0.138	
120R	"				-	0.150	
123R	"				0.106	0.130	C
126R	"				0.157	0.157	P, C
203R	"	362	318	307	-	0.256	
204R	"				0.114	0.268	
190R	F48				-	0.212	
191R	"				-	0.169	
196R	"				-	0.181	
205R	"				0.067	0.181	C
208R	"	374	338	325	-	0.212	

\* Weld parameters are given in Tables VII and VIII

C Cracks

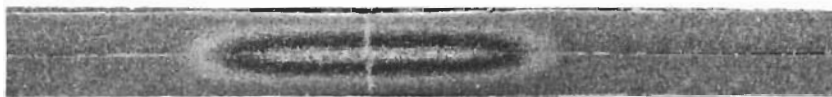
P Porosity

# Contrails



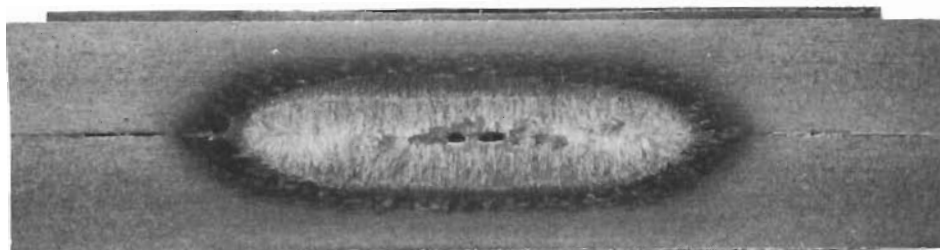
.020 - .020

120R

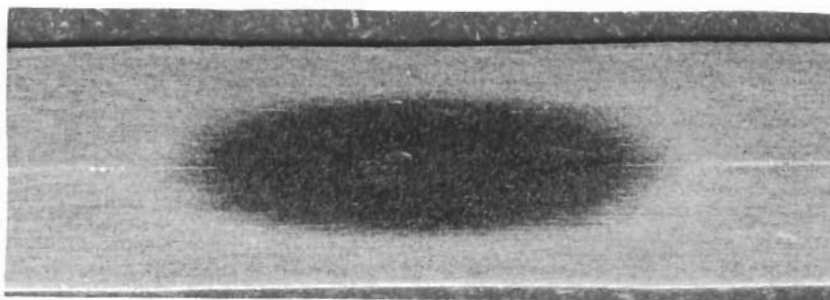


.020 - .020

123R



111R



06060

203R

Figure 76 Photomicrographs of D31 Spot Welds

10X



occurrence in both the 0.020 in. and 0.060 in. D31 sheet. The two lower macrographs show a good fusion weld and a good recrystallization weld in 0.060 in. sheet. A slight increase in the current required to form a fusion spot weld would cause excessive porosity, internal and radial surface cracks and excessive electrode sticking.

Figure 77 illustrates the fusion and recrystallization type spot welds obtained in F48 alloy. Usually the formation of a fused nugget in this alloy was accompanied by transverse cracks, some of which extended to the outer surfaces. Recrystallization bonds were most effective in minimizing center porosity, cracking and electrode sticking. Results of two tensile shear tests in 0.060 in. sheet are given in Table VIII. These welds were heat treated at 2350°F for 24 hours. Although the welds did not shear apart but failed by cracking across at the edge of the weld the low strength is probably an indication of severe notch sensitivity of F48 in this heat treated condition.

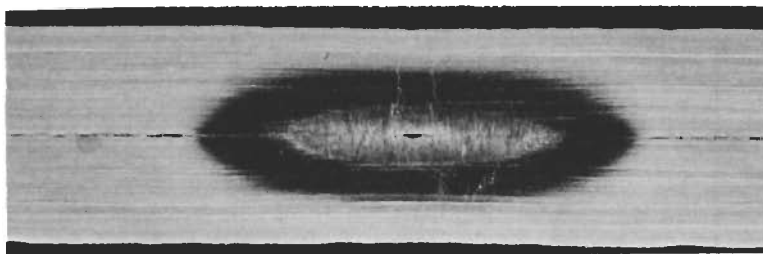
All three of these alloys can be spot welded but as was true with arc fusion welds both D31 and F48 spot welds display brittle behavior. Best results were obtained with solid phase recrystallization type welds rather than fused welds. The long-time low current weld cycle used for recrystallization welds eliminated porosity and minimized electrode sticking. Post heat treatment of the D31 and F48 spot welds increased the tensile shear strength and ductility.

## F. Flash Welds

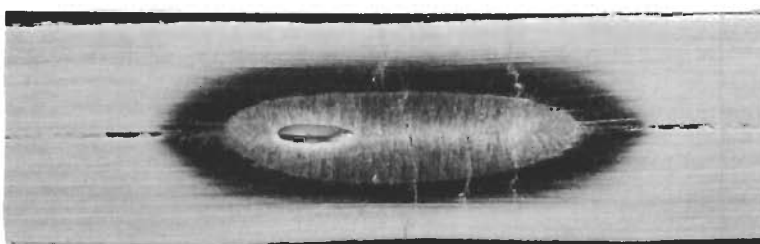
The variables studied during the flash welding portion of this program included flashing distance, upset distance, flashing time, flashing curve, upset current and upset time. The initial flash welding was done on FS82 alloy because fewer weldability problems are encountered. At first it was planned to investigate total flash-off values of 0.3, 0.4, and 0.5 in. starting with the 0.4 in. value. Since the results indicated that adequate flash-off was obtained, lower values of 0.2 and 0.25 in. total flash-off were studied in addition to the 0.4 in. amount.

Setting the value of the acceleration factor ( $a$ ) in the flashing curve determined the initial slope and the flashing acceleration. A low value of ( $a$ ) resulted in a flashing curve starting at a relatively high velocity with a small amount of acceleration during the cycle. With a high value of ( $a$ ) the starting velocity was low but the high acceleration rate developed a higher final velocity than the low acceleration curve. All other factors being the same the total distance traveled, i.e., total flash off, and total flashing time are the same in both cases. The effect of increasing the acceleration factor ( $a$ ) is to cramp the bulk of the flashing toward the end of the cycle. A high acceleration rate minimizes the depth of the heat affected zone while developing adequate interface temperature for proper upsetting. Rapid final flashing can be achieved by shortening the total flashing time for a given amount of flash-off; however, this can result in butting at the start of the cycle if the initial velocity is too great.

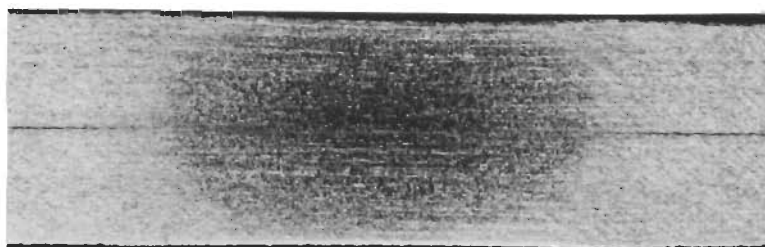
# Contrails



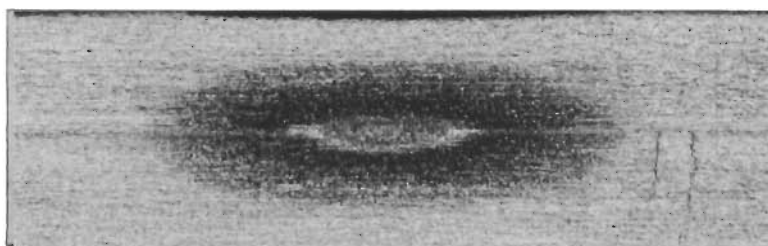
165R



166R



208R



205R

Figure 77 Photomicrographs of F48 Spot Welds 10X

# Contrails

The first sample welded at 6.5 secondary volts butted during the first 50 cycles of weld time, burned open and then flashing began. An excessively bulged joint resulted. All remaining welds were made at a higher voltage, 10.5 volts, to prevent butting. The next three welds made with 0.40 in. total flash-off (0.20 in. per bar) and 1.5 to 2 cycles of upset current at 100% heat were cracked after removing from the welder and could be fractured by hand. Decreasing the upset current magnitude but increasing the time eliminated the severe brittleness and cracks. Bend and tensile tests of several FS82 welds in the as-welded condition displayed low ductility not expected for this material. Metallographic examination of several welds revealed a highly worked directional flow normal to the rolling direction. Some welds with a small amount of upset or low upset heat exhibited what is believed to be a high oxygen phase at the interface as shown in Figure 78. Mechanical test specimens corresponding to these conditions broke while being machined indicating very low ductility. Other tensile and bend specimens corresponding to a microstructure with no oxide phase but similar to the interface structure of Figure 79 exhibited low strength and ductility. From this it is assumed that a high level of oxygen is in solution near the interface but is not obvious as a separate phase. Hardness surveys, Figure 80, across a number of welds show increased hardness at the interface. FS82 weld No. 13 which was upset only 0.15 in. total exhibited the network oxide phase in Figure 78 and the peak interface hardness of 370 DPH in Figure 80. There was no obvious oxide phase in the interface of weld No. 11, but the hardness survey, Figure 80, contained a peak interface hardness of 308 DPH. This indicated that oxygen and possibly hot-cold work was increasing the hardness at this location.

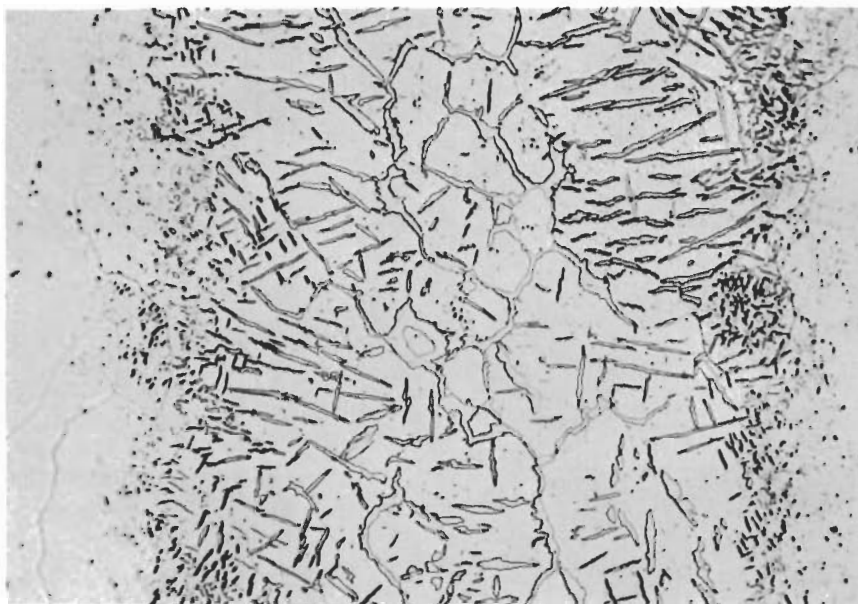
After a 4 hour 2000°F vacuum heat treatment, weld ductility was improved greatly with a slight decrease in ultimate strength. It is presumed that the heat treatment allowed the high oxygen concentration at the interface to be decreased by diffusion.

Welds in D31 and F48 were made at essentially the same parameters as found satisfactory for the FS82 alloy welds. Microstructure and macrographs of these welds are shown in Figures 81 and 82 and hardness surveys are given in Figure 80. Since the need for post heat treatment had been demonstrated previously for other welding methods additional welds made for tensile tests were heat treated as follows: FS82 and FS82HS - 2000°F 4-hours, D31 - 2100°F 24-hours, F48 - #33 - 2350°F 24-hours, #42 - 2500°F 4-hours.

The results of tensile and bend tests on flash weld samples are listed in Table X. Samples not listed were sectioned for metallographic examination. The low tensile strength of 22,300 psi for F48 is considered as unrealistically low because this specimen fractured outside the weld on a 45° plane. This typically brittle mode of fracture occurred on the other samples of this alloy during machining of tensile specimens. Tensile strengths for F48 flash welds 33 and 42 were calculated from the maximum bending load using the flexure formula for the maximum fiber stress in rectangular beams. These results were more reasonable for F48.

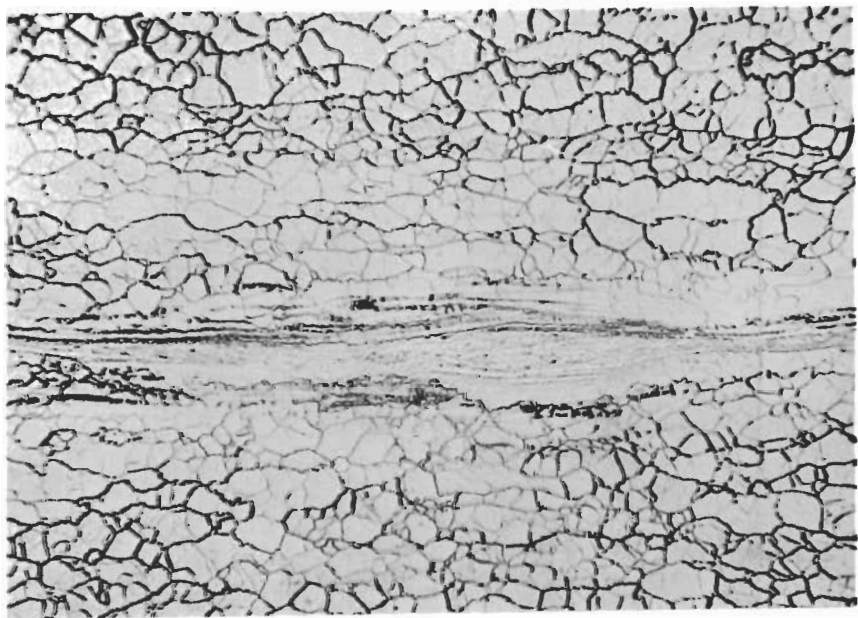
Flash welds were made in FS82, FS82HS and D31 alloys; however, to achieve adequate room temperature ductility post heat treatments were required, 2000°F





Weld 13 FS82

4461



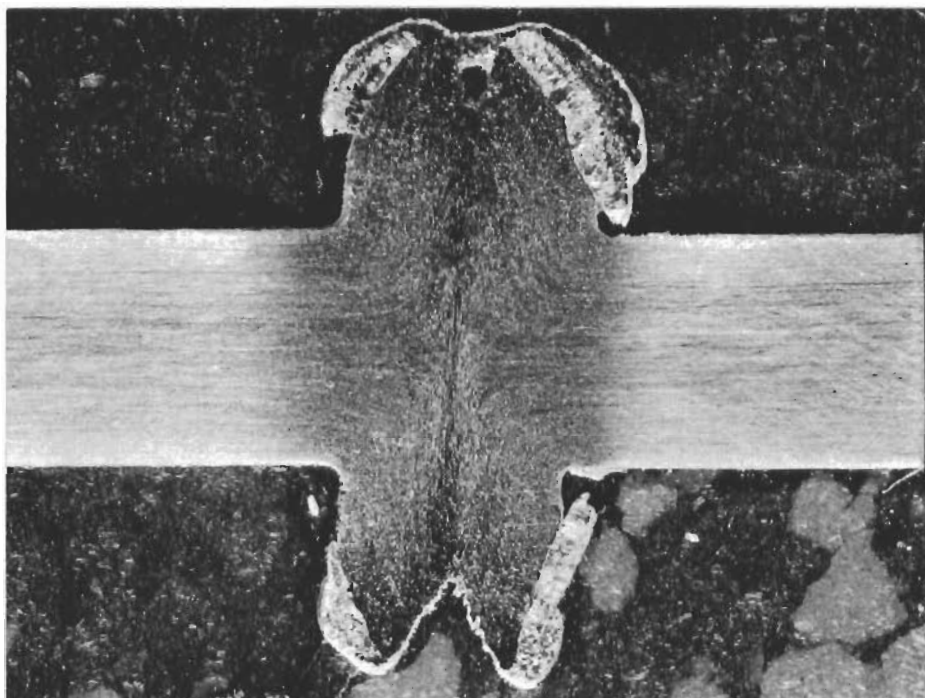
Weld 25 D31

4467

Figure 78 Microstructure of Flash Welds Showing Oxide Phase at Interface

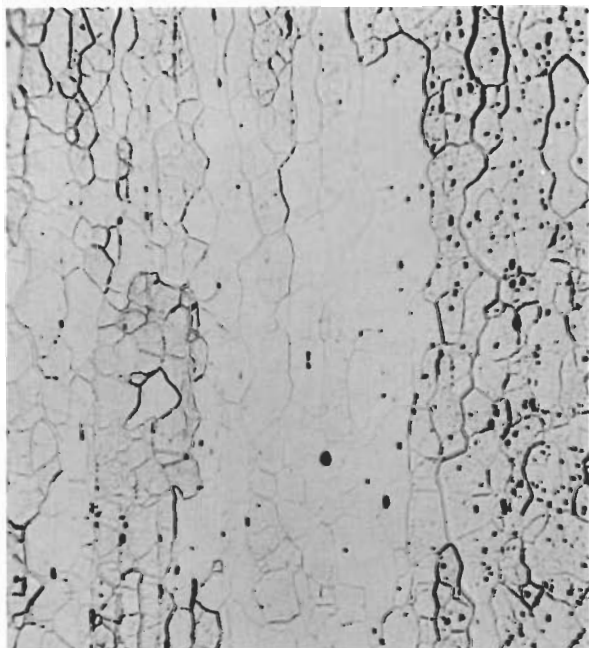
1000X





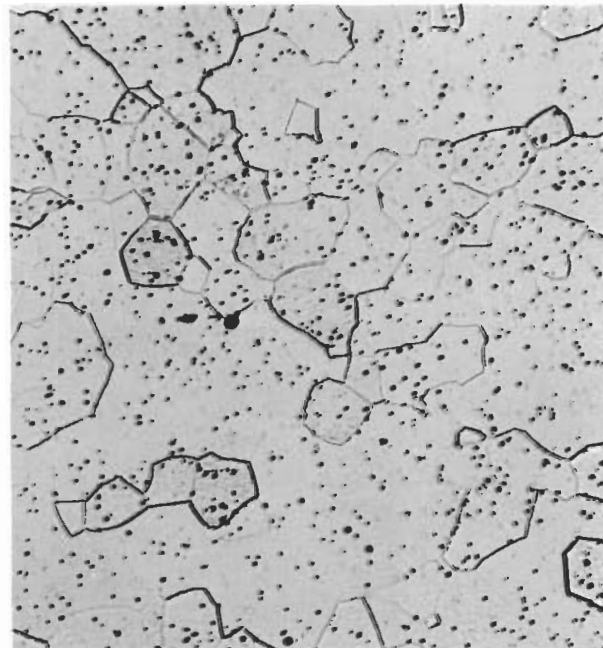
10X

06069-17



Interface

4462



Heat Affected Zone

4463

1000X

Figure 79 Flash Weld in FS82, Weld No. 17

# Contrails

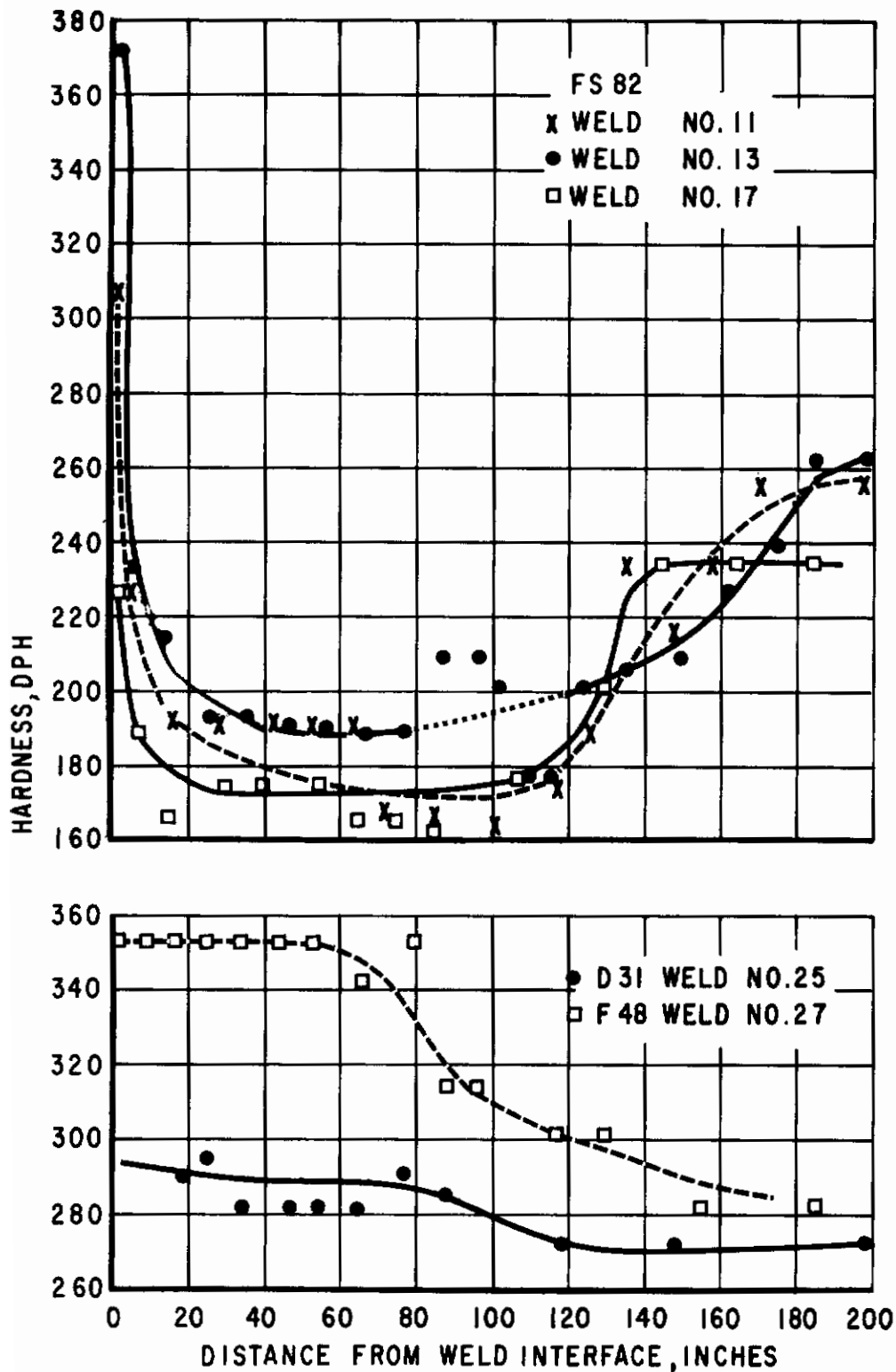
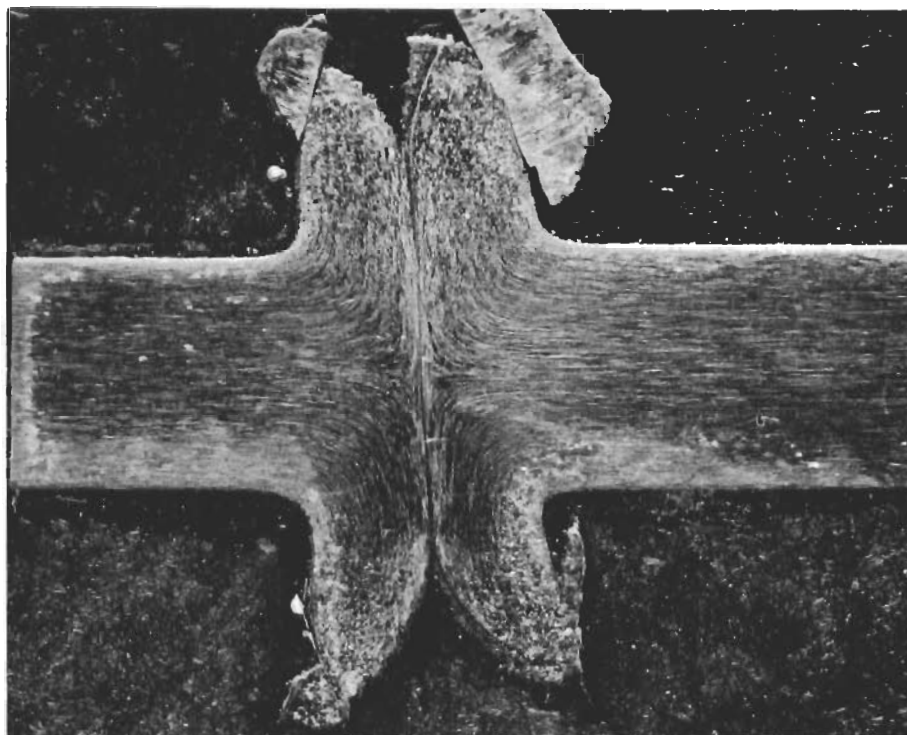


Figure 80. Hardness Surveys of Flash Welds.



10X

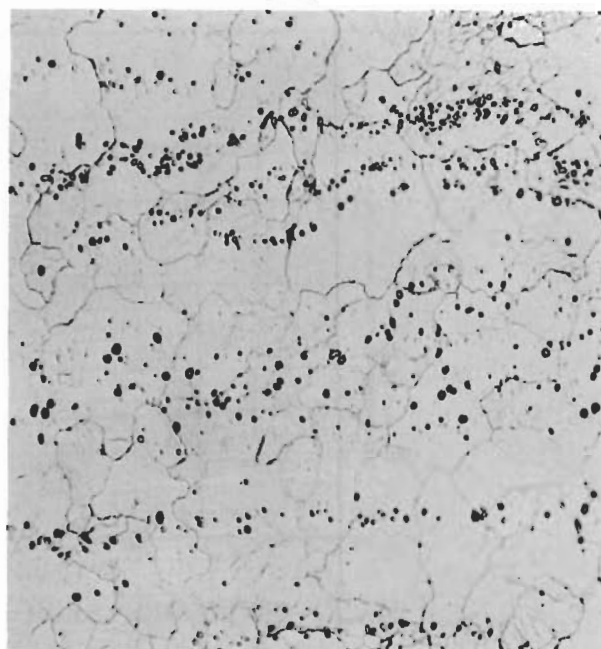
06069-26



Interface

4468

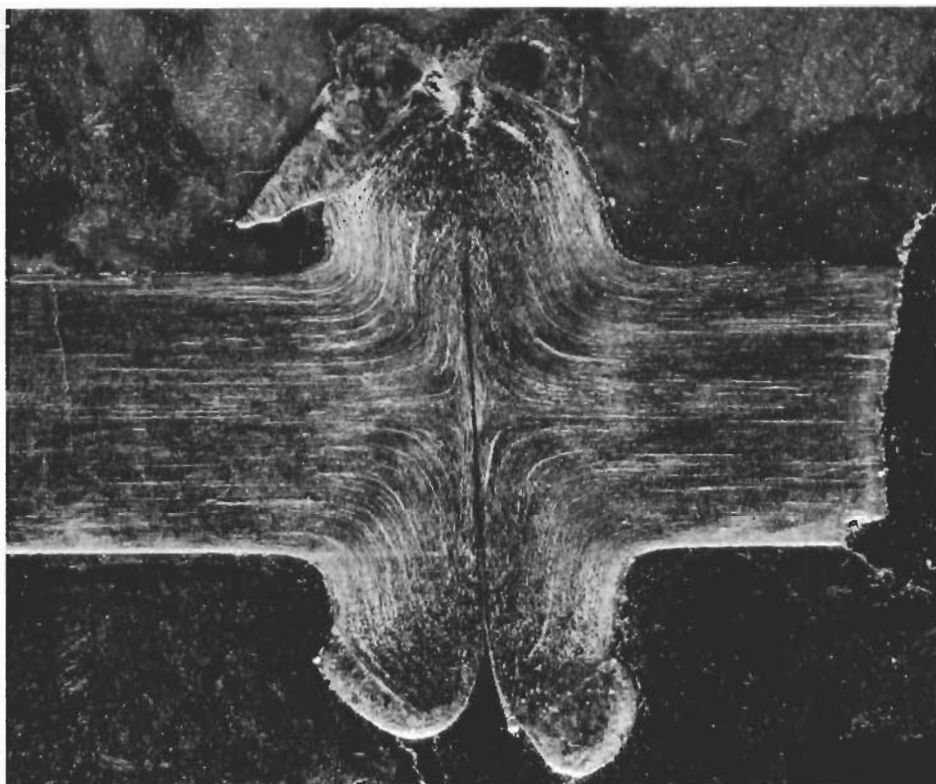
1000X



Heat Affected Zone

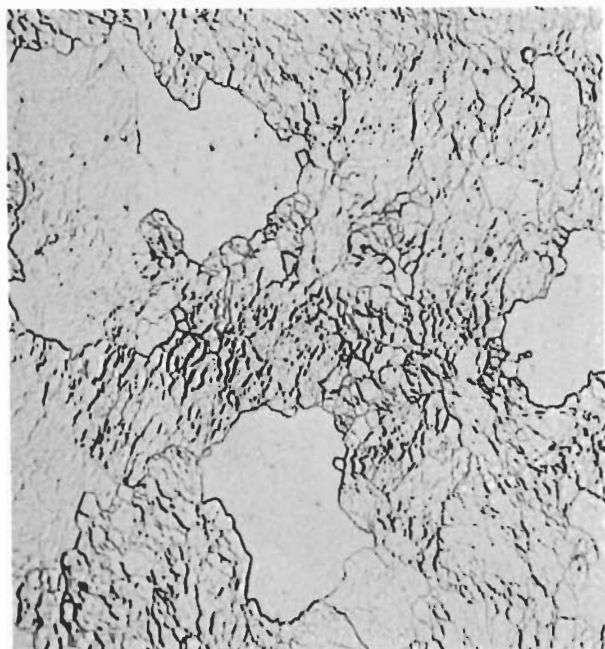
Figure 81 Flash Weld in D31, Weld No. 26





10X

06069-27



Interface

4465



Heat Affected Zone

4466

1000X

Figure 82 Flash Weld in F48, Weld No. 27



TABLE X

FLASH WELD MECHANICAL PROPERTIES

<u>Weld No.</u>	<u>Material</u>	<u>Tensile Strength PSI</u>	<u>Reduction Of Area %</u>	<u>Bend Angle Degrees</u>	<u>Bend Max. Fiber Stress PSI</u>
6	FS82	B	-	B	-
8	FS82	B	-	B	-
10	FS82	13,200	0	0	-
12	FS82	29,200	0	0	-
16	FS82	B	-	B	-
18	FS82	82,300	30.5	0	-
20	FS82	4,600	0	0	-
22	FS82	B	-	B	-
29	FS82	-	-	5	-
30	FS82	-	-	5	-
31*	FS82	71,900	-	-	-
34	FS82	-	-	5	-
35*	FS82	74,100	52.0	-	-
38*	FS82	73,970	69.6	90	-
39*	FS82	75,000	39.6	90	-
25A*	D31	90,600	11.5	-	-
26A	D31	B	-	B	-
40*	D31	92,300	28.3	90	-
41*	D31	92,200	22.9	57	-
27A	F48	B	-	B	-
33*	F48	22,300 a	0.5	0	137,000
42*	F48	B	-	0	115,000
43	F48	B	-	B	-
36*	FS82HS	64,000	52.7	96	-
37*	FS82HS	64,200	49.0	94	-

B - Broke while machining

\* - Heat treated after welding as follows:

FS82 - 2000°F 4-hours

D31 - 2100°F 24-hours

F48 - 33 - 2350°F 24-hours

42 - 2500°F 4-hours

a - Failed on 45° angle in parent sheet

4 hours for FS82 and FS82HS and 2100°F for 24 hours for D31. The F48 welds were not ductile at room temperature even after heat treatment.

## VI SUMMARY

The three alloys included in this investigation are weldable by the TIG process under carefully controlled conditions. However, the bend ductility transition temperature is raised in each of them as a result of welding. For D31 and F48 the 45° bend ductility transition temperature is raised to above 550° and 350°F respectively so that a post heat treatment is required to achieve reasonable ductility at room temperature. Post heat treatments of 2100°F for 24 hours and 2500°F for 4 hours are proven to be most beneficial in lowering the transition temperature of welds in D31 and F48 respectively.

The as-welded 45° transition temperature for FS82 is -100°F; however, this alloy is embrittled by aging in the 1400° to 1800°F temperature range. Ductility is restored in FS82 by overaging at 2000° to 2400°F. A greater loss of ductility occurs in all three alloys when TIG welded outside the vacuum purge atmosphere chamber.

FS82 and 0.020 in. D31 are successfully spot welded by conventional techniques. However, spot welds in 0.060 in. D31 are brittle and require post heat treatment to achieve ductility. Recrystallization type spot welds are superior to fused nugget spot welds in that cracking is eliminated in brittle materials and electrode sticking is minimized.

Flash welds in all materials are brittle as welded but post heat treatments in the FS82 and D31 welds cause a significant improvement in room temperature ductility.

## VII CONCLUSIONS

1. High quality welds can be made in 0.060 in. FS82 and FS82HS alloys at 15 ipm in helium in a vacuum purge atmosphere chamber at 150 - 160 amperes and 14 - 16 arc volts. Under these conditions a bend transition temperature can be expected of -100°F for FS82 and 150°F for FS82HS. Additions of FS82 filler metal raises the transition temperature of FS82 about 70°F and lowers it approximately 50°F for FS82HS. Welds can be made outside the chamber with careful helium shielding at 180 amperes, 16 volts and a speed of 15 ipm. A bend transition temperature of 50°F can be expected for FS82 in this situation. Overaging at 2000°F for 4 hours is recommended if service temperatures in the range of 1400° to 1800°F are expected.

Similar properties can be expected for welds in other sheet thicknesses of this alloy. However, it is necessary to modify the welding parameters according to thickness.

# Contrails

2. Satisfactory welds can be produced in 0.060 in. D31 in a helium atmosphere in a vacuum purge atmosphere chamber at 15 ipm, 150 - 160 amperes and 14 - 15 volts followed by a post heat treatment of 2100°F for 24 hours. A bend transition temperature of approximately 100°F can be expected by following this procedure. If the post heat treatment is omitted, the transition temperature of the weld will be approximately 550°F. Non-chamber welding of D31 is not recommended.

Similar properties can be expected for thinner D31 sheet welded with modified parameters. Thicker D31 sheet may be more susceptible to weld cracking as thickness increases.

3. Maximum as-welded ductility of 0.060 in. F48 alloy can be obtained by welding with a 500°F preheat in a helium atmosphere in a vacuum purge chamber at 134 amperes, 15 arc volts and 15 ipm. A transition temperature of about 350°F can be expected under these conditions. The transition temperature can be lowered to approximately 100°F by post heat treating at 2500°F for 4 hours.

Similar weld properties can be expected for other thicknesses of F48 sheet provided welding parameters are adjusted accordingly. This material may be more susceptible to weld cracking as the thickness increases above 0.060 in.

4. Electron beam welds in these columbium base alloys are significantly more ductile than TIG welds. For 0.060 in. sheet, a welding speed of 40 ipm was satisfactory. Both FS82 and F48 can be welded at 120 ma and 22 kv while D31 can be welded at 100 ma and 20 kv. Transition temperatures of -280°F for FS82, -80°F for FS82HS, 250°F for D31, and 250°F for F48 can be expected with these parameters.

5. FS82 sheet in both 0.020 in. and 0.060 in. thicknesses is ductile as spot welded; however, both D31 and F48 exhibit brittleness in the weld area. Solid phase recrystallization type welds achieved by a low current long time sequence are recommended for D31 and F48 sheet to eliminate weld cracking and porosity. This procedure is helpful in minimizing electrode sticking to the outer sheet surfaces. Post heat treatment of the D31 and F48 welds as suggested for TIG welds, increases the tensile shear strength.

6. The limited investigation of the flash butt welding of these alloys has indicated that FS82, FS82HS, and D31 can be joined with no protective atmosphere. To attain adequate room temperature ductility it is necessary to heat treat FS82 and FS82HS at 2000°F 4-hours and D31 to 2100°F 24-hours. F48 flash welds remained brittle after a 2500°F 4-hour heat treatment. Further work on flash welding these columbium alloys is required, both in air and under a protective atmosphere.

## REFERENCES

1. "Welding Tantalum and Columbium", (L. F. Yntema), Oak Ridge National Laboratory, Tenn., WASH-733, pp 453-476.
2. Nuclear Power Welding Symposium, British Welding Research Assn., Nuclear Power 3: 206-228, May 1958.
3. R. T. Begley, "Development of Columbium Alloys", WADC TR 57-344, Part 4, April 1960.
4. R. T. Begley and W. N. Platte, "Development of Columbium Base Alloys", WADC TR 57-233, Part 4, April 1960.
5. J. Fugardi and J. L. Zambrow, "Cladding and Welding of Stainless Steel to Molybdenum and Columbium", WADS TR 58-674, October 1959.
6. E. A. Franco-Ferreira, "Welding and Brazing", Oak Ridge National Laboratory, Tenn., ORNL-2988, pp 456-458.
7. J. T. Stacey, "Welding Columbium and Columbium Alloy for Hypersonic Flight Vehicles", Western Metalworking, April 1960.
8. R. D. Johnson and L. W. Derry, "An Unusual Feature of the Fusion Welding of Columbium to Vanadium", Nature, MacMillan and Co., London, January 7, 1961.
9. C. F. Burrows, M. M. Schwartz, and L. F. Gagola, "Welding and Brazing of Two Columbium Alloys", Materials in Design Engineering, October 1960.
10. W. R. Young, General Electric Flight Propulsion Laboratory, private communication.
11. H. J. Siegel, McDonnell Aircraft Corporation, private communication.
12. A. F. Trabold and Steven Bank, "Fabrication Studies on Columbium Alloy Sheet", Metal Progress, Vol. 79-5, May 1961.
13. T. L. Robertshaw, M. A. Levinstein, and J. W. Pugh, "Powder Metallurgy of Columbium", ASD Technical Report 61-559, November 1961.
14. S. J. Paprocki, E. L. Hodge, and P. J. Gripshover, "Gas Pressure Bonding", DMIC Report 159, September 25, 1961.
15. S. J. Paprocki, E. L. Hodge, and P. J. Gripshover, "Solid Phase Bonding of Columbium". Paper from Columbium Metallurgy v10, Metallurgical Society of AIME, Interscience, pp 13-30, 1961.



# Contrails

16. S. J. Paprocki, E. L. Hodge, and P. J. Gripshover, "The Bonding of Molybdenum and Columbium-Clad Fuel Elements", BMI-1451, Battelle Memorial Institute, July 12, 1960.
17. J. Byron Jones, Nicholas Maropis and others, "Development of Ultrasonic Welding Equipment for Refractory Metals", Interim Technical Engineering Report, (AD 263 872) (U61-4-5), 1 June-31 August 1961, September 1961.
18. W. E. Weare and R. E. Monroe, "Ultrasonic Welding of Heat Resisting Metals", Welding Journal, Vol. 40, pp 351S-358S.
19. B. R. Rajala and R. J. VanThyne, "Improved Vanadium Base Alloys" ARF 2196-6, Armour Research Foundation.
20. W. R. Young, "Alloy Systems for Brazing of Columbium and Tungsten", ASD Technical Report 61-592.

# Contrails

## APPENDIX

### TABLE A-1

#### PARAMETERS OF WELDS MADE IN VACUUM ATMOSPHERE WELDING CHAMBER

<u>Weld No.</u>	<u>Material</u>	<u>Welding Speed In/Min.</u>	<u>Amps</u>	<u>Volts</u>	<u>Gas</u>	<u>Tungsten Size</u>	<u>Weld Quality</u>
AA-1	FS82	5	195	10.5	A	1/8 pure	1
AB-1	"	"	205	12.5	"	3/32	1
AC-1	"	"	215	12.5	"	"	
AD-1	"	"	220	13.5	"	"	
AE-1	"	"	160	15.5-16.5	He	"	1
AF-1	"	15	"	15	"	"	2
AG-1	"	"	"	"	"	"	
AH-1	"	36	240	17.5	"	"	
CA-1	D31	15	160	12.5	"	"	
CB-1	"	36	250	17.5	"	"	3
CC-1	"	"	245	15.15.5	"	"	3
CA-2	"	"	230	14	"	"	3
CB-2	"	"	242	15	"	"	3
AI-1	FS82	"	290	17	A	"	1
CC-2	D31	"	340	16.5	"	1/8	3
AA-2	FS82	"	345	15.5	"	"	1
CA-3	D31	28.5	200	16.5	He	3/32	3
CB-3	"	21	178	"	"	"	
CB-4	"	5	180	11.5	A	"	2
CC-3	"	15	220	14	"	"	2
CE-1	"	"	215	13.4	"	"	
CC-4	"	36	310	14	"	1/8	3
CE-2	"	"	300	"	"	"	
AB-2	FS82	"	305	"	"	"	1
AD-2	"	"	350	15	"	"	1
AE-2	"	"	380	"	"	"	5
AA-3	"	"	360	"	"	"	6
AG-2	"	"	"	13	"	"	
BD-1	FS82HS	"	370	12.5	"	"	5
BD-2	"	"	330	"	"	"	
AF-2	FS82	15	222	13.5	"	3/32	
BD-3	FS82HS	"	220	14	"	"	
CB-5	D31	"	150	13.5	He	"	
CA-5	"	"	"	13	"	"	
CA-6	"	"	"	"	"	"	3
CE-3	"	"	"	15.5	"	"	
CE-4	"	"	"	13	"	"	4
CE-6	"	"	"	"	"	"	3
CE-5	"	"	"	13.5-14.5	"	"	
CB-7	"	"	"	14.5	"	"	3
AA-4	FS82	"	"	15.5	"	"	

# Contrails

TABLE A-1 (continued)

<u>Weld No.</u>	<u>Material</u>	<u>Welding Speed In/Min.</u>	<u>Amps</u>	<u>Volts</u>	<u>Gas</u>	<u>Tungsten Size</u>	<u>Weld Quality</u>
BD-4	FS82HS	15	150	13-15	He	3/32	
AF-3	FS82	"	"	15.5	"	"	
AH-2	"	"	"	14.5	"	"	
AI-2	"	"	"	15	"	"	1
AC-3	"	"	"	"	"	"	
AH-3	"	"	"	"	"	"	
AE-3	"	"	160	"	"	"	
AD-3	"	"	150	"	"	"	1
AB-3	"	"	168	14.5	"	"	
AA-5	"	"	165	"	"	"	
AB-4	"	"	"	"	"	"	
AF-4	"	"	"	"	"	"	
AG-4	"	"	"	"	"	"	
CC-5	D31	"	"	14.5-15.5	"	"	
CB-8	"	"	"	"	"	"	3
CE-5	"	"	"	"	"	"	
DA-1	F48	"	"	"	"	"	3
DA-2	"	"	"	"	"	"	3
CA-7	D31	"	"	"	"	"	
CB-9	"	"	"	"	"	"	3
CC-6	"	"	"	"	"	"	3
CE-7	"	"	"	"	"	"	
AD-4	FS82	"	"	"	"	"	
AH-4	"	"	"	"	"	"	
BD-5	FS82HS	"	"	"	"	"	
AA-7	FS82	"	"	"	"	"	
BC-1	FS82HS	"	"	"	"	"	
CE-8	D31	5	130	"	"	"	3
DA-3	F48	"	140	15.5	"	"	7
DA-4	"	"	160	14.5-15	"	"	
AE-4	FS82	15	"	"	"	"	
AA-8	"	"	150	"	"	"	
DA-5	F48	15	165	14-14.5	"	"	
DA-6	"	"	"	15	"	"	
DB-1	"	"	"	"	"	"	
DD-1	"	"	160	15.5	"	"	
DC-2	"	"	"	"	"	"	
DC-3	"	"	"	"	"	"	3
AF-7	FS82	"	165	"	"	"	
CC-10	D31	"	160	15	"	"	
AH-8	FS82	"	165	15.5	"	"	
DE-4	F48	"	160	16	"	"	3
DD-4	"	"	170	16.5	"	"	
BC-5	FS82HS	"	160	15	"	"	

# Contrails

TABLE A-1 (continued)

<u>Weld No.</u>	<u>Material</u>	<u>Welding Speed In/Min.</u>	<u>Amps</u>	<u>Volts</u>	<u>Gas</u>	<u>Tungsten Size</u>	<u>Weld Quality</u>
BC-6	FS82HS	15	160	15	He	3/32	
DD-7	F48	"	165	16.5	"	"	
DE-7	"	"	170	"	"	"	
CB-15	D31	"	160	15	"	"	
CC-12	"	"	"	"	"	"	
*AB-13	FS82	"	165	"	"	"	
*DC-6	F48	"	"	"	"	"	
*CB-16	D31	"	160	14.5	"	"	
**CC-13	"	"	"	15.5	"	"	
**DC-7	F48	"	"	16	"	"	
**AB-14	FS82	"	"	15	"	"	
***AH-11	"	"	"	"	"	"	
***CC-14	D31	"	"	14.5	"	"	
***DE-8	F48	"	"	16	"	"	
***DB-5	"	"	"	"	"	"	
CC-7	D31	"	150	14	"	"	3
CB-10	"	"	"	"	"	"	
CE-9	"	"	"	"	"	"	
CA-8	"	"	"	"	"	"	
DA-7	F48	"	165	15	"	"	3
DA-8	"	"	160	"	"	"	3
DB-2	"	"	"	"	"	"	
AF-5	FS82	"	155	"	"	"	
AH-5	"	"	"	"	"	"	
AG-5	"	"	"	"	"	"	
AB-5	"	"	"	"	"	"	
AI-3	"	"	"	"	"	"	
AB-6	"	"	"	"	"	"	
AC-4	"	"	"	"	"	"	
AA-9	"	"	"	"	"	"	
CE-10	D31	"	"	"	"	"	
DA-9	F48	"	"	15.5	"	"	
DB-3	"	"	"	16	"	"	
CA-9	D31	"	150	"	"	"	
CB-10	"	"	155	15.5	"	"	
CC-8	"	"	150	15	"	"	
CE-11	"	36	220	17.5	"	"	3
AI-5	FS82	15	155	15	"	"	1
AB-9	"	"	160	16	"	"	
AB-10	"	"	"	"	"	"	
AG-7	"	"	"	"	"	"	
CA-10	D31	"	165	16	"	"	
CB-12	"	"	"	"	"	"	
AB-11	FS82	"	"	"	"	"	



# Contrails

TABLE A-1 (continued)

<u>Weld No.</u>	<u>Material</u>	<u>Welding Speed In/Min.</u>	<u>Amps</u>	<u>Volts</u>	<u>Gas</u>	<u>Tungsten Size</u>	<u>Weld Quality</u>
AI-6	FS82	15	165	16	He	3/32	
AB-12	"	"	"	15.5	"	"	
AH-6	"	"	"	"	"	"	
AH-7	"	"	"	"	"	"	
AF-6	"	"	"	"	"	"	
BC-3	FS82HS	"	"	14.5	"	"	
BC-4	"	"	"	"	"	"	
DA-10	F48	"	"	15	"	"	3
DE-3	"	"	160	15.5	"	"	
a DC-8	"	"	135	15	"	"	1
a DC-9	"	"	"	"	"	"	
a CB-18	D31	"	140	14.5	"	"	
a CB-17	"	"	150	16	"	"	
a CA-19	"	"	"	"	"	"	
AC-5	FS82	"	170	15.5	"	"	
AD-5	"	"	"	"	"	"	
DE-9	F48	"	176	16.5	"	"	
DD-8	"	"	"	"	"	"	
CA-17	D31	"	168	15.5	"	"	
CC-15	"	"	"	"	"	"	
b AC-6	FS82	"	200	16	"	"	
b AD-6	"	"	190	"	"	"	
b AE-5	"	"	"	16.5	"	"	
b CA-20	D31	"	200	15	"	"	
*CC-15	"	"	190	15.5	"	"	3
d AF-10	FS82	"	"	17	"	"	
d AC-7	"	"	"	16	"	"	
d AA-10	"	"	"	"	"	"	
c CC-16	D31	"	"	16.5	"	"	3
d CA-21	"	"	"	"	"	"	
d AC-8	FS82	"	"	"	"	"	
d DD-9	F48	"	200	18	"	"	
d DD-10	"	"	"	"	"	"	
c AH-12	FS82	"	195	16.5	"	"	
c CA-22	D31	"	"	17	"	"	
c CA-23	"	"	"	"	"	"	
c CB-18	"	"	190	"	"	"	
c DD-11	F48	"	185	"	"	"	
c DD-12	"	"	190	"	"	"	
c CB-19	D31	"	170	17	"	"	
c CA-24	"	"	175	"	"	"	
b BC-6	FS82HS	"	180	16	"	"	
b DC-7	"	"	"	"	"	"	
b BD-6	"	"	"	"	"	"	

TABLE A-1 (continued)

<u>Weld No.</u>	<u>Material</u>	<u>Welding Speed In/Min.</u>	<u>Amps</u>	<u>Volts</u>	<u>Gas</u>	<u>Tungsten Size</u>	<u>Weld Quality</u>
AC-9	FS82	15	168	16.5	He	3/32	
AD-7	"	"	"	"	"	"	
AE-6	"	"	"	"	"	"	
<del>AC</del> -10	"	"	175	16	"	"	
**AE-7	"	"	180	15.5	"	"	
DD-13	Fl8	"	170	16	"	"	
S95A-1	"	"	"	"	"	"	
BC-8	FS82HS	"	160	15	"	"	

- 1 - Insufficient penetration
- 2 - Wide weld bead
- 3 - Transverse cracks
- 4 - Longitudinal cracking
- 5 - Amperage too high, burned holes
- 6 - Weld not satisfactory for testing
- 7 - Severely cracked
- a - Preheat 500°F
- b - FS82 filler wire added to weld puddle
- c - FS80 filler wire added to weld puddle
- d - Pure columbium filler wire added to weld puddle
- ~~1~~ - 2% thoriated tungsten except where noted
- ~~11~~ - FS82 shim used for filler material
- \* - 200 ppm air admitted to chamber atmosphere
- \*\* - 600 ppm air admitted to chamber atmosphere
- \*\*\* - 1300 ppm air admitted to chamber atmosphere

# Contrails

TABLE A-2

PARAMETERS OF WELDS MADE OUTSIDE THE VACUUM ATMOSPHERE PURGE CHAMBER

Weld No.	Alloy	Filler Wire	Amps	Volts	Welding Speed In/Min.	Helium Flow, CFH			Weld Quality
						Torch	Trailer	Back up	
*DE-1	F48	None	220	18	15	32	70	20	2, 3
AB-7	FS82	"	180	16	"	40	"	5	
CC-9	D31	"	"	"	"	"	"	"	
DB-4	F48	"	"	17	"	"	"	"	
AI-4	FS82	"	160	16	5	"	"	"	1
AB-8	"	"	175	"	"	"	"	"	4
CE-12	D31	"	"	"	"	"	"	"	4
DC-1	F48	"	"	"	"	"	"	"	1, 4
CB-11	D31	"	"	"	"	"	"	"	2
AG-6	FS82	"	180	"	"	"	"	2	
DE-2	F48	"	"	"	"	"	"	"	3
*CA-11	D31	"	280	12.5	36	"	80	10	2
*DD-2	F48	"	160	14	15	"	"	"	
**DD-3	"	"	220	"	"	"	"	"	
**CB-13	D31	"	"	"	"	"	"	"	
AH-9	FS82	FS82	"	16	"	40	15	5	
AF-8	"	"	210	"	"	"	"	"	
CA-12	D31	"	190	18	"	"	"	"	2
CA-13	"	"	"	"	"	"	"	"	2
DC-4	F48	"	195	"	"	"	"	"	
DE-5	"	"	"	"	"	"	"	"	2
DD-5	"	Pure Cb	220	16	"	"	"	"	
CE-13	D31	"	"	"	"	"	"	"	
CA-14	"	FS82	200	18	"	"	"	"	
CB-14	"	Pure Cb	220	16	"	"	"	"	
DD-6	F48	"	"	"	"	"	"	"	
CC-11	D31	FS80	"	"	"	"	"	"	2
CE-14	"	"	"	"	"	"	"	"	2
DE-6	F48	"	"	"	"	"	"	"	
DC-5	"	None	180	16	"	"	"	"	
CA-15	D31	"	"	"	"	"	"	"	
CA-16	"	"	"	"	"	"	"	"	
AF-9	FS82	"	"	"	"	"	"	"	
AH-10	"	"	"	"	"	"	"	"	

- 1 Insufficient penetration
- 2 Transverse cracking
- 3 Severely cracked

- 4 Contaminated by air
- \* Preheat 300°F
- \*\* Preheat 450°F

TABLE A-3

PARAMETERS OF WELDS MADE BY THE ELECTRON BEAM PROCESS

<u>Weld No.</u>	<u>KV</u>	<u>MA</u>	<u>Welding Speed In/Min.</u>	<u>Gun Distance From Work In.</u>	<u>Focus</u>
ACEB-1	22	116	40	1.5	62
ACEB-2	22	116	40	1.5	62
AHEB-3	22	140	40	1.5	60
BC2EB-1	22	135	50	1.5	60
ADEB-1	22	132	40	1.5	61
CCEB-4	19	52	20	1.5	60
CCEB-2	21	47	20	1.5	62.5
CA2EB-4	21	50	20	1.5	62.5
CCEB-3	19	155	60	1.5	57
CA2EB-1	25	45	30	1.5	62.5
CA2EB-2	20	100	40	1.5	60
CBEB-2	20	102	40	1.5	60
DC1EB-1	22	135	40	1.5	60
DD1EB-1	26	135	24	1.5	68
DS95AEB-2	22	120	40	1.5	62
DA95AEB-3	22	118	40	1.5	62
DS95AEB-4	22	117	40	1.5	62
DWEB-1	22	135	40	1.5	60
DWEB-2	22	135	40	1.5	60
S95AEB-12	19	150	60	1.5	57
S95AEB-6	20	137	60	1.5	58
S95AEB-9	19	147	60	1.5	57
S95AEB-10	15	117	20	1.5	55



TABLE A-4

FLASH WELDING DATA

<u>Weld No.</u>	<u>Alloy</u>	<u>Initial Die Opening In.</u>	<u>Total Flash- Off In.</u>	<u>Total Upset In.</u>	<u>Flash Curve A</u>	<u>Flash Time Sec.</u>	<u>Upset Heat %</u>	<u>Upset Time Sec.</u>
1	FS82	1.00	0.40	0.20	2.718	3.65	100	1.5
2	FS82	1.00	0.40	0.20	2.718	3.65	100	1.5
3	FS82	1.00	0.40	0.30	2.718	3.65	100	1.5
4	FS82	1.00	0.40	0.25	2.718	3.65	100	1.5
5, 6	FS82	1.00	0.40	0.25	2.718	3.65	70	1.5
7, 8	FS82	1.00	0.40	0.25	2.718	3.65	40	1.5
9, 10	FS82	1.00	0.40	0.25	2.718	3.65	50	4.5
11, 12	FS82	1.00	0.40	0.25	2.718	1.82	50	4.5
13	FS82	1.00	0.20	0.15	2.718	1.30	50	4.5
14	FS82	1.00	0.20	0.25	2.718	1.30	50	4.5
15, 16	FS82	0.75	0.20	0.25	2.718	1.30	50	4.5
17, 18	FS82	0.75	0.20	0.25	5.0	1.30	50	4.5
19, 20	FS82	0.70	0.20	0.20	5.0	1.30	50	4.5
21, 22	FS82	0.70	0.20	0.20	2.718	1.30	50	4.5
23	D31	0.70	0.20	0.20	2.718	1.30	50	4.5
24	D31	1.00	0.40	0.25	2.718	3.65	50	4.5
25, 25A	D31	0.80	0.25	0.25	2.718	1.30	50	4.5
26, 26A	D31	0.80	0.25	0.25	5.0	1.30	50	4.5
27, 27A	F48	0.80	0.25	0.25	2.718	1.30	50	4.5
29	FS82	1.05	0.40	0.30	2.718	3.65	70	4.5
30, 31	FS82	1.05	0.40	0.30	5.0	3.65	70	4.5
32	F48	1.05	0.40	0.25	5.0	3.65	70	4.5
33	F48	1.05	0.40	0.30	5.0	3.65	70	4.5
34, 35	FS82	1.05	0.40	0.30	5.0	3.65	70	4.5
36, 37	FS82HS	1.00	0.40	0.30	5.0	1.82	70	4.5
38, 39	FS82	1.00	0.40	0.30	5.0	1.82	70	4.5
40, 41	D31	1.00	0.40	0.30	5.0	1.82	70	4.5
42, 43	F48	1.00	0.40	0.30	5.0	1.82	70	4.5